Supporting Information for

Enantioselective Cycloaddition of Styrenes with Aldimines Catalyzed by a Chiral Magnesium Potassium Binaphthyldisulfonate Cluster as a Chiral Brønsted Acid Catalyst

Manabu Hatano, Keisuke Nishikawa, and Kazuaki Ishihara*

Graduate School of Engineering, Nagoya University, Furo-cho, Chikusa, Nagoya, 464-8603, Japan.

ishihara@cc.nagoya-u.ac.jp

Table of Contents:

1. General methods.

^{1}H NMR spectra were measured on a JEOL ECS400 (400 MHz) spectrometer at ambient temperature. Data were recorded as follows: chemical shift in ppm from internal tetramethylsilane on the δ scale, multiplicity (s = singlet; d = doublet; t = triplet; q = quartet, m = multiplet, br = broad), coupling constant (Hz), integration, and assignment. ^{13}C NMR spectra were measured on a JEOL ECS400 (100 MHz) spectrometer. Chemical shifts were recorded in ppm from the solvent resonance employed as the internal standard (deuterochloroform at 77.00 ppm). ^{19}F NMR spectra were measured on a JEOL ECS-400 (376 MHz) spectrometer. Chemical shifts were recorded in ppm from the solvent resonance employed as the external standard ($CFCl_3$ at 0 ppm). Optical rotations were measured on Rudolph Autopol IV digital polarimeter. The products were purified by column chromatography on silica gel (E. Merck Art. 9385; Kanto Chemical Co., Inc. 37560). High resolution mass spectral analyses were performed at Chemical Instrument Center, Nagoya University (JEOL JMS-700 (FAB), Bruker Daltonics micrOTOF-QII (ESI)). Infrared (IR) spectra were recorded on a JASCO FT/IR 460 plus spectrometer. ICP-OES analysis was performed with Varian Vista-Pro-AX. For ICP-OES analysis, ultrapure grade nitric acid, methanol, and water were used. High performance liquid chromatography (HPLC) analysis was conducted using Shimadzu LC-10 AD coupled diode array-detector SPD-M20A and chiral column of Daicel CHIRALCEL, CHIRALPAK; AD-H, AD-3, OD-3, and IA-3. X-ray analysis was performed by Rigaku PILATUS-200K. For thin-layer chromatography (TLC) analysis throughout this work, Merck precoated TLC plates (silica gel 60GF254 0.25 mm) were used. Visualization was accomplished by UV light (254 nm), anisaldehyde, $KMnO_4$, and phosphomolybdic acid. Dichloroethane and dichloromethane were freshly distilled in prior to use. Other dry solvents such as acetonitrile, toluene, diethyl ether, DMSO, THF, etc. were purchased and used without further treatment.

2. Preparation of (*R*)-3,3'-Ar$_2$-BINSAs.

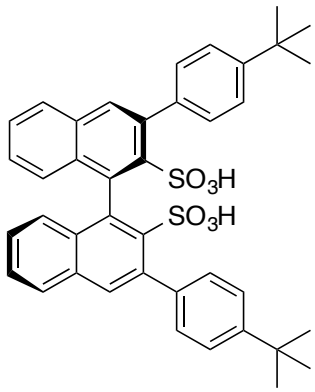

(*R*)-3,3'-Di(4-*tert*-butylphenyl)-(1,1'-binaphthyl)-2,2'-disulfonic acid ((*R*)-1a): The titled compound was prepared according to our reported procedure.[1] Pale brown soild. ^{1}H NMR (400 MHz, CD_3OD) δ 1.39 (s, 18H), 7.06 (d, *J* = 8.7 Hz, 2H), 7.22 (t, *J* = 7.3 Hz, 2H), 7.42 (d, *J* = 8.2 Hz, 4H), 7.49 (t, *J* = 7.3 Hz, 2H), 7.54 (d, *J* = 8.7 Hz, 4H), 7.79 (s, 2H), 7.88 (d, *J* = 7.8 Hz, 2H). ^{13}C NMR (100 MHz, CD_3OD) δ 31.9 (6C), 35.3 (2C), 124.9 (4C), 127.6 (2C), 128.6 (2C), 128.7 (2C), 129.1 (2C), 130.7 (4C), 133.1 (2C), 134.0 (2C), 134.6 (2C), 138.3 (2C), 138.7 (2C), 140.1 (2C), 141.3 (2C). 150.3 (2C). IR (KBr) 3421, 2962, 1698, 1511, 1363, 1165, 1095, 1033 cm^{-1}. M.p. 171-174 °C (decomposition). $[\alpha]_D^{26}$ = +66.8 (*c* 1.0, MeOH, (*R*)). HRMS (FAB–) calcd for $C_{40}H_{37}O_6S_2$ $[M\text{-}H]^-$ 677.2032, found 677.2024.

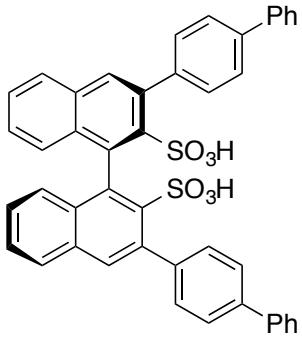

(*R*)-3,3'-Di(4-biphenyl)-(1,1'-binaphthyl)-2,2'-disulfonic acid ((*R*)-1b):[1] The titled compound was prepared in our report.[1] Pale brown soild. ^{1}H NMR (400 MHz, CD_3OD) δ 7.10 (d, *J* = 8.6 Hz, 2H), 7.27 (t, *J* = 7.0 Hz, 2H), 7.33 (t, *J* = 7.3 Hz, 2H), 7.44 (t, *J* = 7.8 Hz, 4H), 7.51 (t, *J* = 7.8 Hz, 2H), 7.62-7.67 (m, 4H), 7.68-7.74 (m, 8H), 7.86 (s, 2H), 7.91 (d, *J* = 8.2 Hz, 2H). ^{13}C NMR (100 MHz, CD_3OD) Many peaks overlapped. δ 126.5, 127.7, 127.9, 128.1, 128.7, 128.8, 129.1, 129.8, 131.6, 132.9, 134.1, 134.6, 138.5, 138.7, 139.7, 140.6, 142.4, 143.3. IR (KBr) 3382, 1697, 1486, 1220, 1164, 1033 cm^{-1}. M.p. 220-224 °C (decomposition). $[\alpha]_D^{27}$ = +17.2 (*c* 1.0, MeOH, (*R*)). HRMS (FAB–) calcd for $C_{44}H_{29}O_6S_2$ $[M–H]^-$ 717.1406, found 717.1391.

3. General procedure for the catalytic enantioselective cycloaddition of styrenes with aldimines (Schemes 1 and 2).

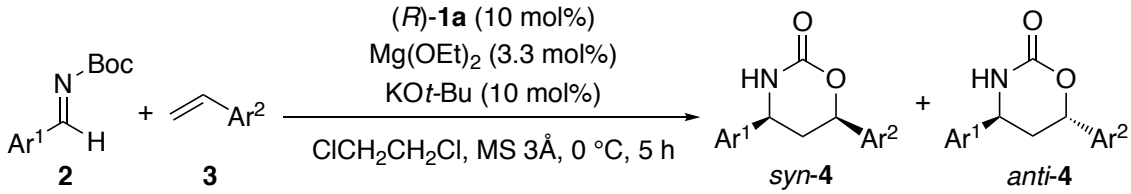

(*R*)-**1a** (13.6 mg, 0.020 mmol, 10 mol%) was placed in a Schlenk test tube under a nitrogen atmosphere and dissolved in dry dichloroethane (2 mL). To a stirred solution were added magnesium ethoxide (0.10 *M* in methanol, 66.7 μL, 0.0067 mmol, 3.3 mol%) and potassium *tert*-butoxide (1.0 *M* in methanol, 20 μL, 0.020 mmol, 10 mol%) at room temperature, and the solution was stirred for 1 h. The volatiles were removed *in vacuo*, and then dichloroethane (1 mL) was added and removed *in vacuo* again. This solvent-removal sequence was repeated twice, and the magnesium/potassium salt of (*R*)-**1a** was obtained *in situ* as pale yellow solid. Then dichloroethane (20 mL) and well-activated MS 3Å (50 mg) were added at 0 °C, and the suspension was stirred at 0 °C for 30 min. Styrene **3** (4.0 mmol) was then added to the suspension, and the mixture was stirred at 0 °C for 30 min. Aldimine **2**[2] (0.20 mmol), which was dissolved in dichloroethane (2 mL) in advance when **2** is solid, was then added at 0 °C, and the mixture was stirred at 0 °C for 5–20 h. The resulting reaction mixture was quenched with triethylamine (0.2 mL) at 0 °C, and filtered through a pad of Celite. The organic phase was concentrated under reduced pressure, and the resultant residue was purified by silica gel column chromatography (eluent: *n*-hexane:EtOAc = 5:1 to 1:15) to give the desired product **4**. *(R)-**1a** was recovered (ca. 90–95%) through the same chromatography using chloroform/methanol.* The enantiomeric purity of **4** was determined by chiral HPLC analysis.

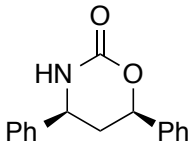

(4*S*,6*R*)-4,6-Diphenyl-1,3-oxazinan-2-one (*syn*-4a):[3–5] 91% yield (5 h), *syn*:*anti* = >99:<1, 96% ee (*syn*). Colorless soild. ^{1}H NMR (400 MHz, $CDCl_3$) δ 2.07 (dt, *J* = 14.2, 11.5 Hz, 1H), 2.41 (dm, *J* = 14.2 Hz, 1H), 4.78 (dd, *J* = 11.5, 4.6 Hz, 1H), 5.31 (br, 1H), 5.45 (dd, *J* = 11.5, 1.8 Hz, 1H), 7.27-7.48 (m, 10H). ^{13}C NMR (100 MHz, $CDCl_3$) δ 39.2, 55.7, 78.5, 125.8 (2C), 126.1 (2C), 128.6 (4C), 129.1 (2C), 138.5, 140.5, 154.3. IR (KBr) 3211, 3107, 2924, 1699, 1455, 1404, 1305, 1285, 1148, 1058 cm^{-1}. M.p. 187-188 °C. $[\alpha]_D^{25}$ = 19.6 (*c* 1.00, $CHCl_3$, 96% ee, (4*S*,6*R*)). HPLC analysis; IA-3, *n*-hexane/*i*-PrOH = 7/3, 1.0 mL/min, 210 nmm t_R = 9.9 min (major, 4*S*,6*R*), 18.6 min (minor, 4*R*,6*S*). HRMS (FAB+) calcd for $C_{16}H_{16}NO_2$ $[M+H]^+$ 254.1181, found

254.1181. *syn/anti*-Isomers were identified by ^{1}H NMR analysis of the authentic sample by using $HBF_4 \cdot Et_2O$ (10 mol%); δ 4.78 (dd, *J* = 11.5, 4.6 Hz, 1H, PhC*H*–N (*syn*)), 4.63 (m, 1H, PhC*H*–N (*anti*)), *syn:anti* = 75:25.

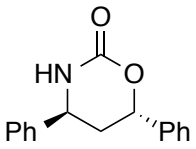

(4*S*,6*S*)-4,6-Diphenyl-1,3-oxazinan-2-one (*anti*-4a):[4] Colorless soild. ^{1}H NMR was consistent with previously reported values.[4] ^{1}H NMR (400 MHz, $CDCl_3$) δ 2.25 (m, 1H), 2.47 (dm, 1H), 4.64 (m, 1H), 5.35 (m, 1H), 5.37 (br, 1H), 7.29-7.42 (m, 10H).

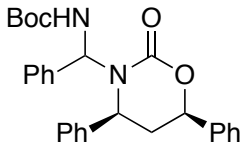

***tert*-Butyl (((4*S*,6*R*)-2-oxo-4,6-diphenyl-1,3-oxazinan-3-yl)(phenyl)methyl)carbamate (5a):** A single diastereomer was obtained, although the stereochemistry was unknown. Colorless soild. ^{1}H NMR (400 MHz, $CDCl_3$) δ 1.50 (s, 9H), 2.36-2.51 (m, 2H), 5.15 (dd, *J* = 10.8, 6.0 Hz, 1H), 5.39 (dd, *J* = 10.5, 3.2 Hz, 1H), 5.90 (d, *J* = 9.6 Hz, 1H), 6.25 (d, *J* = 10.1 Hz, 1H), 7.15-7.45 (m, 15H). ^{13}C NMR (100 MHz, $CDCl_3$) δ 28.4 (3C), 40.1, 63.0, 68.0, 77.8, 80.2, 125.8 (3C), 126.8 (2C), 127.5, 127.9 (2C), 128.2 (2C), 128.7, 128.8 (2C), 129.0 (2C), 138.0, 138.5 (2C), 153.5, 155.7. LRMS (FAB+) calcd for $C_{28}H_{31}N_2O_4$ $[M+H]^+$ 459, found 459.

To confirm the stereochemistry, compound **5a** was transformed into *syn*-**4a** through the hydrolysis with HCl in 86% yield as below.

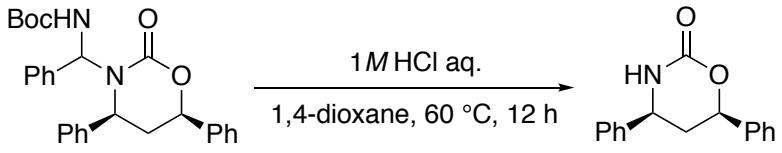

5a *syn*-**4a**, 85%

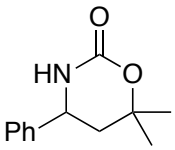

6,6-Dimethyl-4-phenyl-1,3-oxazinan-2-one (6a):[5] Colorless soild. ^{1}H NMR was consistent with previously reported values.[6] ^{1}H NMR (400 MHz, $CDCl_3$) δ 1.44 (s, 3H), 1.52 (s, 3H), 1.83 (dd, *J* = 13.8, 11.8 Hz, 1H), 2.02 (m, 1H), 4.62 (dd, *J* = 11.8, 4.7 Hz, 1H), 5.76 (br, 1H), 7.31-7.47

(m, 5H).

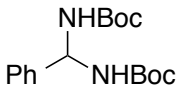

Di-*tert*-butyl (phenylmethylene)dicarbamate (7a):[7] Colorless soild. ^{1}H NMR was consistent with previously reported values.[7] ^{1}H NMR (400 MHz, $CDCl_3$) δ 1.42 (s, 18H), 5.55 (br, 1H), 6.07-6.11 (m, 1H), 7.29-7.42 (m, 5H).

4. Screening of (*R*)-3,3-Ar$_2$-BINSAs 1 in the probe reaction of 3a with 2a.

Table S1 summarizes the screening of (*R*)-3,3-Ar$_2$-BINSAs **1** for the cluster catalyst (3.3 mol%) in the probe reaction of **3a** with **2a**. The catalyst derived from (*R*)-**1b** (entry 4) was slightly less effective than the optimized catalyst derived from (*R*)-**1a** (entry 1). The catalysts derived from (*R*)-**1c**, (*R*)-**1d**, and (*R*)-**1e** showed almost no catalytic activities (entries 5–7). Steric hindrance of (*R*)-**1c** might make it difficult to generate the possible cluster catalyst (entry 5). Less sterically hindered (*R*)-**1d** might not be effective for stabilizing the corresponding cluster catalyst (entry 6). The low solubility of the catalyst derived from (*R*)-**1e** might be a possible reason for the low

Table S1. Screening of (*R*)-3,3-Ar$_2$-BINSAs (**1**).[a]

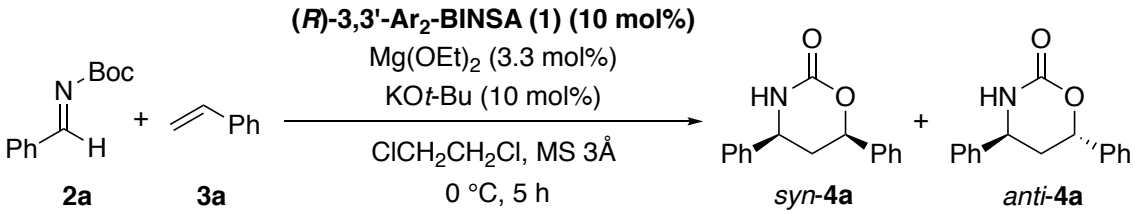

2a **3a** *syn*-**4a** *anti*-**4a**

entry	(*R*)-**1**	Ar	yield (%)	*syn*-**4a**:*anti*-**4a**	ee (%) of *syn*-**4a**
1	(*R*)-**1a**	**4-*t*-BuC$_6$H$_4$**	**91**	**>99:<1**	**96**
2[b]	(*R*)-**1a**	4-*t*-BuC$_6$H$_4$	63	>99:<1	93
3[c]	(*R*)-**1a**	4-*t*-BuC$_6$H$_4$	67	>99:<1	89
4	(*R*)-**1b**	4-PhC$_6$H$_4$	90	>99:<1	90
5	(*R*)-**1c**	3,5-Ph$_2$C$_6$H$_3$	0	–	–
6	(*R*)-**1d**	Ph	10	83:17	24
7	(*R*)-**1e**	H	8	80:20	–12

[a] The reaction was carried out with **2a** (0.20 mmol), **3a** (4 mmol) in dichloroethane at 0 °C for 5 h in the presence of 3.3 mol% of the catalyst and MS 3Å. [b] 2 mmol of **3a** was used. [c] 1.7 mol% of the catalyst was used.

catalytic activity (entry 7). When styrene **3a** was reduced to 2 mmol (i.e., 10 equiv), the yield was decreased (63%) although enantioselectivity was almost the same (93% ee) (entry 2). When the catalytic amount was reduced to 1.7 mol%, both the yield and enantioselectivity were decreased (63% yield, 89% ee) (entry 3). Overall, at least in this probe reaction of **2a** and **3a**, 20 equiv of **3a** and 3.3 mol% of the catalyst were necessary. Also see, Eq. 7 in the paper with the use of 4-methylstyrene **3b**, where 2 equiv of **3b** and 1.7 mol% of catalyst could be used. Therefore, the loading amounts of catalyst and styrene would strongly depend on the reactivity of styrene.

5. Screening of solvents in the probe reaction of 3a with 2a.

Table S2 summarizes the screening of solvents, such as chloroform, dichloromethane, dichloroethane, toluene, diethyl ether, and acetonitrile in the probe reaction of **3a** with **2a**. As a result, dichloromethane and dichloroethane were much more effective than the other solvents. Moreover, dichloroethane was slightly more effective than dichloromethane with respect to the chemical yield of **4a**, although the enantioselectivities were the same.

Table S2. Screening of solvents.[a]

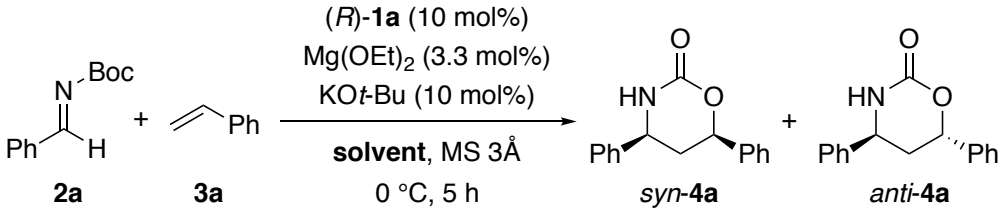

2a **3a** *syn*-**4a** *anti*-**4a**

entry	solvent	yield (%)	*syn*-**4a**:*anti*-**4a**	ee (%) of *syn*-**4a**
1	$CHCl_3$	9	89:11	10
2	CH_2Cl_2	84	99:1	96
3	**$ClCH_2CH_2Cl$**	**91**	**>99:<1**	**96**
4	toluene	8	81:19	–2
5	Et_2O	0	–	–
6	CH_3CN	0	–	–

[a] The reaction was carried out with **2a** (0.20 mmol), **3a** (4 mmol) in solvent at 0 °C for 5 h in the presence of 3.3 mol% of the catalyst and MS 3Å.

6. Screening of metal salts in the probe reaction of 3a with 2a.

Screening of alkali metal salts (10 mol%) was performed with the combined use of (*R*)-**1a** (10 mol%) and $Mg(OEt)_2$ (3.3 mol%) in the probe reaction of **3a** with **2a** (Table S3, entries 1–4). Li(I) and Cs(I) salts were much less effective than Na(I) and K(I) salts (entries 1 and 4). Moreover, K(I) salt was more effective than Na(I) salt for *syn/anti*-selectivity and the enantioselectivity of *syn*-**4a** (entries 2 and 4). Next, Ca(II) and Zn(II) salts with the combined use of (*R*)-**1a** (10 mol%) and $K(O\textit{t}\text{-Bu})_2$ (3.3 mol%) were examined in the probe reaction of **3a** with **2a** (entries 5 and 6). As a result, both the yields and enantioselectivities of **4a** were low, although these catalysts were soluble under the reaction conditions.

Table S3. Screening of alkali metal salts.[a]

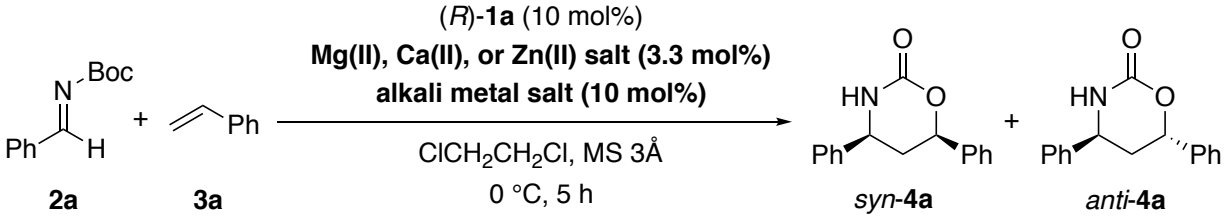

2a **3a** *syn*-**4a** *anti*-**4a**

entry	Mg(II), Ca(II), or Zn(II) salt (mol%)	alkali metal salt (mol%)	yield (%)	*syn*-**4a**:*anti*-**4a**	ee (%) of *syn*-**4a**
1	$Mg(OEt)_2$ (3.3)	LiO*i*-Pr (10)	14	92:8	54
2	$Mg(OEt)_2$ (3.3)	NaOMe (10)	90	95:5	90
3	**$Mg(OEt)_2$ (3.3)**	**KO*t*-Bu (10)**	**91**	**>99:<1**	**96**
4	$Mg(OEt)_2$ (3.3)	Cs_2CO_3 (5)	10	88:12	21
5	$Ca(O\textit{i}\text{-Pr})_2$ (3.3)	KO*t*-Bu (10)	43	91:9	43
6	Et_2Zn (3.3)	KO*t*-Bu (10)	57	88:12	22

[a] The reaction was carried out with **2a** (0.20 mmol), **3a** (4 mmol) in dichloroethane at 0 °C for 5 h in the presence of 3.3 mol% of the catalyst and MS 3Å.

7. Screening of the reaction temperature and molecular sieves in the probe reaction of 3a with 2a.

First, we examined the effect of molecular sieves on the optimized 3:1:3 complex of (*R*)-**1a**/Mg/K (3.3 mol%) in the probe reaction of **3a** with **2a** (Table S4). At –10 °C, no significant differences were observed between the presence and absence of MS 3Å (entries 1 and 2). However, at 0 °C, a significant difference in the yield of **4a** was observed between the presence and absence of MS 3Å (entries 3 and 4); **4a** was obtained in 56% yield with 95% ee in the absence of MS 3Å (entry 3), whereas **4a** was obtained in 91% yield with 96% ee in the presence of MS 3Å (entry 4). These results showed that the removal of adventitious water *in situ*, which would easily decompose **2a** under our acidic reaction conditions, is very important. MS 4Å and MS 5Å were slightly less effective than MS 3Å with respect to the yield, *syn/anti*-selectivity, and/or enantioselectivity (entries 5 and 6). Next, we conducted the reaction at a higher temperature with the use of MS 3Å. As a result, at 10 °C, the reaction proceeded smoothly, but the yield and enantioselectivity were slightly decreased (entry 7). Interestingly, the reaction did not proceed at 25 °C (entry 8). In contrast, in the absence of MS 3Å, the reaction proceeded almost smoothly, and **4a** was obtained in 75% yield with 88% ee (entry 9). These results in entries 8 and 9 may be due to the leaching of alkali metal ions from MS 3Å at 25 °C, since MS 3Å is $\mathbf{K_9Na_3}[(AlO_2)_{12}(SiO_2)_{12}]$. Probably, ion-exchange between H^+ of the catalyst and K^+ (or Na^+) of MS 3Å would generate inactive species *in situ*, like the complexes in the X-ray analysis (entry 8).

Table S4. Screening of reaction temperature and molecular sieves.[a]

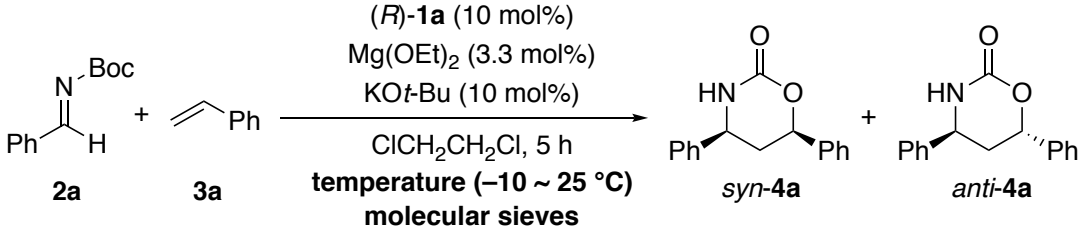

2a **3a** *syn*-**4a** *anti*-**4a**

entry	molecular sieves	temperature (°C)	yield (%)	*syn*-**4a**:*anti*-**4a**	ee (%) of *syn*-**4a**
1	–	–10	36	>99:<1	94
2	MS 3Å	–10	38	>99:<1	94
3	–	0	56	>99:<1	95
4	**MS 3Å**	**0**	**91**	**>99:<1**	**96**
5	MS 4Å	0	84	>99:<1	95
6	MS 5Å	0	89	96:4	86
7	MS 3Å	10	89	>99:<1	93
8	MS 3Å	25	0	–	–
9	–	25	75	95:5	88

[a] The reaction was carried out with **2a** (0.20 mmol), **3a** (4 mmol) in dichloroethane at –10 to 25 °C for 5 h in thepresence of 3.3 mol% of the catalyst and in the presence or absence of molecular sieves.

Note that MS 4Å is $\mathbf{Na_{12}}[(AlO_2)_{12}(SiO_2)_{12}]$ and MS 5Å is $Ca_{4.5}\mathbf{Na_3}[(AlO_2)_{12}(SiO_2)_{12}]$. Based on the screening of K(I), Na(I), Mg(II), and Ca(II) in Table S3, the combined use of K(I) and Mg(II) gave better results than other combinations. Therefore, the use of MS 3Å, $\mathbf{K_9}Na_3[(AlO_2)_{12}(SiO_2)_{12}]$, might be reasonable since only MS 3Å involves mainly K^+ ions. Undesired ion-exchange between K^+ of the catalyst and Na^+ (or Ca^{2+}) of MS 4Å or MS 5Å might generate less active catalysts, such as a 3:1:4 complex of (*R*)-**1a**/Mg/K(Na).

We further examined the effect of MS 3Å on catalysts in terms of drying ability as well as K^+ (or Na^+) leaching ability (Table S5). In the presence of MS 3Å, the yields were generally improved due to the removal of water, although the product ratio of *syn*-**4a** and *anti*-**4a** was not essentially influenced (entries 2, 4, 6, 8, and 10). Moreover, in some cases, the enantioselectivities were also improved (entries 5 vs. 6 and 7 vs. 8). For example, *with the use of a 2:1 complex of (R)-**1a**/Mg,* the product was obtained *in 90% yield with 78% ee in the presence of MS 3Å (entry 6)*, whereas the product was obtained *in 73% yield with 48% ee in the absence of MS 3Å (entry 5)*. In contrast, *with the use of a 3:1:3 complex of (R)-**1a**/Mg/K, the enantioselectivities were essentially the same (95–96% ee) in either the presence or absence of MS 3Å*, although the yields were significantly improved *(entries 9 and 10)*. These improved enantioselectivities might

Table S5. Effect of molecular sieves (MS 3Å) to catalysts.[a]

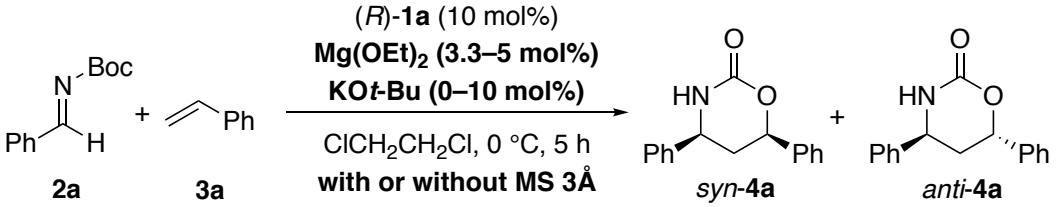

entry	Mg^{2+} (mol%)	K^+ (mol%)	(*R*)-**1a**:Mg:K (Initial ratio)	MS 3Å	yield (%)	*syn*-**4a**:*anti*-**4a**	ee (%) of *syn*-**4a**
1	0	0	1:0:0	without	52	76:24	–4
2	0	0	1:0:0	**with**	**69**	80:20	–2
3	0	10	1:0:1	without	57	91:9	4
4	0	10	1:0:1	**with**	**81**	76:24	–2
5	5	0	2:1:0	without	73	92:8	48
6	5	0	2:1:0	**with**	**90**	94:6	**78**
7	5	5	2:1:1	without	65	>99:<1	82
8	5	5	2:1:1	**with**	**83**	95:5	**89**
9	3.3	10	3:1:3	without	56	>99:<1	95
10	3.3	10	3:1:3	**with**	**91**	>99:<1	96

[a] The reaction was carried out with **2a** (0.20 mmol), **3a** (4 mmol) in dichloroethane at 0 °C for 5 h in the presence of 3.3 mol% of catalysts and in the presence or absence of MS 3Å. For convenience to understand the catalysts, possible structures of the catalysts are shown below, although the positions of H^+ and K^+ ions were not determined.

Table S5 (Continued).

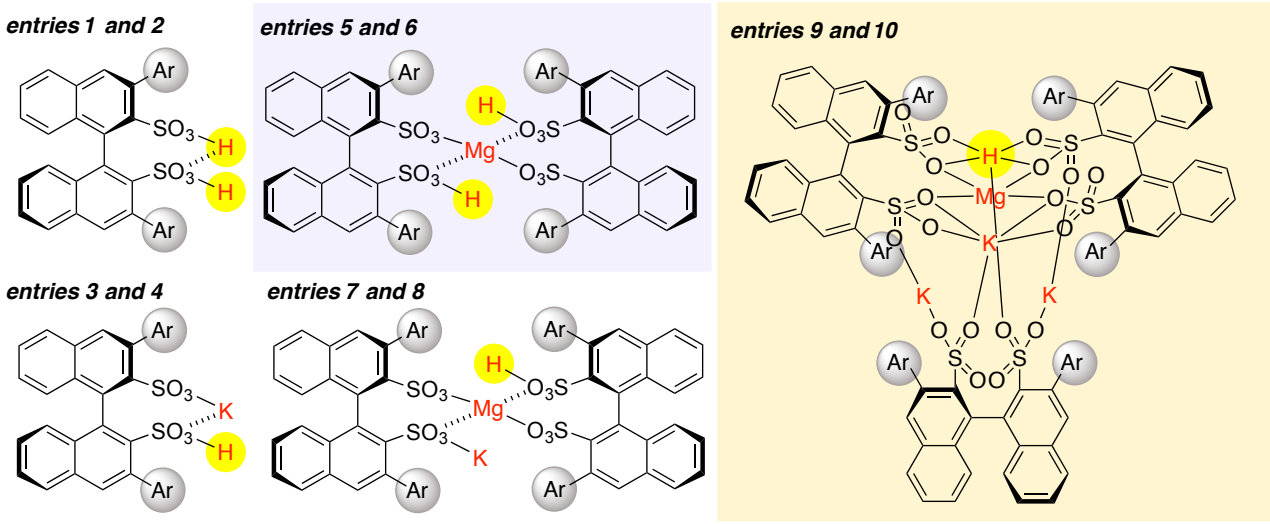

For these complexes shown, the positions of H^+ and K^+ ions were not determined.

be due to the leaching of alkali ions from MS 3Å (**K_9Na_3**[$(AlO_2)_{12}(SiO_2)_{12}$]). Accordingly, some 'undesired' or 'unoptimized' catalysts might change to 'desired' or optimized' catalysts *in situ* in the presence of MS 3Å. To confirm whether or not leaching really occurred, a trace element analysis was conducted by ICP-OES for the representative catalysts in entries 5, 6, 9, and 10 in Table S5. As a result, *the value of K^+ increased when MS 3Å was used for a 2:1 complex of (R)-**1a**/Mg (Table S6, entry 1 vs. entry 2).* In contrast, *there was little, if any, change in the value of K^+ when MS 3Å was used for a 3:1:3 complex of (R)-**1a**/Mg/K (Table S6, entry 3 vs. entry 4)*.

Table S6. Trace element analysis by ICP-OES (Inductively coupled plasma-optical emission spectroscopy)[a]

entry	Corresponding batch	(*R*)-**1a**:Mg:K (Initial ratio)	MS 3Å	K^+	Na^+	Mg^{2+}	Ca^{2+}
1	Table S5, entry 5	2:1:0	**without**	**0.5**	1.1	40.1	1.0
2	Table S5, entry 6	2:1:0	**with**	**9.6**	1.3	38.5	1.0
3	Table S5, entry 9	3:1:3	**without**	**63.1**	2.0	29.4	0.4
4	Table S5, entry 10	3:1:3	**with**	**67.7**	2.4	29.3	0.4

[a] Values in ppm (mg/L).

Overall, these results in Table S6 suggest that K^+ ion, unlike Na^+ ion, would be selectively leached from MS 3Å. As a result, a 2:1 complex of (*R*)-**1a**/Mg would incorporate K^+ ion and release H^+. Thus, 'undesired' catalysts, which do not originally contain K^+, might occasionally incorporate K^+ leached due to the effect of MS 3Å to spontaneously generate 'desired' catalysts.

Conclusion: *The optimum 3:1:3 complex of (R)-**1a**/Mg/K would not be further affected by MS 3Å in terms of the leaching of K^+ ion under the standard reaction conditions (Table S6, entry 3 vs entry 4).* Thus, we can ignore the ion-leaching effect of MS 3Å under the standard (optimized) reaction conditions.

Sample preparation for ICP-OES: (*R*)-**1a** (13.6 mg, 0.020 mmol) was placed in a Schlenk test tube under a nitrogen atmosphere and dissolved in dry dichloroethane (2 mL). To a stirred solution were added magnesium ethoxide (0.10 *M* in methanol, 66.7 μL, 0.0067 mmol) and potassium *tert*-butoxide (1.0 *M* in methanol, 20 μL, 0.020 mmol) and at room temperature, and the solution was stirred for 1 h. The volatiles were removed *in vacuo*, and then dichloroethane (1 mL) was added and removed *in vacuo* again. This solvent-removal sequence was repeated twice, and the magnesium/potassium salt of (*R*)-**1a** was obtained *in situ* as pale yellow solid.

[With MS 3Å] Then, dichloroethane (20 mL) and well-activated MS 3Å (50 mg) were added at 0 °C, and the suspension was stirred at 0 °C for 30 min. 14.7 mL of the resulting mixture passed through a membrane filter (200 mm mesh) to remove MS 3Å, and the volatile was removed from the filtrate *in vacuo*.
[Without MS 3Å] Then, dichloroethane (20 mL) was added at 0 °C, and the solution was stirred at 0 °C for 30 min. 14.7 mL of the resulting mixture passed through a membrane filter (200 mm mesh), and the volatile was removed from the filtrate *in vacuo*.

The resulting solid was diluted with methanol (0.5 mL) and 1% HNO_3 aqueous solution (9.5 mL), and passed through a membrane filter (200 mm mesh) just before ICP-OES mesurement (final concentration: *ca.* 1000 mg/L for (*R*)-**1a**). Calibration was executed by using a commercially available ICP standard solution including K^+, Na^+, Mg^{2+}, Ca^{2+}, Sr^{2+}, Ba^{2+} ions (each 100 mg/L in 0.1 mol/L HNO_3). The analytical results are shown in Table S6. Data was collected as a semi-quantitative method. Therefore, the values are almost qualitative, and absolute values between different ions cannot be evaluated.

8. Screening of other aldimines.

Some other aldimines were examined. Instead of *N*-Boc aldimine **2a** (Eq. S1), *N*-Cbz aldimine **S1** and *N*-Ts aldimine **S3** were used under our optimized reaction conditions (Eqs. S2 and S3). As a result, the corresponding desired products were not obtained in either case. Next, *N*-Bz aldimine **S5** was used (Eq. S4). However, the yield of the corresponding product **S6** was low (3% yield). Moreover, according to the report by Terada and Momiyama,[8] we used more reactive *N*-(3,5-difluorobenzate)aldimine **S7** and α-methylstyrene **8a** (Eq. S5). As a result, the corresponding product was obtained, but in improved yield (26%) with 38% ee. Overall, our catalyst system was particularly effective with the use of *N*-Boc aldimine.

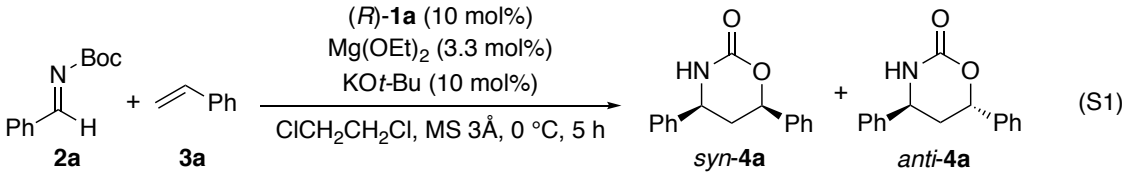

(S1)

91%, *syn*-**4a**:*anti*-**4a** = >99:1, 96% ee (*syn*-**4a**)
(Our standard result)

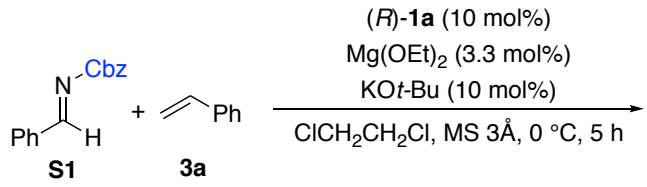

(S2)

S2, 0% (Complex mixture)

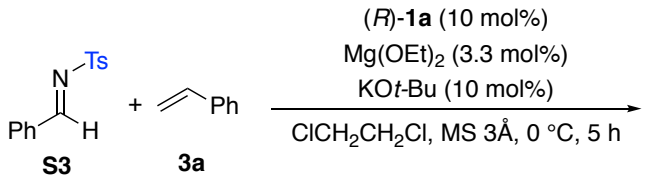

(S3)

S4, 0% (No reaction)

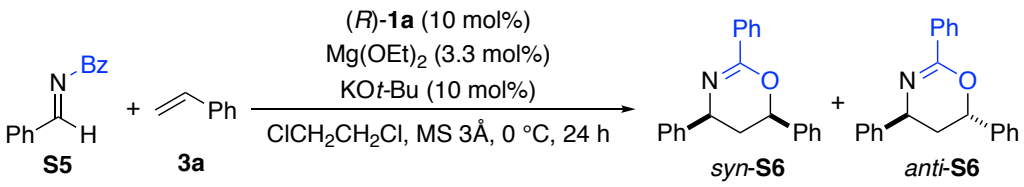

(S4)

3%, *syn*:*anti* = 19/1, 2% ee (*syn*)

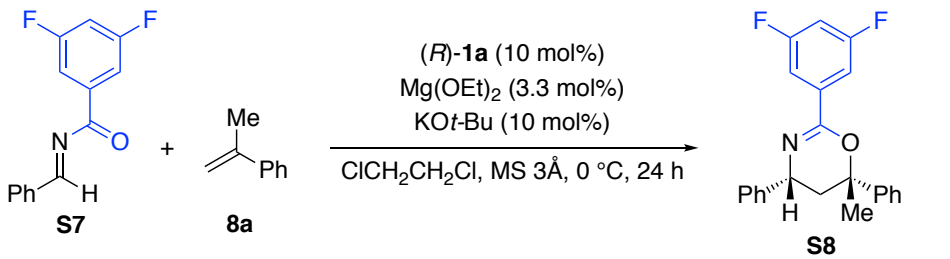

(S5)

26%, *cis*:*trans* = >20:1
38% ee (*cis*)

9. Products in Scheme 1.

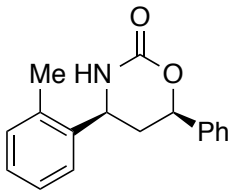

(4*S*,6*R*)-6-Phenyl-4-(*o*-tolyl)-1,3-oxazinan-2-one (*syn*-4b): 80% yield (5 h), *syn:anti* = >99:<1, 98% ee (*syn*). Colorless soild. ^{1}H NMR (400 MHz, $CDCl_3$) δ 2.00 (dt, *J* = 14.2, 11.5 Hz, 1H), 2.37-2.44 (m, 1H), 2.40 (s, 3H), 5.04 (dd, *J* = 11.5, 4.6 Hz, 1H), 5.18 (br, 1H), 5.45 (dd, *J* = 11.5, 1.8 Hz, 1H), 7.18 (d, *J* = 7.3 Hz, 1H), 7.23 (t, *J* = 7.3 Hz, 1H), 7.29 (d, *J* = 7.3 Hz, 1H), 7.17-7.47 (m, 5H), 7.46 (d, *J* = 7.8 Hz, 1H). ^{13}C NMR (100 MHz, $CDCl_3$) δ 19.1, 37.5, 51.9, 78.7, 125.1, 126.0 (2C), 127.2, 128.3, 128.7 (3C), 131.0, 134.8, 138.5, 138.6, 154.4. IR (KBr) 3219, 3108, 2934, 1691, 1401, 1301, 1286, 1148, 1051 cm^{-1}. M.p. 201-202 °C. $[\alpha]_D^{26}$ = –19.6 (*c* 1.00, $CHCl_3$, 98% ee, (4*S*,6*R*)). HPLC analysis; IA-3, *n*-hexane/*i*-PrOH = 7/3, 1.0 mL/min, 254 nm, t_R = 9.9 min (major, 4*S*,6*R*), 14.2 min (minor, 4*R*,6*S*). HRMS (FAB+) calcd for $C_{17}H_{18}NO_2$ $[M+H]^+$ 268.1338, found 268.1339. *syn/anti*-Isomers were identified by ^{1}H NMR analysis of the authentic sample by using $HBF_4 \cdot Et_2O$ (10 mol%); δ 5.04 (dd, *J* = 11.5, 4.6 Hz, 1H, ArC*H*–N (*syn*)), 4.89 (m, 1H, ArC*H*–N (*anti*)), *syn:anti* = 81:19.

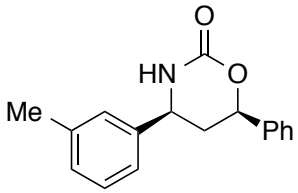

(4*S*,6*R*)-6-Phenyl-4-(*m*-tolyl)-1,3-oxazinan-2-one (*syn*-4c): 98% yield (5 h), *syn:anti* = >99:<1, 94% ee (*syn*). Colorless soild. ^{1}H NMR (400 MHz, $CDCl_3$) δ 2.06 (dt, *J* = 14.2, 11.5 Hz, 1H), 2.37 (s, 3H), 2.37-2.43 (m, 1H), 4.73 (dd, *J* = 11.5, 4.6 Hz, 1H), 5.23 (br, 1H), 5.44 (dd, *J* = 11.9, 1.8 Hz, 1H), 7.13-7.20 (m, 3H), 7.28-7.43 (m, 6H). ^{13}C NMR (100 MHz, $CDCl_3$) δ 21.5, 39.3, 55.9, 78.6, 123.2, 125.9 (2C), 126.7, 128.7 (3C), 129.1, 129.5, 138.5, 139.1, 140.5, 154.1. IR (KBr) 3283, 3159, 2929, 1726, 1694, 1455, 1396, 1317, 1303, 1288, 1142, 1048 cm^{-1}. M.p. 215-216 °C. $[\alpha]_D^{26}$ = +14.0 (*c* 1.00, $CHCl_3$, 94% ee, (4*S*,4*R*)). HPLC analysis; IA-3, *n*-hexane/*i*-PrOH = 7/3, 1.0 mL/min, 210 nm, t_R = 10.3 min (major, 4*S*,6*R*), 18.7 min (minor, 4*R*,6*S*). HRMS (FAB+) calcd for $C_{17}H_{18}NO_2$ $[M+H]^+$ 268.1338, found 268.1332. *syn/anti*-Isomers were identified by ^{1}H NMR analysis of the authentic sample by using $HBF_4 \cdot Et_2O$ (10 mol%); δ 4.73 (dd, *J* = 11.5, 4.6 Hz, 1H, ArC*H*–N (*syn*)), 4.60 (m, 1H, ArC*H*–N (*anti*)), *syn:anti* = 79:21.

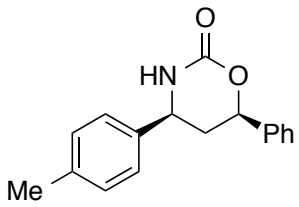

(4*S*,6*R*)-6-Phenyl-4-(*p*-tolyl)-1,3-oxazinan-2-one (*syn*-4d): 96% yield (5 h), *syn:anti* = >99:<1, 96% ee (*syn*). Colorless soild. ^{1}H NMR (400 MHz, $CDCl_3$) δ 2.05 (dt, *J* = 14.2, 11.5 Hz, 1H), 2.36 (s, 3H), 2.36-2.42 (m, 1H), 4.73 (dd, *J* = 11.5, 4.6 Hz, 1H), 5.24 (br, 1H), 5.43 (dd, *J* = 11.9, 1.8 Hz, 1H), 7.17-7.26 (m, 4H), 7.28-7.43 (m, 5H). ^{13}C NMR (100 MHz, $CDCl_3$) δ 21.2, 39.3, 55.7, 78.6, 125.9 (2C), 126.1 (2C), 128.6, 128.7 (2C), 129.9 (2C), 137.5, 138.6, 138.7, 154.0. IR (KBr) 3272, 3154, 2923, 1726, 1687, 1456, 1396, 1317, 1301, 1146, 1051 cm^{-1}. M.p. 193-194 °C. $[\alpha]_D^{26}$ = +20.8 (*c* 1.00, $CHCl_3$, 96% ee, (4*S*,6*R*)). HPLC analysis; IA-3, *n*-hexane/*i*-PrOH = 7/3, 1.0 mL/min, 210 nm, t_R = 11.5 min (major, 4*S*,6*R*), 23.2 min (minor, 4*R*,6*S*). HRMS (FAB+) calcd for $C_{17}H_{18}NO_2$ $[M+H]^+$ 268.1338, found 268.1332. *syn/anti*-Isomers were identified by ^{1}H NMR analysis of the authentic sample by using $HBF_4 \cdot Et_2O$ (10 mol%); δ 4.73 (dd, *J* = 11.5, 4.6 Hz, 1H, ArC*H*–N (*syn*)), 4.60 (m, 1H, ArC*H*–N (*anti*)), *syn:anti* = 86:14

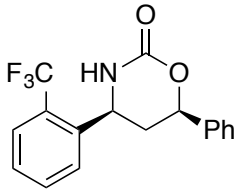

(4*S*,6*R*)-6-Phenyl-4-(2-(trifluoromethyl)phenyl)-1,3-oxazinan-2-one (*syn*-4e): 100% yield (5 h), *syn:anti* = >99:<1, 99% ee (*syn*). Colorless soild. ^{1}H NMR (400 MHz, $CDCl_3$) δ 2.02 (dt, *J* = 14.2, 11.9 Hz, 1H), 2.49 (dm, *J* = 14.2 Hz, 1H), 5.21 (dd, *J* = 11.9, 4.6 Hz, 1H), 5.30 (br, 1H), 5.46 (dd, *J* = 11.9, 1.8 Hz, 1H), 7.30-7.50 (m, 6H), 7.65 (t, *J* = 7.8 Hz, 1H), 7.68 (d, *J* = 7.8 Hz, 1H), 7.78 (d, *J* = 7.8 Hz, 1H). ^{13}C NMR (100 MHz, $CDCl_3$) δ 39.1, 51.2, 78.3, 124.2 (q, J_{C-F} = 273.5 Hz), 125.5 (2C), 126.0 (q, J_{C-F} = 5.8 Hz), 127.6 (2C), 127.7 (q, J_{C-F} = 30.0 Hz), 128.5, 128.6 (2C), 133.0, 138.2, 139.6, 154.5. ^{19}F NMR (376 MHz, $CDCl_3$) δ –59.8. IR (KBr) 3411, 3273, 1726, 1698, 1457, 1375, 1313, 1164, 1119, 1051, 1035 cm^{-1}. M.p. 203-205 °C. $[\alpha]_D^{23}$ = +13.2 (*c* 1.00, $CHCl_3$, 99% ee, (4*S*,6*R*)). HPLC analysis; IA-3, *n*-hexane/*i*-PrOH = 7/3, 1.0 mL/min, 254 nm, t_R = 9.6 min (major, 4*S*,6*R*), 16.7 min (minor, 4*R*,6*S*). HRMS (FAB+) calcd for $C_{17}H_{14}F_3NNaO_2$ $[M+Na]^+$ 344.0874, found 344.0849. *syn/anti*-Isomers were identified by ^{1}H NMR analysis of the authentic sample by using $HBF_4 \cdot Et_2O$ (10 mol%); δ 5.21 (dd, *J* = 11.9, 4.6 Hz, 1H, ArC*H*–N (*syn*)), 5.04-5.10 (m, 1H, ArC*H*–N (*anti*)), *syn:anti* = 71:29.

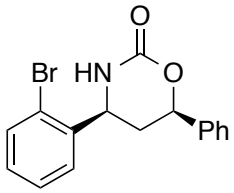

(4*S*,6*R*)-4-(2-Bromophenyl)-6-phenyl-1,3-oxazinan-2-one (*syn*-4f): 98% yield (5 h), *syn:anti* = 98:2, 97% ee (*syn*). Colorless soild. ^{1}H NMR (400 MHz, $CDCl_3$) δ 1.89 (dt, *J* = 14.2, 11.5 Hz, 1H), 2.62 (dm, *J* = 14.2 Hz, 1H), 5.23 (dd, *J* = 11.5, 4.6 Hz, 1H), 5.34 (br, 1H), 5.47 (dd, *J* = 11.5, 1.8 Hz, 1H), 7.21 (t, *J* = 7.3 Hz, 2H), 7.32-7.45 (m, 5H), 7.54 (d, *J* = 7.8 Hz, 1H), 7.56 (d, *J* = 8.2 Hz, 1H). ^{13}C NMR (100 MHz, $CDCl_3$) δ 36.8, 54.7, 78.4, 122.4, 126.0 (2C), 126.8, 128.6, 128.7 (3C), 129.9, 133.4, 138.3, 139.5, 154.5. IR (KBr) 3213, 3108, 2937, 1694, 1397, 1301, 1285, 1148, 1053 cm^{-1}. M.p. 181-182 °C. $[\alpha]_D^{27}$ = –84.0 (*c* 1.00, $CHCl_3$, 97% ee, (4*S*,6*R*)). HPLC analysis; IA-3, *n*-hexane/*i*-PrOH = 7/3, 1.0 mL/min, 210 nm, t_R = 11.8 min (major, 4*S*,6*R*), 21.9 min (minor, 4*R*,6*S*). HRMS (FAB+) calcd for $C_{16}H_{15}{}^{79}BrNO_2$ $[M+H]^+$ 332.0286, found 332.0292; $C_{16}H_{15}{}^{81}BrNO_2$ $[M+H]^+$ 334.0266, found 334.0258. *syn/anti*-Isomers were identified by ^{1}H NMR analysis of the authentic sample by using $HBF_4{\cdot}Et_2O$ (10 mol%); δ 5.23 (dd, *J* = 11.5, 4.6 Hz, 1H, ArC*H*–N (*syn*)), 5.07 (m, 1H, ArC*H*–N (*anti*)), *syn:anti* = 73:27.

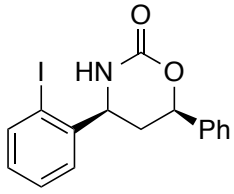

(4*S*,6*R*)-4-(2-Iodophenyl)-6-phenyl-1,3-oxazinan-2-one (*syn*-4g): 100% yield (5 h), *syn:anti* = >99:<1, 99% ee (*syn*). Colorless soild. ^{1}H NMR (400 MHz, $CDCl_3$) δ 1.85 (dt, *J* = 13.7, 11.5 Hz, 1H), 2.61 (dm, *J* = 14.2 Hz, 1H), 5.06 (dd, *J* = 11.5, 4.6 Hz, 1H), 5.29 (br, 1H), 5.47 (d, *J* = 11.9 Hz, 1H), 7.04 (t, *J* = 7.3 Hz, 1H), 7.34-7.45 (m, 6H), 7.50 (d, *J* = 7.8 Hz, 1H), 7.85 (d, *J* = 8.2 Hz, 1H). ^{13}C NMR (100 MHz, $CDCl_3$) δ 37.0, 59.5, 78.4, 97.7, 126.0 (2C), 126.5, 128.7 (3C), 129.5, 130.3, 138.3, 140.1, 142.2, 154.5. IR (KBr) 3208, 3099, 2933, 1693, 1466, 1396, 1299, 1285, 1147, 1053 cm^{-1}. M.p. 216-217 °C. $[\alpha]_D^{26}$ = –92.4 (*c* 1.00, $CHCl_3$, 99% ee, (4*S*,6*R*)). HPLC analysis; IA-3, *n*-hexane/*i*-PrOH = 7/3, 1.0 mL/min, 254 nm, t_R = 12.2 min (major, 4*S*,6*R*), 20.3 min (minor, 4*R*,6*S*). HRMS (FAB+) calcd for $C_{16}H_{15}INO_2$ $[M+H]^+$ 380.0148, found 380.0155. *syn/anti*-Isomers were identified by ^{1}H NMR analysis of the authentic sample by using $HBF_4{\cdot}Et_2O$ (10 mol%); δ 5.06 (dd, *J* = 11.5, 4.6 Hz, 1H, ArC*H*–N (*syn*)), 4.90 (m, 1H, ArC*H*–N (*anti*)), *syn:anti* = 71:29.

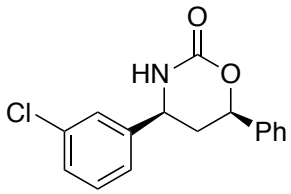

(4*S*,6*R*)-4-(3-Chlorophenyl)-6-phenyl-1,3-oxazinan-2-one (*syn*-4h): 98% yield (5 h), *syn:anti* = 98:2, 95% ee (*syn*). Colorless soild. ^{1}H NMR (400 MHz, $CDCl_3$) δ 2.04 (dt, *J* = 14.2, 11.5 Hz, 1H), 2.41 (dm, *J* = 14.2 Hz, 1H), 4.76 (dd, *J* = 11.5, 4.6 Hz, 1H), 5.38 (br, 1H), 5.43 (dd, *J* = 11.5, 2.3 Hz, 1H), 7.26-7.28 (m, 2H), 7.31-7.42 (m, 7H). ^{13}C NMR (100 MHz, $CDCl_3$) δ 39.1, 55.2, 78.4, 124.3, 125.9 (2C), 126.4, 128.7 (3C), 128.8, 130.5, 135.0, 138.3, 142.7, 154.3. IR (KBr) 3268, 3159, 2927, 1691, 1470, 1393, 1288, 1147, 1045 cm^{-1}. M.p. 201-202 °C. $[\alpha]_D^{27}$ = +19.6 (*c* 1.00, $CHCl_3$, 95% ee, (4*S*,6*R*)). HPLC analysis; OD-3, *n*-hexane/*i*-PrOH = 7/3, 1.0 mL/min, 254 nm, t_R = 12.7 min (minor, 4*R*,6*S*), 16.3 min (major, 4*S*,6*R*). HRMS (FAB+) calcd for $C_{16}H_{15}ClNO_2$ $[M+H]^+$ 288.0791, found 288.0790. *syn/anti*-Isomers were identified by ^{1}H NMR analysis of the authentic sample by using $HBF_4 \cdot Et_2O$ (10 mol%); δ 4.76 (dd, *J* = 11.5, 4.6 Hz, 1H, ArC*H*–N (*syn*)), 4.62-4.65 (m, 1H, ArC*H*–N (*anti*)), *syn:anti* = 71:29.

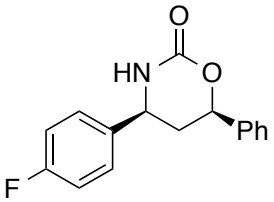

(4*S*,6*R*)-4-(4-Fluorophenyl)-6-phenyl-1,3-oxazinan-2-one (*syn*-4i): 97% yield (5 h), *syn:anti* = >99:<1, 96% ee (*syn*). Colorless soild. ^{1}H NMR (400 MHz, $CDCl_3$) δ 2.04 (dt, *J* = 14.2, 11.9 Hz, 1H), 2.39 (dm, *J* = 14.2 Hz, 1H), 4.77 (dd, *J* = 11.9, 4.6 Hz, 1H), 5.30 (br, 1H), 5.43 (dd, *J* = 11.9, 1.8 Hz, 1H), 7.09 (t, *J* = 8.7 Hz, 2H), 7.32-7.43 (m, 7H). ^{13}C NMR (100 MHz, $CDCl_3$) δ 39.4, 55.2, 78.5, 116.2 (d, *J* = 21.9 Hz, 2C), 125.9 (2C), 127.9 (d, *J* = 8.6 Hz, 2C), 128.7 (3C), 136.3 (d, *J* = 1.9 Hz), 138.4, 154.0, 162.8 (d, *J* = 246.0 Hz). ^{19}F NMR (376 MHz, $CDCl_3$) δ –113.6. IR (KBr) 3244, 3129, 2927, 1699, 1657, 1508, 1396, 1304, 1226, 1058 cm^{-1}. M.p. 183-184 °C. $[\alpha]_D^{26}$ = +14.8 (*c* 1.00, $CHCl_3$, 96% ee, (4*S*,6*R*)). HPLC analysis; IA-3, *n*-hexane/*i*-PrOH = 7/3, 1.0 mL/min, 210 nm, t_R = 11.2 min (major, 4*S*,6*R*), 17.9 min (minor, 4*R*,6*S*). HRMS (FAB+) calcd for $C_{16}H_{15}FNO_2$ $[M+H]^+$ 272.1087, found 272.1092. *syn/anti*-Isomers were identified by ^{1}H NMR analysis of the authentic sample by using $HBF_4 \cdot Et_2O$ (10 mol%); δ 4.77 (dd, *J* = 11.9, 4.6 Hz, 1H, ArC*H*–N (*syn*)), 4.62 (m, 1H, ArC*H*–N (*anti*)), *syn:anti* = 88:12.

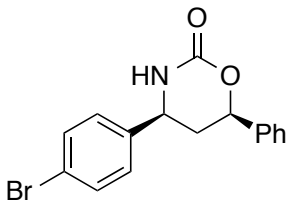

(4*S*,6*R*)-4-(4-Bromophenyl)-6-phenyl-1,3-oxazinan-2-one (*syn*-4j): 98% yield (5 h), *syn:anti* = >99:<1, 95% ee (*syn*). Colorless soild. ^{1}H NMR (400 MHz, $CDCl_3$) δ 2.03 (dt, *J* = 14.2, 11.5 Hz, 1H), 2.36-2.42 (dm, *J* = 14.2 Hz, 1H), 4.75 (dd, *J* = 11.5, 4.6 Hz, 1H), 5.31 (br, 1H), 5.43 (d, *J* = 11.9 Hz, 1H), 7.22-7.28 (m, 2H), 7.32-7.43 (m, 5H), 7.50-7.56 (m, 2H). ^{13}C NMR (100 MHz, $CDCl_3$) δ 39.1, 55.3, 78.5, 122.6, 125.9 (2C), 127.8 (2C), 128.7 (3C), 132.3 (2C), 138.3, 139.6, 154.2. IR (KBr) 3255, 3146, 2923, 2923, 1722, 1688, 1486, 1455, 1412, 1391, 1292, 1047, 1008 cm^{-1}. M.p. 177-179 °C. $[\alpha]_D^{26}$ = +50.4 (*c* 1.00, $CHCl_3$, 95% ee, (4*S*,6*R*)). HPLC analysis; IA-3, *n*-hexane/*i*-PrOH = 7/3, 1.0 mL/min, 210 nm, t_R = 10.7 min (major, 4*S*,6*R*), 14.3 min (minor, 4*R*,6*S*). HRMS (FAB+) calcd for $C_{16}H_{15}{}^{79}BrNO_2$ $[M+H]^+$ 332.0286, found 332.0289; $C_{16}H_{15}{}^{81}BrNO_2$ $[M+H]^+$ 334.0266, found 334.0268. *syn/anti*-Isomers were identified by ^{1}H NMR analysis of the authentic sample by using $HBF_4{\cdot}Et_2O$ (10 mol%); δ 4.75 (dd, *J* = 11.5, 4.6 Hz, 1H, ArC*H*–N (*syn*)), 4.62 (m, 1H, ArC*H*–N (*anti*)), *syn:anti* = 88:12.

Crystal data of *syn*-4j (Figure S1): Compound *syn*-**4j** was recrystallized from *n*-hexane–dichloromethane at room temperature for 2 days. Formula $C_{16}H_{14}BrNO_2$, colorless, crystal dimensions 0.50 × 0.40 × 0.15 mm^3, monoclinic, space group $P2_1$ (#4), *a* = 10.513(3) Å, *b* = 6.0756(16) Å, *c* = 12.045(4) Å, α = 90.00°, β = 109.543(5)°, γ = 90.00°, *V* = 725.0(4) $Å^3$, *Z* = 2, ρ_{calc} = 1.522 g cm^{-3}, F(000) = 336, μ(MoKα) = 2.835 mm^{-1}, *T* = 123 K. 6325 reflections collected, 3150 independent reflections with $I > 2\sigma(I)$ ($2\theta_{max}$ = 27.567°), and 185 parameters were used for the solution of the structure. The non-hydrogen atoms were refined anisotropically. R_1 = 0.0326 and wR_2 = 0.0644. GOF = 0.850. Flack x parameter = 0.013(9). Crystallographic data (excluding structure factors) for the structure reported in this paper have been deposited with

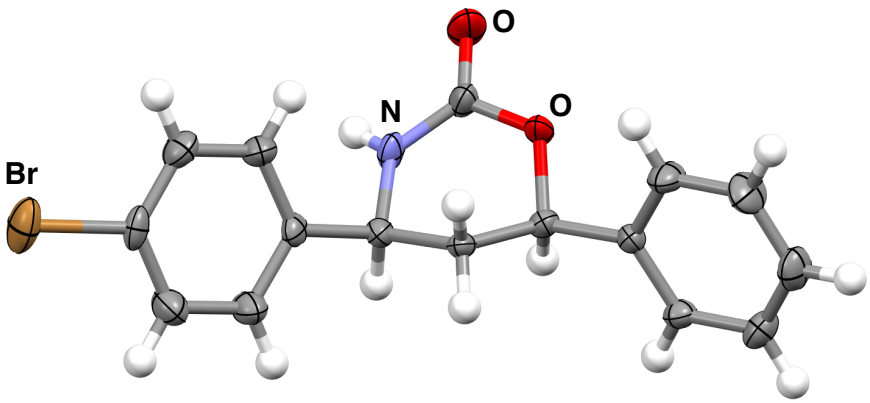

Figure S1. OPTEP drawing of *syn*-**4j**.

the Cambridge Crystallographic Data Centre as supplementary publication no. CCDC-1546387). Copies of the data can be obtained free of charge on application to CCDC, 12 Union Road, Cambridge CB2 1EZ, UK [Web page: http://www.ccdc.cam.ac.uk/].

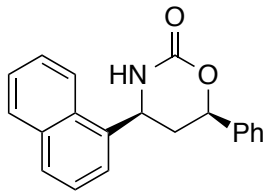

(4*S*,6*R*)-4-(Naphthalen-1-yl)-6-phenyl-1,3-oxazinan-2-one (*syn*-4k): 99% yield (5 h), *syn:anti* = >99:<1, 98% ee (*syn*). Colorless soild. ^{1}H NMR (400 MHz, $CDCl_3$) δ 2.21 (dt, *J* = 14.2, 11.5 Hz, 1H), 2.41 (dm, *J* = 14.2 Hz, 1H), 5.37 (br, 1H), 5.60 (dd, *J* = 11.9, 1.9 Hz, 1H), 5.65 (dd, *J* = 11.5, 4.6 Hz, 1H), 7.31-7.41 (m, 3H), 7.42-7.47 (m, 2H), 7.50-7.62 (m, 3H), 7.67 (d, *J* = 7.3 Hz, 1H), 7.86 (d, *J* = 8.2 Hz, 1H), 7.92 (d, *J* = 7.8 Hz, 1H), 8.05 (d, *J* = 8.2 Hz, 1H). ^{13}C NMR (100 MHz, $CDCl_3$) δ 37.8, 51.8, 78.8, 121.8, 122.9, 125.8, 126.0 (2C), 126.2, 126.9, 128.7 (3C), 129.1, 129.4, 130.1, 134.0, 136.1, 138.4, 154.4. IR (KBr) 3221, 3105, 2923, 1693, 1408, 1378, 1301, 1286, 1143, 1055 cm^{-1}. M.p. 220-221 °C. $[\alpha]_D^{27}$ = –126.0 (*c* 1.00, $CHCl_3$, 98% ee, (4*S*,6*R*)). HPLC analysis; IA-3, *n*-hexane/*i*-PrOH = 7/3, 1.0 mL/min, 280 nm, t_R = 11.0 min (major, 4*S*,6*R*), 18.1 min (minor, 4*R*,6*S*). HRMS (FAB+) calcd for $C_{20}H_{18}NO_2$ $[M+H]^+$ 304.1338, found 304.1337. *syn/anti*-Isomers were identified by ^{1}H NMR analysis of the authentic sample by using $HBF_4 \cdot Et_2O$ (10 mol%); δ 5.60 (dd, *J* = 11.9, 1.9 Hz, 1H, ArC*H*–N (*syn*)), 5.29 (m, 1H, ArC*H*–N (*anti*)), *syn:anti* =70:30.

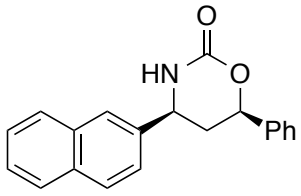

(4*S*,6*R*)-4-(Naphthalen-2-yl)-6-phenyl-1,3-oxazinan-2-one (*syn*-4l): 100% yield (5 h), *syn:anti* = >99:<1, 97% ee (*syn*). Colorless soild. ^{1}H NMR (400 MHz, $CDCl_3$) δ 2.17 (dt, *J* = 14.2, 11.9 Hz, 1H), 2.48 (dm, *J* = 14.6 Hz, 1H), 4.95 (dd, *J* = 11.4, 4.6 Hz, 1H), 5.36 (br, 1H), 5.50 (d, *J* = 11.9 Hz, 1H), 7.30-7.57 (m, 8H), 7.83-7.87 (m, 3H), 7.89 (d, *J* = 8.2 Hz, 1H). ^{13}C NMR (100 MHz, d_6-DMSO) δ 38.1, 54.5, 77.2, 124.7, 125.0, 126.0, 126.2 (2C), 126.3, 127.6, 127.8, 128.2, 128.3, 128.5 (2C), 132.6, 132.9, 139.3, 139.5, 153.2 IR (KBr) 3276, 3156, 3054, 1723, 1692, 1403, 1372, 1318, 1303, 1048 cm^{-1}. M.p. 220-221 °C. $[\alpha]_D^{22}$ = 72.0 (*c* 0.10, $CHCl_3$, 97% ee, (4*S*,6*R*)). HPLC analysis; IA-3, *n*-hexane/*i*-PrOH = 7/3, 1.0 mL/min, 254 nm, t_R = 14.0 min (major, 4*S*,6*R*), 23.6 min (minor, 4*R*,6*S*). HRMS (FAB+) calcd for $C_{20}H_{18}NO_2$ $[M+H]^+$ 304.1338, found 304.1337. *syn/anti*-Isomers were identified by ^{1}H NMR analysis of the authentic sample

by using $HBF_4 \cdot Et_2O$ (10 mol%); δ 4.95 (dd, *J* = 11.4, 4.6 Hz, 1H, ArC*H*–N (*syn*)), 4.84 (m, 1H, ArC*H*–N (*anti*)), *syn:anti* = 83:17.

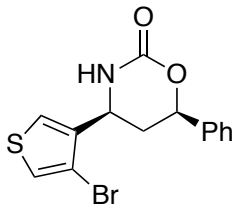

(4*S*,6*R*)-4-(4-Bromothiophen-3-yl)-6-phenyl-1,3-oxazinan-2-one (*syn*-4m): 91% yield (20 h), *syn:anti* = >99:<1, 95% ee (*syn*). Pale yellow soild. ^{1}H NMR (400 MHz, $CDCl_3$) δ 2.00 (dt, *J* = 14.2, 11.9 Hz, 1H), 2.57 (dm, *J* = 14.2 Hz, 1H), 4.94 (dd, *J* = 11.9, 4.6 Hz, 1H), 5.45 (dd, *J* = 11.9, 1.8 Hz, 1H), 5.45 (br, 1H), 7.32-7.45 (m, 7H). ^{13}C NMR (100 MHz, $CDCl_3$) δ 36.8, 51.2, 78.4, 109.4, 122.4, 124.8, 126.0 (2C), 128.7 (3C), 138.3, 139.8, 154.5. IR (KBr) 3221, 3115, 2921, 2885, 1713, 1684, 1409, 1360, 1284, 1143, 1043 cm^{-1}. M.p. 175-177 °C (decomposition). $[\alpha]_D^{24}$ = –29.2 (*c* 1.00, $CHCl_3$, 95% ee, (4*S*,6*R*)). HPLC analysis; IA-3, *n*-hexane/*i*-PrOH = 7/3, 1.0 mL/min, 210 nm, t_R = 10.8 min (major, 4*S*,6*R*), 15.1 min (minor, 4*R*,6*S*). HRMS (ESI+) calcd for $C_{14}H_{13}{}^{81}BrNO_2S$ $[M+H]^+$ 339.9830, found 339.9837. *syn/anti*-Isomers were identified by ^{1}H NMR analysis of the authentic sample by using $HBF_4 \cdot Et_2O$ (10 mol%); δ 4.94 (dd, *J*= 11.9, 4.6 Hz, 1H, ArC*H*–N (*syn*)), 4.81 (m, 1H, ArC*H*–N (*anti*)), *syn:anti* = 77:23.

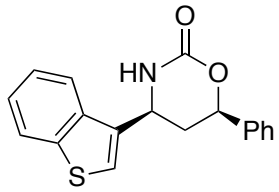

(4*S*,6*R*)-4-(Benzo[*b*]thiophen-3-yl)-6-phenyl-1,3-oxazinan-2-one (*syn*-4n): 87% yield (20 h), *syn:anti* = 98:2, 91% ee (*syn*). Colorless soild. ^{1}H NMR (400 MHz, $CDCl_3$) δ 2.29 (dt, *J* = 14.2, 11.5 Hz, 1H), 2.59 (dm, *J* = 14.2 Hz, 1H), 5.25 (dd, *J* = 11.5, 4.6 Hz, 1H), 5.49 (br, 1H), 5.53 (dd, *J* = 11.5, 2.3 Hz, 1H), 7.32-7.47 (m, 7H), 7.48 (s, 1H), 7.82 (m, 1H), 7.90 (m, 1H). ^{13}C NMR (100 MHz, $CDCl_3$) δ 36.9, 50.7, 78.6, 121.3, 123.2, 123.4, 124.5, 125.0, 125.9 (2C), 128.7 (3C), 135.2, 136.3, 138.3, 141.2, 154.2. IR (KBr) 3244, 3107, 2925, 1706, 1457, 1428, 1403, 1296, 1148, 1059 cm^{-1}. M.p. 210-213 °C (decomposition). $[\alpha]_D^{25}$ = –42.8 (*c* 1.00, $CHCl_3$, 91% ee, (4*S*,6*R*)). HPLC analysis; AD-3, *n*-hexane/*i*-PrOH = 7/3, 1.0 mL/min, 210 nm, t_R = 9.2 min (major, 4*S*,6*R*), 18.5 min (minor, 4*R*,6*S*). HRMS (FAB+) calcd for $C_{18}H_{16}NO_2S$ $[M+H]^+$ 310.0902, found 310.0896. *syn/anti*-Isomers were identified by ^{1}H NMR analysis of the authentic sample by using $HBF_4 \cdot Et_2O$ (10 mol%); δ 5.25 (dd, *J* = 11.5, 4.6 Hz, 1H, ArC*H*–N (*syn*)), 5.13 (m, 1H, ArC*H*–N (*anti*)), *syn:anti* = 88:12.

10. Products in Scheme 2.

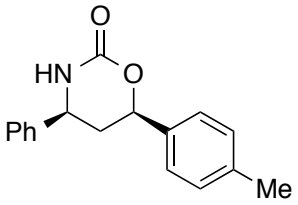

(4*S*,6*R*)-4-Phenyl-6-(*p*-tolyl)-1,3-oxazinan-2-one (*syn*-8a):[5] 95% yield (5 h), *syn:anti* = 94:6, 89% ee (*syn*). Colorless soild. ^{1}H NMR (400 MHz, $CDCl_3$) δ 2.06 (dt, *J* = 14.2, 11.5 Hz, 1H), 2.38 (dm, *J* = 14.2 Hz, 1H), 2.35 (s, 3H), 4.76 (dd, *J* = 11.5, 4.6 Hz, 1H), 5.25-5.30 (br, 1H), 5.41 (dd, *J* = 11.5, 1.8 Hz, 1H), 7.18 (d, *J* = 7.8 Hz, 2H), 7.30 (d, *J* = 8.2 Hz, 2H), 7.33-7.42 (m, 5H). ^{13}C NMR (100 MHz, $CDCl_3$) δ 21.2, 39.2, 55.9, 78.5, 125.9 (2C), 126.1 (2C), 128.7, 129.2 (2C), 129.3 (2C), 135.5, 138.5, 140.6, 154.2. IR (KBr) 3227, 3114, 2919, 1715, 1456, 1400, 1304, 1147, 1058 cm^{-1}. M.p. 188-190 °C. $[\alpha]_D^{26}$ = +10.4 (*c* 1.00, $CHCl_3$, 89% ee, (4*S*,6*R*)). HPLC analysis; IA-3, *n*-hexane/*i*-PrOH = 7/3, 210 nm, 1.0 mL/min, t_R = 12.4 min (major, 4*S*,6*R*), 25.6 min (minor, 4*R*,6*S*). HRMS (FAB+) calcd for $C_{17}H_{18}NO_2$ $[M+H]^+$ 268.1338, found 268.1339. *syn/anti*-Isomers were identified by ^{1}H NMR analysis of the authentic sample by using $HBF_4 \cdot Et_2O$ (10 mol%); δ 4.76 (dd, *J* = 11.5, 4.6 Hz, 1H, PhC*H*–N (*syn*)), 4.63 (m, 1H, PhC*H*–N (*anti*)), *syn:anti* = 63:37.

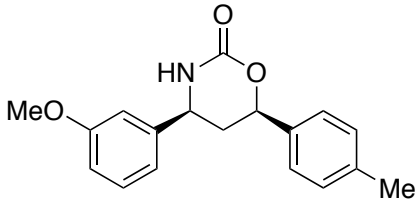

(4*S*,6*R*)-4-(3-Methoxyphenyl)-6-(p-tolyl)-1,3-oxazinan-2-one (*syn*-8b): 84% yield (20 h), *syn:anti* = 90:10 (Inseparable through the silica gel column chromatography), 89% ee (*syn*). Colorless soild. ^{1}H NMR (400 MHz, $CDCl_3$) δ 2.06 (dt, *J* = 14.2, 11.5 Hz, 1H), 2.35 (s, 3H), 2.37 (m, 1H), 3.82 (s, 3H), 4.73 (dd, *J* = 11.5, 4.1 Hz, 1H), 5.35 (br, 1H), 5.39 (d, *J* = 11.5 Hz, 1H), 6.88 (d, *J* = 7.8 Hz, 1H), 6.89 (s, 1H), 6.94 (d, *J* = 7.8 Hz, 1H), 7.18 (d, *J* = 7.8 Hz, 2H), 7.25-7.34 (m, 3H). ^{13}C NMR (100 MHz, $CDCl_3$) δ 21.2, 39.0, 55.3, 55.7, 78.4, 111.5, 114.0, 118.2, 125.8 (2C), 129.3 (2C), 130.2, 135.5, 138.4, 142.2, 154.3, 160.1. IR (KBr) 3319, 2968, 1715, 1597, 1459, 1392, 1302, 1256, 1154, 1051 cm^{-1}. M.p. 148-149 °C. $[\alpha]_D^{26}$ = +26.0 (*c* 1.00, $CHCl_3$, 89% ee, (4*S*,6*R*)). HPLC analysis; IA-3, *n*-hexane/*i*-PrOH = 7/3, 1.0 mL/min, 210 nm, t_R = 13.4 min (major, 4*S*,6*R*), 33.6 min (minor, 4*R*,6*S*). HRMS (FAB+) calcd for $C_{18}H_{20}NO_3$ $[M+H]^+$ 298.1443, found 298.1439. *syn/anti*-Isomers were identified by ^{1}H NMR analysis of the authentic sample by using $HBF_4 \cdot Et_2O$ (10 mol%); δ 4.73 (dd, *J* = 11.5, 4.1 Hz, 1H, ArC*H*–N (*syn*)), 4.61 (m, 1H, ArC*H*–N (*anti*)), *syn:anti* = 63/37.

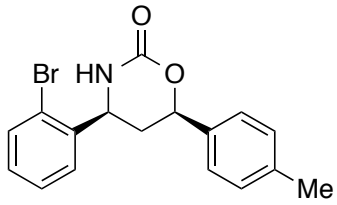

(4*S*,6*R*)-4-(4-Bromothiophen-3-yl)-6-(*p*-tolyl)-1,3-oxazinan-2-one (*syn*-8c): 99% yield (5 h), *syn:anti* = >99:<1, 98% ee (*syn*). Colorless soild. ^{1}H NMR (400 MHz, $CDCl_3$) δ 1.89 (dt, *J* = 14.2, 11.9 Hz, 1H), 2.35 (s, 3H), 2.60 (dm, *J* = 14.2 Hz, 1H), 5.21 (dd, *J* = 11.5, 4.6 Hz, 1H), 5.24 (br, 1H), 5.43 (dd, *J* = 11.9, 1.8 Hz, 1H), 7.18 (d, *J* = 8.2 Hz, 2H), 7.21 (d, *J* = 7.8 Hz, 1H), 7.31 (d, *J* = 8.2 Hz, 2H), 7.40 (t, *J* = 7.3 Hz, 1H), 7.53 (d, *J* = 7.8 Hz, 1H), 7.57 (d, *J* = 7.8 Hz, 1H). ^{13}C NMR (100 MHz, $CDCl_3$) δ 21.3, 36.7, 54.7, 78.4, 122.4, 126.0 (2C), 126.8, 128.6, 129.3 (2C), 129.9, 133.4, 135.3, 138.6, 139.6, 154.6. IR (KBr) 3216, 3111, 2936, 1698, 1468, 1397, 1302, 1285, 1151, 1054, 1023 cm^{-1}. M.p. 151-153 °C. $[\alpha]_D^{22}$ = –79.2 (*c* 1.00, $CHCl_3$, 98% ee, (4*S*,6*R*)). HPLC analysis; IA-3, *n*-hexane/*i*-PrOH = 7/3, 1.0 mL/min, 210 nm, t_R = 12.3 min (major, 4*S*,6*R*), 27.3 min (minor, 4*R*,6*S*). HRMS (ESI+) calcd for $C_{17}H_{16}{}^{79}BrNNaO_2$ $[M+Na]^+$ 368.0257, found 368.0253; $C_{17}H_{16}{}^{81}BrNNaO_2$ $[M+Na]^+$ 370.0238, found 370.0240. *syn/anti*-Isomers were identified by ^{1}H NMR analysis of the authentic sample by using $HBF_4{\cdot}Et_2O$ (10 mol%); δ 5.21 (dd, *J* = 11.5, 4.6 Hz, 1H, ArC*H*–N (*syn*)), 5.04 (m, 1H, ArC*H*–N (*anti*)), *syn:anti* = 62:38.

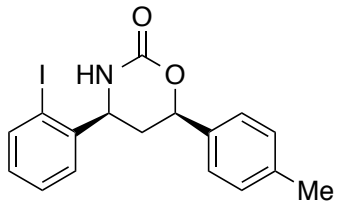

(4*S*,6*R*)-4-(4-Bromothiophen-3-yl)-6-(*p*-tolyl)-1,3-oxazinan-2-one (*syn*-8d): 99% yield (5 h), *syn:anti* = >99:<1, 97% ee (*syn*). Colorless soild. ^{1}H NMR (400 MHz, $CDCl_3$) δ 1.84 (dt, *J* = 13.7, 11.5 Hz, 1H), 2.35 (s, 3H), 2.58 (dm, *J* = 14.2 Hz, 1H), 5.04 (dd, *J* = 11.5, 4.6 Hz, 1H), 5.29 (br, 1H), 5.43 (dd, *J* = 11.9, 1.4 Hz, 1H), 7.04 (t, *J* = 7.6 Hz, 1H), 7.19 (d, *J* = 8.2 Hz, 2H), 7.31 (d, *J* = 8.2 Hz, 2H), 7.43 (t, *J* = 7.8 Hz, 1H), 7.50 (d, *J* = 7.8 Hz, 1H), 7.84 (d, *J* = 7.8 Hz, 1H). ^{13}C NMR (100 MHz, $CDCl_3$) δ 21.3, 36.9, 59.5, 78.4, 97.7, 126.0 (2C), 126.5, 129.4 (2C), 129.5, 130.3, 135.3, 138.6, 140.1, 142.3, 154.5. IR (KBr) 3215, 3103, 2927, 1697, 1396, 1301, 1149, 1055, 1009 cm^{-1}. M.p. 206-208 °C. $[\alpha]_D^{26}$ = –130.0 (*c* 1.00, $CHCl_3$, 97% ee, (4*S*,6*R*)). HPLC analysis; IA-3, *n*-hexane/*i*-PrOH = 7/3, 1.0 mL/min, 254 nm, t_R = 13.9 min (major, 4*S*,6*R*), 25.0 min (minor, 4*R*,6*S*). HRMS (FAB+) calcd for $C_{17}H_{17}INO_2$ $[M+H]^+$ 394.0304, found 394.0303. *syn/anti*-Isomers were identified by ^{1}H NMR analysis of the authentic sample by using $HBF_4{\cdot}Et_2O$ (10 mol%); δ 5.04 (dd, *J* = 11.5, 4.6 Hz, 1H, ArC*H*–N (*syn*)), 4.86 (m, 1H, ArC*H*–N (*anti*)), *syn:anti* = 57:43.

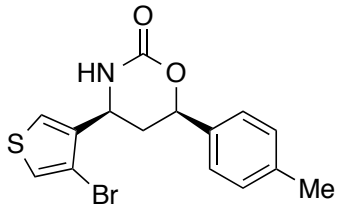

(4*S*,6*R*)-4-(4-Bromothiophen-3-yl)-6-(*p*-tolyl)-1,3-oxazinan-2-one (*syn*-8e): 84% yield (5 h), *syn:anti* = 95:5, 85% ee (*syn*). Colorless soild. ^{1}H NMR (400 MHz, $CDCl_3$) δ 1.99 (dt, *J* = 14.2, 11.5 Hz, 1H), 2.36 (s, 3H), 2.57 (dm, *J* = 14.2 Hz, 1H), 4.92 (dd, *J* = 11.0, 4.6 Hz, 1H), 5.41 (d, *J* = 11.9 Hz, 1H), 5.46 (br, 1H), 7.19 (d, *J* = 8.2 Hz, 2H), 7.30 (d, *J* = 8.2 Hz, 2H), 7.34 (d, *J* = 3.2 Hz, 1H), 7.36 (d, *J* = 3.2 Hz, 1H). ^{13}C NMR (100 MHz, $CDCl_3$) δ 21.3, 36.8, 51.2, 78.4, 109.5, 122.3, 124.9, 126.0 (2C), 129.4 (2C), 135.3, 138.6, 140.0, 154.3. IR (KBr) 3230, 3099, 3077, 2919, 1699, 1518, 1410, 1294, 1146, 1055 cm^{-1}. M.p. 166-168 °C (decomposition). $[\alpha]_D^{25}$ = –18.0 (*c* 1.00, $CHCl_3$, 85% ee, (4*S*,6*R*)). HPLC analysis; OD-3, *n*-hexane/*i*-PrOH = 9/1, 1.0 mL/min, 210 nm, t_R = 44.2 min (major, 4*S*,6*R*), 68.1 min (minor, 4*R*,6*S*). HRMS (ESI+) calcd for $C_{15}H_{14}{}^{79}BrNNaO_2S$ $[M+Na]^+$ 373.9820, found 373.9830; $C_{15}H_{14}{}^{81}BrNNaO_2S$ $[M+Na]^+$ 375.9801, found 375.9807. *syn/anti*-Isomers were identified by ^{1}H NMR analysis of the authentic sample by using $HBF_4{\cdot}Et_2O$ (10 mol%); δ 4.92 (dd, *J* = 11.0, 4.6 Hz, 1H, ArC*H*–N (*syn*)), 4.79 (m, 1H, ArC*H*–N (*anti*)), *syn:anti* = 56:44.

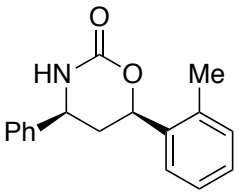

(4*S*,6*R*)-4-Phenyl-6-(*o*-tolyl)-1,3-oxazinan-2-one (*syn*-8f): 83% yield, *syn:anti* = 93:7 (Inseparable through the silica gel column chromatography), 78% ee (*syn*). Colorless soild. ^{1}H NMR (400 MHz, $CDCl_3$) δ 2.05 (dt, *J* = 14.2, 11.9 Hz, 1H), 2.36 (dm, *J* = 14.2 Hz, 1H), 2.40 (s, 3H), 4.77 (dd, *J* = 11.9, 4.6 Hz, 1H), 5.31 (br, 1H), 5.64 (dd, *J* = 11.9, 1.8 Hz, 1H), 7.17 (m, 1H), 7.20-7.27 (m, 3H), 7.32-7.44 (m, 4H), 7.49 (m, 1H). ^{13}C NMR (100 MHz, $CDCl_3$) δ 19.1, 37.9, 55.9, 75.6, 125.7, 126.1 (2C), 126.5, 128.4, 128.7, 129.2 (2C), 130.6, 134.5, 136.4, 140.6, 154.5. IR (KBr) 3229, 3114, 2928, 1702, 1456, 1399, 1287, 1147, 1048 cm^{-1}. M.p. 188-190 °C. $[\alpha]_D^{26}$ = +28.8 (*c* 1.00, $CHCl_3$, 78% ee, (4*S*,6*R*)). HPLC analysis; IA-3, *n*-hexane/*i*-PrOH = 7/3, 1.0 mL/min, 210 nm, t_R = 9.4 min (major, 4*S*,6*R*), 25.9 min (minor, 4*R*,6*S*). HRMS (FAB+) calcd for $C_{17}H_{18}NO_2$ $[M+H]^+$ 268.1338, found 268.1335. *syn/anti*-Isomers were identified by ^{1}H NMR analysis of the authentic sample by using $HBF_4{\cdot}Et_2O$ (10 mol%); δ 5.64 (dd, *J* = 11.9, 1.8 Hz, 1H, PhC*H*–N (*syn*)), 5.47 (dd, *J* = 9.8, 2.8 Hz, 1H, PhC*H*–N (*anti*)), *syn:anti* = 79:21.

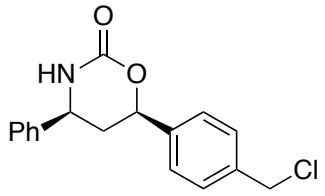

(4*S*,6*R*)-6-(4-(Chloromethyl)phenyl)-4-phenyl-1,3-oxazinan-2-one (*syn*-8g): 82% yield (20 h), *syn:anti* = >99:<1, 92% ee (*syn*). Colorless soild. ^{1}H NMR (400 MHz, $CDCl_3$) δ 2.04 (dt, *J* = 13.7, 11.5 Hz, 1H), 2.40 (dm, *J* = 13.7 Hz, 1H), 4.55 (s, 2H), 4.77 (dd, *J* = 11.5, 4.6 Hz, 1H), 5.30 (br, 1H), 5.45 (dd, *J* = 11.5, 1.8 Hz, 1H), 7.31-7.44 (m, 9H). ^{13}C NMR (100 MHz, $CDCl_3$) δ 39.1, 45.8, 55.7, 78.1, 126.1 (2C), 126.2 (2C), 128.7, 128.9 (2C), 129.2 (2C), 137.8, 138.8, 140.4, 154.1. IR (KBr) 3241, 3113, 2925, 1700, 1401, 1291, 1206, 1144, 1059 cm^{-1}. M.p. 223-225 °C. $[\alpha]_D^{26}$ = +33.6 (*c* 1.00, $CHCl_3$, 92% ee, (4*S*,6*R*)). HPLC analysis; IA-3, *n*-hexane/*i*-PrOH = 7/3, 1.0 mL/min, 210 nm, t_R = 19.8 min (major, 4*S*,6*R*), 63.0 min (minor, 4*R*,6*S*). HRMS (FAB+) calcd for $C_{17}H_{17}ClNO_2$ $[M+H]^+$ 302.0948, found 302.0935. *syn/anti*-Isomers were identified by ^{1}H NMR analysis of the authentic sample by using $HBF_4 \cdot Et_2O$ (10 mol%); δ 5.45 (dd, *J* = 11.5, 1.8 Hz, 1H, PhC*H*–N (*syn*)), 5.35 (dd, *J* = 8.7, 3.2 Hz, 1H, PhC*H*–N (*anti*)), *syn:anti* = 77:23.

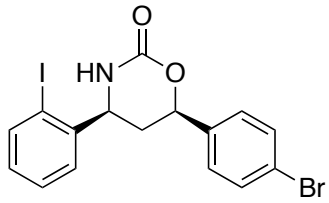

(4*S*,6*R*)-6-(4-Bromophenyl)-4-(2-iodophenyl)-1,3-oxazinan-2-one (*syn*-8h): 96% yield (20 h), *syn:anti* = >99:<1, 96% ee (*syn*). Colorless soild. ^{1}H NMR (400 MHz, $CDCl_3$) δ 1.80 (dt, *J* = 14.2, 11.5 Hz, 1H), 2.59 (dm, *J* = 14.2 Hz, 1H), 5.05 (dd, *J* = 11.5, 4.6 Hz, 1H), 5.33 (br, 1H), 5.43 (dd, *J* = 11.5, 1.8 Hz, 1H), 7.05 (dt, *J* = 7.6, 1.8 Hz, 1H), 7.31 (d, *J* = 8.2 Hz, 2H), 7.42-7.53 (m, 4H), 7.85 (dd, *J* = 8.1, 0.9 Hz, 1H). ^{13}C NMR (100 MHz, $CDCl_3$) δ 36.8, 59.3, 77.6, 97.6, 122.6, 126.4, 127.6 (2C), 129.5, 130.3, 131.8 (2C), 137.3, 140.0, 142.0, 154.4. IR (KBr) 3242, 3120, 3060, 1710, 1440, 1392, 1297, 1148, 1065, 1011 cm^{-1}. M.p. 164-165 °C. $[\alpha]_D^{26}$ = –85.2 (*c* 1.00, $CHCl_3$, 96% ee, (4*S*,6*R*)). HPLC analysis; IA-3, *n*-hexane/*i*-PrOH = 7/3, 1.0 mL/min, 210 nm, t_R = 15.9 min (major, 4*S*,6*R*), 36.8 min (minor, 4*R*,6*S*). HRMS (FAB+) calcd for $C_{16}H_{14}{}^{79}BrINO_2$ $[M+H]^+$ 457.9253, found 457.9251; $C_{16}H_{14}{}^{81}BrINO_2$ $[M+H]^+$ 459.9232, found 459.9215. *syn/anti*-Isomers were identified by ^{1}H NMR analysis of the authentic sample by using $HBF_4 \cdot Et_2O$ (10 mol%); δ 5.05 (dd, *J* = 11.5, 4.6 Hz, 1H, ArC*H*–N (*syn*)), 4.85-4.88 (m, 1H, ArC*H*–N (*anti*)), *syn:anti* = 79:21.

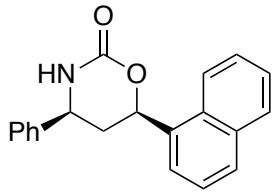

(4*S*,6*R*)-6-(Naphthalen-1-yl)-4-phenyl-1,3-oxazinan-2-one (*syn*-8i):[5] 81% yield (5 h), *syn:anti* = 99:1, 96% ee (*syn*). Colorless soild. ^{1}H NMR (400 MHz, $CDCl_3$) δ 2.19 (dt, *J* = 14.2, 11.5 Hz, 1H), 2.64 (dm, *J* = 14.2 Hz, 1H), 4.92 (dd, *J* = 11.5, 4.6 Hz, 1H), 5.42 (br, 1H), 6.22 (dd, *J* = 11.5, 1.8 Hz, 1H), 7.32-7.42 (m, 5H), 7.49-7.59 (m, 3H), 7.76 (d, *J* = 7.3 Hz, 1H), 7.84 (d, *J* = 8.2 Hz, 1H), 7.90 (d, *J* = 8.7 Hz, 1H), 7.97 (d, *J* = 8.7 Hz, 1H). ^{13}C NMR (100 MHz, $CDCl_3$) δ 38.6, 55.9, 75.4, 122.2, 123.4, 125.5, 125.8, 126.1 (2C), 126.6, 128.6, 129.0, 129.1 (3C), 129.8, 133.7, 133.9, 140.5, 154.5. IR (KBr) 3237, 3120, 2927, 1706, 1400, 1303, 1147, 1078, 1051 cm^{-1}. M.p. 212-214 °C. $[\alpha]_D^{23}$ = +160.0 (*c* 1.00, $CHCl_3$, 96% ee, (4*S*,6*R*)). HPLC analysis; IA-3, *n*-hexane/*i*-PrOH = 7/3, 1.0 mL/min, 280 nm, t_R = 10.1 min (major, 4*S*,6*R*), 14.2 min (minor, 4*R*,6*S*). HRMS (FAB+) calcd for $C_{20}H_{18}NO_2$ $[M+H]^+$ 304.1338, found 304.1334. *syn/anti*-Isomers were identified by ^{1}H NMR analysis of the authentic sample by using $HBF_4 \cdot Et_2O$ (10 mol%); δ 6.22 (dd, *J* = 11.5, 1.8 Hz, 1H, PhC*H*–N (*syn*)), 6.10 (dd, *J* = 8.2, 3.2 Hz, 1H, PhC*H*–N (*anti*)), *syn:anti* = 81:19.

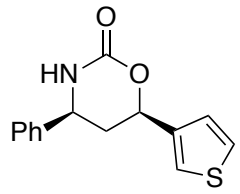

(4*S*,6*R*)-4-phenyl-6-(thiophen-3-yl)-1,3-oxazinan-2-one (*syn*-8j): 96% yield, *syn*:*anti* = 96:4 (Inseparable through the silica gel column chromatography), 95% ee (*syn*). Colorless soild. ^{1}H NMR (400 MHz, $CDCl_3$) δ 2.12 (dt, *J* = 14.2, 11.9 Hz, 1H), 2.47 (dm, *J* = 14.2 Hz, 1H), 4.75 (dd, *J* = 11.9, 4.6 Hz, 1H), 5.30 (br, 1H), 5.54 (dd, *J* = 11.9, 1.8 Hz, 1H), 7.12 (d, *J* = 5.6 Hz, 1H), 7.32-7.43 (m, 7H). ^{13}C NMR (100 MHz, $CDCl_3$) δ 38.3, 55.6, 74.9, 122.3, 125.4, 126.1 (2C), 126.6, 128.7, 129.2 (2C), 139.6, 140.5, 154.0. IR (KBr) 3272, 3156, 2927, 2866, 1725, 1406, 1298, 1146, 1058 cm^{-1}. M.p. 177-179 °C. $[\alpha]_D^{25}$ = –20.0 (*c* 1.00, $CHCl_3$, 95% ee, (4*S*,6*R*)). HPLC analysis; IA-3, *n*-hexane/*i*-PrOH = 7/3, 1.0 mL/min, 210 nm, t_R = 14.7 min (major, 4*S*,6*R*), 26.5 min (minor, 4*R*,6*S*). HRMS (FAB+) calcd for $C_{14}H_{14}NO_2S$ $[M+H]^+$ 260.0745, found 260.0740. *syn/anti*-Isomers were identified by ^{1}H NMR analysis of the authentic sample by using $HBF_4 \cdot Et_2O$ (10 mol%); δ 4.75 (dd, *J* = 11.9, 4.6 Hz, 1H, PhC*H*–N (*syn*)), 4.66 (m, 1H, PhC*H*–N (*anti*)), *syn*:*anti* = 61:39.

11. Product from α-methylstyrene 9 in Eq. 2.

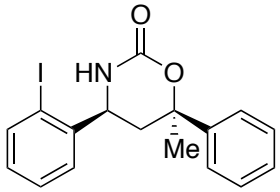

(4*S*,6*R*)-4-(2-Iodophenyl)-6-methyl-6-phenyl-1,3-oxazinan-2-one (*syn*-10): 81% yield, *syn:anti* = 95:5, 85% ee (*syn*). Colorless soild. ^{1}H NMR (400 MHz, $CDCl_3$) δ 1.86-1.92 (m, 1H), 1.88 (s, 3H), 2.61 (dd, *J* = 14.2, 4.6 Hz, 1H), 5.07 (dd, *J* = 11.0, 4.6 Hz, 1H), 5.47 (br, 1H), 6.98-7.02 (m, 1H), 7.25-7.36 (m, 5H), 7.45 (d, *J* = 7.8 Hz, 2H), 7.83 (d, *J* = 8.2 Hz, 1H). ^{13}C NMR (100 MHz, $CDCl_3$) δ 26.5, 40.4, 57.0, 81.5, 97.6, 124.1 (2C), 126.9, 127.6, 128.5 (2C), 129.3, 130.0, 139.9, 141.8, 144.1, 154.3. IR (KBr) 3230, 3114, 3060, 2979, 2928, 1701, 1463, 1440, 1392, 1331, 1296, 1092, 1070 cm^{-1}. M.p. 134-135 °C. $[\alpha]_D^{27}$ = –94.8 (*c* 1.00, $CHCl_3$, 85% ee, (4*S*,6*R*)). HPLC analysis; IA-3, *n*-hexane/*i*-PrOH = 7/3, 1.0 mL/min, 254 nm, t_R = 9.4 min (major, 4*S*,6*R*), 16.2 min (minor, 4*R*,6*S*). HRMS (FAB+) calcd for $C_{17}H_{17}INO_2$ $[M+H]^+$ 394.0304, found 394.0303. *syn/anti*-Isomers were identified by ^{1}H NMR analysis of the authentic sample by using $HBF_4 \cdot Et_2O$ (10 mol%); δ 5.07 (dd, *J* = 11.0, 4.6 Hz, 1H, ArC*H*–N (*syn*)), 4.36 (dd, *J* = 11.9, 4.6 Hz, 1H, ArC*H*–N (*anti*)), *syn*:*anti* = 76:24.

12. Reaction of β-methylstyrene 11 for the mechanistic insights (Eq. 3).

To determine the stereochemistry of 1,3-*syn*-2,3-*anti*-**12** and 1,3-*syn*-2,3-*syn*-**12**, we examined the NOE effect in ^{1}H NMR ($CDCl_3$) analysis, as shown in Figure S2. In particular, we observed reasonable NOEs between *syn*-protons in 1,3-*syn*-2,3-*anti*-**12** and 1,3-*syn*-2,3-*syn*-**12**, respectively. Moreover, X-ray analysis was conducted for 1,3-*syn*-2,3-*anti*-**12**, and the absolute stereochemistry was determined unambiguously (Figure S3).

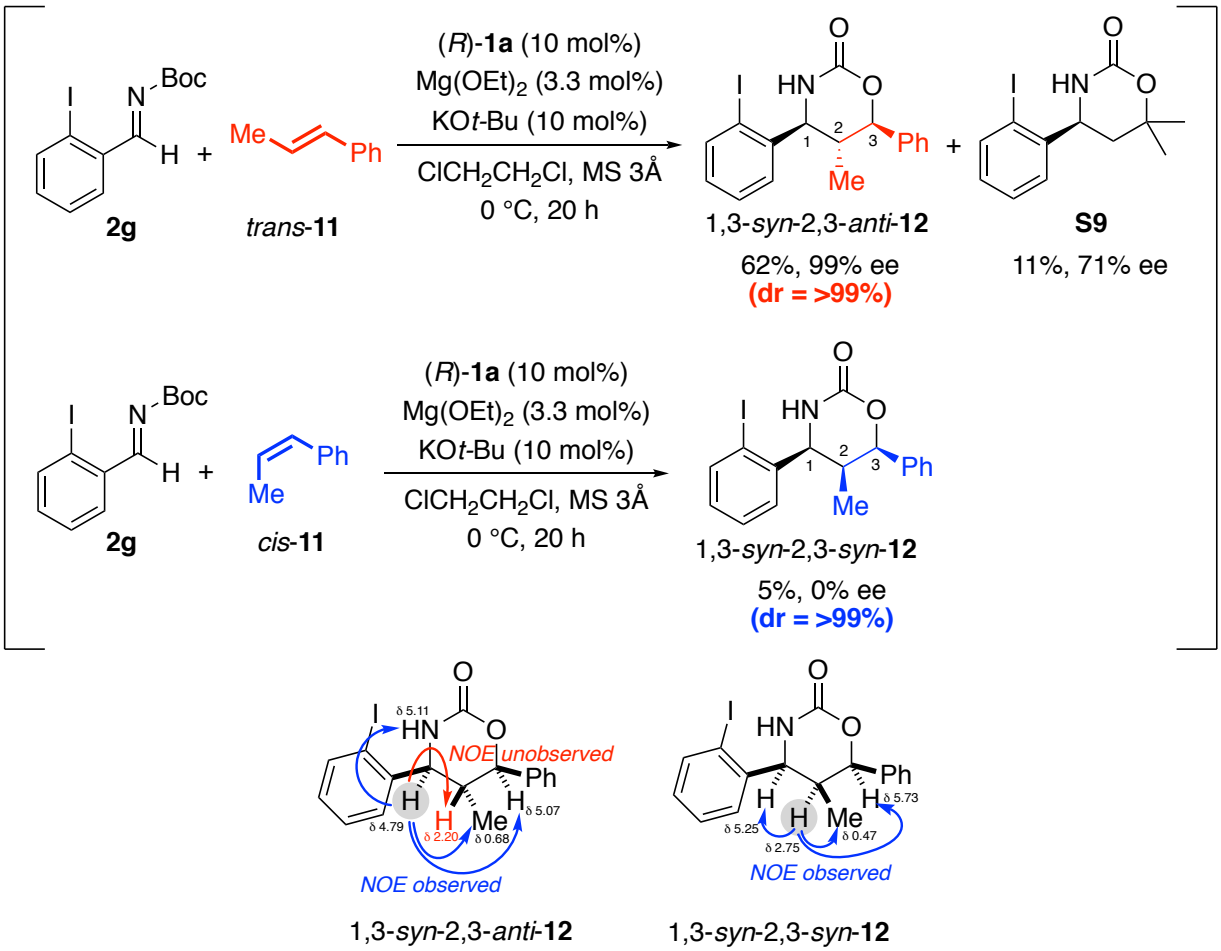

Figure S2. NOE experiment for compounds 1,3-*syn*-2,3-*anti*-**12** and 1,3-*syn*-2,3-*syn*-**12**.

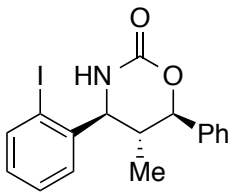

(4*S*,5*R*,6*R*)-4-(2-Iodophenyl)-5-methyl-6-phenyl-1,3-oxazinan-2-one (1,3-*syn*-2,3-*anti*-12): 62% yield (20 h), dr = >99%, 99% ee. Colorless soild. ^{1}H NMR (400 MHz, $CDCl_3$) δ 0.68 (d, J = 6.9 Hz, 3H), 2.20 (m, 1H), 4.79 (d, J = 10.1 Hz, 1H), 5.07 (d, J = 10.5 Hz, 1H), 5.11 (br, 1H),

7.05 (m, 1H), 7.32-7.47 (m, 7H), 7.87 (d, J = 7.8 Hz, 1H). ^{13}C NMR (100 MHz, $CDCl_3$) δ 12.9, 41.4, 62.2, 84.7, 100.2, 127.5 (2C), 128.5, 128.7 (2C), 129.1, 129.5, 130.6, 137.3, 140.3, 141.7, 153.6. IR (KBr) 3413, 3233, 3134, 1701, 1395, 1037 cm^{-1}. M.p. 231-234 °C. $[\alpha]_D^{26}$ = –59.6 (*c* 1.00, $CHCl_3$, 99% ee). HPLC analysis; IA-3, *n*-hexane/*i*-PrOH = 7/3, 1.0 mL/min, 210 nm, t_R = 10.0 min (major, 4*S*,5*R*,6*R*), 14.7 min (minor, 4*R*,5*S*,6*S*). HRMS (FAB+) calcd for $C_{17}H_{17}INO_2$ $[M+H]^+$ 394.0304, found 394.0314. *syn/anti*-Isomers were identified by ^{1}H NMR analysis of the authentic sample by using $HBF_4{\cdot}Et_2O$ (10 mol%); δ 0.68 (d, J = 6.9 Hz, 3H, CH_3 (*syn-trans*)), 0.90 (d, J = 6.9 Hz, 3H, CH_3 (*anti-trans*)), *syn-trans:anti-trans* = 61:39.

Crystal data of 1,3-*syn*-2,3-*anti*-12 (Figure S3): Compound 1,3-*syn*-2,3-*anti*-**12** was recrystallized from *n*-hexane–dichloromethane at room temperature for 2 days. Formula $C_{34}H_{32}I_2N_2O_4$, colorless, crystal dimensions 0.30 × 0.10 × 0.10 mm^3, monoclinic, space group *C*2 (#5), a = 19.657(3) Å, b = 7.8904(13) Å, c = 20.662(3) Å, α = 90.00°, β = 100.247(3)°, γ = 90.00°, V = 3153.6(8) Å^3, Z = 4, ρ_{calc} = 1.656 g cm^{-3}, F(000) = 1552, μ(MoKα) = 2.035 mm^{-1}, T = 123 K. 13313 reflections collected, 6441 independent reflections with $I > 2\sigma(I)$ ($2\theta_{max}$ = 27.828°), and 390 parameters were used for the solution of the structure. The non-hydrogen atoms were refined anisotropically. R_1 = 0.0414 and wR_2 = 0.1069. GOF = 1.251. Flack x parameter = 0.039(6). Crystallographic data (excluding structure factors) for the structure reported in this paper have been deposited with the Cambridge Crystallographic DataCentre as supplementary publication no. CCDC-1546388). Copies of the data can be obtained free of charge on application to CCDC, 12 Union Road, Cambridge CB2 1EZ, UK [Web page: http://www.ccdc.cam.ac.uk/].

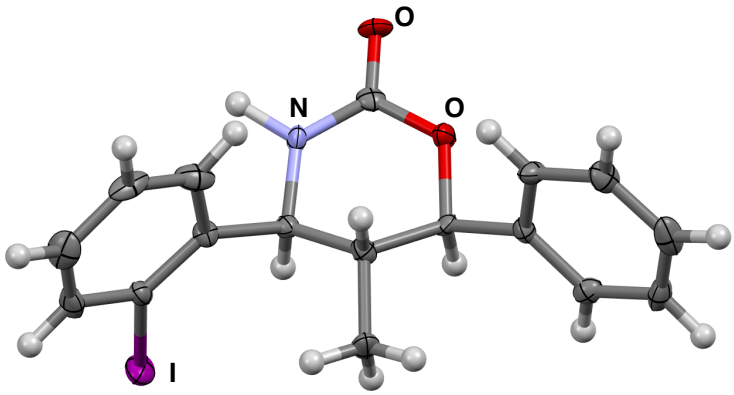

Figure S3. OPTEP drawing of 1,3-*syn*-2,3-*anti*-**12**.

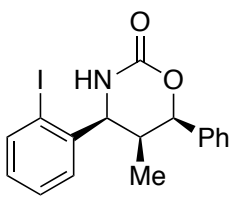

(4*S*,5*S*,6*R*)-4-(2-Iodophenyl)-5-methyl-6-phenyl-1,3-oxazinan-2-one (1,3-*syn*-2,3-*syn*-12): 5% yield (20 h), dr = >99%, 0% ee. Colorless soild. ^{1}H NMR (400 MHz, $CDCl_3$) δ 0.47 (d, J = 6.9

Hz, 3H), 2.75 (m, 1H), 5.25 (d, J = 4.6 Hz, 1H), 5.26 (br, 1H), 5.73 (d, J = 2.3 Hz, 1H), 7.06 (td, J = 7.3, 1.8 Hz, 1H), 7.30-7.46 (m, 7H), 7.89 (d, J = 7.8, 1.4 Hz, 1H). ^{13}C NMR (100 MHz, $CDCl_3$) δ 5.6, 33.7, 63.4, 81.0, 98.0, 125.4 (2C), 127.7, 128.0, 128.5 (2C), 128.7, 130.2, 137.4, 139.7, 140.3, 154.3. IR (KBr) 3241, 3120, 2976, 1705, 1456, 1397, 1333, 1275, 1161, 1100, 1012 cm^{-1}. M.p. 196-198 °C. HRMS (FAB+) calcd for $C_{17}H_{17}INO_2$ $[M+H]^+$ 394.0304, found 394.0295

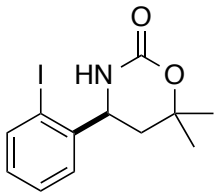

4-(2-Iodophenyl)-6,6-dimethyl-1,3-oxazinan-2-one (S9): Colorless soild. ^{1}H NMR (400 MHz, $CDCl_3$) δ 1.46 (s, 3H), 1.54-1.62 (m, 1H), 1.57 (s, 3H), 2.25 (ddd, J = 13.7, 4.6, 1.8 Hz, 1H), 4.94 (dd, J = 11.5, 4.6 Hz, 1H), 5.22 (br, 1H), 7.04 (td, J = 7.3, 1.8 Hz, 1H), 7.42 (t, J = 7.8 Hz, 1H), 7.46 (dd, J = 7.2, 2.3 Hz, 1H), 7.84 (d, J = 8.2 Hz, 1H). ^{13}C NMR (100 MHz, $CDCl_3$) δ 25.2, 29.4, 40.0, 57.0, 78.8, 97.6, 126.7, 129.5, 130.1, 139.9, 142.3, 154.3. IR (KBr) 3222, 3103, 2978, 2925, 1697, 1394, 1303, 1129, 1104, 1010 cm^{-1}. M.p. 168-171 °C. HRMS (FAB+) calcd for $C_{12}H_{15}INO_2$ $[M+H]^+$ 332.0148, found 332.0141.

Since the reaction of *cis*-**11** with **2g** was very sluggish when a 3:1:3 mixture of (*R*)-**1a**/Mg/K was used, 1,3-*syn*-2,3-*syn*-**12** was obtained in only 5% yield, as shown above. Therefore, HBF_4-catalysis was also conducted for the reactions of *trans*-**11** with **2g** and *cis*-**11** with **2g** (Eqs. S6 and S7). As a result, 1,3-*syn*-2,3-***anti***-**12** (34% yield) and 1,3-*anti*-2,3-***anti***-**12** (8% yield) were obtained selectively when ***trans***-**11** was used (Eq. S6). In contrast, 1,3-*syn*-2,3-***syn***-**12** (58% yield) and 1,3-*anti*-2,3-***syn***-**12** (2% yield) were obtained selectively when ***cis***-**11** was used (Eq. S7). These results supported the concerted reaction pathway.

Procedure for HBF_4·Et_2O catalysis: Aldimine **2g** (66.2 mg, 0.20 mmol), *trans*-β-methylstyrene (*trans*-**11**) or *cis*-β-methylstyrene (*cis*-**11**) (519 μL, 4.0 mmol), and $MgSO_4$ (100 mg) were placed in a Schlenk tube under a nitrogen atmosphere and dissolved in dry dichloromethane (10 mL). To the solution was added tetrafluoroboric acid diethyl ether complex (2.7 μL, 0.020 mmol, 10 mol%), and the mixture was stirred at room temperature for 20 h. The resulting reaction mixture was quenched with triethylamine (0.2 mL) at room temperature, and filtered through a pad of Celite. The organic phase was concentrated under reduced pressure, and the resultant residue was purified by silica gel column chromatography (eluent: *n*-hexane:EtOAc = 5:1 to 1:15) to give the desired product.

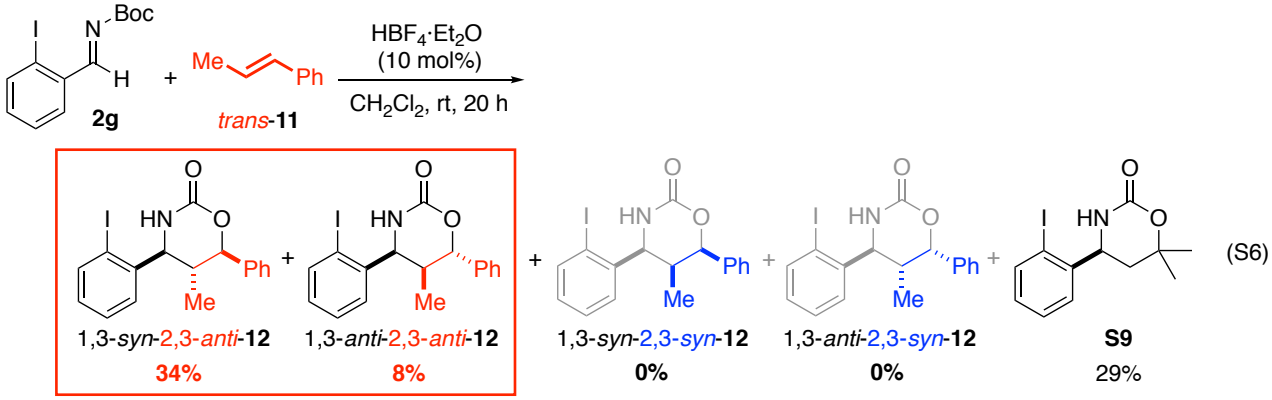

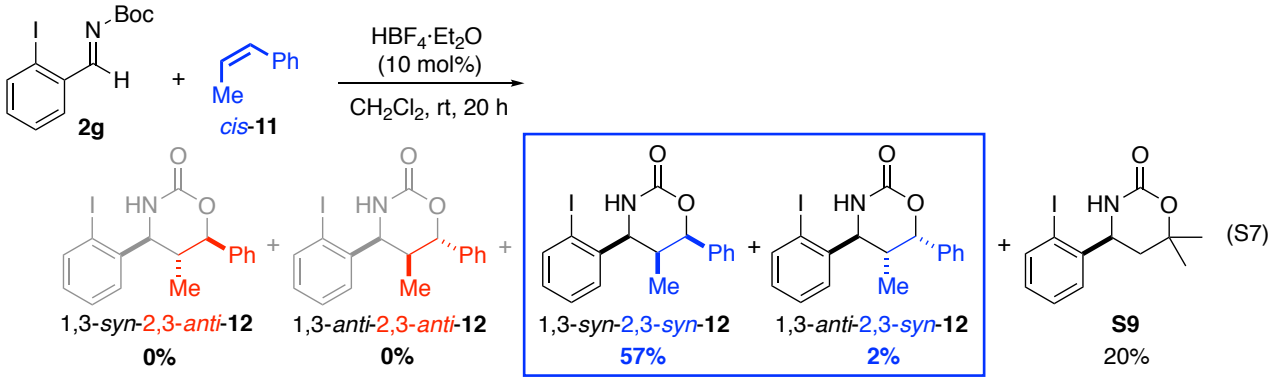

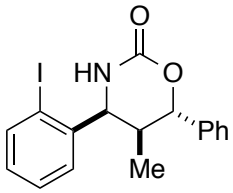

(4*S,5*S**,6*S**)-4-(2-Iodophenyl)-5-methyl-6-phenyl-1,3-oxazinan-2-one (1,3-*anti*-2,3-*anti*-12):** Colorless soild. ^{1}H NMR (400 MHz, $CDCl_3$) δ 0.90 (d, *J* = 6.9 Hz, 3H), 2.73 (m, 1H), 4.70 (d, *J* = 5.0 Hz, 1H), 5.21 (br, 1H), 5.37 (d, *J* = 4.1 Hz, 1H), 7.05 (m, 1H), 7.32-7.47 (m, 7H), 7.81-7.83 (m, 1H).

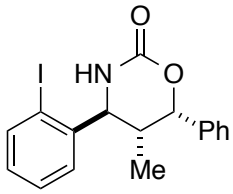

(4*S,5*R**,6*S**)-4-(2-Iodophenyl)-5-methyl-6-phenyl-1,3-oxazinan-2-one (1,3-*anti*-2,3-*syn*-12):** Colorless soild. ^{1}H NMR (400 MHz, $CDCl_3$) δ 1.09 (d, *J* = 6.9 Hz, 3H), 3.15 (m, 1H), 5.25 (m, 1H), 5.78 (m, 1H), 6.05 (br, 1H), 7.05 (m, 1H), 7.32-7.47 (m, 7H), 7.82 (m, 1H).

13. Product from indene 13 in Eq. 4.

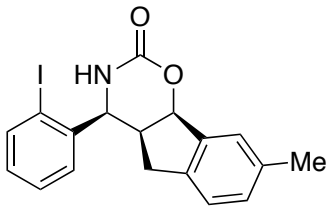

(4*S*,4a*S*,9b*R*)-4-(2-Iodophenyl)-8-methyl-4,4a,5,9b-tetrahydroindeno[2,1-e][1,3]oxazin-2(3*H*)-one (*syn*-14): With (*R*)-**1a**-derived catalyst: 91% yield (20 h), dr = >99%, 77% ee. With (*R*)-**1b**-derived catalyst: 95% yield (20 h), dr = >99%, 82% ee. (20 h). Colorless soild. ^{1}H NMR (400 MHz, $CDCl_3$) δ 2.25 (dd, *J* = 15.6, 7.8 Hz, 1H), 2.35 (s, 3H), 3.02 (dd, *J* = 15.6, 10.1 Hz, 1H), 3.34 (m, 1H), 5.22 (br, 1H), 5.28 (d, *J* = 4.1 Hz, 1H), 5.74 (d, *J* = 5.5 Hz, 1H), 7.04-7.13 (m, 3H), 7.32 (s, 1H), 7.41-7.48 (m, 2H), 7.91 (d, *J* = 8.2 Hz, 1H). ^{13}C NMR (100 MHz, $CDCl_3$) δ 21.3, 30.3, 39.8, 58.7, 83.3, 97.9, 124.8, 126.4, 127.0, 129.1, 130.1, 130.9, 137.1, 139.2, 140.1, 140.2 (2C), 155.0. IR (KBr) 3224, 3110, 2954, 2923, 1698, 1494, 1461, 1439, 1393, 1278, 1262, 1166, 1046, 1011 cm^{-1}. M.p. 220 °C (decomposition). $[\alpha]_D^{25}$ = –178.4 (*c* 0.50, $CHCl_3$, 77% ee (4*S*,4a*S*,9b*R*)). HPLC analysis; IA-3, *n*-hexane/*i*-PrOH = 7/3, 1.0 mL/min, 210 nm, t_R = 14.1 min (major, 4*S*,4a*S*,9b*R*), 18.9 min (minor, 4*R*,4a*R*,9b*S*). HRMS (ESI+) calcd for $C_{18}H_{17}INO_2$ $[M+H]^+$ 406.0298, found 406.0280. Diastereomers were identified by ^{1}H NMR analysis of the authentic sample by using $HBF_4 \cdot Et_2O$ (10 mol%); δ 5.74 (d, *J* = 5.5 Hz, 1H, OC*H*) (*major*, *syn*-4*S**,4a*S**,9b*R**), 5.57 (d, *J* = 5.5 Hz, 1H, OC*H*) (*minor*, *anti*-4*S**,4a*R**,9b*S**), *syn:anti* = 91:9. Enantiopurity of compound **14** was improved by a following procedure. Compound **14** (77.0 mg, 0.19 mmol, dr = >99%, 82% ee) was dissolved in THF/$CHCl_3$ (v/v = 1/1, 2 mL) at room temperature. Hexane (2 mL) was slowly added to the solution, and white prepicipate was formed. The prepicipate was filtered and the resulting filtrate was concentrated under reduced pressure to give compound **14** (66.5 mg, 82% yield based on imine **2g**, dr = >99%, 98% ee).

To determine the stereochemistry of *syn*-**14**, we performed an NOE effect on ^{1}H NMR ($CDCl_3$) analysis as shown in Figure S4. In particular, we could observe the reasonable NOEs.

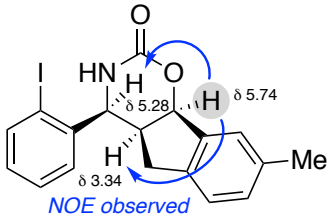

Figure S4. NOE experiment for compound *syn*-**14.**

14. Transformation to 1,3-amino alcohols 16 (Scheme 3, Eqs. 5 and 6).

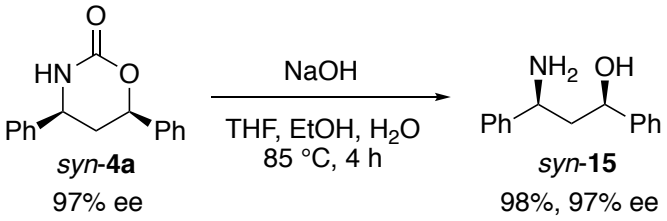

(1*R*,3*S*)-3-Amino-1,3-diphenylpropan-1-ol) (*syn*-15):[9] The solution of *syn*-**4a** (25.3 mg, 0.10 mmol) and sodium hydroxide (5 mg, 0.12 mmol) in THF (1 mL), ethanol (0.5 mL), and water (25 μL) was heated at 85 °C for 4 h. After cooling to room temperature, volatiles were removed under reduced pressure. Water (10 mL) was added to the resultant residue, and the mixture was extracted with dichloromethane (5 mL × 2). The combined extracts were dried over Na_2SO_4. The organic phase was concentrated under reduced pressure, and the resultant residue was purified by silica gel column chromatography (eluent: $CHCl_3$:MeOH = 30:1 to 1:1) to give the desired product as colorless soild (22.3 mg, 98% yield). The enantiomeric purity was determined by chiral HPLC analysis. ^{1}H NMR (400 MHz, $CDCl_3$) δ 1.3-2.0 (br, 2H), 1.89-2.02 (m, 2H), 2.6-4.0 (br, 1H), 4.18 (dd, *J* = 10.1, 3.7 Hz, 1H), 5.04 (dd, *J* = 9.6, 2.8 Hz, 1H), 7.22-7.27 (m, 4H), 7.31-7.36 (m, 4H), 7.40 (d, *J* = 7.3 Hz, 2H). ^{13}C NMR (100 MHz, $CDCl_3$) δ 46.5, 57.3, 77.4, 125.5 (2C), 126.7 (2C), 127.2, 127.4, 128.4 (2C), 128.9 (2C), 145.0, 146.8. IR (KBr) 3345, 3273, 3026, 2915, 2851, 1601, 1492, 1448, 1431, 1375, 1092, 1059, 1038 cm^{-1}. M.p. 118-120 °C. $[\alpha]_D^{22}$ = +1.2 (*c* 1.00, MeOH, 97% ee). [lit. $[\alpha]_D$ = +4.9 (*c* 2.0, MeOH, 100% ee, (1*R*,3*S*))].[10] HPLC analysis; OD-3, *n*-hexane/*i*-PrOH = 9/1, 0.8 mL/min, 210 nm, t_R = 40.5 min (minor, 1*S*,3*R*), 44.1 min (major, 1*R*,3*S*). HRMS (FAB+) calcd for $C_{15}H_{18}NO$ $[M+H]^+$ 228.1388, found 228.1381.

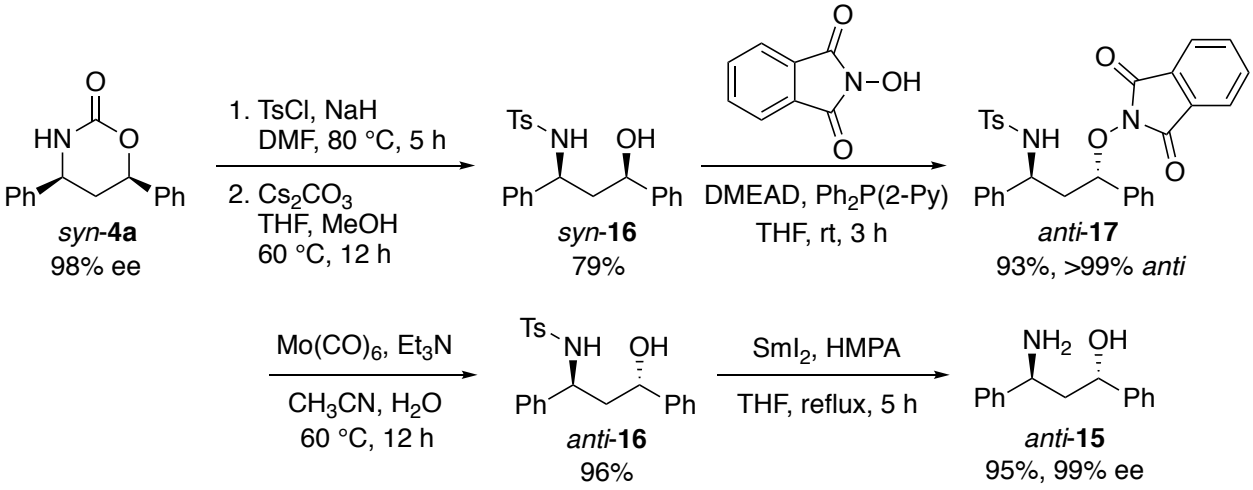

***N*-((1*S*,3*R*)-3-Hydroxy-1,3-diphenylpropyl)-4-methylbenzenesulfonamide (*syn*-16):**[11] To a suspension of sodium hydride (60% oil dispersion, 80 mg, 2.0 mmol) in *N*,*N*-dimethylformamide (DMF) (5 mL) at 0 °C was slowly added a solution of *syn*-**4a** (253 mg, 1.0 mmol) in DMF (5 mL), and the mixture was stirred at 0 °C for 1 h. *p*-Toluenesulfonyl chloride (381 mg, 2.0 mmol) was added to the resulting yellow suspension at 0 °C, and the mixture was heated at 80 °C for 5 h. Then, the reaction mixture was cooled to room temperature, and diluted with water (10 mL). The mixture was extracted with ethyl acetate (5 mL × 2), and the combined extracts were dried over Na_2SO_4. The organic phase was concentrated under reduced pressure, and the resultant residue was purified by neutral silica gel column chromatography (eluent: *n*-hexane:EtOAc = 9:1 to 1:1) to give Ts-protected product (345 mg, 85% yield), which was used without further purification in the next step. The solution of Ts-protected product (345 mg, 0.85 mmol) and cesium carbonate (110 mg, 0.34 mmol) in THF (5 mL) and methanol (5 mL) was stirred at 60 °C for 12 h. After cooling to room temperature, the mixture was concentrated under reduced pressure. The resultant residue was extracted with dichloromethane (5 mL × 2), and the combined extracts were dried over Na_2SO_4. The organic phase was concentrated under reduced pressure, and the resultant residue was purified by silica gel column chromatography (eluent: $CHCl_3$:MeOH = 30:1 to 10:1) to give the product *syn*-**16** as colorless soild (301.1 mg, 93% yield). ^{1}H NMR (400 MHz, $CDCl_3$) δ 1.91 (dm, *J* = 14.2 Hz, 1H), 2.11 (m, 1H), 2.23 (m, 1H), 2.37 (s, 3H), 4.55 (ddd, *J* = 8.5, 5.5, 5.0 Hz, 1H), 4.60 (dt, *J* = 10.0, 3.2 Hz, 1H), 5.85 (brd, *J* = 4.6 Hz, 1H), 7.07-7.18 (m, 7H), 7.22-7.28 (m, 3H), 7.31 (t, *J* = 7.3 Hz, 2H), 7.53 (d, *J* = 8.7 Hz, 2H). ^{13}C NMR (100 MHz, $CDCl_3$) δ 21.5, 46.3, 57.7, 73.2, 125.7 (2C), 126.8 (2C), 127.3 (2C), 127.5, 128.0, 128.4 (2C), 128.7 (2C), 129.3 (2C), 137.4, 140.8, 143.0, 143.9. IR (KBr) 3503, 3175, 1457, 1430, 1325, 1152, 1089, 1069 cm^{-1}. M.p. 99-100 °C. $[\alpha]_D^{25}$ = –8.8 (*c* 1.00, $CHCl_3$, 98% ee). HRMS (FAB+) calcd for $C_{22}H_{24}NO_3S$ $[M+H]^+$ 382.1477, found 382.1469.

***N*-((1*S*,3*S*)-3-((1,3-Dioxoisoindolin-2-yl)oxy)-1,3-diphenylpropyl)-4-methylbenzenesulfonamide (*anti*-17):** To a stirred, cooled (0 °C) mixture of *syn*-**16** (175 mg, 0.459 mmol), diphenyl-2-pyridylphosphine (242 mg, 0.917 mmol), and *N*-hydroxyphthalimide (150 mg, 0.917 mmol) in THF (5 mL) was added bis(2-methoxyethyl) azodicarboxylate (DMEAD)[12] (215 mg, 0.917 mmol), and the mixture was stirred at room temperature for 3 h. The reaction mixture was diluted with ethyl acetate (10 mL), and then washed with 1 *M* HCl aqueous solution (10 mL× 2) and water (10 mL × 2). The combined extracts were dried over Na_2SO_4. The organic phase was concentrated under reduced pressure, and the resultant residue was purified by silica gel column chromatography (eluent: *n*-hexane:EtOAc = 9:1 to 1:1) to give the product *anti*-**17** as colorless soild (225 mg, 93% yield). ^{1}H NMR (400 MHz, $CDCl_3$) δ 2.34 (m, 1H), 2.37 (s, 3H), 2.63 (m, 1H), 4.63 (q, *J* = 8.2 Hz, 1H), 5.12 (dd, *J* = 8.2, 4.1 Hz, 1H), 6.04 (d, *J* = 8.2 Hz, 1H), 7.11-7.32 (m, 12H), 7.56 (d, *J* = 8.2 Hz, 2H), 7.67-7.70 (m, 4H). ^{13}C NMR (100 MHz, $CDCl_3$) δ 21.5, 42.0, 55.2, 86.5, 123.6 (2C), 126.8 (2C), 127.2 (2C), 127.6, 127.8 (2C), 128.5 (2C), 128.6 (2C), 128.7,

129.2, 129.3 (2C), 134.5 (3C), 137.5, 137.9, 139.5, 142.9, 163.8 (2C). IR (KBr) 3277, 2925, 2850, 1733, 1456, 1375, 1159 cm^{-1}. M.p. 235-237 °C. $[\alpha]_D^{25}$ = –130.0 (*c* 1.00, $CHCl_3$, 98% ee). HRMS (FAB+) calcd for $C_{30}H_{27}N_2O_5S$ $[M+H]^+$ 527.1641, found 527.1655.

***N*-((1*S*,3*S*)-3-Hydroxy-1,3-diphenylpropyl)-4-methylbenzenesulfonamide (*anti*-16):**[11] A mixture of *anti*-**17** (65.7 mg, 0.125 mmol), molybdenumhexacarbonyl (65.9 mg, 0.25 mmol), and triethylamine (174 μL, 1.25 mmol) in CH_3CN/water (15:1, 1.5 mL) was stirred at 80 °C for 12 h. After cooling to room temperature, the volatiles were removed under reduced pressure. The resultant residue was purified by silica gel column chromatography (eluent: $CHCl_3$:MeOH = 30:1 to 10:1) to give the product *anti*-**16** as colorless soild (45.8 mg, 96% yield). ^{1}H NMR (400 MHz, $CDCl_3$) δ 1.98-2.10 (m, 2H), 2.38 (s, 3H), 2.52 (d, *J* = 3.7 Hz, 1H), 4.61 (q, *J* = 8.2 Hz, 1H), 4.83 (m, 1H), 5.66 (brd, *J* = 8.2 Hz, 1H), 7.03-7.07 (m, 2H), 7.15-7.28 (m, 8H), 7.31 (d, *J* = 7.3 Hz, 2H), 7.61 (d, *J* = 8.2 Hz, 2H). ^{13}C NMR (100 MHz, $CDCl_3$) δ 21.5, 45.9, 55.4, 70.6, 125.7 (2C), 126.3 (2C), 127.1 (2C), 127.3, 127.6, 128.5 (4C), 129.4 (2C), 137.5, 140.5, 143.1, 143.7. IR (KBr) 3548, 3327, 1457, 1417, 1320, 1153, 1054 cm^{-1}. M.p. 101-103 °C. $[\alpha]_D^{26}$ = –42.8 (*c* 1.00, $CHCl_3$, 98% ee). HRMS (FAB+) calcd for $C_{22}H_{23}NNaO_3S$ $[M+Na]^+$ 404.1296, found 404.1302.

(1*S*,3*S*)-3-Amino-1,3-diphenylpropan-1-ol (*anti*-15):[9] Samarium(II) iodide (0.10 *M* in THF, 8.9 mL, 0.89 mmol) and hexamethylphosphoramide (HMPA) (0.60 mL, 3.45 mmol) were added to a solution of *anti*-**16** (28.3 mg, 0.0742 mmol) in THF (1 mL) at room temperature. The mixture was stirred under reflux conditions for 5 h until the purple color of the solution disappeared. The mixture was cooled to room temperature, and quenched with saturated $NaHCO_3$ aqueous solution (10 mL). The resultant mixture was extracted with dichloromethane (5 mL × 2), and the combined extracts were dried over Na_2SO_4. The organic phase was concentrated under reduced pressure, and the resultant residue was purified by silica gel column chromatography (eluent: $CHCl_3$:MeOH = 30:1 to 1:1) to give the product *anti*-**15** as colorless soild (16.1 mg, 95% yield). The enantiomeric purity was determined by chiral HPLC analysis. ^{1}H NMR (400 MHz, $CDCl_3$) δ 2.05-2.19 (m, 2H), 2.3-3.2 (br, 3H), 4.16 (dd, *J* = 7.8, 3.7 Hz, 1H), 4.94 (dd, *J* = 6.4, 3.7 Hz, 1H), 7.22-7.29 (m, 4H), 7.31-7.39 (m, 6H). ^{13}C NMR (100 MHz, $CDCl_3$) δ 44.7, 53.2, 70.6, 125.6 (2C), 126.3 (2C), 127.2, 127.9, 128.4 (2C), 128.9 (2C), 141.8, 144.2. IR (KBr) 3350, 3275, 3082, 3025, 2864, 1490, 1454, 1078, 1065, 1004 cm^{-1}. M.p. 123-125 °C. $[\alpha]_D^{26}$ = –15.6 (*c* 1.00, MeOH, 98% ee). [lit. $[\alpha]_D$ = –39.9 (*c* 1.9, MeOH, 100% ee (1*S*,3*S*))].[10] HPLC analysis; OD-3, *n*-hexane/*i*-PrOH = 9/1, 0.8 mL/min, 210 nm, t_R = 24.6 min (minor, 1*R*,3*R*), 25.6 min (major, 1*S*,3*S*). HRMS (FAB+) calcd for $C_{15}H_{18}NO$ $[M+H]^+$ 228.1388, found 228.1381.

15. Transformation to bioactive compound 21 (Scheme 3, Eq. 7).

Gram scale synthesis of *syn*-**8d** could be achieved with the use of **5 mol% of catalysts and 2 molar equivalent of 3b** as shown below.

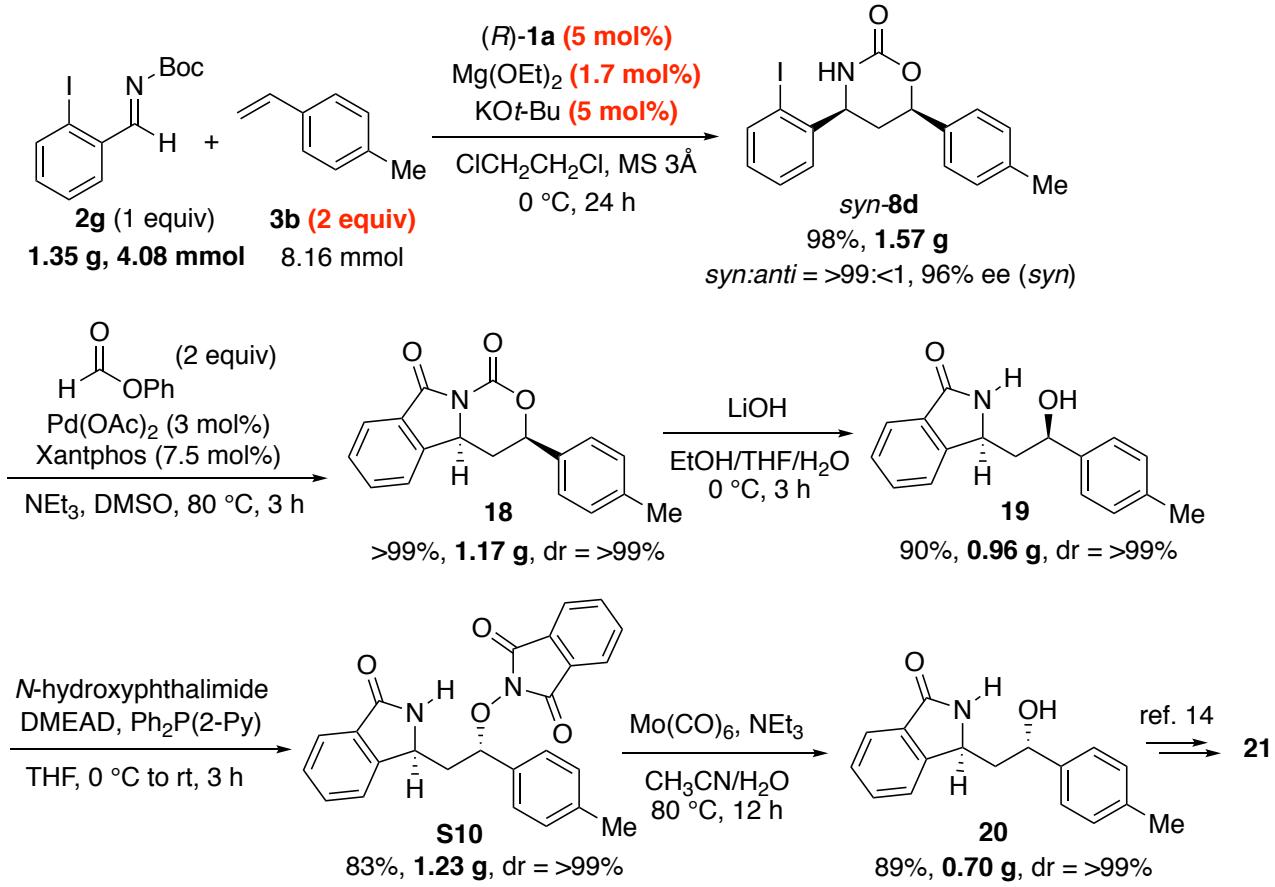

[Gram scale synthesis of *syn*-8d] (*R*)-**1a** (138.5 mg, 0.204 mmol, 5 mol%) was placed in a Schlenk test tube under a nitrogen atmosphere and dissolved in dry dichloroethane (2 mL). To a stirred solution were added magnesium ethoxide (0.10 *M* in methanol, 680 μL, 0.068 mmol, 1.7 mol%) and potassium *tert*-butoxide (1.0 *M* in methanol, 204 μL, 0.204 mmol, 5 mol%) at room temperature, and the solution was stirred for 1 h. The volatiles were removed *in vacuo*, and then dichloroethane (1 mL) was added and removed *in vacuo* again. This solvent-removal sequence was repeated twice, and the magnesium/potassium salt of (*R*)-**1a** was obtained *in situ* as pale yellow solid. Then, dichloroethane (38 mL) and well-activated MS 3Å (100 mg) were added at 0 °C, and the suspension was stirred at 0 °C for 30 min. 4-Methylstyrene **3b** (1.07 mL, 8.16 mmol) was then added to the suspension, and the mixture was stirred at 0 °C for 30 min. Aldimine **2g** (1.35 g, 4.08 mmol), which was dissolved in dichloroethane (2 mL), was then added at 0 °C, and the mixture was stirred at 0 °C for 24 h. The resulting reaction mixture was quenched with triethylamine (1.0 mL) at 0 °C, and filtered through a pad of Celite. The organic phase was concentrated under reduced pressure, and the resultant residue was purified by silica gel column chromatography (eluent: *n*-hexane:EtOAc = 5:1 to 1:15) to give the desired product **8d** in 98%

yield as colorless soild (1.57 g, >99% purity). The enantiomeric purity of **8d** was determined by chiral HPLC analysis (*syn:anti* = >99:<1, 96% ee (*syn*)). (*R*)-**1a** was recovered (133 mg, 99%, >99% purity) through the same chromatography using chloroform/methanol.

(3*R*,4a*S*)-3-(*p*-Tolyl)-4,4a-dihydro-1*H*-[1,3]oxazino[4,3-*a*]isoindole-1,9(3*H*)-dione (18): A synthetic procedure was based on the literature.[13] Compound *syn*-**8d** (1.57 g, 4.00 mmol), palladium(II) acetate (26.9 mg, 0.12 mmol, 3 mol%), and 4,5-bis(diphenylphosphino)-9,9-dimethylxanthene (Xantphos) (173 mg, 0.30 mmol 7.5 mol%) were placed in a 200 mL round-bottom flask under a nitrogen atmosphere. DMSO (50 mL), phenyl formate (976 μL, 8.0 mmol), and triethylamine (1.1 mL, 8.0 mmol) were added to the flask, and the mixture was heated at 80 °C for 3 h. Then, the reaction mixture was cooled to room temperature, and diluted with ethyl acetate (50 mL) and water (50 mL). The mixture was washed with water (25 mL × 2), and the combined extracts were dried over Na_2SO_4. The organic phase was concentrated under reduced pressure, and the resultant residue was purified by silica gel column chromatography (eluent: *n*-hexane:EtOAc = 1:1 to 1:10) to give the desired product **18** as pale brown soild (1.17 g, 100% yield). ^{1}H NMR (400 MHz, $CDCl_3$) δ 1.93 (dt, *J* = 13.7, 11.9 Hz, 1H), 2.36 (s, 3H), 2.88 (dm, *J* = 13.7 Hz, 1H), 5.17 (dd, *J* = 12.4, 2.8 Hz, 1H), 5.66 (dd, *J* = 11.9, 3.7 Hz, 1H), 7.20 (d, *J* = 7.8 Hz, 2H), 7.28 (d, *J* = 7.8 Hz, 2H), 7.53 (dd, *J* = 7.8, 0.9 Hz, 1H), 7.59 (t, *J* = 7.8 Hz, 1H), 7.73 (dt, *J* = 7.6, 0.9 Hz, 1H), 8.04 (d, *J* = 7.8 Hz, 1H). ^{13}C NMR (100 MHz, $CDCl_3$) δ 21.2, 35.7, 57.2, 81.6, 122.4, 125.7, 125.9 (2C), 129.5 (2C), 129.7, 129.9, 134.5, 134.9, 139.0, 143.1, 146.9, 165.9. IR (KBr) 2946, 1764, 1382, 1290, 1264, 1225, 1178, 1094, 1051, 1002 cm^{-1}. M.p. 225-226 °C. $[\alpha]_D^{26}$ = –34.4 (*c* 1.00, $CHCl_3$, 96% ee). HRMS (FAB+) calcd for $C_{18}H_{16}NO_3$ $[M+H]^+$ 294.1130 found 294.1130.

(*S*)-3-((*R*)-2-Hydroxy-2-(*p*-tolyl)ethyl)isoindolin-1-one (19):[14] To a stirred, cooled (0 °C) solution of **18** (1.17 g, 4.00 mmol) in THF (10 mL), ethanol (10 mL), and water (5 mL) was added lithium hydroxide (95.7 mg, 4.0 mmol), and the mixture was stirred at 0 °C for 3 h. The reaction mixture was quenched with saturated NH_4Cl aqueous solution (50 mL) at 0 °C, and extracted with dichloromethane (50 mL × 2). The combined extracts were dried over Na_2SO_4. The organic phase was concentrated under reduced pressure, and the resultant residue was purified by silica gel column chromatography (eluent: *n*-hexane:EtOAc = 1:1 to 1:15) to give the product **19** as colorless soild (0.959 g, 90% yield). ^{1}H NMR (400 MHz, $CDCl_3$) δ 1.88 (dt, *J* = 14.2, 10.5 Hz, 1H), 2.21-2.37 (m, 2H), 2.35 (s, 3H), 4.76 (dd, *J* = 10.5, 1.8 Hz, 1H), 5.06 (dt, *J* = 10.1, 2.8 Hz, 1H), 7.10 (br, 1H), 7.19 (d, *J* = 7.8 Hz, 2H), 7.28 (d, *J* = 7.8 Hz, 2H), 7.41 (d, *J* = 6.9 Hz, 1H), 7.46 (t, *J* = 7.3 Hz, 1H), 7.54 (td, *J* = 7.8, 1.4 Hz, 1H), 7.86 (d, *J* = 7.8 Hz, 1H). ^{13}C NMR (100 MHz, $CDCl_3$) δ 21.2, 43.9, 56.8, 74.5, 122.4, 123.9, 125.7 (2C), 128.2, 129.4 (2C), 131.8, 131.9, 137.8, 141.3, 147.5, 170.5. IR (KBr) 3420, 3258, 2919, 1687, 1469, 1404, 1080 cm^{-1}. M.p. 63-65 °C. $[\alpha]_D^{28}$ = +20.4 (*c* 1.00, $CHCl_3$, 96% ee). HRMS (FAB+) calcd for $C_{17}H_{18}NO_2$ $[M+H]^+$ 268.1338,

found 268.1328.

2-((*S*)-2-((*S*)-3-Oxoisoindolin-1-yl)-1-(*p*-tolyl)ethoxy)isoindoline-1,3-dione (S10): To a stirred, cooled (0 °C) mixture of **19** (0.959 g, 3.59 mmol), diphenyl-2-pyridylphosphine (1.89 g, 7.2 mmol), and *N*-hydroxyphthalimide (1.17 g, 7.2 mmol) in THF (36 mL) was added bis(2-methoxyethyl) azodicarboxylate (DMEAD)[12] (1.75 g, 7.2 mmol), and the mixture was stirred at room temperature for 3 h. The reaction mixture was diluted with dichloromethane (50 mL), and then washed with 1 *M* HCl aqueous solution (50 mL× 2) and water (50 mL × 2). The combined extracts were dried over Na_2SO_4. The organic phase was concentrated under reduced pressure, and the resultant residue was purified by silica gel column chromatography (eluent: *n*-hexane:EtOAc = 1:1 to 1:10) to give the product **S10** as colorless soild (1.23 g, 83% yield). ^{1}H NMR (400 MHz, $CDCl_3$) δ 1.74 (ddd, *J* = 14.9, 11.3, 1.6 Hz, 1H), 2.32 (s, 3H), 2.78 (ddd, *J* = 15.1, 11.4, 1.8 Hz, 1H), 5.16 (dd, *J* = 11.5, 2.8 Hz, 1H), 5.41 (dd, *J* = 11.5, 3.7 Hz, 1H), 7.16 (d, *J* = 7.8 Hz, 2H), 7.40 (d, *J* = 7.8 Hz, 2H), 7.42-7.50 (m, 2H), 7.55 (t, *J* = 7.3 Hz, 1H), 7.71 (br, 1H), 7.71-7.79 (m, 4H), 7.89 (d, *J* = 7.8 Hz, 1H). ^{13}C NMR (100 MHz, $CDCl_3$) δ 21.2, 41.5, 53.1, 86.9, 122.2, 123.6 (2C), 123.9, 127.5 (2C), 128.2, 128.6, 129.2 (2C), 131.7, 131.8 (2C), 134.5, 134.6 (2C), 139.2, 147.5, 163.8 (2C), 170.7. IR (KBr) 3363, 2919, 1724, 1697, 1467, 1411, 1374, 1188, 1130, 1082 cm^{-1}. M.p. 190-193 °C. $[\alpha]_D^{28}$ = –289.9 (*c* 1.00, $CHCl_3$, 96% ee). HRMS (FAB+) calcd for $C_{25}H_{21}N_2O_4$ $[M+H]^+$ 413.1501, found 413.1504.

(*S*)-3-((*S*)-2-Hydroxy-2-(*p*-tolyl)ethyl)isoindolin-1-one (20):[14] A mixture of **S10** (1.23 g, 2.98 mmol), molybdenumhexacarbonyl (1.58 mg, 6.0 mmol), and triethylamine (4.2 μL, 30 mmol) in CH_3CN/water (15:1, 30 mL) was stirred at 80 °C for 12 h. After cooling to room temperature, the volatiles were removed under reduced pressure. The resultant residue was purified by silica gel column chromatography (eluent: *n*-hexane:EtOAc = 1:1 to 1:10) to give the product **20** as colorless soild (0.700 g, 88% yield, 98% ee). ^{1}H NMR, MS, IR data were consistent with previously reported values.[14] ^{1}H NMR (400 MHz, $CDCl_3$) δ 1.79 (br, 1H), 1.83 (m, 1H), 2.34 (s, 3H), 2.43 (m, 1H), 4.82 (dd, *J* = 10.5, 2.3 Hz, 1H), 5.07 (m, 1H), 7.17 (d, *J* = 7.8 Hz, 2H), 7.30 (d, *J* = 7.8 Hz, 2H), 7.35 (d, *J* = 7.3 Hz, 1H), 7.43 (t, *J* = 7.8 Hz, 1H), 7.52 (t, *J* = 7.3 Hz, 1H), 7.53 (br, 1H), 7.81 (d, *J* = 7.8 Hz, 1H). ^{13}C NMR (100 MHz, $CDCl_3$) δ 21.2, 44.0, 54.1, 71.5, 122.4, 123.9, 125.5 (2C), 128.1, 129.3 (2C), 131.6, 131.9, 137.4, 141.1, 148.2, 171.4. IR (KBr) 3207, 1666, 1472, 1415, 1370, 1327, 1200, 1144, 1065 cm^{-1}. M.p. 183-184 °C. $[\alpha]_D^{28}$ = –52.4 (*c* 1.00, $CHCl_3$, 98% ee). HRMS (FAB+) calcd for $C_{17}H_{18}NO_2$ $[M+H]^+$ 268.1338, found 268.1339. HPLC analysis; OD-3, *n*-hexane/*i*-PrOH = 7/3, 1.0 mL/min, 254 nm, t_R = 5.8 min (major, *S*,*S*), 8.0 min (minor, *R*,*R*). Compound **20** would be transformed to compound **21** by the known procedures.[14]

16. ^{1}H NMR analysis of (*R*)-1a/Mg/K complexes.

^{1}H NMR (CD_2Cl_2) analysis was performed for some complexes (Figure S5). Figures S5a–d show the results with (*R*)-**1a** alone, a 1:1 complex of (*R*)-**1a**/K, a 1:2 complex of (*R*)-**1a**/K, and a 1:1 complex of (*R*)-**1a**/Mg, respectively. (*R*)-**1a** alone (Figure S5a) shows a relatively sharp spectrum, while the others (Figures S5b–c) show relatively broad peaks.

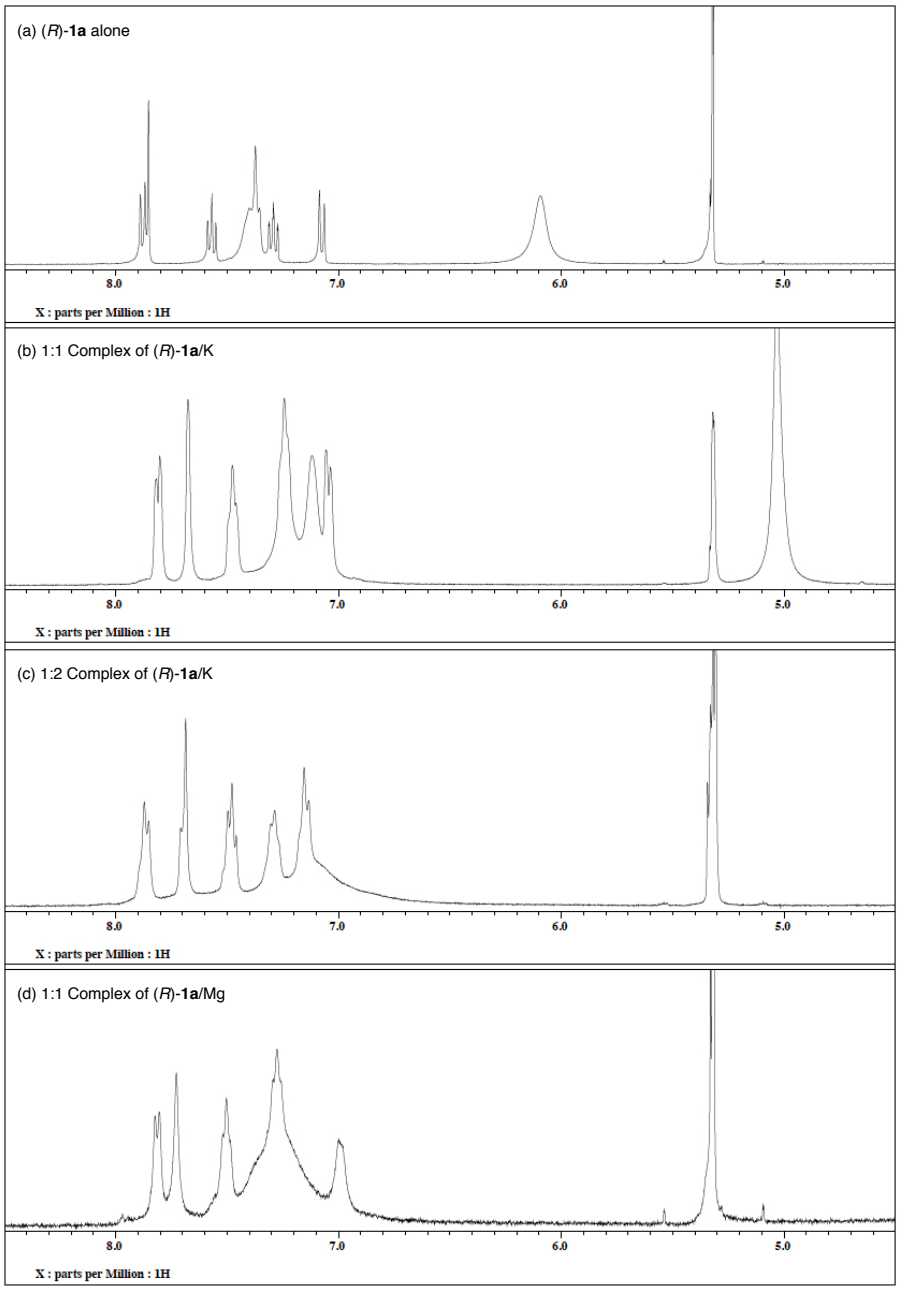

Figure S5. ^{1}H NMR (CD_2Cl_2) analysis of (*R*)-**1a**/Mg/K complexes. (a) (*R*)-**1a** alone. (b) A 1:1 complex of (*R*)-**1a**/K. (c) A 1:2 complex of (*R*)-**1a**/K. (d) A 1:1 complex of (*R*)-**1a**/Mg.

Figures S5e–h show the results with a 2:1 complex of (*R*)-**1a**/Mg, a 2:1:1 complex of (*R*)-**1a**/Mg/K, a 2:1:2 complex of (*R*)-**1a**/Mg/K, and a 3:1:3 complex of (*R*)-**1a**/Mg/K, respectively. The 2:1 complex of (*R*)-**1a**/Mg (Figure S5e) and 2:1:1 complex of (*R*)-**1a**/Mg/K (Figure S5f) showed relatively broad spectra. Cluster species, the 3:1:3 complex of (*R*)-**1a**/Mg/K (Figure S5h) and its component, a 2:1:2 complex of (*R*)-**1a**/Mg/K (Figure S5g), showed relatively sharp spectra. However, overall, wce did not find clear evidence for a possible cluster structure of the active species, a 3:1:3 complex of (*R*)-**1a**/Mg/K.

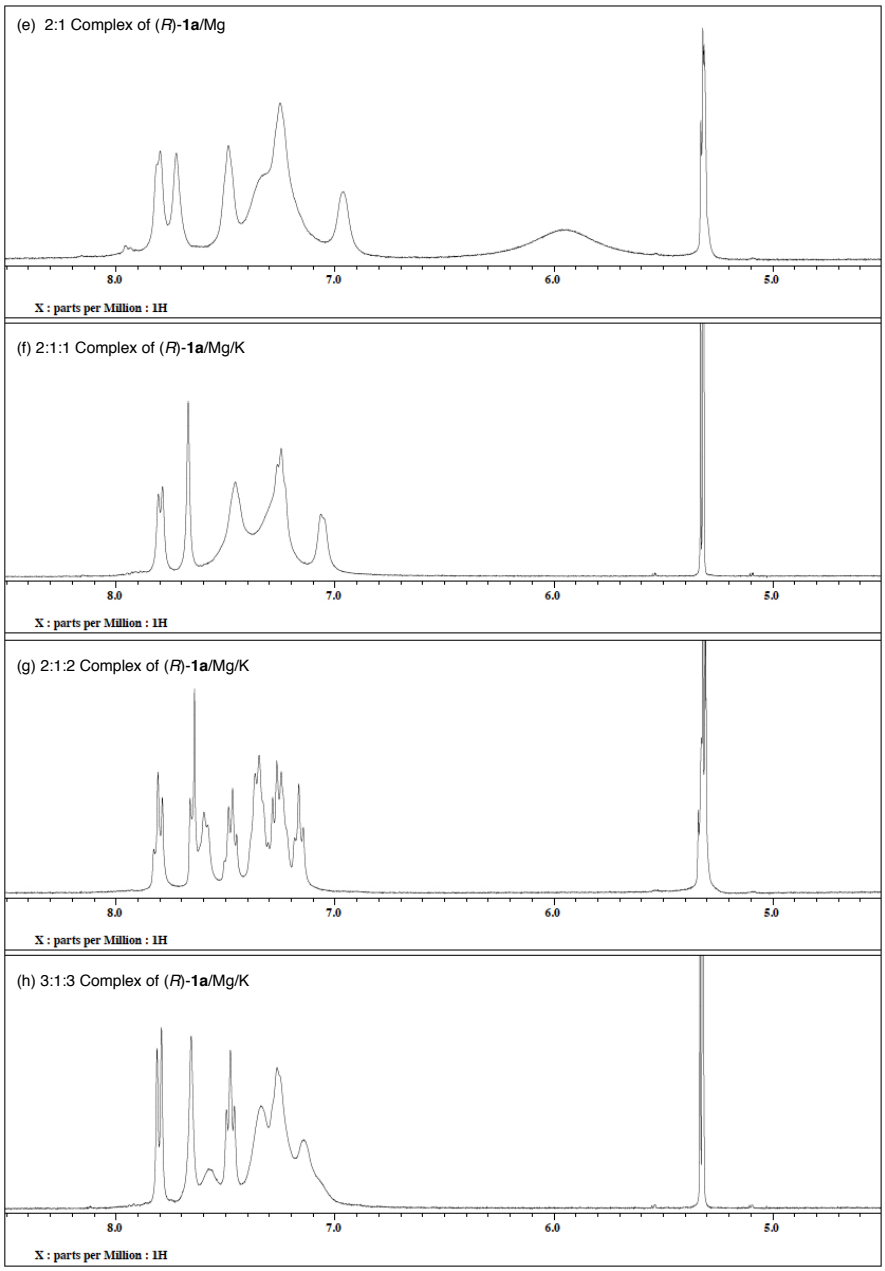

Figure S5 (Continued). (e) A 2:1 complex of (*R*)-**1a**/Mg. (f) A 2:1:1 complex of (*R*)-**1a**/Mg/K. (g) A 2:1:2 complex of (*R*)-**1a**/Mg/K (a possible core species of the cluster). (h) A 3:1:3 complex of (*R*)-**1a**/Mg/K (the possible cluster).

17. ESI-MS analysis of a 3:1:3 complex of (*R*)-1a/Mg/K.

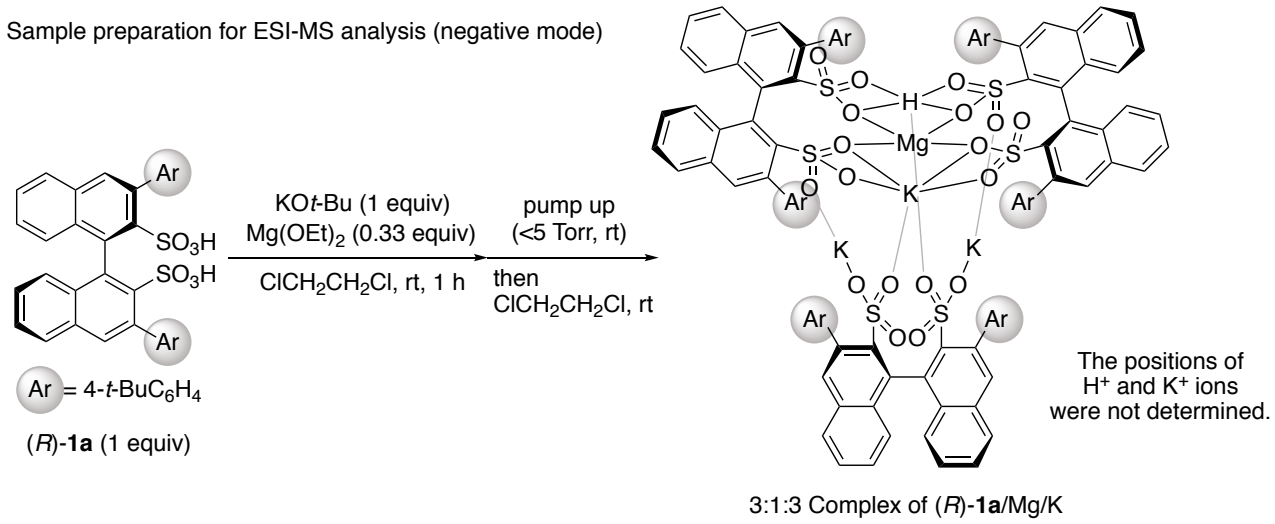

Sample preparation for ESI-MS analysis: (*R*)-**1a** (13.6 mg, 0.020 mmol) was placed in a Schlenk test tube under a nitrogen atmosphere and dissolved in dry dichloroethane (2 mL). To a stirred solution were added magnesium ethoxide (0.10 *M* in methanol, 66.7 μL, 0.0067 mmol) and potassium *tert*-butoxide (1.0 *M* in methanol, 20 μL, 0.020 mmol) at room temperature, and the solution was stirred for 1 h. The volatiles were removed *in vacuo*, and then dichloroethane (1 mL) was added and removed *in vacuo* again. This solvent-removal sequence was repeated twice, and the magnesium/potassium salt of (*R*)-**1a** was obtained *in situ* as pale yellow solid. Then dichloroethane (2 mL) was added at room temperature, and stirred for 10 min. 20 μL of the resulting mixture was diluted with dichloroethane (1 mL) in a well-dried test tube (final concentration: ca. 0.2 m*M*), and passed through a membrane filter (200 mm mesh) just before injection.

The spectrum (negative mode) is shown in Figure S6. Correlation of the theoretical ion distribution for the major peaks (*m/z* = 2150~2220) is shown in Figure S7. As shown in Figures S6 and S7, not only Mg^{2+}/K^+ and Mg^{2+}/Na^+, but also K^+/Na^+ exchanges occurred in (*R*)-**1a**/Mg/K complexes during the analysis due to Na^+ that remained in the ESI-MS instrument. Among these peaks, the desired peak of a 3:1:3 complex of (*R*)-**1a**/Mg/K also could be identified as $C_{120}H_{108}MgK_3O_{18}S_6^-$ [3{(*R*)-**1a**} – 6H + Mg + 3K]$^-$ (*m/z* = 2171.5339 (found), 2171.4644 (calc.)).

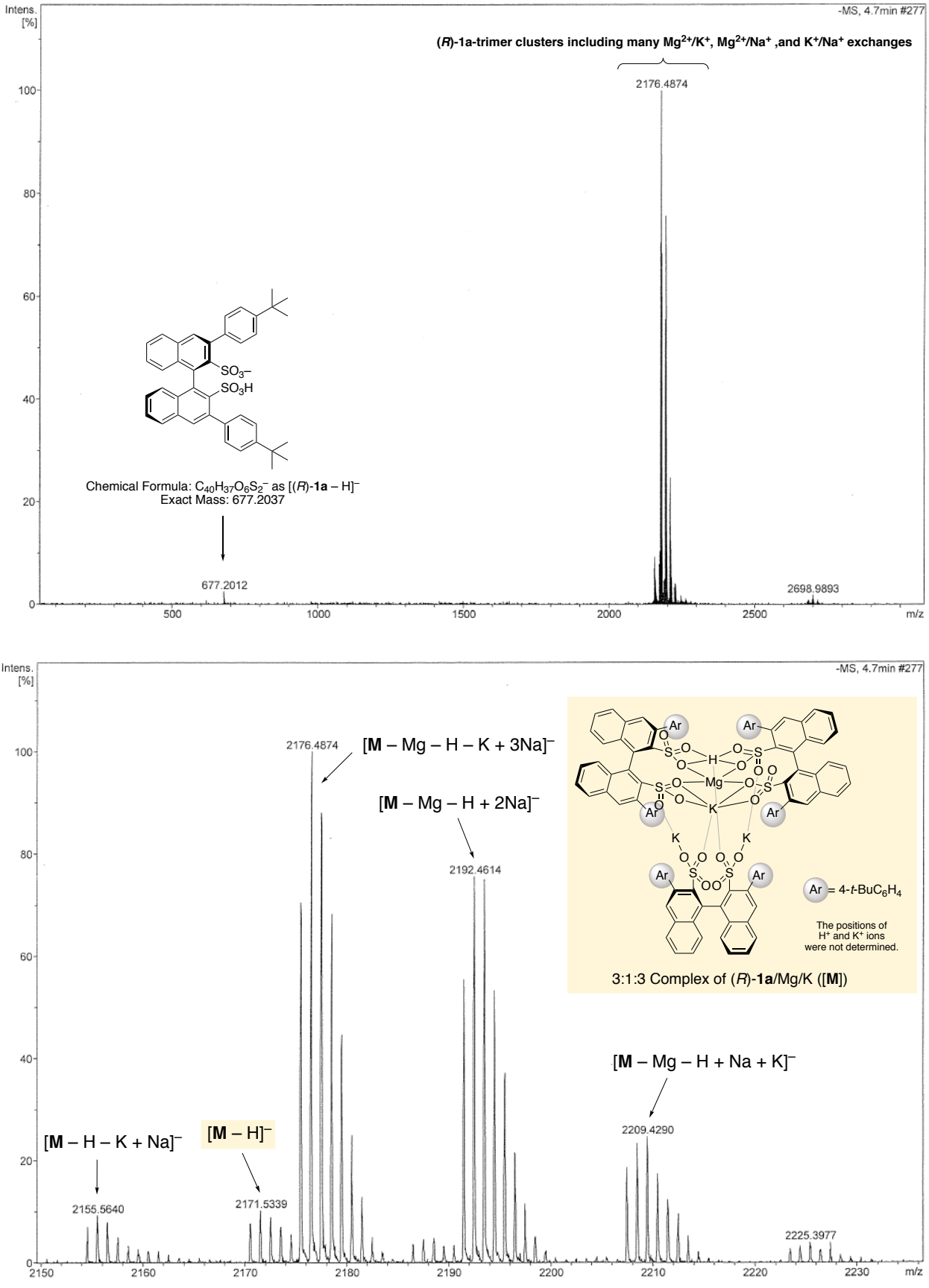

Figure S6. ESI-MS (negative mode) spectrum of a 3:1:3 complex of (*R*)-**1a**/Mg/K.

Theoretical distribution of $C_{120}H_{108}K_2MgNaO_{18}S_6^-$ as [3{(*R*)-1a**} – 6H + Mg + Na + 2K]$^-$**

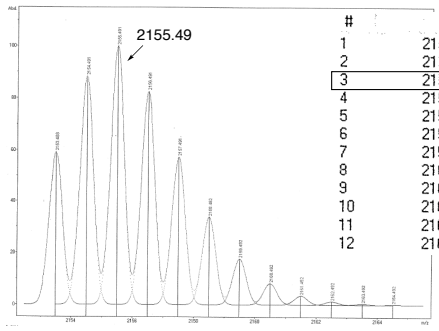

#	m/z	Abundance
1	2153.487668	59.181
2	2154.490705	88.301
3	2155.490690	100.000
4	2156.491417	82.548
5	2157.491485	57.313
6	2158.491692	33.884
7	2159.491719	17.695
8	2160.491767	8.263
9	2161.491770	3.501
10	2162.491783	1.358
11	2163.491799	0.486
12	2164.491835	0.161

Theoretical distribution of $C_{120}H_{108}K_3Na_2O_{18}S_6^-$ as [3{(*R*)-1a**} – 6H + 2Na + 3K]$^-$**

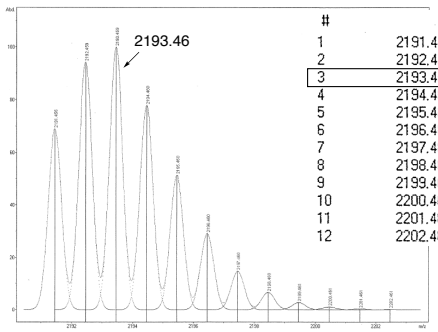

#	m/z	Abundance
1	2191.456102	68.974
2	2192.459348	94.189
3	2193.459285	100.000
4	2194.460066	77.861
5	2195.460138	51.424
6	2196.460368	29.080
7	2197.460411	14.599
8	2198.460478	6.581
9	2199.460501	2.702
10	2200.460533	1.018
11	2201.460567	0.355
12	2202.460621	0.115

Theoretical distribution of $C_{120}H_{108}K_3MgO_{18}S_6^-$ as [3{(*R*)-1a**} – 6H + Mg + 3K]$^-$**

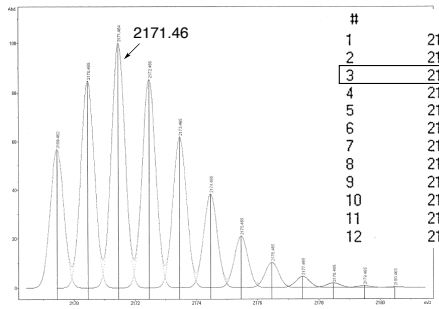

#	m/z	Abundance
1	2169.461605	56.751
2	2170.464642	84.682
3	2171.464427	100.000
4	2172.465169	85.281
5	2173.465123	61.890
6	2174.465307	38.212
7	2175.465255	20.938
8	2176.465258	10.271
9	2177.465191	4.583
10	2178.465142	1.874
11	2179.465083	0.708
12	2180.465041	0.249

Theoretical distribution of $C_{120}H_{108}K_4NaO_{18}S_6^-$ as [3{(*R*)-1a**} – 6H + Na + 4K]$^-$**

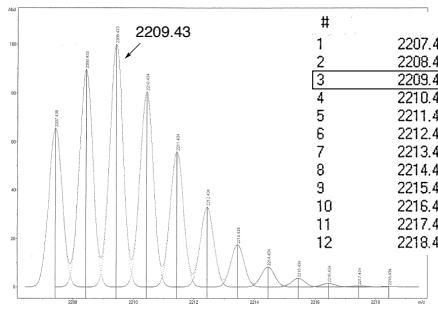

#	m/z	Abundance
1	2207.430039	65.696
2	2208.433285	89.721
3	2209.432983	100.000
4	2210.433794	80.647
5	2211.433739	55.863
6	2212.433952	33.056
7	2213.433911	17.443
8	2214.433934	8.269
9	2215.433885	3.578
10	2216.433855	1.423
11	2217.433814	0.524
12	2218.433791	0.180

Theoretical distribution of $C_{120}H_{108}K_2Na_3O_{18}S_6^-$ as [3{(*R*)-1a**} – 6H + 3Na + 2K]$^-$**

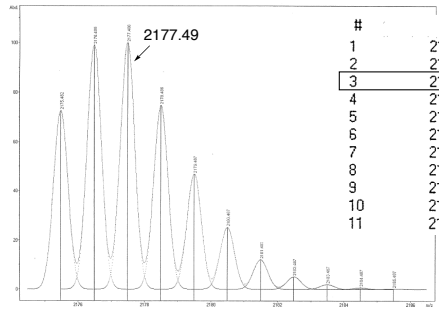

#	m/z	Abundance
1	2175.482165	72.596
2	2176.485411	99.126
3	2177.485613	100.000
4	2178.486377	74.783
5	2179.486580	46.899
6	2180.486845	25.204
7	2181.486975	11.978
8	2182.487103	5.106
9	2183.487205	1.979
10	2184.487315	0.703
11	2185.487437	0.231

Figure S7. Theoretical ion distribution for the major peaks in ESI-MS spectrum of a 3:1:3 complex of (*R*)-**1a**/Mg/K.

18. X-ray analysis of (*R*)-1a/Mg/K complexes.

Preparation of a X-ray sample: (*R*)-**1a** (13.6 mg, 0.020 mmol) was placed in a Schlenk test tube under a nitrogen atmosphere and dissolved in dry dichloroethane (2 mL). To a stirred solution were added di-*n*-butylmagnesium (1.0 *M* in heptane, 13.2 μL, 0.0132 mmol) and potassium *tert*-butoxide (1.0 *M* in THF, 13.2 μL, 0.0132 mmol) at room temperature, and the solution was stirred for 1 h. The volatiles were removed *in vacuo*, and then dichloroethane (1 mL) was added and removed *in vacuo* again. This solvent-removal sequence was repeated twice. Then water (5.4 μL, 0.30 mmol), THF (0.5 mL), and *n*-heptane (0.5 mL) were added at room temperature, and the solution passed through a membrane filter (0.50 μm pore size). The solution was settled at room temperature, and a single crystal was obtained within 12 h.

X-ray analysis: We could obtain a good crystal, which was relatively stable in the mother liquor but extremely unstable in the absence of the mother liquor. The crystal decomposed under the analysis conditions even at 123 K, and gradually provided a powder pattern. However, we ultimately succeeded in the X-ray analysis, although the R_1 value (0.1095) was not so excellent. As a result, cif-check check CIF/PLATON still showed some Alert A errors. These errors might be caused by the huge structure itself (Z = 2, $C_{120}H_{108}K_{3.5}Mg_{1.5}O_{21.5}S_6$, which is subject to symmetric expansion.) and disorder of some parts of the structures, and we could not determine all of thehydrogens, such as SO_3H and H_2O. Moreover, we used SQUEEZE since the solvents are also so badly disordered that they cannot be modeled even with restraints. Therefore, we cannot fully discuss the detailed parameters of the compounds such as bond distances, angles, and torsions, although there should be no serious difficulties in roughly understanding the structures of these complexes.

Crystal data of (*R*)-1a/Mg/K complexes (Figure S8): Formula $C_{120}H_{108}K_{3.5}Mg_{1.5}O_{21.5}S_6$, pale yellow, crystal dimensions 0.30 × 0.30 × 0.20 mm^3, monoclinic, space group *C*2 (#5), a = 19.261(2) Å, b = 25.280(3) Å, c = 32.387(4) Å, α = 90.00°, β = 104.025(2)°, γ = 90.00°, V = 15300(3) $Å^3$, Z = 2, ρ_{calc} = 0.981 g cm^{-3}, F(000) = 4722, μ(MoKα) = 0.242 mm^{-1}, T = 123 K. 28622 reflections collected, 15869 independent reflections with $I > 2\sigma(I)$ ($2\theta_{max}$ = 27.540°), and 1394 parameters were used for the solution of the structure. The non-hydrogen atoms were refined anisotropically. R_1 = 0.1095 and wR_2 = 0.2703. GOF = 1.673. Flack x parameter = 0.099(15). Crystallographic data (excluding structure factors) for the structure reported in this paper have been deposited with the Cambridge Crystallographic Data Centre as supplementary publication no. CCDC-1546867. Copies of the data can be obtained free of charge on application to CCDC, 12 Union Road, Cambridge CB2 1EZ, UK [Web page: http://www.ccdc.cam.ac.uk/].

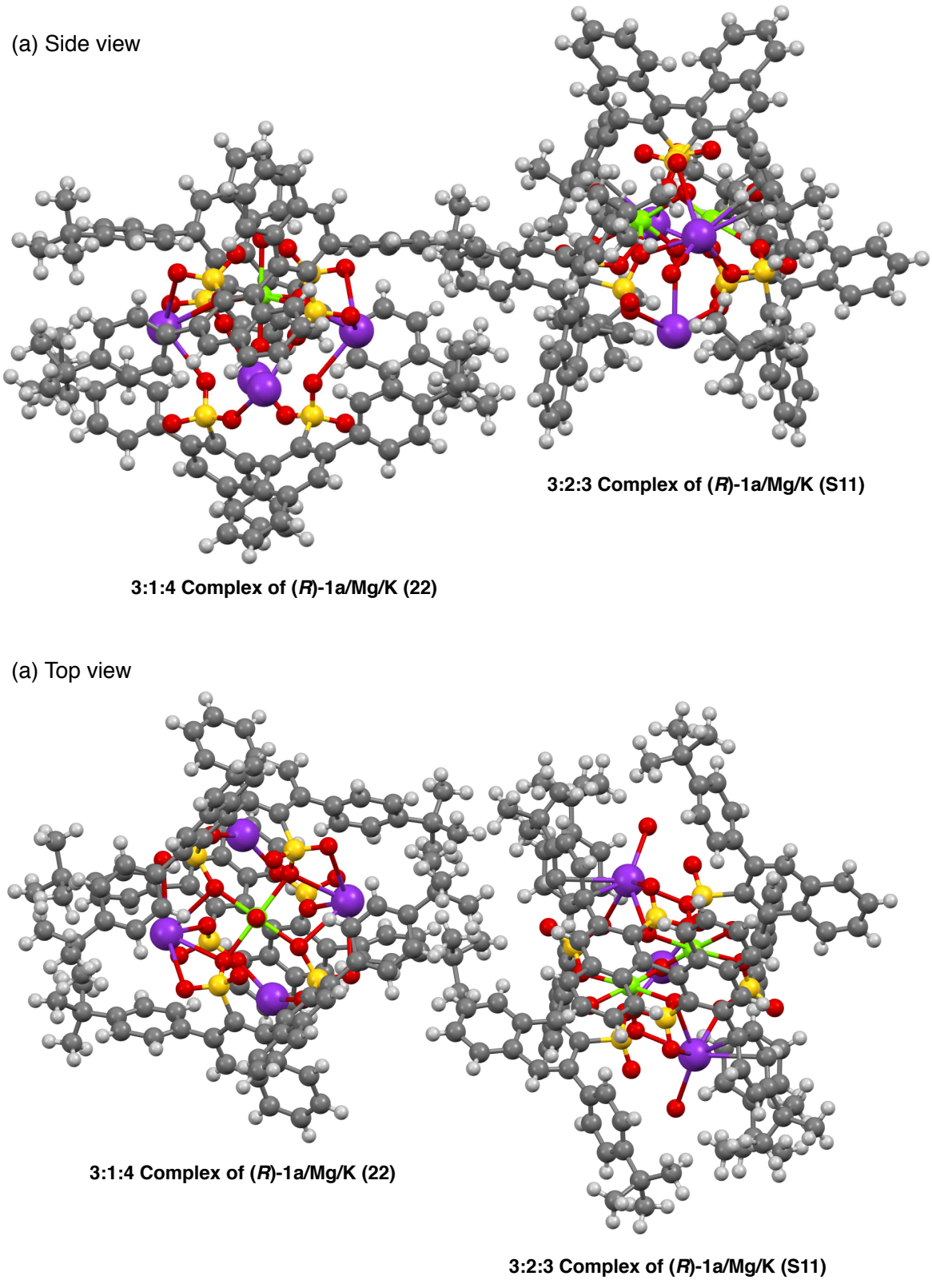

Figure S8. X-ray drawings of (*R*)-**1a**/Mg/K complexes (red = O, green = Mg, yellow = S, purple = K).

(a) Structual formula.

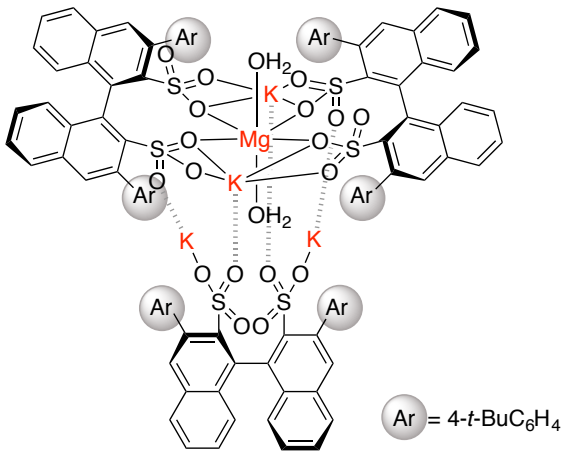

(b) Structual drawing in wireflame style.

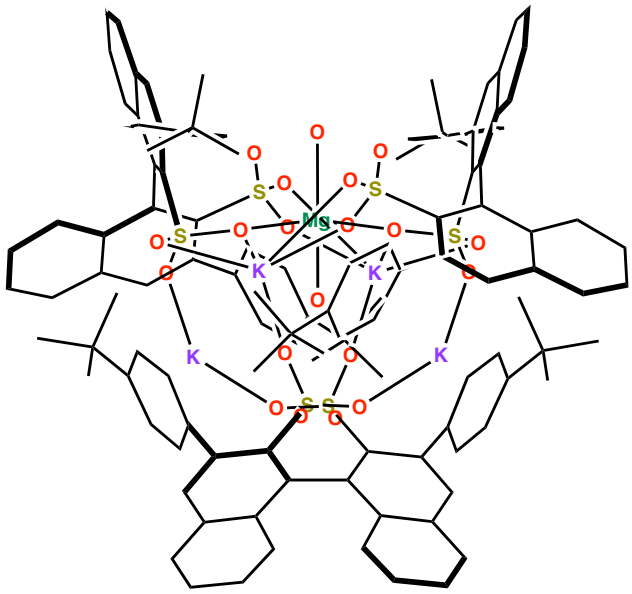

(c) Structual drawing in capped sticks and ball/sticks styles.

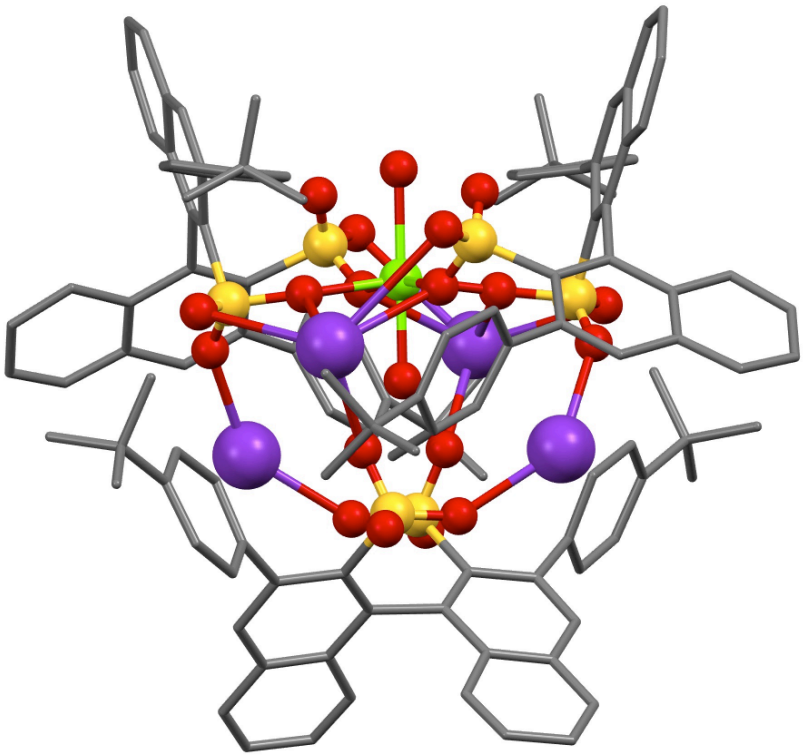

Figure S9. X-ray drawings of a 3:1:4 complex of (*R*)-**1a**/Mg/K (**22**) as one crystal conponent. Hydrogens are omitted for clarity.

(a) Structual formula

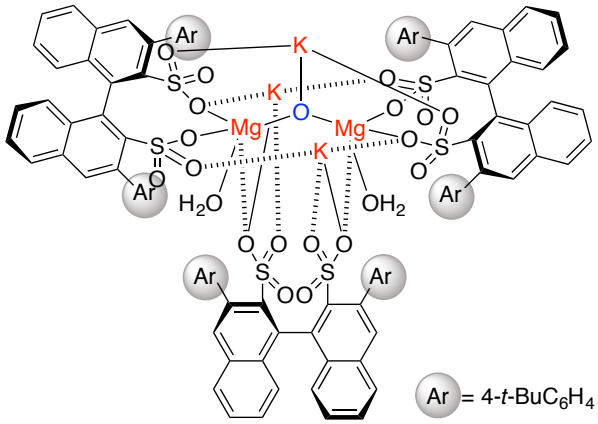

(b) Structual drawing in wireflame style

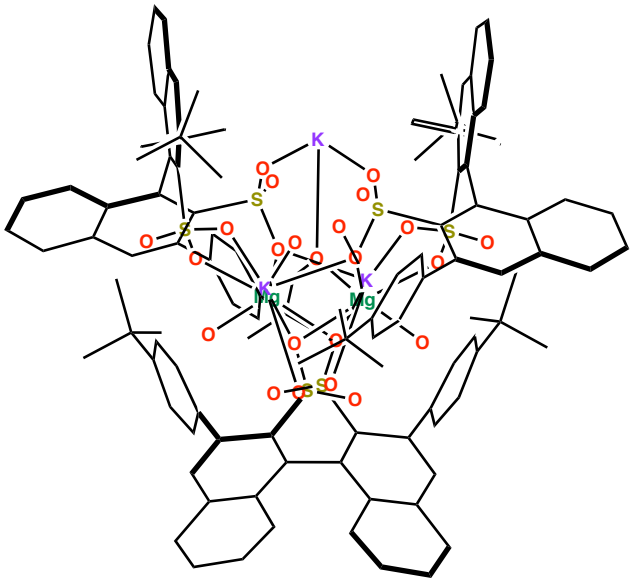

(c) Structual drawing in capped sticks and ball and sticks style

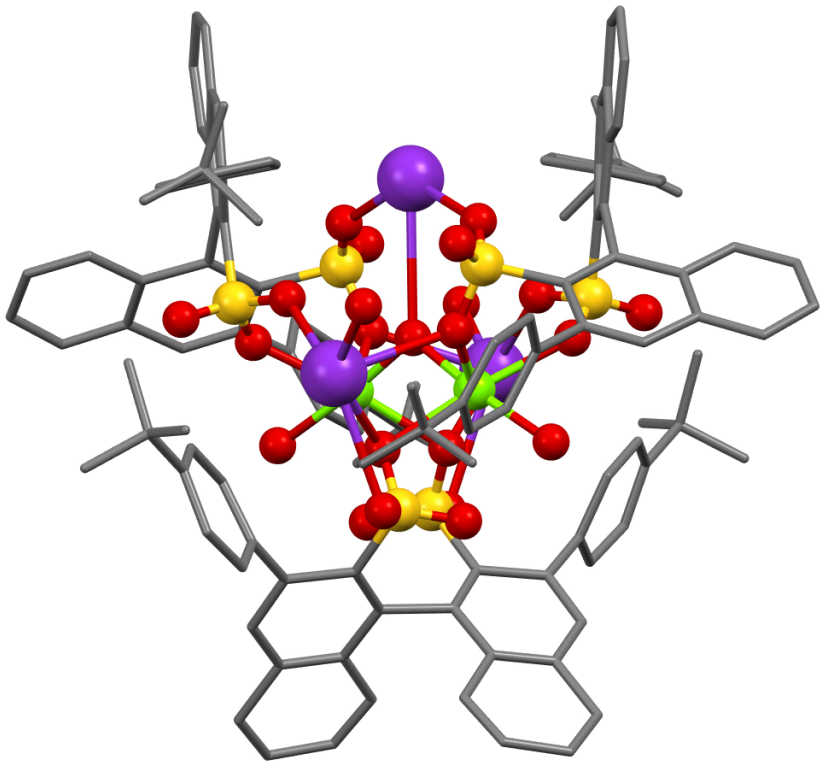

Figure S10. X-ray drawings of a 3:2:3 complex of (*R*)-**1a**/Mg/K (**S11**) as the other crystal conponent. Hydrogens are omitted for clarity. One SO_3H proton, which is supposed to be here, cannot be determined.

19. Control experiments with the use of various (*R*)-1a/Mg/K complexes.

Based on the X-ray analysis of the (*R*)-**1a**/Mg/K clusters, we examined a probe reaction with the use of the most relevant (*R*)-**1a**/Mg/K complexes (i.e., mono-Mg(II) complexes and di-Mg(II) complexes) in the absence of MS 3Å (Table S7).

[For mono-Mg(II) complexes] First, the use of a 3:1:4 complex of (*R*)-**1a**/Mg/K, which had the same ratio as complex **22** as seen in X-ray analysis and involved no SO_3H proton, did not show catalytic activity (entry 1). In sharp contrast, the use of a 3:1:3 complex of (*R*)-**1a**/Mg/K (i.e., our optimized ratio), which included one SO_3H proton, showed great catalytic activity, and *syn*-**4a** was obtained with 95% ee (entry 2). Moreover, other mono-Mg(II) complexes, such as a 3:1:2 complex of (*R*)-**1a**/Mg/K and a 3:1:1 complex of (*R*)-**1a**/Mg/K, which included two and three SO_3H protons, respectively, were examined (entries 3 and 4). As a result, *syn*-**4a** was obtained with 89% ee and 84% ee, respectively (entries 3 and 4). Overall, *mono-Mg(II) complexes with one, two, or three SO_3H protons showed catalytic activities, and in particular a **3:1:3 complex of (R)-1a/Mg/K with one SO_3H proton** gave better results than the others (entry 2 vs. entries 3 and 4).* However, due to the complex equilibrium of the catalyst components, it is not possible to unequivocally determine that a 3:1:2 complex of (*R*)-**1a**/Mg/K is a real active species.

[For di-Mg(II) complexes] Next, we found that the use of a 3:2:3 complex of (*R*)-**1a**/Mg/K, which had the same ratio as complex **S11** as seen in X-ray analysis and would involve one SO_3H proton, did not show catalytic activity (entry 5). Moreover, the use of a 3:2:2 complex of (*R*)-**1a**/Mg/K, which involved two SO_3H proton, also did not show catalytic activity (entry 6). Therefore, *di-Mg(II) complexes should **not** be active species in this reaction.*

Table S7. Screening of the ratio of magnesium and potassium ions to (*R*)-**1a**.

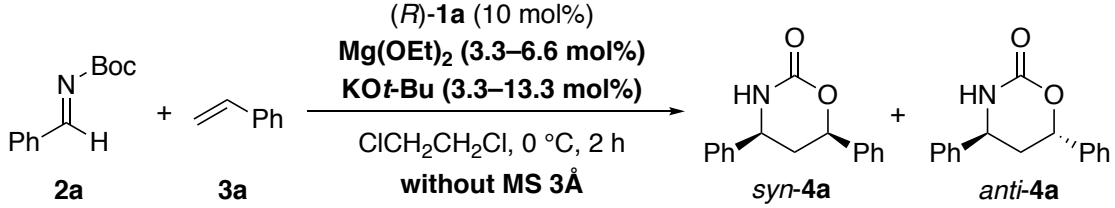

entry	Mg^{2+} (mol%)[b]	K^+ (mol%)[c]	(*R*)-**1a**:Mg:K	yield (%)	*syn*:*anti* of **4a**	ee (%) of *syn*-**4a**
1	3.3	13.3	3:**1**:4	**0**	–	–
2	3.3	10	3:**1**:3	56	**>99:<1**	**95**
3	3.3	6.6	3:**1**:2	52	>99:<1	89
4	3.3	3.3	3:**1**:1	63	>20:<1	84
5	6.6	10	3:**2**:3	**0**	–	–
6	6.6	6.6	3:**2**:2	**0**	–	–

[a] The reaction was conducted in dichloroethane at 0 °C for 2 h on a 0.20 mmol scale of **2a** in the absence of MS 3Å. [b] $Mg(OEt)_2$ was used as a magnesium source as described in the general reation procedure. [c] KO*t*-Bu was used as a potassium source as described in the general reation procedure.

Table S7 (Continued). The structures below have not been derermined and are drawn based on speculations. In particular, the positions of proton and potassium ions were not determined except for the complex in entry 1.

entry 1 3:1:4 Complex of (*R*)-**1a**/Mg/K

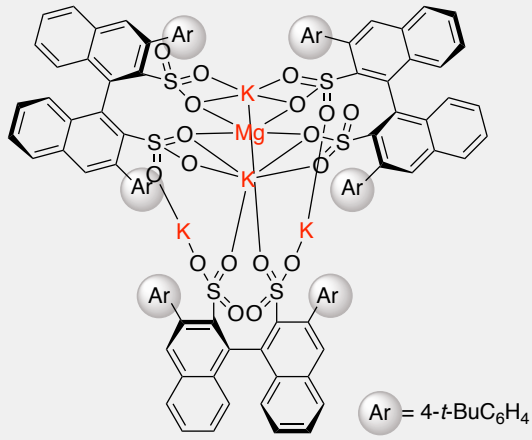

Inactive

entry 2 3:1:3 Complex of (*R*)-**1a**/Mg/K

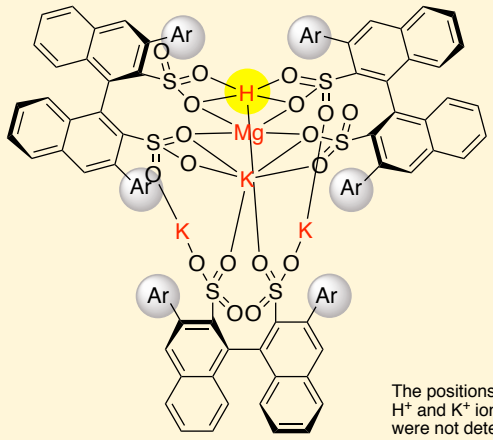

More active

entry 3 3:1:2 Complex of (*R*)-**1a**/Mg/K

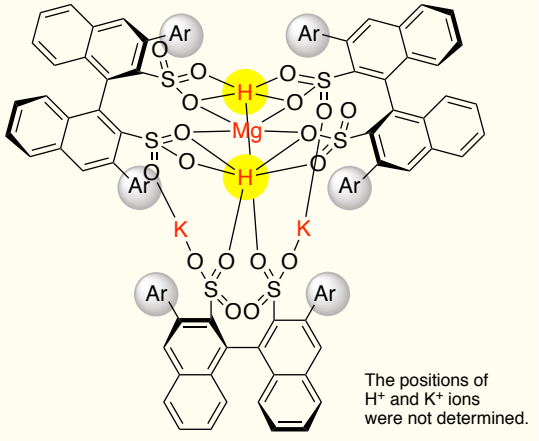

Less active

entry 4 3:1:1 Complex of (*R*)-**1a**/Mg/K

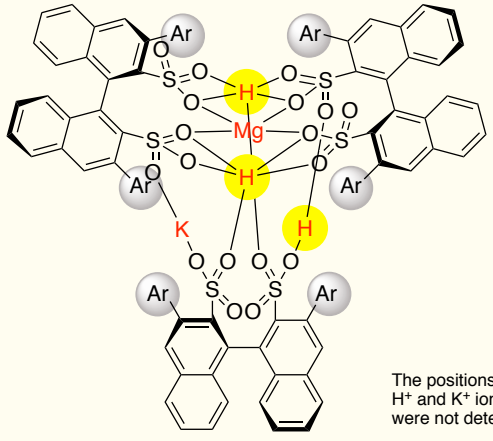

Less active

entry 5 3:2:3 Complex of (*R*)-**1a**/Mg/K

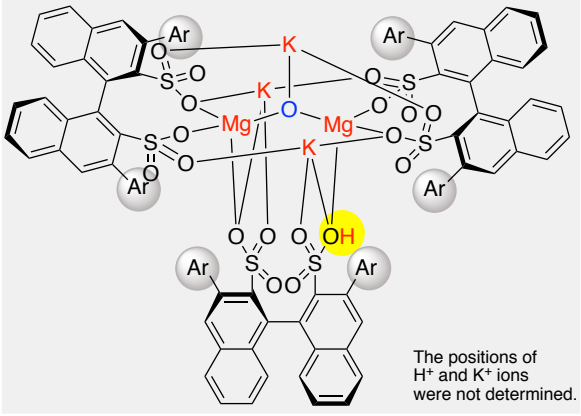

Inactive

entry 6 3:2:2 Complex of (*R*)-**1a**/Mg/K

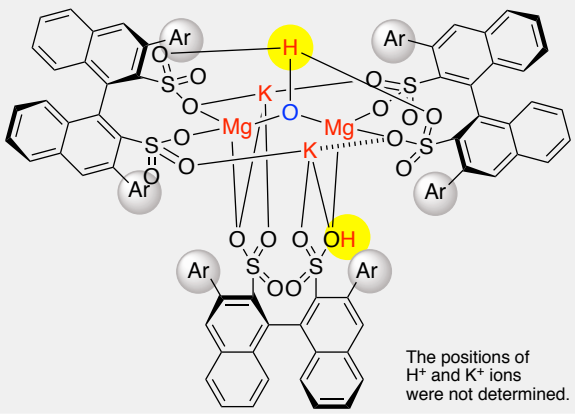

Inactive

20. Kinetics study.

An initial rate kinetics study was conducted according to the established procedure in the literature.[15] As a result, first-order dependency (1.18) on the initial concentration of the catalyst components was observed by plotting ln n_{obs} (m*M*·min^{-1}) versus ln [3:1:3 complex of (*R*)-**1a**/Mg/K (m*M*)] (Figure S13). Zero-order dependency (0.0135) on the initial concentration of the aldimine **2a** was observed by plotting ln n_{obs} (m*M*·min^{-1}) versus ln [**2a** (m*M*)] (Figure S15). First-order dependency (0.978) on the initial concentration of the styrene **3a** was observed by plotting ln n_{obs} (m*M*·min^{-1}) versus ln [**3a** (m*M*)] (Figure S17).

To make sense of these observations, we can consider possible reaction steps under the assumption of a 3:1:3 complex of (*R*)-**1a**/Mg/K (first-order) (Figure S11). First, a 3:1:3 complex of (*R*)-**1a**/Mg/K (first-order) might coordinate and activate aldimine **2a** (zero-order), which should not be a rate-determining step. Next, the corresponding **2a**-activated 3:1:3 complex of (*R*)-**1a**/Mg/K (first-order) might react with styrene **3a** (first-order); this should be a rate-determining step.

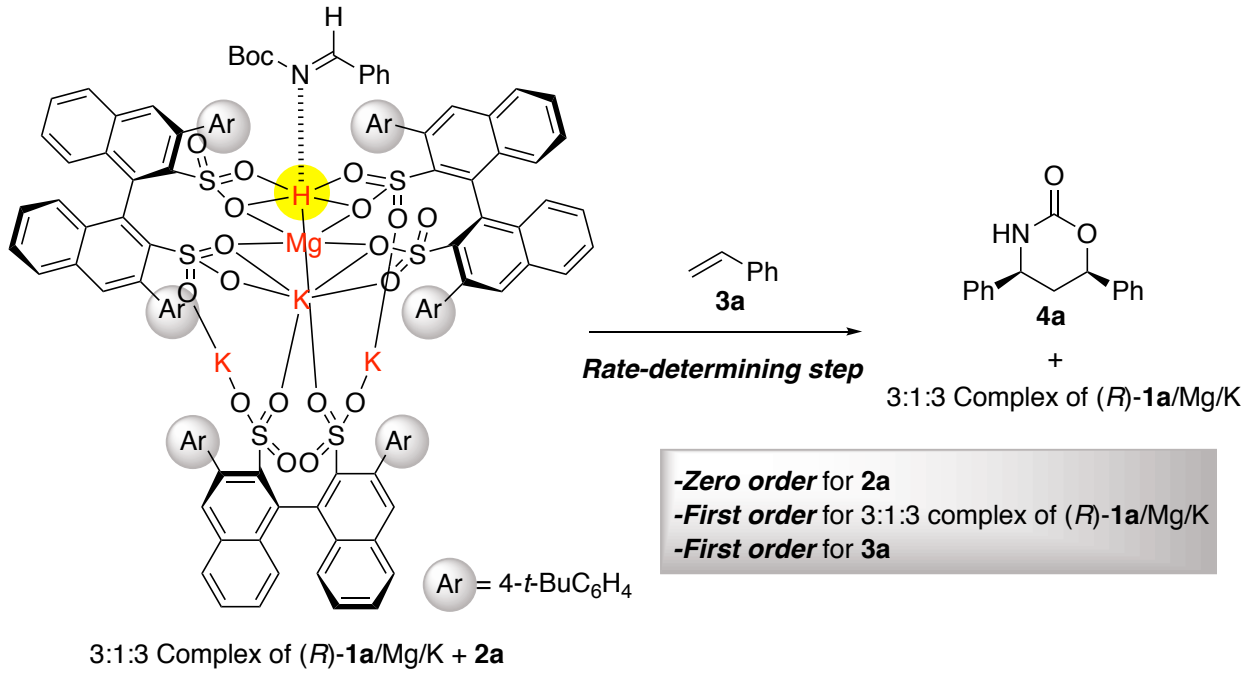

Figure S11. Summary of kinetics study and possible rate determing step.

(1) Kinetics study using 3:1:3 complex of (*R*)-1a/Mg/K.

0.333 mM/[3:1:3 complex of (R)-1a/Mg/K] concentration: (*R*)-**1a** (13.6 mg, 0.020 mmol, 10 mol%) was placed in a Schlenk test tube under a nitrogen atmosphere and dissolved in dry dichloroethane (2 mL). To a stirred solution were added magnesium ethoxide (0.10 *M* in methanol, 66.7 μL, 0.0067 mmol, 3.3 mol%) and potassium *tert*-butoxide (1.0 *M* in methanol, 20 μL, 0.020 mmol, 10 mol%) at room temperature, and the solution was stirred for 1 h. The volatiles were removed *in vacuo*, and then dichloroethane (1 mL) was added and removed *in vacuo* again. This solvent-removal sequence was repeated twice, and the magnesium/potassium salt of (*R*)-**1a** was obtained *in situ* as pale yellow solid. Then dichloroethane (20 mL) and well-activated MS 3Å (50 mg) were added at 0 °C, and the suspension was stirred at 0 °C for 30 min. Styrene **3a** (463 μL, 4.0 mmol) was added to the suspension, and the mixture was stirred at 0 °C for 30 min. Aldimine **2a** (41.1 mg, 0.20 mmol) was added at 0 °C, and the mixture was stirred at 0 °C for 120 min. After stirring for the indicated period, small amount of reaction mixture was sampled via syringe and poured into triethylamine (ca. 100 μL) to quench the reaction. The volatiles were removed under reduced pressure, and the residue was dissolved into $CDCl_3$ to measure the conversion yield, which was determined by NMR analysis of peaks derived from **2a** (8.85 ppm, s, 1H, PhC*H*=N) and **4a** (4.78 ppm, dd, *J* = 11.5, 4.6 Hz, 1H, PhC*H*–N).

0.167 mM/[3:1:3 complex of (R)-1a/Mg/K] concentration*:* (*R*)-**1a** (6.8 mg, 0.010 mmol), magnesium ethoxide (0.10 *M* in methanol, 33.3 μL, 0.0033 mmol), potassium *tert*-butoxide (1.0 *M* in methanol, 10 μL, 0.010 mmol), styrene **3a** (463 μL, 4.0 mmol), aldimine **2a** (41.1 mg, 0.20 mmol), and dichloroethane (20 mL) were used.

0.667 mM/[3:1:3 complex of (R)-1a/Mg/K] concentration*:* (*R*)-**1a** (27.2 mg, 0.040 mmol), magnesium ethoxide (0.10 *M* in methanol, 133.3 μL, 0.0133 mmol), potassium *tert*-butoxide (1.0 *M* in methanol, 40 μL, 0.040 mmol), styrene **3a** (463 μL, 4.0 mmol), aldimine **2a** (41.1 mg, 0.20 mmol), and dichloroethane (20 mL) were used.

A 3:1:3 complex of (*R*)-**1a**/Mg/K (m*M*) vs. time (min) plot is shown in Figure S12. Initial rate kinetics study of cycloaddition of **3a** with **2a** was conducted by assuming pseudo first-order consumption of **2a** to give **4a**. As a result, first-order dependency (1.18) in the initial concentration of the catalyst components was observed by plotting ln ν_{obs} (m$M \cdot min^{-1}$) versus ln [3:1:3 complex of (*R*)-**1a**/Mg/K (m*M*)] (Figure S13). Overall, this observation might strongly assist that the active species would be a 3:1:3 complex of (*R*)-**1a**/Mg/K, which would provide the single active proton center in the transition states, without decomposition to its components.

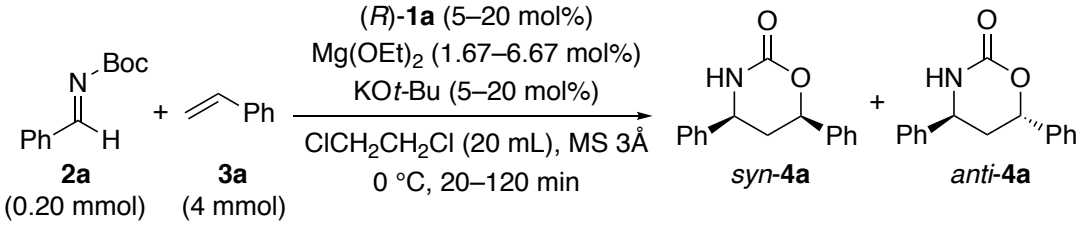

Catalyst concentration (m*M*)	ν_{obs} [m*M* min^{-1}]
0.167	0.0195
0.333	0.0440
0.667	0.100

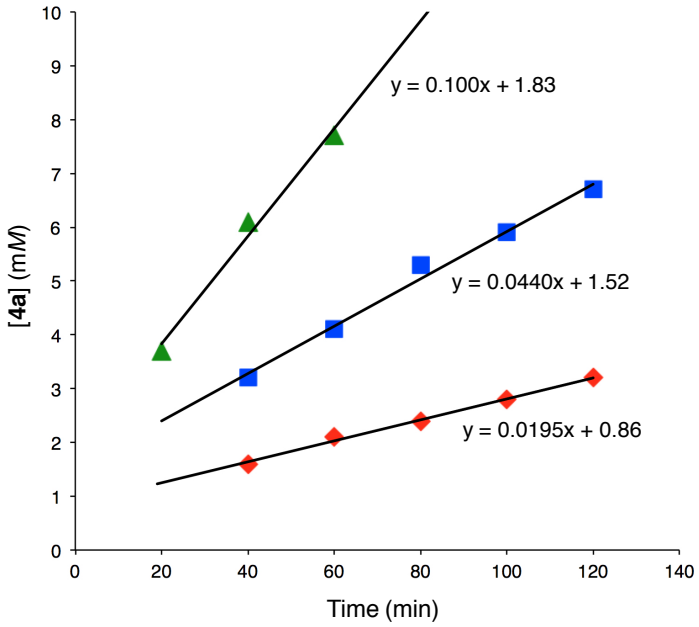

Figure S12. Plot of [**4a**] (m*M*) vs. time (min) with variable catalyst concentration.

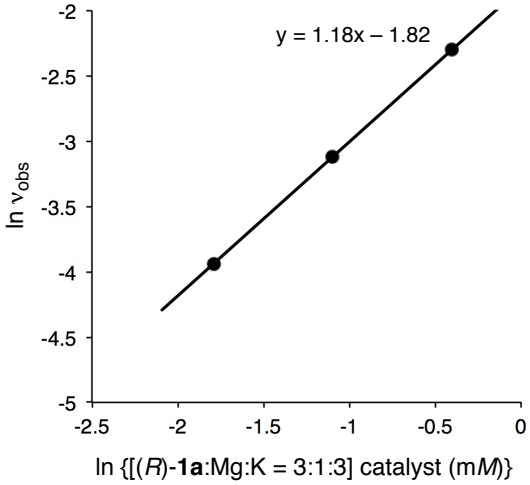

Figure S13. Plot of ln ν_{obs} (m*M*·min^{-1}) vs. ln [3:1:3 complex of (*R*)-**1a**/Mg/K (m*M*)].

(2) Kinetic study of aldimine 2a.

10 mM/[aldimine 2a] concentration: (*R*)-**1a** (13.6 mg, 0.020 mmol, 10 mol%) was placed in a Schlenk test tube under a nitrogen atmosphere and dissolved in dry dichloroethane (2 mL). To a stirred solution were added magnesium ethoxide (0.10 *M* in methanol, 66.7 μL, 0.0067 mmol, 3.3 mol%) and potassium *tert*-butoxide (1.0 *M* in methanol, 20 μL, 0.020 mmol, 10 mol%) at room temperature, and the solution was stirred for 1 h. The volatiles were removed *in vacuo*, and then dichloroethane (1 mL) was added and removed *in vacuo* again. This solvent-removal sequence was repeated twice, and the magnesium/potassium salt of (*R*)-**1a** was obtained *in situ* as pale yellow solid. Then dichloroethane (20 mL) and well-activated MS 3Å (50 mg) were added at 0 °C, and the suspension was stirred at 0 °C for 30 min. Styrene **3a** (463 μL, 4.0 mmol) was added to the suspension, and the mixture was stirred at 0 °C for 30 min. Aldimine **2a** (41.1 mg, 0.20 mmol) was added at 0 °C, and the mixture was stirred at 0 °C for 120 min. After stirring for the indicated period, small amount of reaction mixture was sampled via syringe and poured into triethylamine (ca. 100 μL) to quench the reaction. The volatiles were removed under reduced pressure, and the residue was dissolved into $CDCl_3$ to measure the conversion yield, which was determined by NMR analysis of peaks derived from **2a** (8.85 ppm, s, 1H, PhC*H*=N) and **4a** (4.78 ppm, dd, J = 11.5, 4.6 Hz, 1H, PhC*H*–N).

5 mM/[aldimine 2a] concentration*:* (*R*)-**1a** (13.6 mg, 0.020 mmol), magnesium ethoxide (0.10 *M* in methanol, 66.7 μL, 0.0067 mmol), potassium *tert*-butoxide (1.0 *M* in methanol, 20 μL, 0.020 mmol), styrene **3a** (463 μL, 4.0 mmol), aldimine **2a** (20.5 mg, 0.10 mmol), and dichloroethane (20 mL) were used.

20 mM/[aldimine 2a] concentration*:* (*R*)-**1a** (13.6 mg, 0.020 mmol), magnesium ethoxide (0.10 *M* in methanol, 66.7 μL, 0.0067 mmol), potassium *tert*-butoxide (1.0 *M* in methanol, 20 μL, 0.020 mmol), styrene **3a** (463 μL, 4.0 mmol), aldimine **2a** (82.1 mg, 0.40 mmol), and dichloroethane (20 mL) were used.

A **2a** (m*M*) vs. time (min) plot is shown in Figure S14. Initial rate kinetics study of cycloaddition of **3a** with **2a** was conducted by assuming pseudo first-order consumption of **2a** to give **4a**. As a result, zero-order dependency (0.0135) in the initial concentration of the aldimine **2a** was observed by plotting ln ν_{obs} (m$M \cdot min^{-1}$) versus ln [**2a** (m*M*)] (Figure S15).

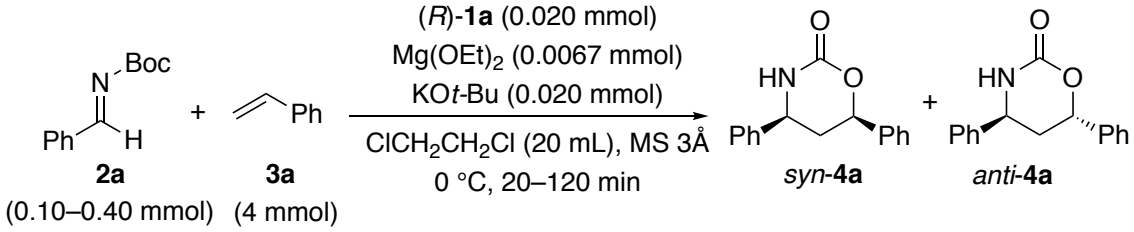

2a concentration (m*M*)	ν_{obs} [m*M* min^{-1}]
5	0.0425
10	0.0440
20	0.0433

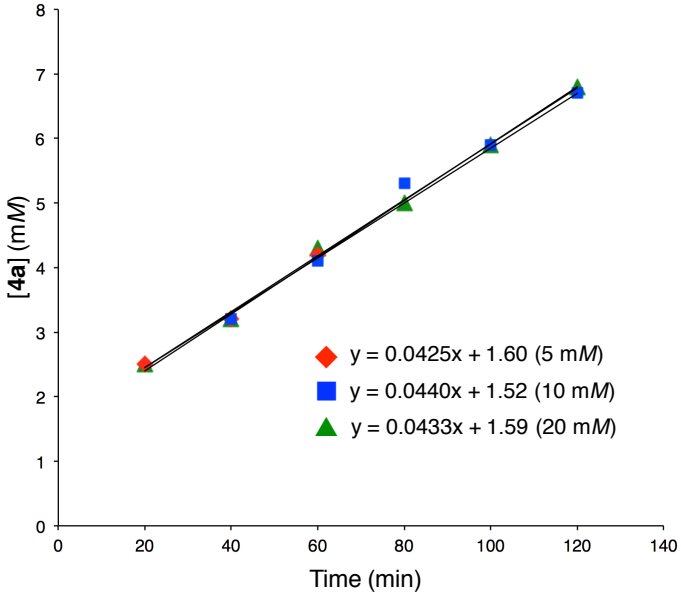

Figure S14. Plot of [**4a**] (m*M*) vs. time (min) with variable **2a** concentration.

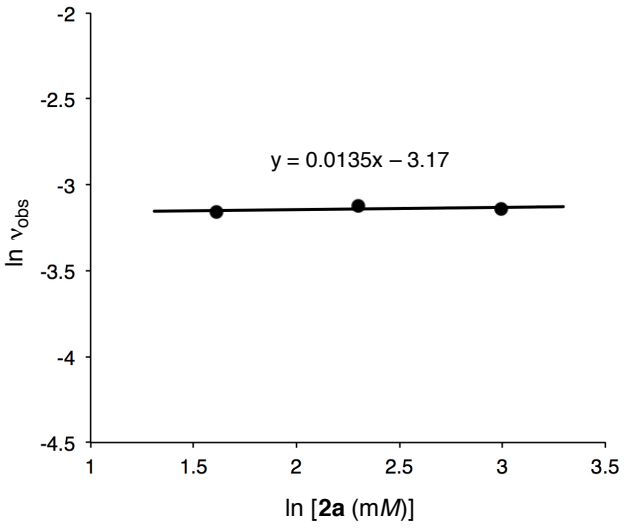

Figure S15. Plot of ln ν_{obs} (m*M*·min^{-1}) vs. ln [**2a** (m*M*)].

(3) Kinetic study of styrene 3a.

200 mM/[styrene 3a] concentration: (*R*)-**1a** (13.6 mg, 0.020 mmol, 10 mol%) was placed in a Schlenk test tube under a nitrogen atmosphere and dissolved in dry dichloroethane (2 mL). To a stirred solution were added magnesium ethoxide (0.10 *M* in methanol, 66.7 μL, 0.0067 mmol, 3.3 mol%) and potassium *tert*-butoxide (1.0 *M* in methanol, 20 μL, 0.020 mmol, 10 mol%) at room temperature, and the solution was stirred for 1 h. The volatiles were removed *in vacuo*, and then dichloroethane (1 mL) was added and removed *in vacuo* again. This solvent-removal sequence was repeated twice, and the magnesium/potassium salt of (*R*)-**1a** was obtained *in situ* as pale yellow solid. Then dichloroethane (20 mL) and well-activated MS 3Å (50 mg) were added at 0 °C, and the suspension was stirred at 0 °C for 30 min. Styrene **3a** (463 μL, 4.0 mmol) was added to the suspension, and the mixture was stirred at 0 °C for 30 min. Aldimine **2a** (41.1 mg, 0.20 mmol) was added at 0 °C, and the mixture was stirred at 0 °C for 120 min. After stirring for the indicated period, small amount of reaction mixture was sampled via syringe and poured into triethylamine (ca. 100 μL) to quench the reaction. The volatiles were removed under reduced pressure, and the residue was dissolved into $CDCl_3$ to measure the conversion yield, which was determined by NMR analysis of peaks derived from **2a** (8.85 ppm, s, 1H, PhC*H*=N) and **4a** (4.78 ppm, dd, J = 11.5, 4.6 Hz, 1H, PhC*H*–N).

100 mM/[styrene 3a] concentration*:* (*R*)-**1a** (13.6 mg, 0.020 mmol), magnesium ethoxide (0.10 *M* in methanol, 66.7 μL, 0.0067 mmol), potassium *tert*-butoxide (1.0 *M* in methanol, 20 μL, 0.020 mmol), styrene **3a** (231 μL, 2.0 mmol), and aldimine **2a** (41.1 mg, 0.20 mmol) were used.

400 mM/[styrene 3a] concentration*:* (*R*)-**1a** (13.6 mg, 0.020 mmol), magnesium ethoxide (0.10 *M* in methanol, 66.7 μL, 0.0067 mmol), potassium *tert*-butoxide (1.0 *M* in methanol, 20 μL, 0.020 mmol), styrene **3a** (926 μL, 8.0 mmol), and aldimine **2a** (41.1 mg, 0.20 mmol) were used.

A **3a** (m*M*) vs. time (min) plot is shown in Figure S16. Initial rate kinetics study of cycloaddition of **3a** with **2a** was conducted by assuming pseudo first-order consumption of **2a** to give **4a**. As a result, first-order dependency (0.978) in the initial concentration of the styrene **3a** was observed by plotting ln ν_{obs} (mM·min^{-1}) versus ln [**3a** (m*M*)] (Figure S17).

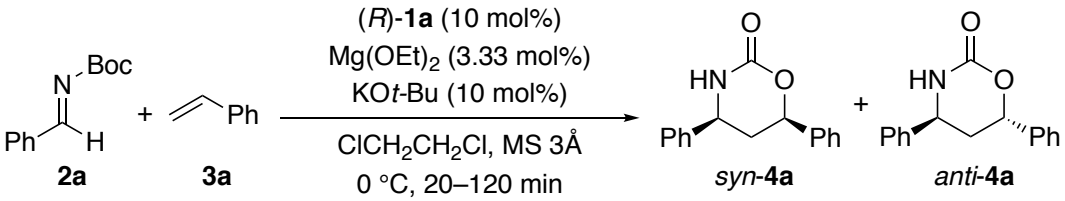

3a concentration (m*M*)	ν_{obs} [m*M* min^{-1}]
100	0.0245
200	0.0440
400	0.0950

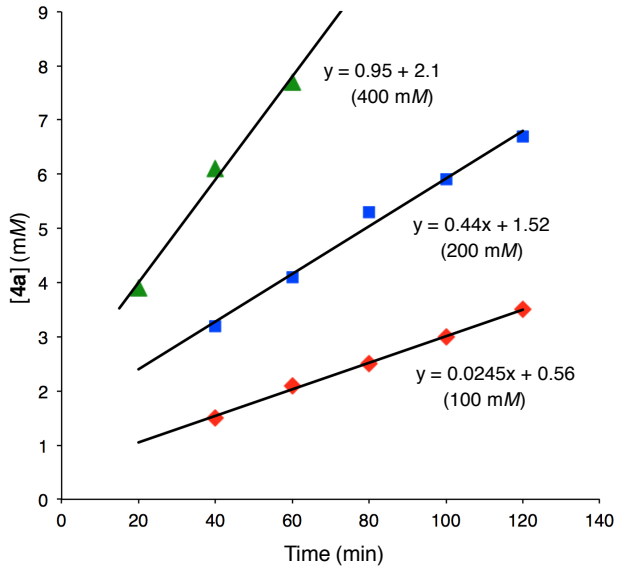

Figure S16. Plot of [**4a**] (m*M*) vs. time (min) with variable **3a** concentration.

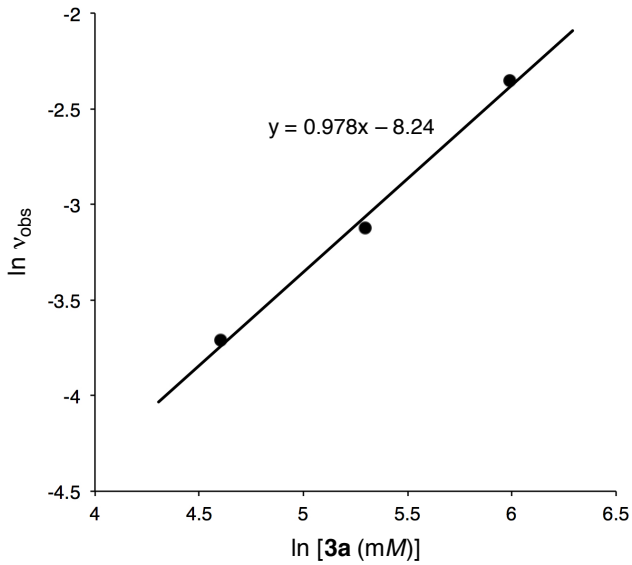

Figure S17. Plot of ln ν_{obs} (m*M*·min^{-1}) vs. ln [**3a** (m*M*)].

21. Control experiments with the use of catalysts and additives (Eqs. 9 and 10).

To confirm whether or not one proton in the SO_3H moiety would be the active center in the 3:1:3 complex of (*R*)-**1a**/Mg/K, we performed the following experiments (1), (2), and (3).

(1) Effect of the addition of trifluoromethanesulfonic acid (3.3 mol%) or *p*-toluenesulfonic acid (3.3 mol%) on the catalytic reaction of a 3:1:4 complex of (*R*)-**1a**/Mg/K (3.3 mol%).

As shown in Eq. 9, the addition of a strong acid such as trifluoromethanesulfonic acid (TfOH) dramatically restored the catalytic activity of an inactive 3:1:4 complex of (*R*)-**1a**/Mg/K. Moreover, the addition of a much weaker acid such as *p*-toluenesulfonic acid (*p*-TsOH) did not strongly promote the reaction, and *syn*-**4a** was obtained in 7% yield with 89% ee (Eq. S8). As seen in Table S8, *p*-TsOH alone did not promote the reaction. Therefore, these results also might support the presence of proton-catalysis, after the proton-exchange reaction.

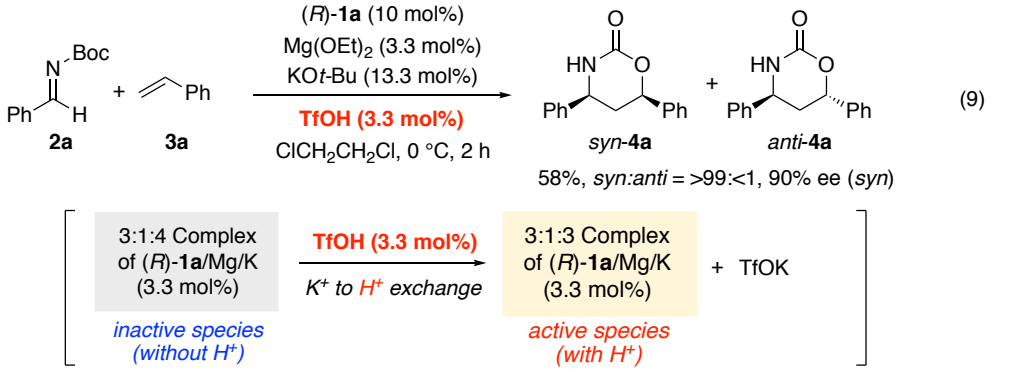

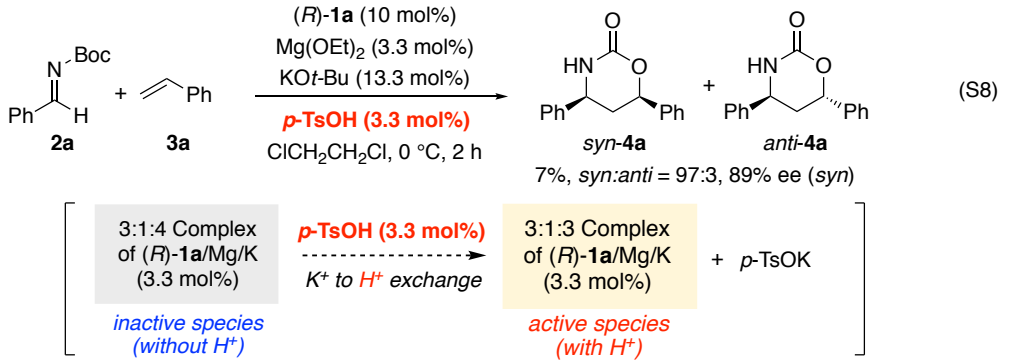

[Procedure of Eq. 9] (*R*)-**1a** (14.0 mg, 0.0206 mmol, 10 mol%) was placed in a Schlenk test tube under a nitrogen atmosphere and dissolved in dry dichloroethane (2 mL). To a stirred solution were added magnesium ethoxide (0.10 *M* in methanol, 68.7 μL, 0.00687 mmol, 3.3 mol%) and potassium *tert*-butoxide (1.0 *M* in methanol, 27.5 μL, 0.0275 mmol, 13.3 mol%) at room temperature, and the solution was stirred for 1 h. The volatiles were removed *in vacuo*, and then dichloroethane (1 mL) was added and removed *in vacuo* again. This solvent-removal sequence was repeated twice, and the magnesium/potassium salt of (*R*)-**1a** was obtained *in situ* as pale yellow solid. Then dichloroethane (20 mL) and trifluoromethanesulfonic acid (0.6 μL, 0.00687 mmol,

3.3 mol%) were added at room temperature, and the solution was stirred at room temperature for 30 min. Styrene **3a** (463 μL, 4.0 mmol) was then added to the solution at 0 °C, and the mixture was stirred at 0 °C for 30 min. Then aldimine **2a** (42.2 mg, 0.206 mmol) was added at 0 °C, and the mixture was stirred at 0 °C for 2 h. The resulting reaction mixture was quenched with triethylamine (0.2 mL) at 0 °C, and the organic phase was concentrated under reduced pressure. The resultant residue was purified by silica gel column chromatography (eluent: *n*-hexane:EtOAc = 5:1 to 1:15) to give the desired product **4a** in 58% yield (30.3 mg). The enantiomeric purity of **4a** was determined by chiral HPLC analysis (*syn*:*anti* = >99:<1, 90% ee (*syn*)).

[Procedure of Eq. S8] Based on the samed procedure, *p*-toluenesulfonic acid monohydrate (1.2 mg, 0.00687 mmol, 3.3 mol%) was used in place of trifluoromethanesulfonic acid. The desired product **4a** was obtained in 7% yield (3.7 mg). The enantiomeric purity of **4a** was determined by chiral HPLC analysis (*syn:anti* = 97:3, 89% ee (*syn*)).

(2) Effect of the addition of 2,6-di-*tert*-butylpyridine (3.3 mol%) on the catalytic reaction of a 3:1:3 complex of (*R*)-**1a**/Mg/K (3.3 mol%).

As shown in Eq. 10, the addition of 2,6-di-*tert*-butylpyridine completely deactivated the catalytic activity of a 3:1:3 complex of (*R*)-**1a**/Mg/K. This result might support proton-catalysis.

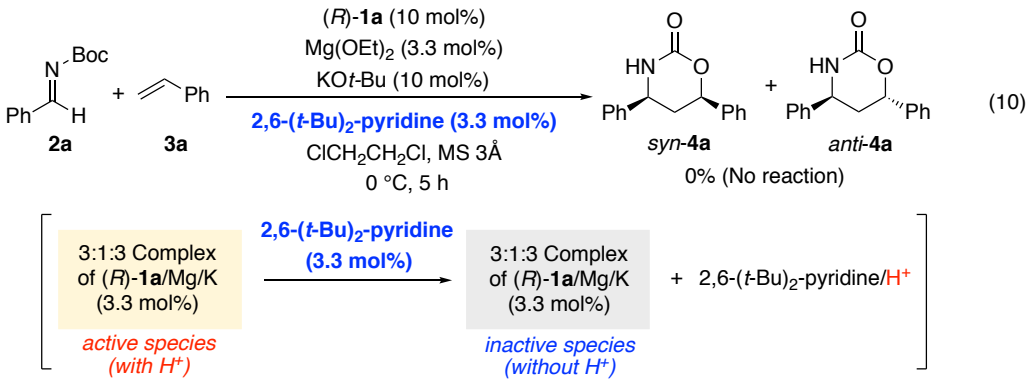

[Procedure of Eq. 10] (*R*)-**1a** (13.6 mg, 0.020 mmol, 10 mol%) was placed in a Schlenk test tube under a nitrogen atmosphere and dissolved in dry dichloroethane (2 mL). To a stirred solution were added magnesium ethoxide (0.10 *M* in methanol, 66.7 μL, 0.0067 mmol, 3.3 mol%) and potassium *tert*-butoxide (1.0 *M* in methanol, 20 μL, 0.020 mmol, 10 mol%) at room temperature, and the solution was stirred for 1 h. The volatiles were removed *in vacuo*, and then dichloroethane (1 mL) was added and removed *in vacuo* again. This solvent-removal sequence was repeated twice, and the magnesium/potassium salt of (*R*)-**1a** was obtained *in situ* as pale yellow solid. Then dichloroethane (20 mL), well-activated MS 3Å (50 mg), and 2,6-di-*tert*-butylpyridine (1.5 μL, 0.0067 mmol, 3.3 mol%) were added at room temperature, and the solution was stirred at room temperature for 30 min. Styrene **3a** (463 μL, 4.0 mmol) was then added to the solution at

0 °C, and the mixture was stirred at 0 °C for 30 min. Then aldimine **2a** (41.1 mg, 0.20 mmol) was added at 0 °C, and the mixture was stirred at 0 °C for 5 h. The resulting reaction mixture was quenched with triethylamine (0.2 mL) at 0 °C, and the organic phase was concentrated under reduced pressure. The resultant residue was analyzed by ^{1}H NMR measurement. As a result, no desired product was obtained and starting materials were fully recovered.

(3) Effect of the addition of methallyltrimethylsilane (10 mol%) on the catalytic reaction of a 3:1:3 complex of (*R*)-**1a**/Mg/K (3.3 mol%).

As shown in Eq. 10, the addition of methallyltrimethylsilane completely deactivated the catalytic activity of a 3:1:3 complex of (*R*)-**1a**/Mg/K. This result also might support the proton-catalysis.

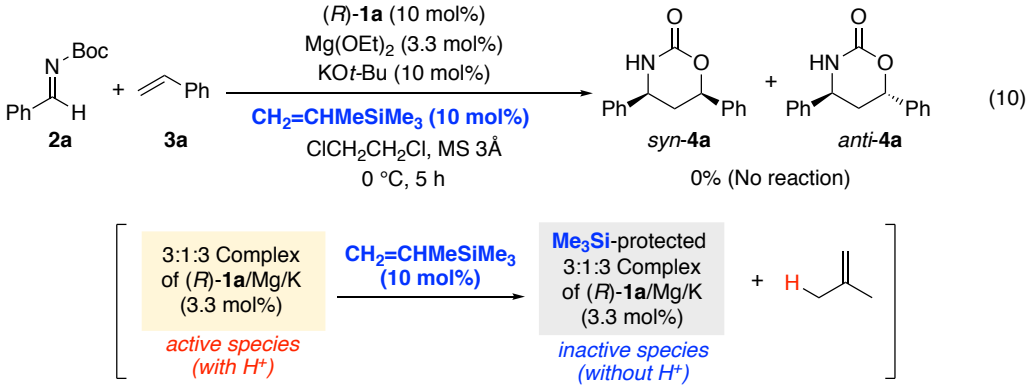

[Procedure of Eq. 10] (*R*)-**1a** (13.6 mg, 0.020 mmol, 10 mol%) was placed in a Schlenk test tube under a nitrogen atmosphere and dissolved in dry dichloroethane (2 mL). To a stirred solution were added magnesium ethoxide (0.10 *M* in methanol, 66.7 μL, 0.0067 mmol, 3.3 mol%) and potassium *tert*-butoxide (1.0 *M* in methanol, 20 μL, 0.020 mmol, 10 mol%) at room temperature, and the solution was stirred for 1 h. The volatiles were removed *in vacuo*, and then dichloroethane (1 mL) was added and removed *in vacuo* again. This solvent-removal sequence was repeated twice, and the magnesium/potassium salt of (*R*)-**1a** was obtained *in situ* as pale yellow solid. Then dichloroethane (20 mL), well-activated MS 3Å (50 mg), and methallyltrimethylsilane (3.6 μL, 0.020 mmol, 10 mol%) were added at room temperature, and the solution was stirred at room temperature for 30 min. Styrene **3a** (463 μL, 4.0 mmol) was then added to the solution at 0 °C, and the mixture was stirred at 0 °C for 30 min. Then aldimine **2a** (41.1 mg, 0.20 mmol) was added at 0 °C, and the mixture was stirred at 0 °C for 5 h. The resulting reaction mixture was quenched with triethylamine (0.2 mL) at 0 °C, and the organic phase was concentrated under reduced pressure. The resultant residue was analyzed by ^{1}H NMR measurement. As a result, no desired product was obtained and starting materials were fully recovered.

22. Control experiments with the use of achiral Brønsted acids and Lewis acids.

To confirm whether or not the proton in the SO_3H moiety would be the active center in the 3:1:3 complex of (*R*)-**1a**/Mg/K (i.e., to confirm whether Mg(II) and K(I) are unlikely to be active centers), we examined some achiral Brønsted acids as well as achiral Lewis acids (Table S8). As a result, the reaction did not proceed in the presence of weak Brønsted acids, such as CH_3SO_3H, *p*-TsOH, $(PhO)_2PO_2H$, CF_3CO_2H, and CH_3CO_2H (entries 2–6). On the other hand, stronger Brønsted acids, such as $HBF_4{\cdot}Et_2O$, TfOH, and Tf_2NH, promoted the reaction, and the yields were improved in the order $HBF_4{\cdot}Et_2O$ < TfOH < Tf_2NH (entries 7–9). Strong Lewis acids, such as $Mg(ClO_4)_2$ and $BF_3{\cdot}Et_2O$, which are conventionally used in *N*-Boc-cleavage reactions,[16] were also examined (entries 11 and 12). As a result, $BF_3{\cdot}Et_2O$ promoted the reaction moderately (32% yield), although the *syn/anti*-diastereoselectivity was low (67:32), whereas $Mg(ClO_4)_2$ did not

Table S8. Control experiments with achiral acid catalysts.[a]

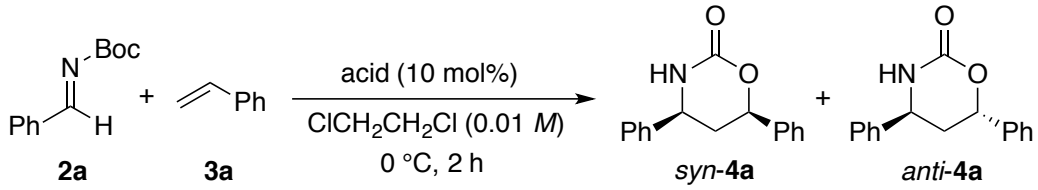

entry	acid	pK_a in H_2O[b]	pK_a in DMSO[c]	yield (%)	*syn*-**4a**:*anti*-**4a**
1	–	–	–	0	–
2	CH_3CO_2H	4.76	–	0	–
3	CF_3CO_2H	0.26	–	0	–
4	$(PhO)_2PO_2H$	0.26[d]	–	0	–
5	*p*-TsOH	–1.34	–	0	–
6	CH_3SO_3H	–2.0	–	0	–
7	$HBF_4{\cdot}Et_2O$	–4.9[e]	–10.3	30	75:25
8	TfOH	–13.0	–11.4	70	71:29
9	Tf_2NH	–	–11.9	84	80:20
11[f]	$Mg(ClO_4)_2$	–	–	0	–
12[f]	$BF_3{\cdot}Et_2O$	–	–	32	67:33
13	(*R*)-**1a**:Mg:K = 3:1:3 (3.3 mol%)	–	–	56	>99:<1

[a] The reaction was carried out with **2a** (0.20 mmol), **3a** (4 mmol) in dichloroethane at 0 °C for 2 h in the presence of 10 mol% of the catalyst. [b] Gryko, D.; Zimnicka, M.; Lipiński, R. *J. Org. Chem.* **2007**, *72*, 964. [c] Kütt, A.; Rodima, T.; Saame, J.; Raamat, E.; Mäemets, V.; Kaljurand, I.; Koppel, I. A.; Garlyauskayte, R. Y.; Yagupolskii, Y. L.; Yagupolskii, L. M.; Bernhardt, E.; Willner, H.; Leito, I. *J. Org. Chem.* **2011**, *76*, 391. [d] Krašovec, F.; Jan, J. *Croat. Chem. Acta* **1963**, *35*, 183. [e] Klähn, M.; Seduraman, A.; Wu, P. *J. Phys. Chem. B* **2011**, *115*, 8231. [f] MS 3Å was used.

promote the reaction. Overall these results strongly support the notion that strong Brønsted acids would facilitate the reaction more efficiently than Lewis acids. Moreover, the Brønsted acidity of our 3:1:3 complex of (*R*)-**1a**/Mg/K (entry 13) might be stronger than those of *p*-TsOH (entry 5) and CH_3SO_3H (entry 6), and weaker than those of TfOH (entry 8) and Tf_2NH (entry 9).

23. Control experiments with the use of chiral Brønsted acids

Moreover, other chiral Brønsted acid catalysts were examined (Table S9). As a result, highly regarded chiral phosphoric acid **S12** (TRIP)[17] did not promote the reaction due to the weak Brønsted acidity (entry 3). Even chiral phosphoric acid **S13**,[18] which would have stronger Brønsted acidity than **S12**, was not effective (entry 4). Moreover, chiral phosphoramides **S14** and **S15**,[19] as stronger Brønsted acid catalysts, promoted the reaction, although the yield, *syn/anti*-ratio, and enantioselectivity of **4a** were not good (entries 5–8). Highly Brønsted acidic chiral disulfonimide catalyst **S16**[20] also promoted the reaction, but the *syn/anti*-ratio and enantioselectivity of **4a** were decreased (entries 9 and 10). Finally, our previous methodology using (*R*)-BINSA ammonium salts was examined. As a result, **S17**[21] slightly promoted the reaction with low selectivities, whereas no reaction occurred when we used less acidic **S18**[22].

Table S9. Screening of other chiral catalysts.[a]

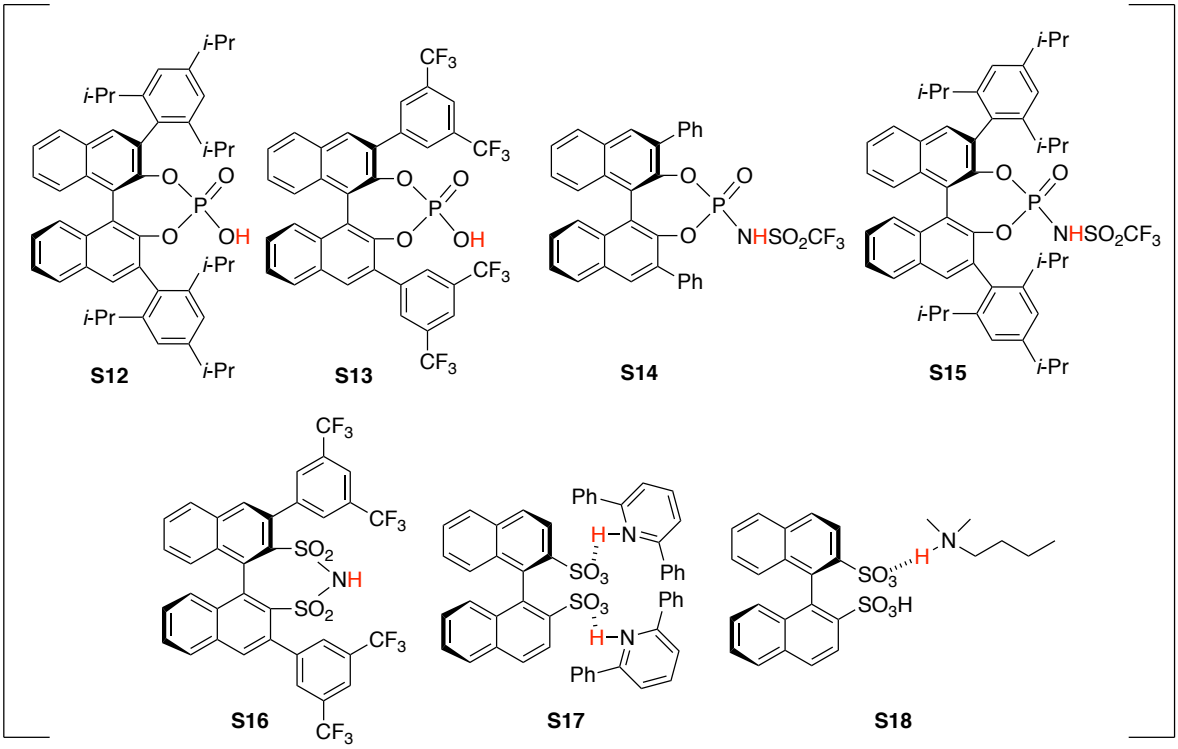

Table S9 (Continued).

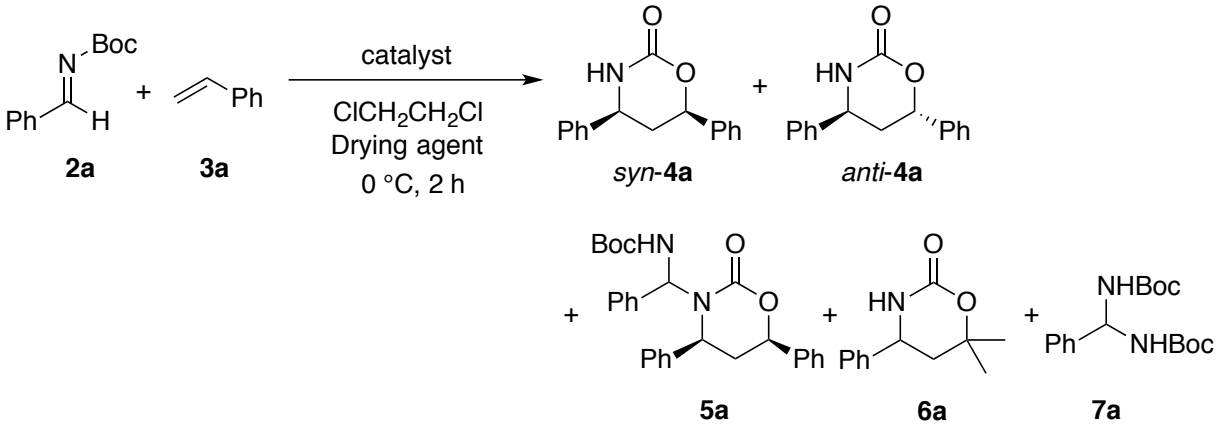

Entry	Catalyst	Drying agent	Yield (%) of **4a**/**5a**/**6a**/**7a** by ^{1}H NMR	Isolated yield (%) of *syn*-**4a**	*syn*-**4a**:*anti*-**4a**	ee (%) of *syn*-**4a**
1[b]	3:1:3 complex of (*R*)-**1a**/Mg/K	–	59/0/0/20	56	>99:<1	95
2[b]	3:1:3 complex of (*R*)-**1a**/Mg/K	MS 3Å	**92/4/0/0**	**91**	**>99:<1**	**96**
3	**S12**	–	0/0/0/47	0	–	–
4	**S13**	–	0/0/0/20	0	–	–
5	**S14**	–	57/0/22/22	55	84:16	–21
6	**S14**	MS 3Å	47/10/7/0	47	88:12	–24
7	**S15**	–	42/0/5/21	40	87:13	40
8	**S15**	MS 3Å	55/3/12/0	30	87:13	24
9	**S16**	–	31/6/0/18	31	74:26	19
10	**S16**	MS 3Å	43/9/5/0	42	78:22	18
11	**S17**	–	12/4/0/34	12	84:16	–17
12	**S17**	MS 3Å	26/8/3/0	25	87:13	–18
13	**S18**	–	0/0/0/0	0	–	–
14	**S18**	MS 3Å	0/0/0/0	0	–	–

[a] The reaction was carried out with **2a** (0.20 mmol), **3a** (4 mmol) in dichloroethane at 0 °C for 2 h in the presence of 10 mol% of the catalyst unless otherwise noted. [b] Reaction time was 5 h. (*R*)-**1** (10 mol%), KO*t*-Bu (10 mol%), and $Mg(OEt)_2$ (3.3 mol%) were used as a catalyst.

24. Re-investigation of our previous works.

To confirm whether or not chiral BINSA ammonium salt catalysts might dissolve the drying agents and take up the corresponding metal ions, we re-investigated our previous works (1) and (2), as shown following the conclusion.

> **Conclusion:** Our previous reactions with chiral BINSA ammonium salt catalysts might not be affected by $MgSO_4$. Chiral BINSA ammonium salts might be fairly neutralized, and would have much weaker Brønsted acidity than the original chiral BINSA alone. Therefore, chiral BINSA ammonium salts in the presence of $MgSO_4$ under mixing conditions may not easily dissolve $MgSO_4$. However, the Brønsted acidity of the corresponding chiral BINSA ammonium salts would strongly depend on the basicity of the selected amines. Therefore, we must be careful regarding catalyst preparation and/or the reaction conditions to avoid leaching Mg^{2+} when we use strong Brønsted acids. Equal attention should be paid to other drying agents, such as Na_2SO_4, molecular sieves, etc.

(1) Direct Mannich-type reaction of aldimine S1 and acetylacetone S19.[21]

The original data for the reaction of aldimine **S1** with acetylacetone **S19** are shown in Eq. S9. **S20** was obtained in 91% yield with 90% ee in the presence of chiral BINSA ammonium salt catalyst and $MgSO_4$ in dichloromethane at 0 °C.[21] When the reaction was conducted without $MgSO_4$, **S20** was obtained in 50% yield with 93% ee (Eq. S10). The yield was decreased since adventitious water decomposed **S1** at 0 °C. Next, we examined the reaction with the chiral BINSA Mg(II) salt, which was prepared in advance from (*R*)-BINSA, $Mg(OEt)_2$, and 2,6-Ph_2-pyridine, in the presence of $MgSO_4$ (Eq. S11). As a result, **S20** was obtained quantitatively but the enantioselectivity was only 37% ee. These results strongly suggest that $MgSO_4$ in this catalysis would not be dissolved and thus would not be involved in the complexation of the chiral BINSA ammonium salt catalyts.

[Reaction procedure] A well-dried pylex Schlenk tube was charged with (*R*)-1,1'-binaphthyl-2,2'-disulfonic acid (BINSA) (1.0 mg, 0.0025 mmol) and 2,6-diphenylpyridine (1.2 mg, 0.005 mmol) under nitrogen atmosphere. 2 mL of acetonitrile was added, and the solution was stirred at room temperature for 15 min. The volatile solvent was removed *in vacuo*, and then $MgSO_4$ (50 mg) and 1.5 mL of dichloromethane were added, and the suspension was stirred at room temperature for 30 min. The mixture was cooled to 0 °C, and aldomine **S1** (89.7 mg, 0.375 mmol) in dichloromethane (0.5 mL) was added *via* a cannula, and then acetylacetone **S19** (25.0 mg, 0.25 mmol) in dichloromethane (0.5 mL) was added over 1 h (A syringe pump is

useful if available.). After that, the resultant mixture was stirred at 0 °C for 30 min, by monitoring the TLC. 10 mL of saturated $NaHCO_3$ aqueous solution was poured into the reaction mixture, the product was extracted with ehyl acetate (15 mL × 2). The combined extracts were washed with brine (10 mL) and dried over Na_2SO_4. The organic phase was concentrated under reduced pressure and the crude product was purified by silica gel column chromatography (eluent: hexane/EtOAc = 3/1), to give the desired product **S20** (77.2 mg, 91% yield). The enantiomeric purity was determined by chiral HPLC (AD-H; hexane/EtOH = 9/1, 1.0 mL/min, tR = 47.3 min (minor, *S*), 52.3 min (major, *R*), 90% ee (*R*)).

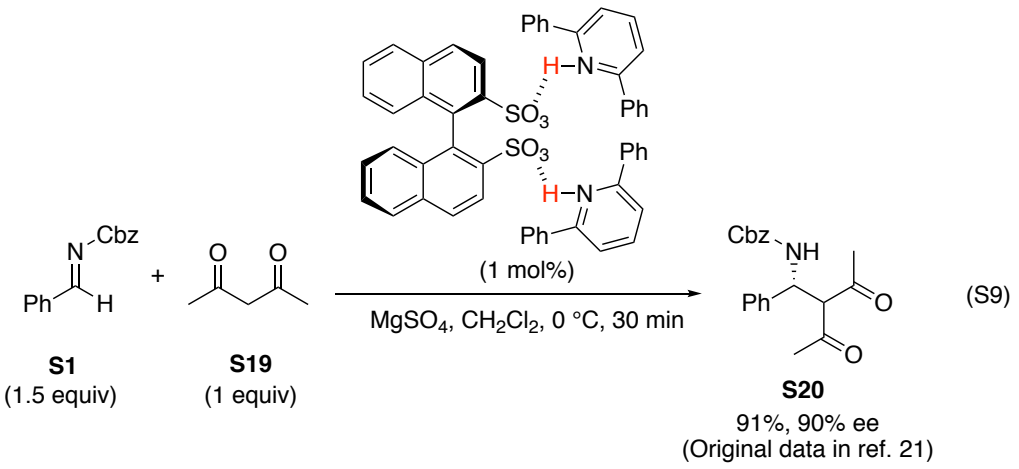

(2) Aza-Friedel–Crafts reaction of pyrrole S21 with aldimine S1.[21]

The original data for the reaction of pyrrole **S21** with aldimine **S1** are shown in Eq. S12. **S22** was obtained in 84% yield with 89% ee in the presence of chiral BINSA ammonium salt catalyst and $MgSO_4$ in dichloromethane at –78 °C.[22] When the reaction was conducted without $MgSO_4$, **S22** was obtained in 86% yield with 85% ee (Eq. S13). In this case, the yield was not decreased (*cf.* Eq. S10) despite the presence of adventitious water, since the reaction temperature was –78 °C. Next, we examined the reaction with the chiral BINSA Mg(II) salt, which was prepared in advance from (*R*)-BINSA, $Mg(OEt)_2$, and *N*,*N*-Me_2NBu in the presence of $MgSO_4$ (Eq. S14). As a result, **S22** was scarcely obtained (5% yield) and the enantioselectivity was only 1% ee. These results

strongly suggest that $MgSO_4$ in this catalysis also would not affect the complexation of the chiral BINSA ammonium salt catalyst.

[Reaction procedure] A well-dried pyrex Schlenk tube was charged with (*R*)-BINSA (4.1 mg, 0.01 mmol) and *N*,*N*-dimethylbutylamine (1.4 μL, 0.01 mmol) under a nitrogen atmosphere. 2 mL of acetonitrile was added, and the solution was stirred at room temperature for 30 min. The volatile solvent was removed *in vacuo* at room temperature for 1 h, and then $MgSO_4$ (40 mg), 1.5 mL of dichloromethane, and *n*-benzylpyrrole **S21** (30.8 μL 0.20 mmol) were added. The mixture was cooled to –78 °C and stirred for 30 min. Aldimine **S1** (71.8 mg, 0.30 mmol) in dichloromethane (0.5 mL) was added *via* a cannula. The resultant mixture was then stirred at –78 °C for 30 min. 1 mL of saturated $NaHCO_3$ aqueous solution was poured into the reaction mixture, and the product was extracted with ethyl acetate (15 mL × 2). The combined extracts were washed with brine (10 mL) and dried over $MgSO_4$. The organic phase was concentrated under reduced pressure and the crude product was purified by silica gel column chromatography (eluent: *n*-hexane/AcOEt = 3/1 to 1/1) to give the desired product **S22** (66.7 mg, 84% yield). The enantiomeric purity was determined by chiral HPLC (AD-H, *n*-hexane/*i*-PrOH = 9/1, 1.0 mL/min, t_R = 22.9 min (minor, *R*), 26.1 min (major, *S*), 89% ee (*S*)).

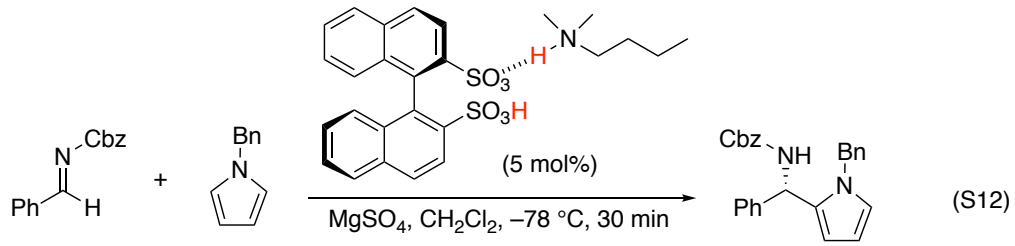

S1 (1.5 equiv) **S21** (1 equiv) **S22** 84%, 89% ee (Original data in ref. 22) (S12)

S1 (1.5 equiv) + **S21** (1 equiv) (*R*)-BINSA (5 mol%), *N*,*N*-Me_2NBu (5 mol%), CH_2Cl_2, –78 °C, 30 min, **(Without $MgSO_4$)** → **S22** **86%, 85% ee** (S13)

S1 (1.5 equiv) + **S21** (1 equiv) (*R*)-BINSA (5 mol%), **$Mg(OEt)_2$ (5 mol%)**, *N*,*N*-Me_2NBu (5 mol%), **$MgSO_4$**, CH_2Cl_2, –78 °C, 30 min → **S22** **5%, 1% ee** (S14)

26. Additional mechanistic consideration.

For another possible mechanism, formation of **S23**[5] cannot be completely ruled out as shown Eq. S15, although unstable **S23** might readily decompose to **S24** by releasing CO_2.

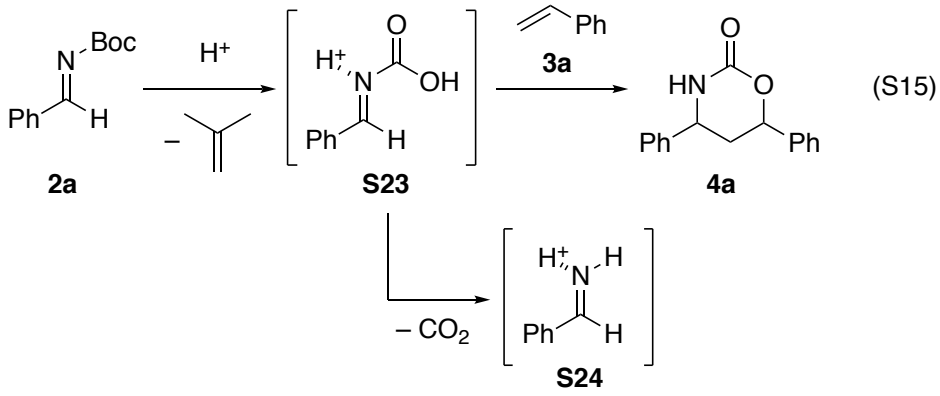

(S15)

Therefore, we additionally examined another substrate with β-H on the *N*-CO_2 moiety (Eq. S16). As a result, *N*-CO_2Et-aldimine, which might be let to **S23**, was not effective under our standard conditions, and **4a** was not obtained since a reaction gave a complex mixture. This result might strongly suggest that nucleophilicity of *N*-protected intermediate **S25** in the concertet pathway should be important, although steric factor of *N*-CO_2R might also affected the results. In anyway, at this preliminaly stage, we cannot conclude the mechamism, and further investigation should be necessary.

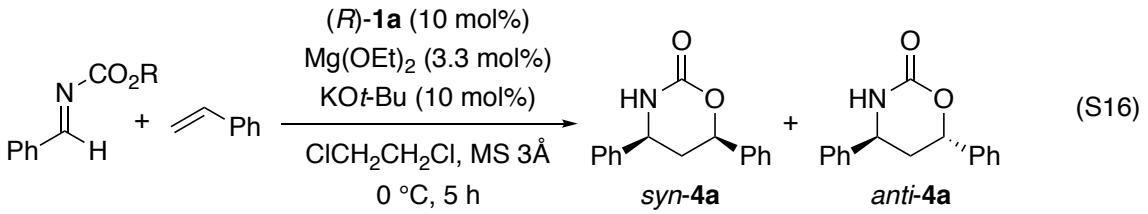

(S16)

R = *t*-Bu: 91%, *syn*:*anti* = >99:<1, 96% ee (*syn*)
R = Et: 0% (Complex mixture)

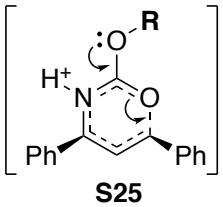

27. References.

(1) Hatano, M.; Ozaki, T.; Nishikawa, K.; Ishihara, K. *J. Org. Chem.* **2013**, *78*, 10405.

(2) Wenzel, A. G.; Jacobsen, E. N. *J. Am. Chem. Soc.* **2002**, *124*, 12964.

(3) Richter, H.; Fröhlich, R.; Daniliuc, C.-G.; Mancheño. O. G. *Angew. Chem. Int. Ed.* **2012**, *51*, 8656.

(4) Kochi, T.; Tang, T. P.; Ellman, J. A. *J. Am. Chem. Soc.* **2002**, *124*, 6518.

(5) Uddin, N.; Ulicki, J. S.; Foersterling, F. H.; Hossain, M. M. *Tetrahedron Lett.* **2011**, *52*, 4353.

(6) Davies, S. G.; Garner, A. C.; Roberts, P. M.; Smith, A. D.; Sweet, M. J.; Thomson, J. E. *Org. Biomol. Chem.* **2006**, *4*, 2753.

(7) Kano, T.; Yurino, T.; Asakawa, D.; Maruoka, K. *Angew. Chem. Int. Ed.* **2013**, *52*, 5532.

(8) Momiyama, N.; Okamoto, H.; Kikuchi, J.; Korenaga, T.; Terada, M. *ACS Catal.* **2016**, *6*, 1198.

(9) Narasaka, K.; Ukaji, Y.; Yamazaki, S. *Bull. Chem. Soc. Jpn.* **1986**, *59*, 525.

(10) Lanter, J. C.; Chen, H.; Zhang, X.; Sui, Z. *Org. Lett.* **2005**, *7*, 5905.

(11) Tokizane, M.; Sato, K.; Ohta, T.; Ito, Y. *Tetrahedron: Asymmetry* **2008**, *19*, 2519.

(12) (a) Sugimura, T.; Hagiya, K. *Chem. Lett.* **2007**, *36*, 566. (b) Hagiya, K.; Muramoto, N.; Misaki, T.; Sugimura, T. *Tetrahedron* **2009**, *65*, 6109.

(13) Konishi, H.; Nagase, H.; Manabe, K. *Chem. Commun.* **2015**, *51*, 1854.

(14) (a) Müller, A.; Polborn, K.; Wanner, K. T. *J. Heterocyclic Chem.* **2007**, *44*, 575. (b) Müller, A.; Höfner, G.; Renukappa-Gutke, T.; Parsons, C. G.; Wanner, K. T. *Bioorg. Med. Chem. Lett.* **2011**, *21*, 5795.

(15) Mashiko, T.; Kumagai, N.; Shibasaki, M. *J. Am. Chem. Soc.* **2009**, *131*, 14990.

(16) Wuts, P. G. M. *Greene's Protective Groups in Organic Synthesis (Fifth Edition), John Wiley & Sons*, **2014**.

(17) Martin, N. J. A.; List, B. *J. Am. Chem. Soc.* **2006**, *128*, 13368.

(18) Akiyama, T.; Morita, H.; Itoh, J.; Fuchibe, K. *Org. Lett.* **2005**, *7*, 2583.

(19) Nakashima, D.; Yamamoto, H. *J. Am. Chem. Soc.* **2006**, *128*, 9626.

(20) García-García, P.; Lay, F.; García-García, P.; Rabalakos, C.; List, B. *Angew. Chem. Int. Ed.* **2009**, *48*, 4363.

(21) Hatano, M.; Maki, T.; Moriyama, K.; Arinobe, M.; Ishihara, K. *J. Am. Chem. Soc.* **2008**, *130*, 16858.

(22) Hatano, M.; Sugiura, Y.; Akakura, M.; Ishihara, K. *Synlett* **2011**, *2011*, 1247.

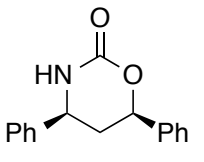

(*syn*-**4a**)

IA-3,
n-hexane/*i*-PrOH = 7/3,
1.0 mL/min, 210 nm

Racemic *syn*-**4a**

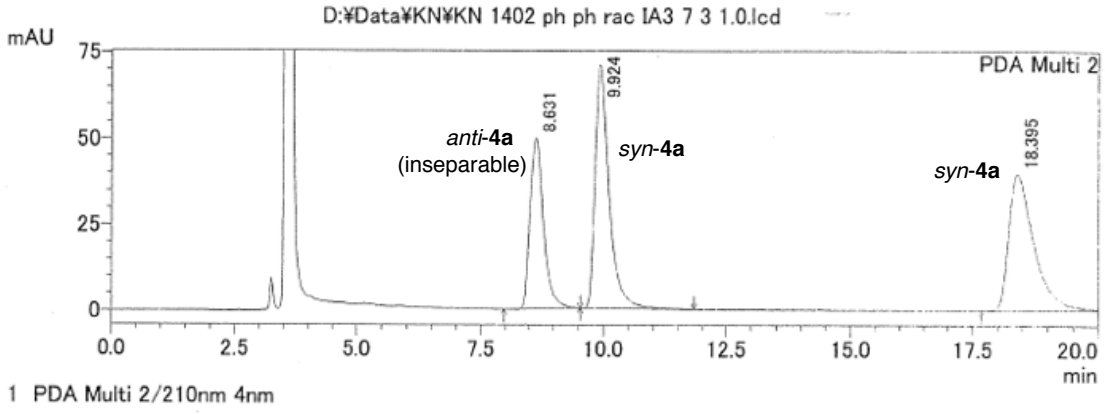

syn-**4a** by the catalysis

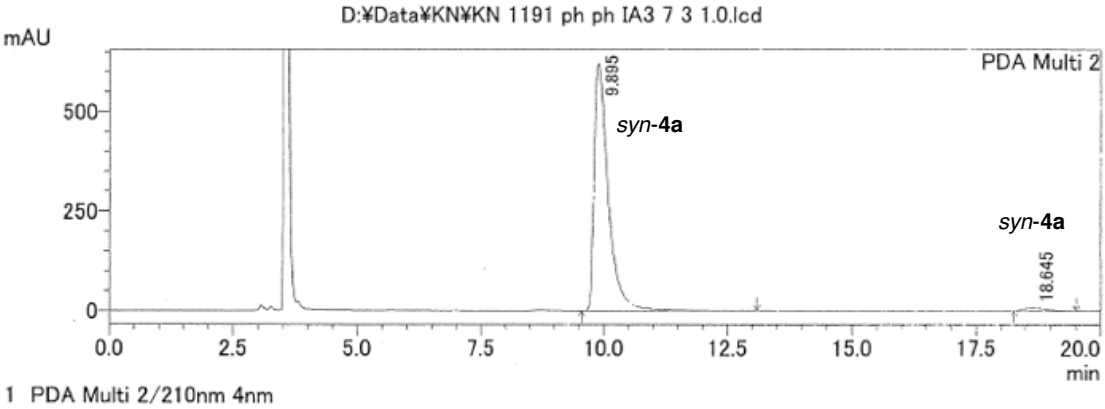

Peak Table

PDA Ch2 210nm 4nm

Peak No	RT (min)	Area	Height (mV)	% Area
1	9.895	12448185	621978	98.116
2	18.645	238998	7569	1.884
Total		12687183	629547	100.000

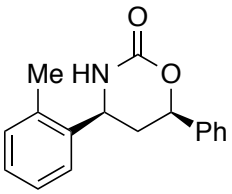

(*syn*-**4b**)

IA-3,
n-hexane/*i*-PrOH = 7/3,
1.0 mL/min, 254 nm

Racemic *syn*-**4b**

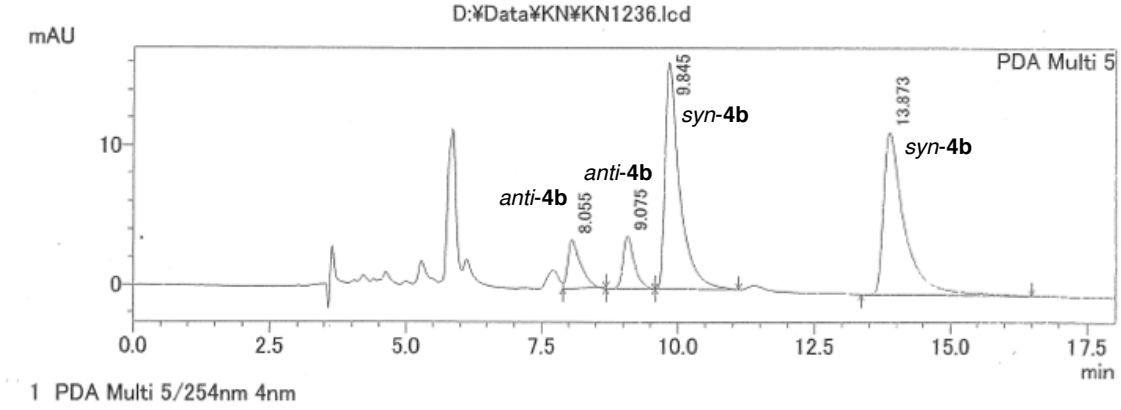

syn-**4b** by the catalysis

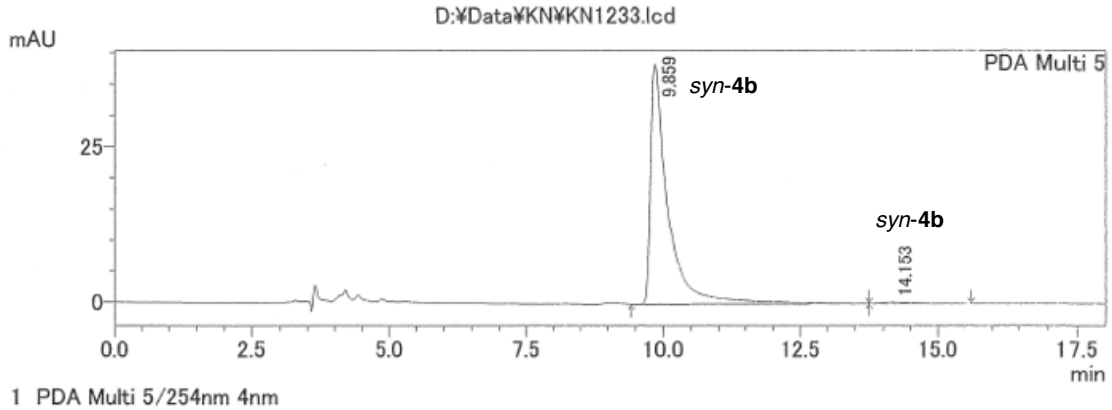

Peak Table

PDA Ch5 254nm 4nm

Peak No	RT (min)	Area	Height (mV)	% Area
1	9.859	821348	38470	99.128
2	14.153	7225	221	0.872
Total		828573	38692	100.000

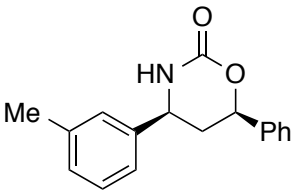

(*syn*-**4c**)

IA-3,
n-hexane/*i*-PrOH = 7/3,
1.0 mL/min, 210 nm

Racemic *syn*-**4c**

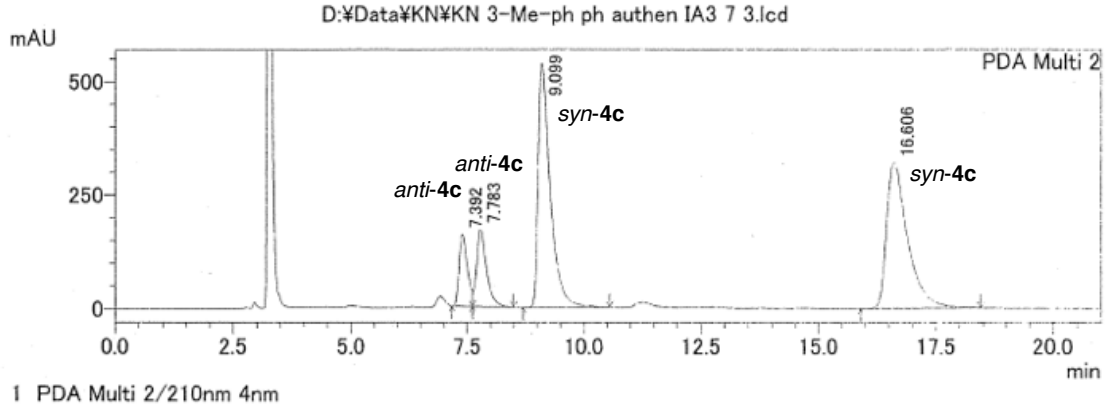

syn-**4c** by the catalysis

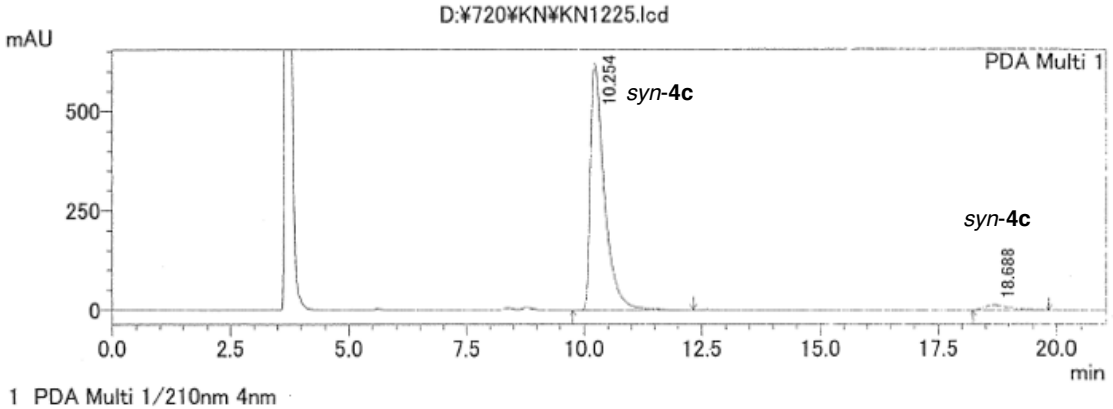

Peak Table

SPD-M20A Ch1 210nm 4nm

Peak No.	RT (min)	Area	Height (mV)	% Area
1	10.254	12953716	484657	96.925
2	18.688	410897	11909	3.075
Total		13364613	496567	100.000

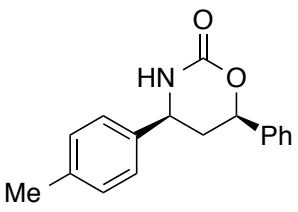

(*syn*-**4d**)

IA-3,
n-hexane/*i*-PrOH = 7/3,
1.0 mL/min, 210 nm

Racemic *syn*-**4d**

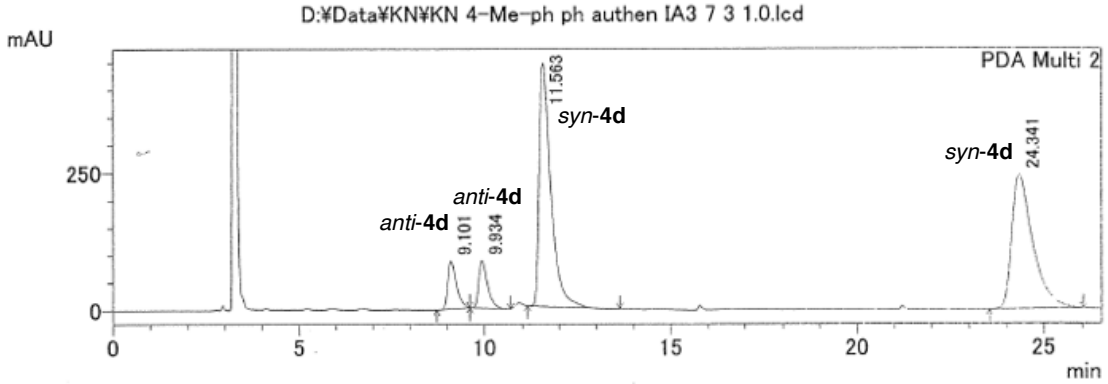

syn-**4d** by the catalysis

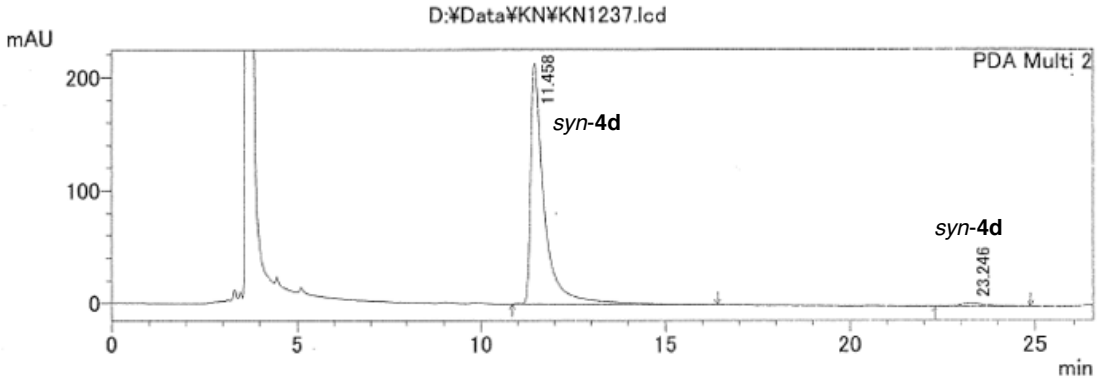

Peak Table

PDA Ch2 210nm 4nm

Peak No	RT (min)	Area	Height (mV)	% Area
1	11.458	5516904	213734	97.833
2	23.246	122181	3016	2.167
Total		5639084	216751	100.000

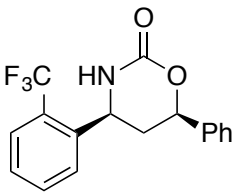

(*syn*-**4e**)

IA-3,
n-hexane/*i*-PrOH = 7/3,
1.0 mL/min, 254 nm

Racemic *syn*-**4e**

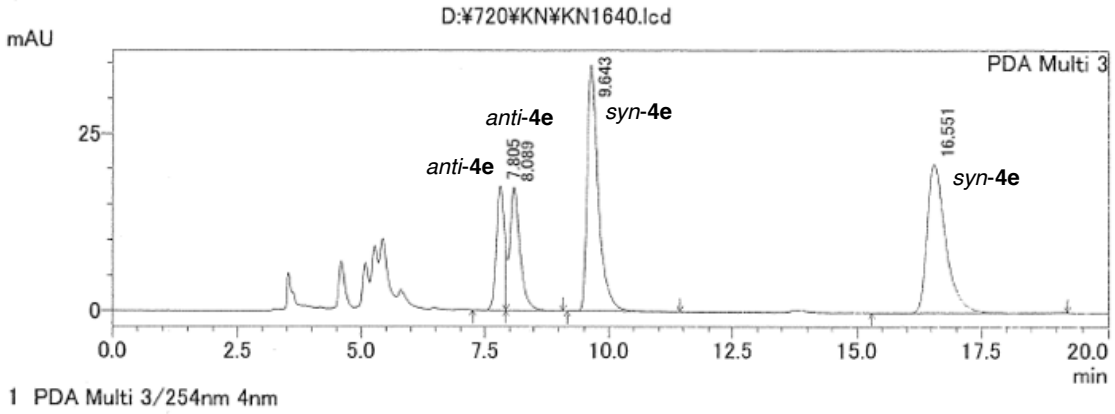

syn-**4e** by the catalysis

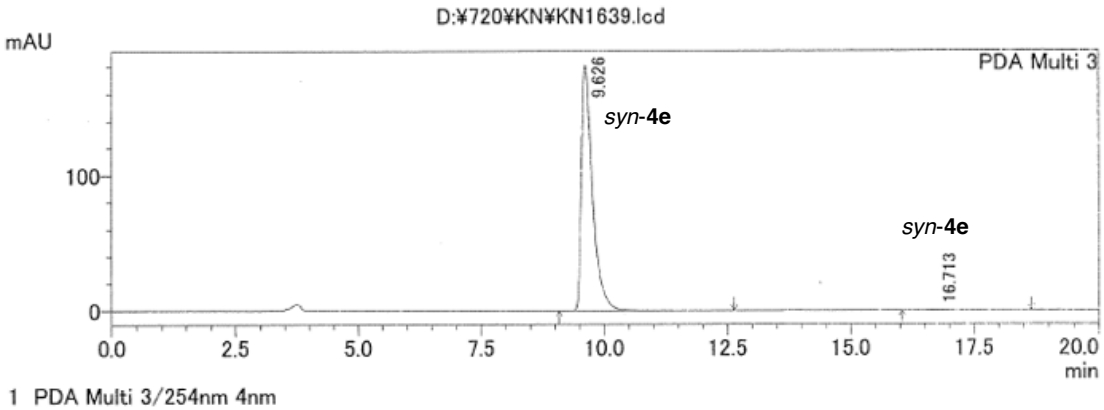

Peak Table

SPD-M20A Ch3 254nm 4nm

Peak No.	RT (min)	Area	Height (mV)	% Area
1	9.626	2871414	181193	99.589
2	16.713	11855	423	0.411
Total		2883269	181616	100.000

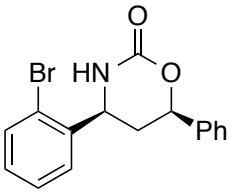

(*syn*-**4f**)

IA-3,
n-hexane/*i*-PrOH = 7/3,
1.0 mL/min, 210 nm

Racemic *syn*-**4f**

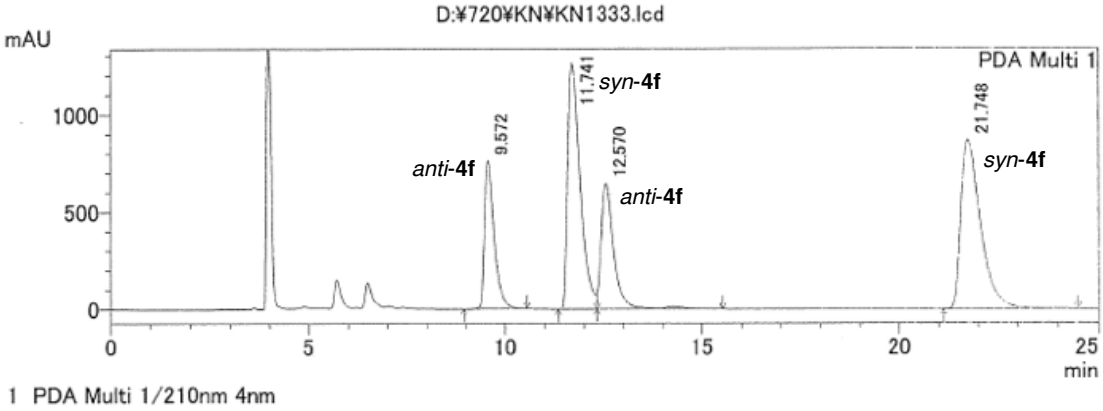

syn-**4f** by the catalysis

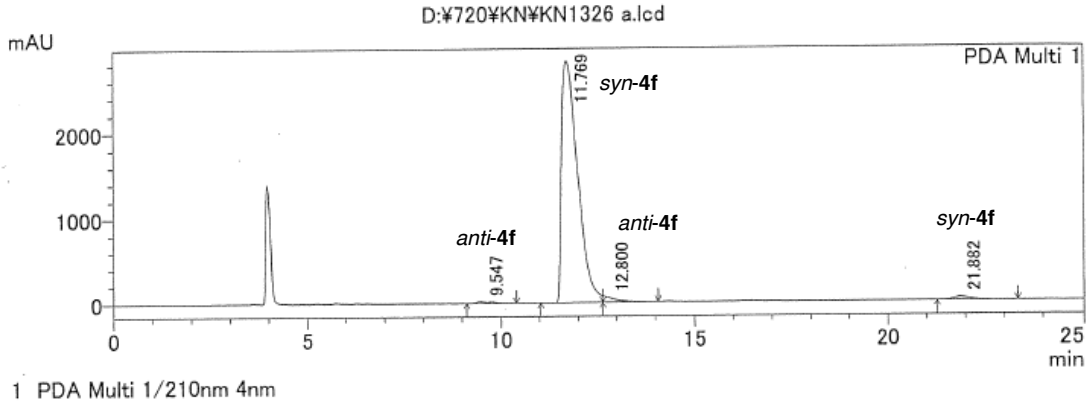

Peak Table

SPD-M20A Ch1 210nm 4nm

Peak No.	RT (min)	Area	Height (mV)	% Area
1	9.547	690588	22044	0.819
2	11.769	80852396	2735193	95.878
3	12.800	1589657	65157	1.885
4	21.882	1195746	34411	1.418
Total		84328386	2856805	100.000

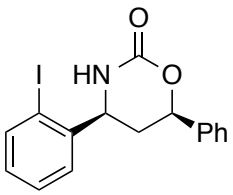

(*syn*-**4g**)

IA-3,
n-hexane/*i*-PrOH = 7/3,
1.0 mL/min, 254 nm

Racemic *syn*-**4g**

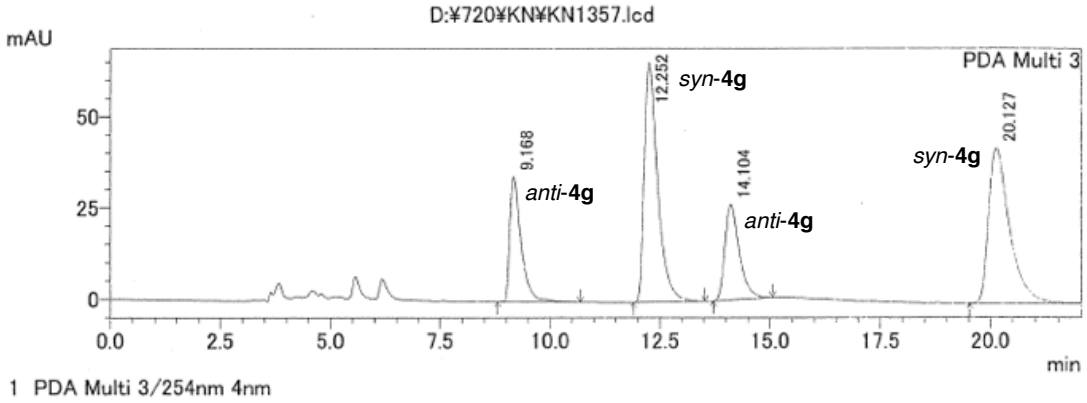

syn-**4g** by the catalysis

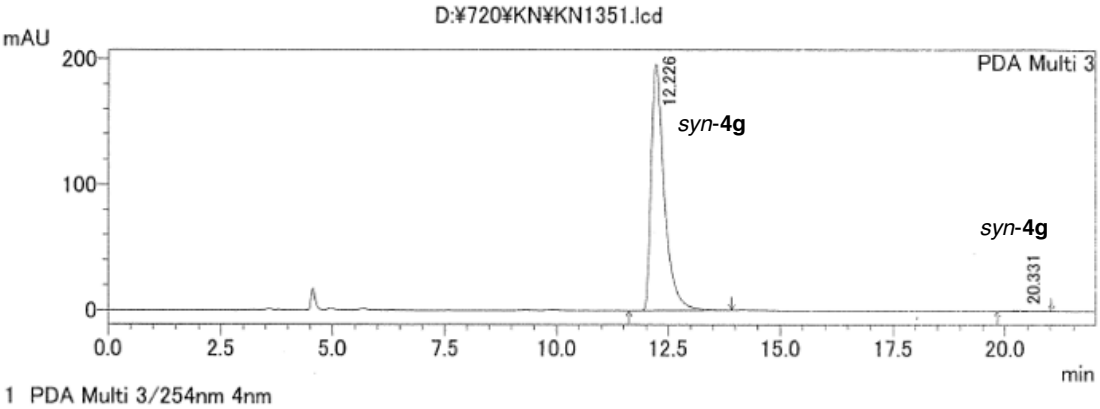

Peak Table

SPD-M20A Ch3 254nm 4nm

Peak No.	RT (min)	Area	Height (mV)	% Area
1	12.226	4090115	195947	99.471
2	20.331	21761	707	0.529
Total		4111876	196654	100.000

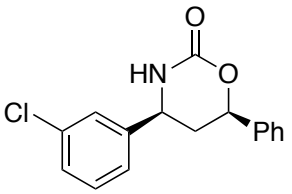

(*syn*-**4h**)

OD-3,
n-hexane/*i*-PrOH = 7/3,
1.0 mL/min, 254 nm

Racemic *syn*-**4h**

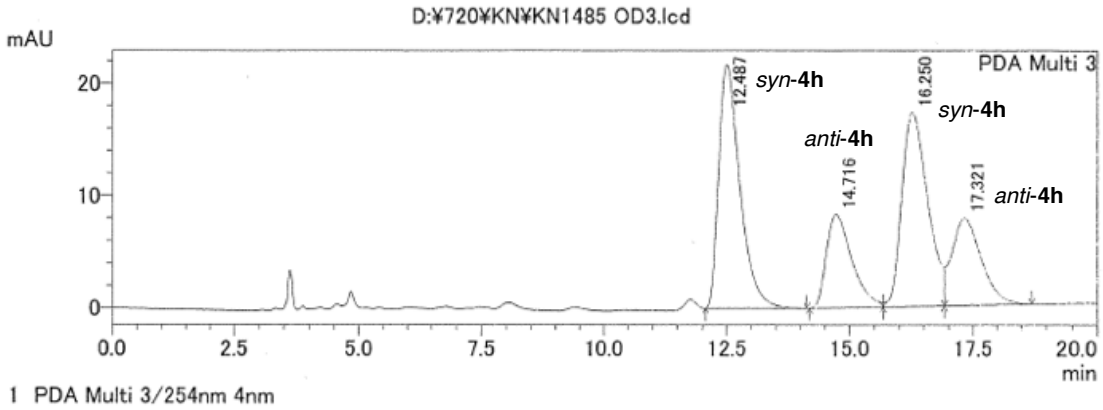

syn-**4h** by the catalysis

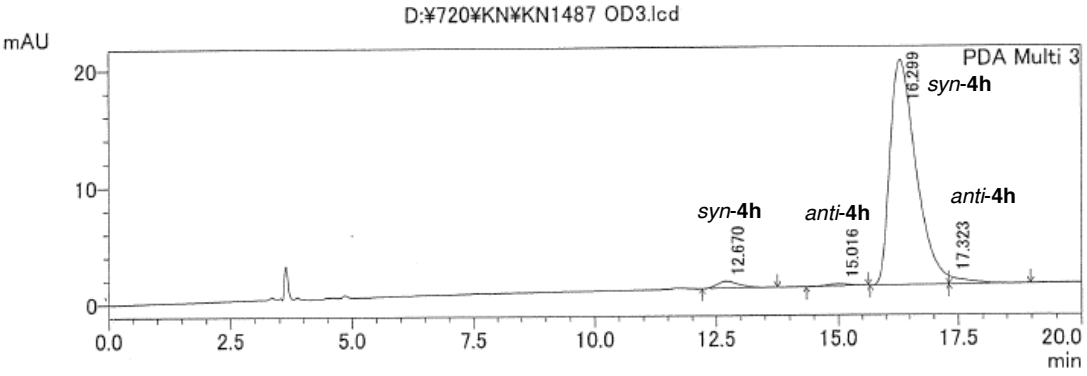

Peak Table

SPD-M20A Ch3 254nm 4nm

Peak No.	RT (min)	Area	Height (mV)	% Area
1	12.670	19169	600	2.491
2	15.016	5852	181	0.760
3	16.299	727379	19183	94.526
4	17.323	17101	676	2.222
Total		769500	20640	100.000

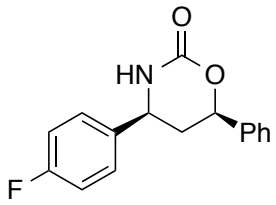

(*syn*-**4i**)

IA-3,
n-hexane/*i*-PrOH = 7/3,
1.0 mL/min, 210 nm

Racemic *syn*-**4i**

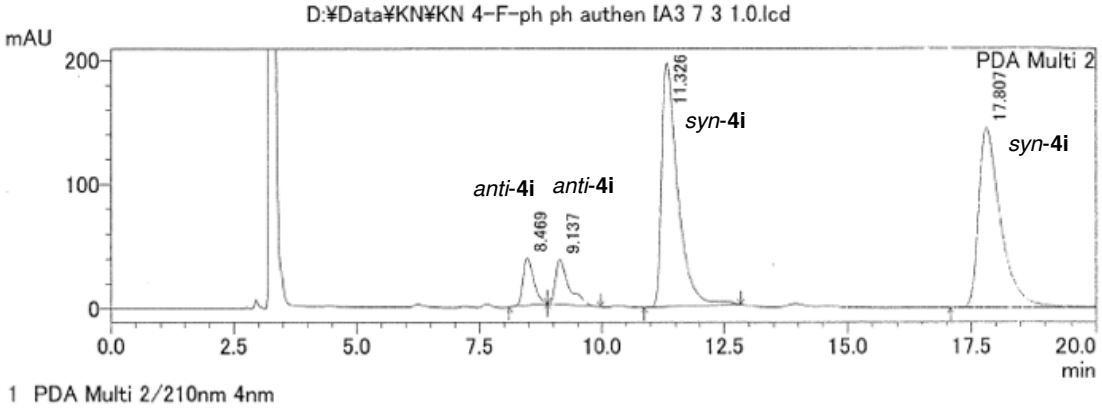

syn-**4i** by the catalysis

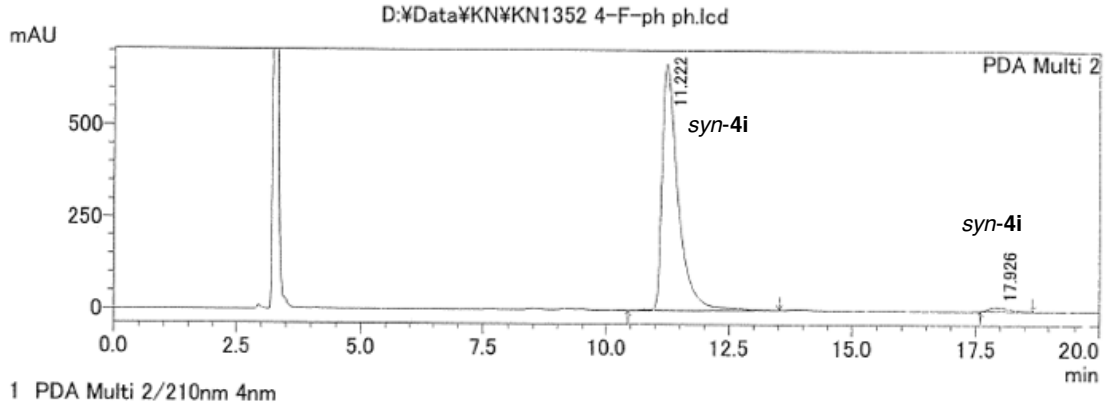

Peak Table

PDA Ch2 210nm 4nm

Peak No	RT (min)	Area	Height (mV)	% Area
1	11.222	15325621	667068	97.977
2	17.926	316390	11367	2.023
Total		15642011	678435	100.000

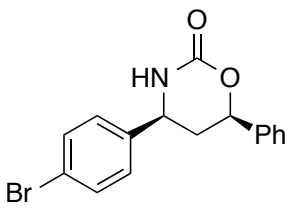

(*syn*-**4j**)

IA-3,
n-hexane/*i*-PrOH = 7/3,
1.0 mL/min, 210 nm

Racemic *syn*-**4j**

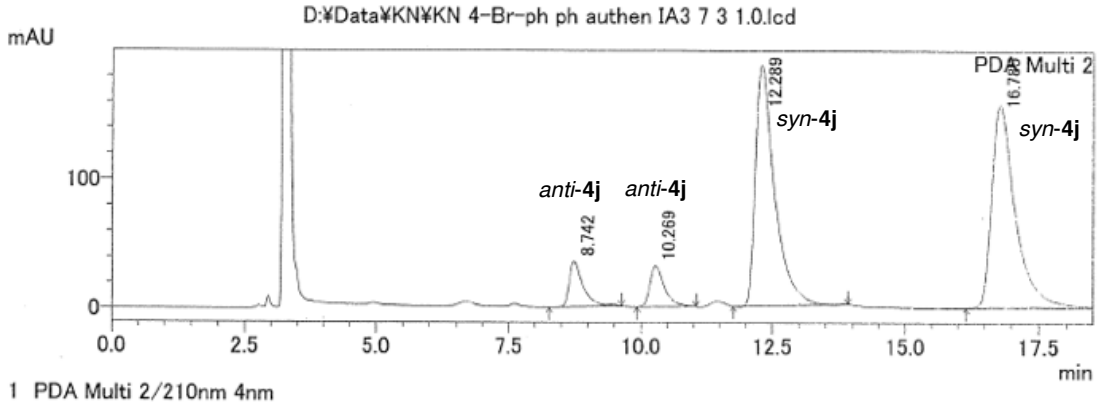

syn-**4j** by the catalysis

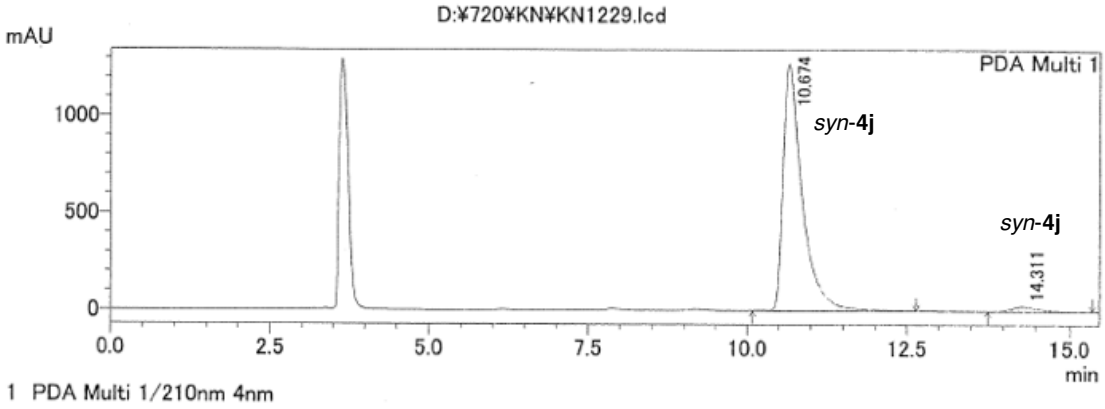

Peak Table

SPD-M20A Ch1 210nm 4nm

Peak No.	RT (min)	Area	Height (mV)	% Area
1	10.674	26252799	1146607	97.573
2	14.311	653106	23464	2.427
Total		26905905	1170070	100.000

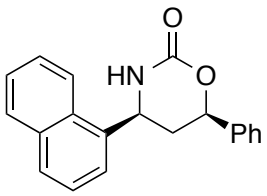

(*syn*-**4k**)

IA-3,
n-hexane/*i*-PrOH = 7/3,
1.0 mL/min, 280 nm

Racemic *syn*-**4k**

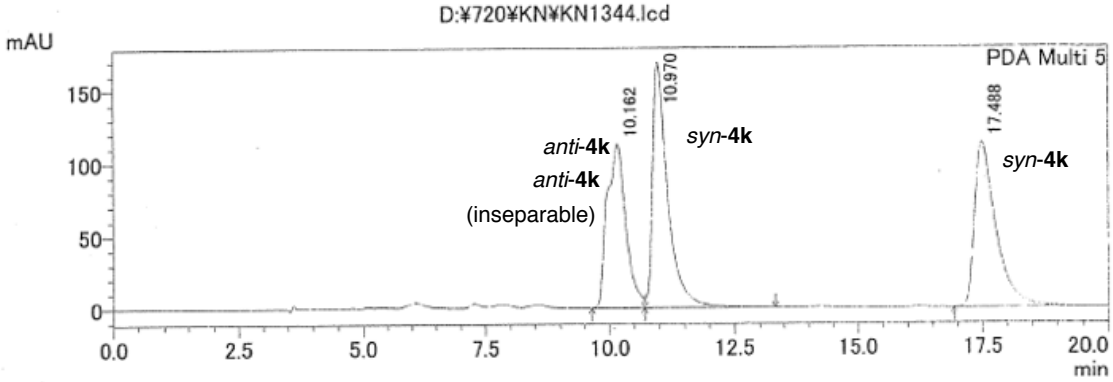

1 PDA Multi 5/280nm 4nm

syn-**4k** by the catalysis

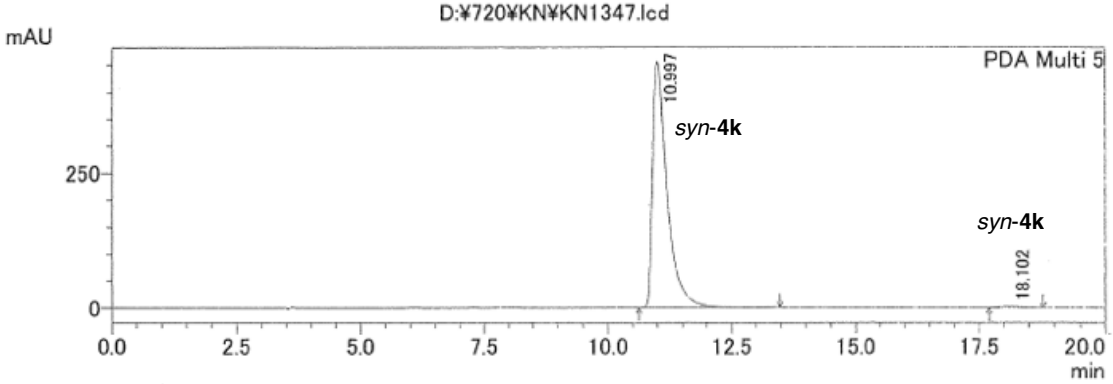

1 PDA Multi 5/280nm 4nm

Peak Table

SPD-M20A Ch5 280nm 4nm

Peak No.	RT (min)	Area	Height (mV)	% Area
1	10.997	9262626	456599	99.012
2	18.102	92464	3124	0.988
Total		9355089	459723	100.000

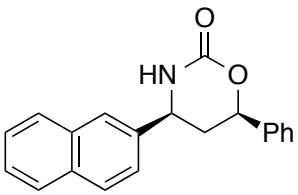

(*syn*-**4l**)

IA-3,
n-hexane/*i*-PrOH = 7/3,
1.0 mL/min, 254 nm

Racemic *syn*-**4l**

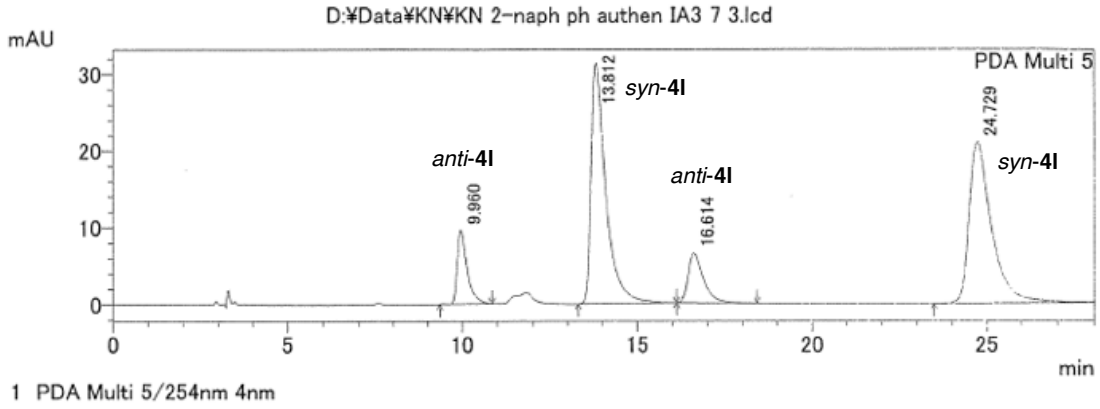

syn-**4l** by the catalysis

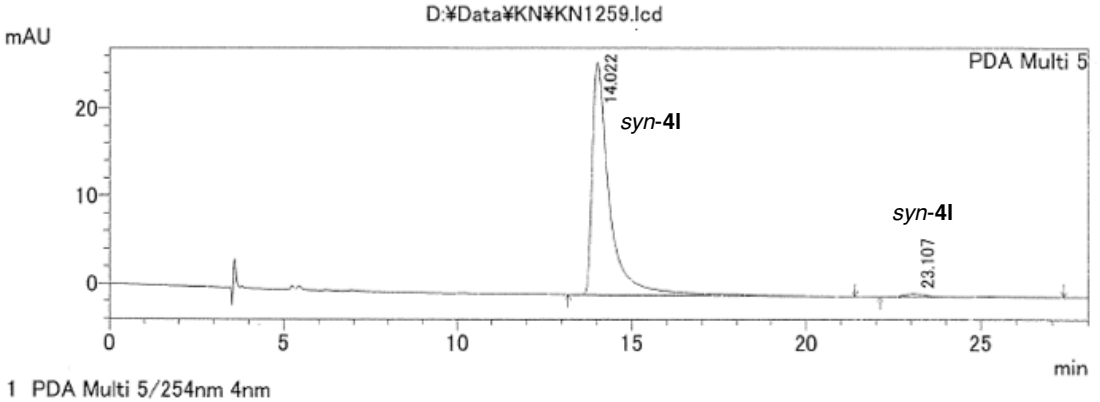

Peak Table

PDA Ch5 254nm 4nm

Peak No	RT (min)	Area	Height (mV)	% Area
1	14.022	925460	26587	98.319
2	23.107	15822	353	1.681
Total		941282	26940	100.000

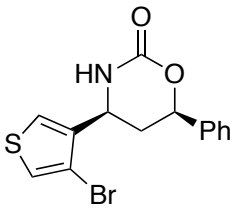

(*syn*-**4m**)

IA-3,
n-hexane/*i*-PrOH = 7/3,
1.0 mL/min, 210 nm

Racemic *syn*-**4m**

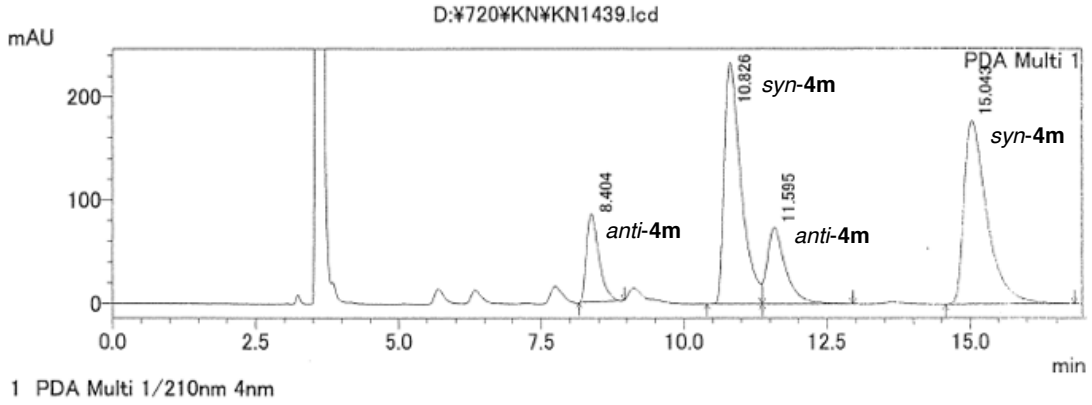

syn-**4m** by the catalysis

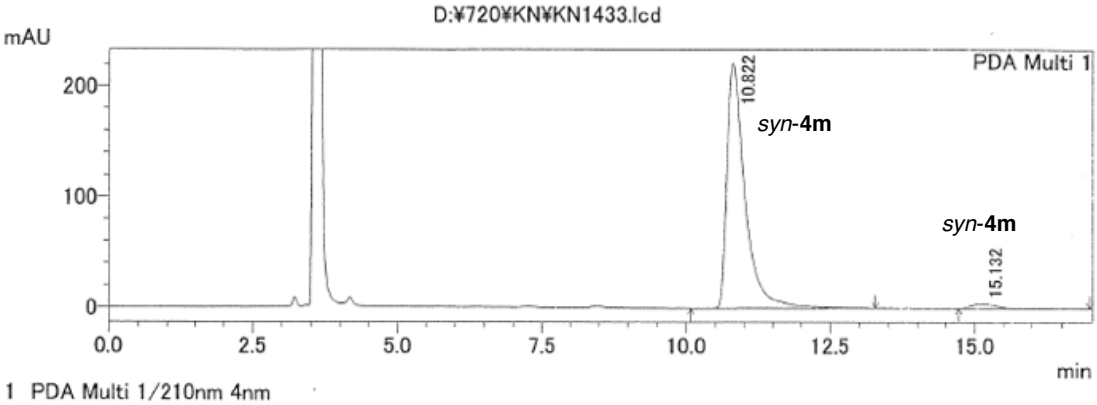

Peak Table

SPD-M20A Ch1 210nm 4nm

Peak No.	RT (min)	Area	Height (mV)	% Area
1	10.822	4789950	206488	97.416
2	15.132	127055	4175	2.584
Total		4917004	210663	100.000

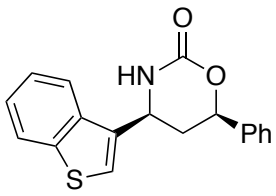

(*syn*-**4n**)

AD-3,
n-hexane/*i*-PrOH = 7/3,
1.0 mL/min, 210 nm

Racemic *syn*-**4n**

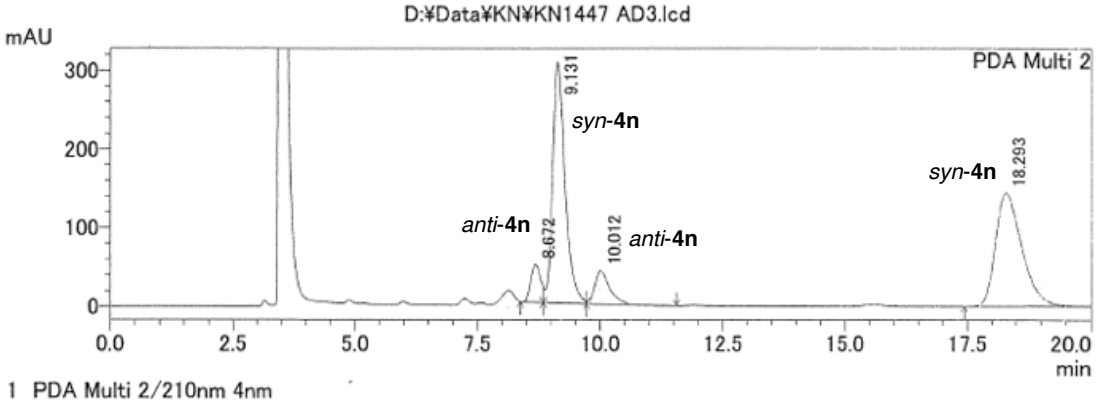

syn-**4n** by the catalysis

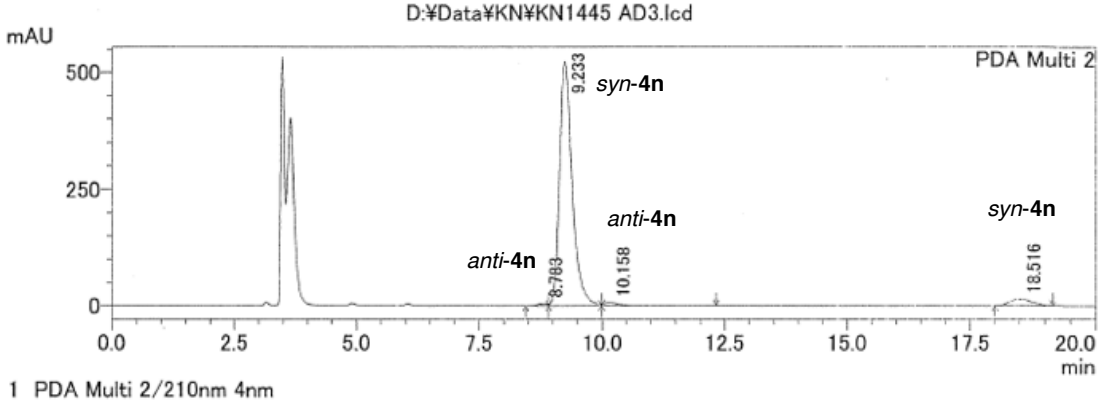

Peak Table

PDA Ch2 210nm 4nm

Peak No	RT (min)	Area	Height (mV)	% Area
1	8.783	60416	4465	0.613
2	9.233	9194264	524142	93.360
3	10.158	172724	6099	1.754
4	18.516	420801	13323	4.273
Total		9848205	548030	100.000

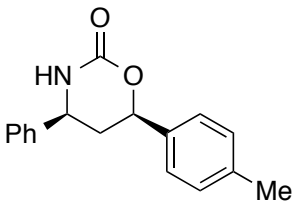

(*syn*-**8a**)

IA-3,
n-hexane/*i*-PrOH = 7/3,
1.0 mL/min, 210 nm

Racemic *syn*-**8a**

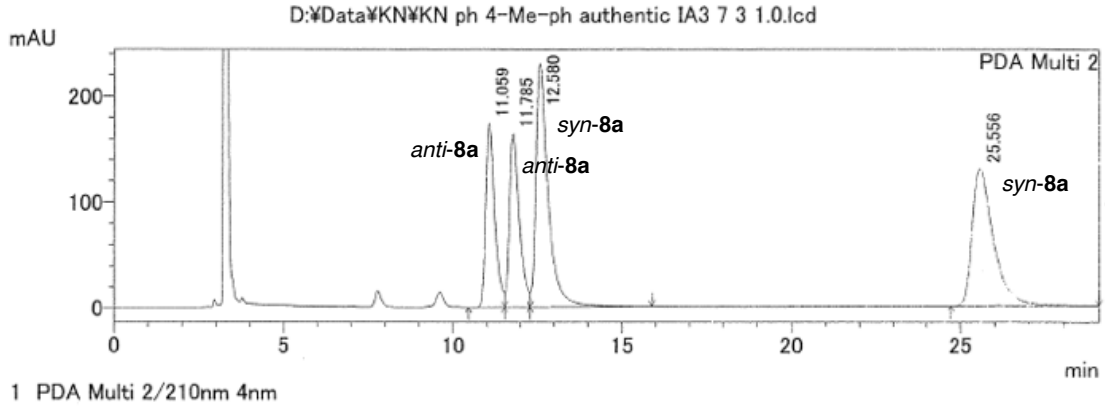

syn-**8a** by the catalysis

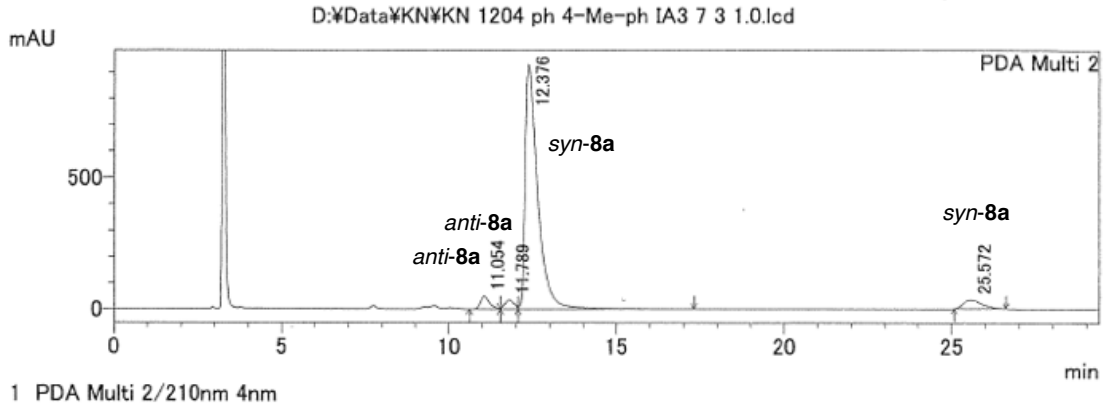

Peak Table

PDA Ch2 210nm 4nm

Peak No	RT (min)	Area	Height (mV)	% Area
1	11.054	920988	49110	3.443
2	11.789	668226	35609	2.498
3	12.376	23835475	931721	89.105
4	25.572	1325254	33846	4.954
Total		26749943	1050286	100.000

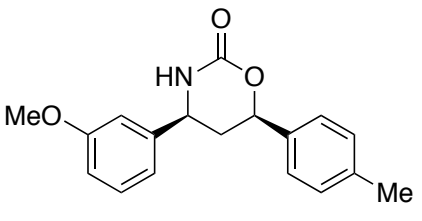

(*syn*-**8b**)

IA-3,

n-hexane/*i*-PrOH = 7/3,

1.0 mL/min, 210 nm

Racemic *syn*-**8b**

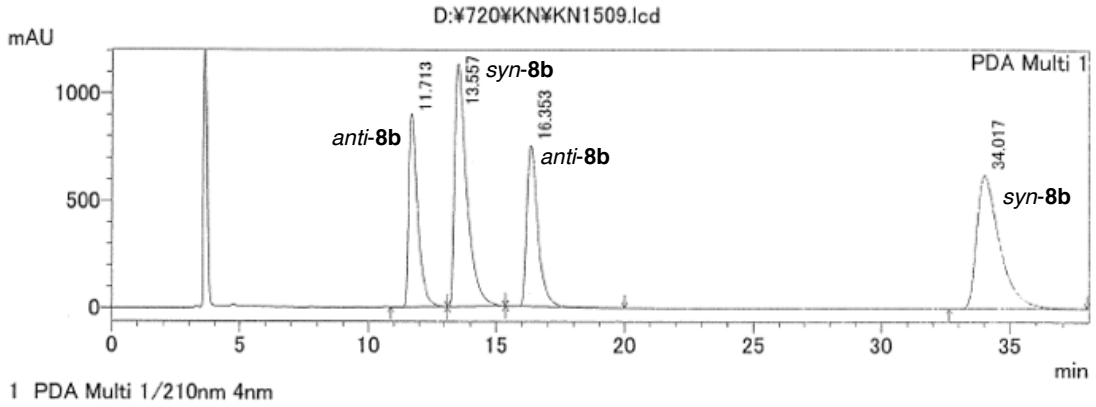

syn-**8b** by the catalysis

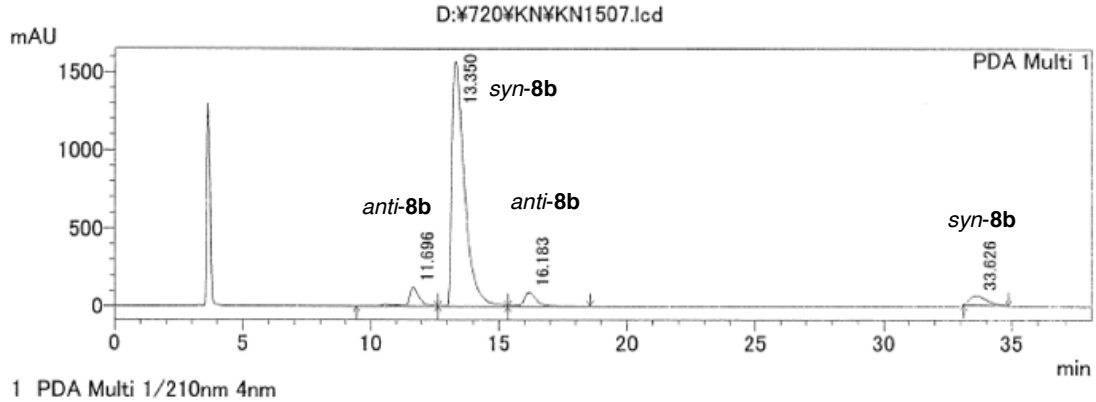

Peak Table

SPD-M20A Ch1 210nm 4nm

Peak No.	RT (min)	Area	Height (mV)	% Area
1	11.696	3522958	105957	5.651
2	13.350	52805847	1491468	84.701
3	16.183	2994248	82382	4.803
4	33.626	3020512	59274	4.845
Total		62343564	1739082	100.000

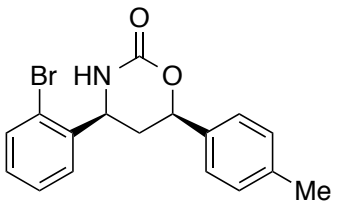

(*syn*-**8c**)

IA-3,

n-hexane/*i*-PrOH = 7/3,

1.0 mL/min, 210 nm

Racemic *syn*-**8c**

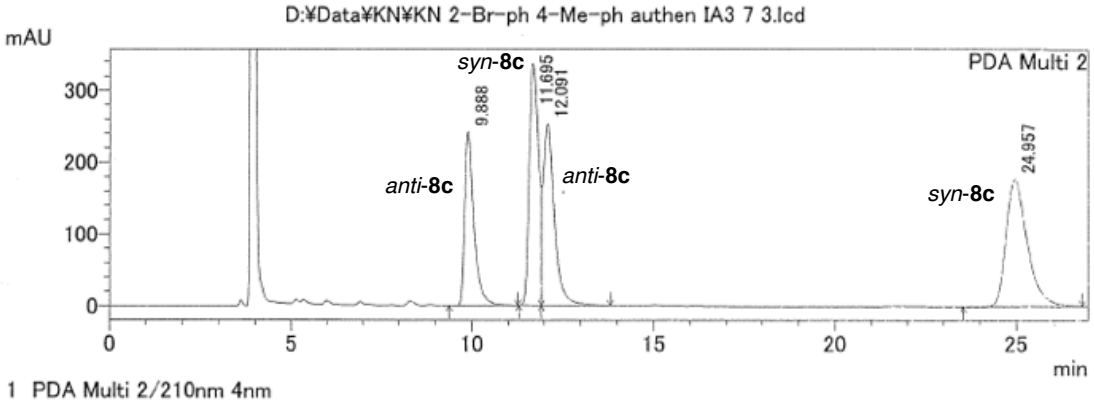

syn-**8c** by the catalysis

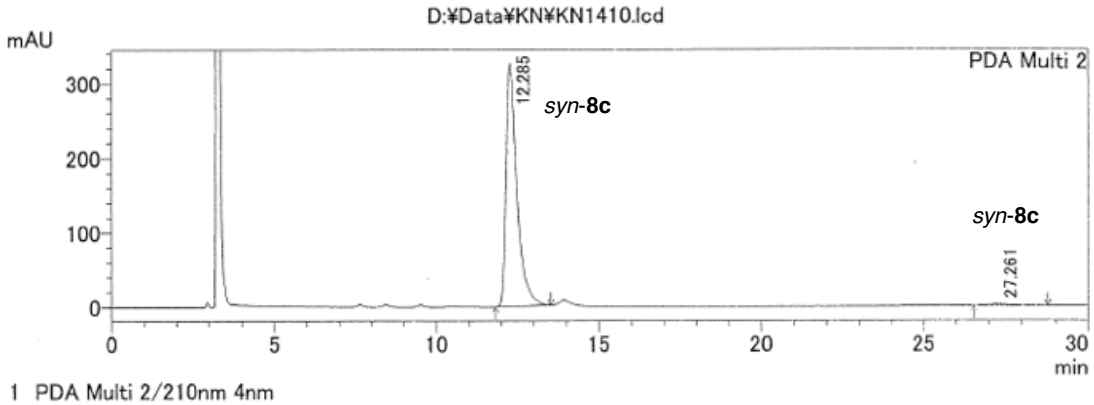

Peak Table

PDA Ch2 210nm 4nm

Peak No	RT (min)	Area	Height (mV)	% Area
1	12.285	7501461	325569	98.796
2	27.261	91395	2178	1.204
Total		7592856	327746	100.000

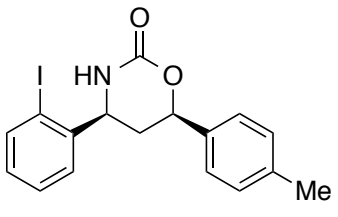

(*syn*-**8d**)

IA-3,

n-hexane/*i*-PrOH = 7/3,

1.0 mL/min, 254 nm

Racemic *syn*-**8d**

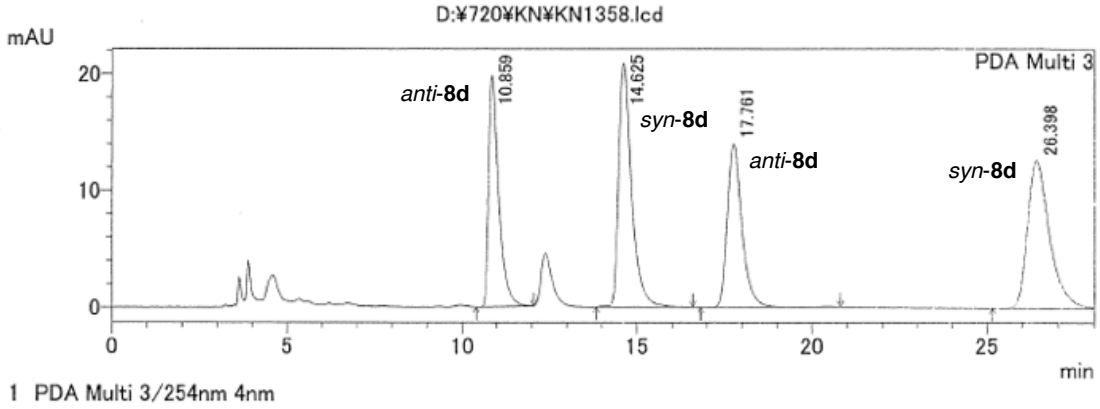

syn-**8d** by the catalysis

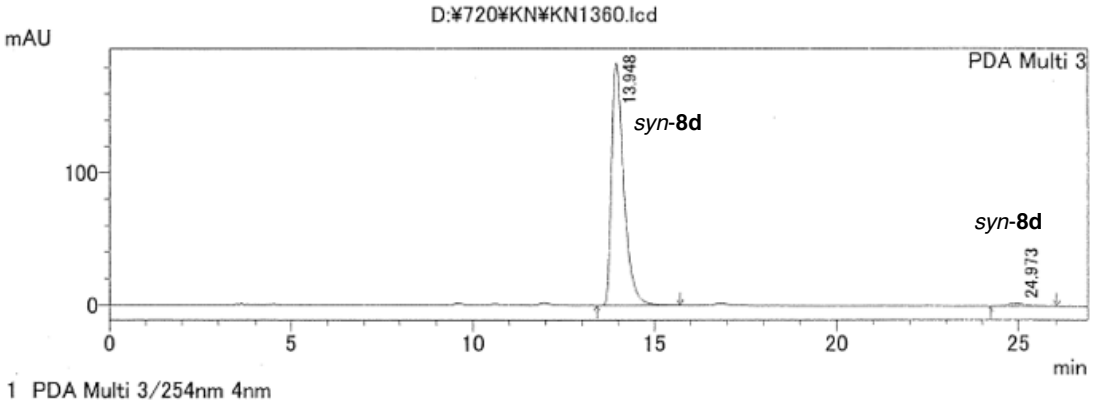

Peak Table

SPD-M20A Ch3 254nm 4nm

Peak No.	RT (min)	Area	Height (mV)	% Area
1	13.948	4222081	183974	98.503
2	24.973	64174	1686	1.497
Total		4286255	185660	100.000

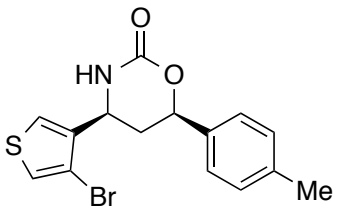

(*syn*-**8e**)

OD-3,

n-hexane/*i*-PrOH = 9/1,

1.0 mL/min, 210 nm

Racemic *syn*-**8e**

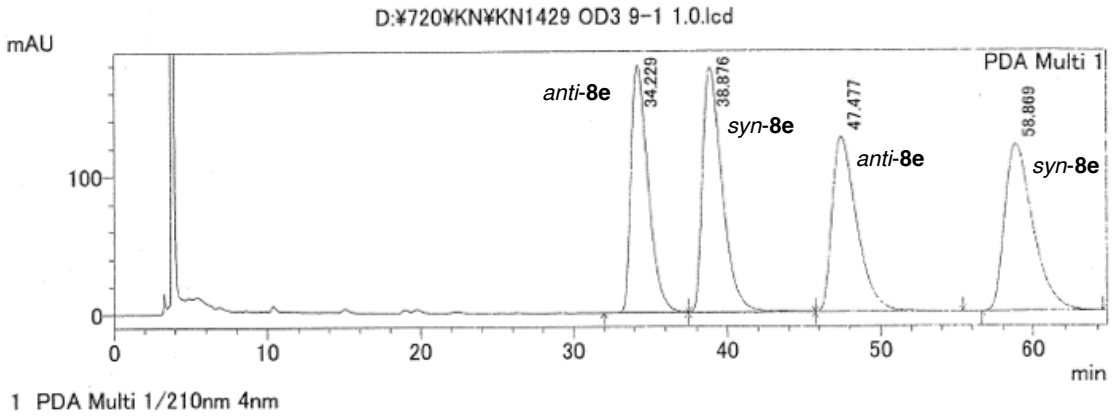

syn-**8e** by the catalysis

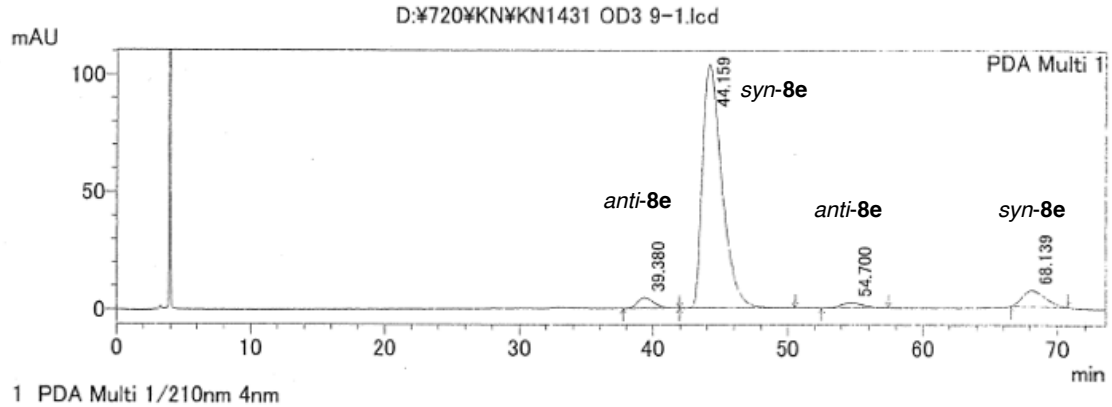

Peak Table

SPD-M20A Ch1 210nm 4nm

Peak No.	RT (min)	Area	Height (mV)	% Area
1	39.380	379731	4452	3.238
2	44.159	10273345	102365	87.605
3	54.700	254449	2113	2.170
4	68.139	819357	6773	6.987
Total		11726882	115703	100.000

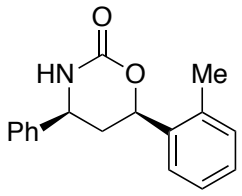

(*syn*-**8f**)

IA-3,
n-hexane/*i*-PrOH = 7/3,
1.0 mL/min, 210 nm

Racemic *syn*-**8f**

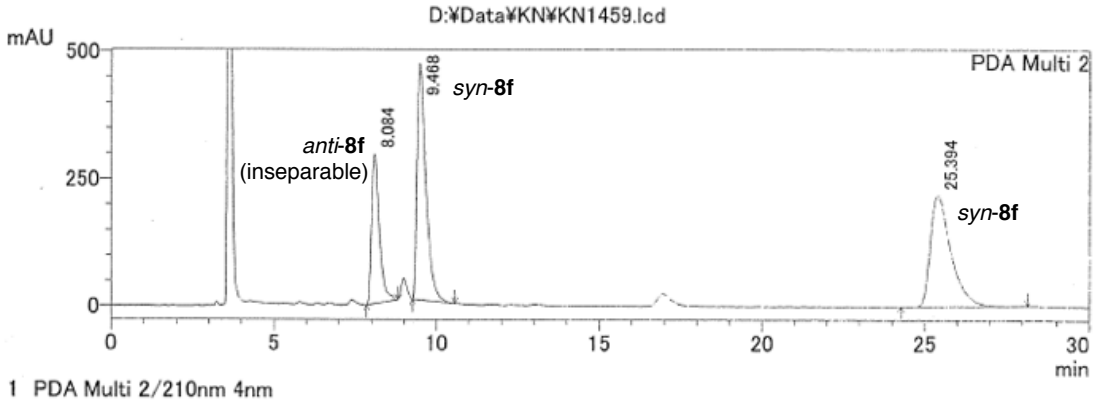

syn-**8f** by the catalysis

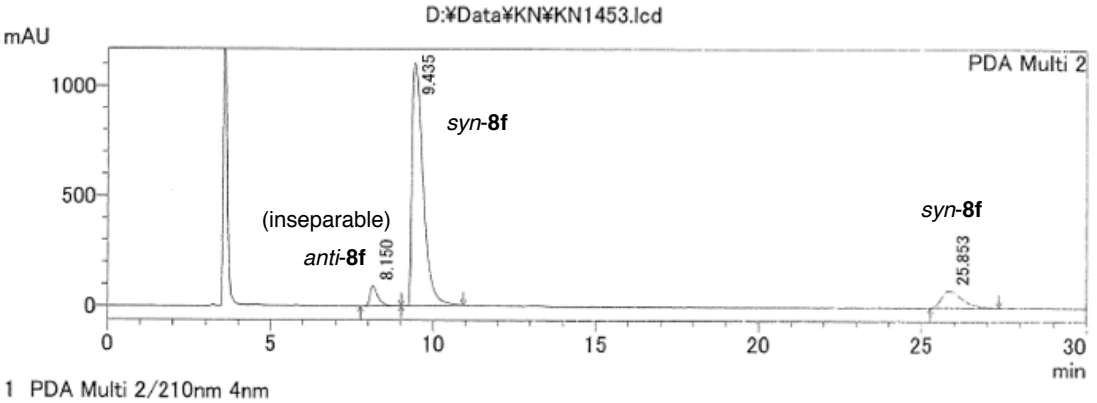

Peak Table

PDA Ch2 210nm 4nm

Peak No	RT (min)	Area	Height (mV)	% Area
1	8.150	1529512	91976	4.924
2	9.435	26239851	1106620	84.480
3	25.853	3290898	76839	10.595
Total		31060260	1275434	100.000

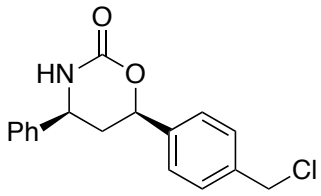

(*syn*-**8g**)

IA-3,
n-hexane/*i*-PrOH = 7/3,
1.0 mL/min, 210 nm

Racemic *syn*-**8g**

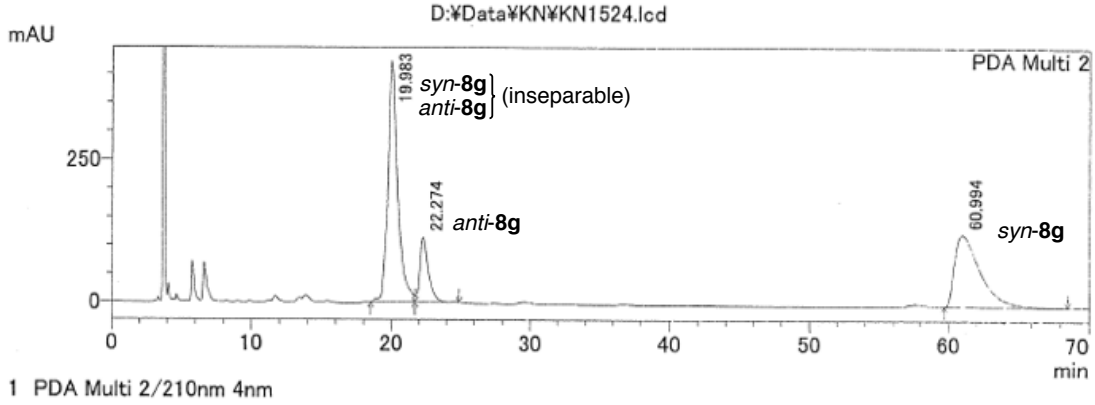

syn-**8g** by the catalysis

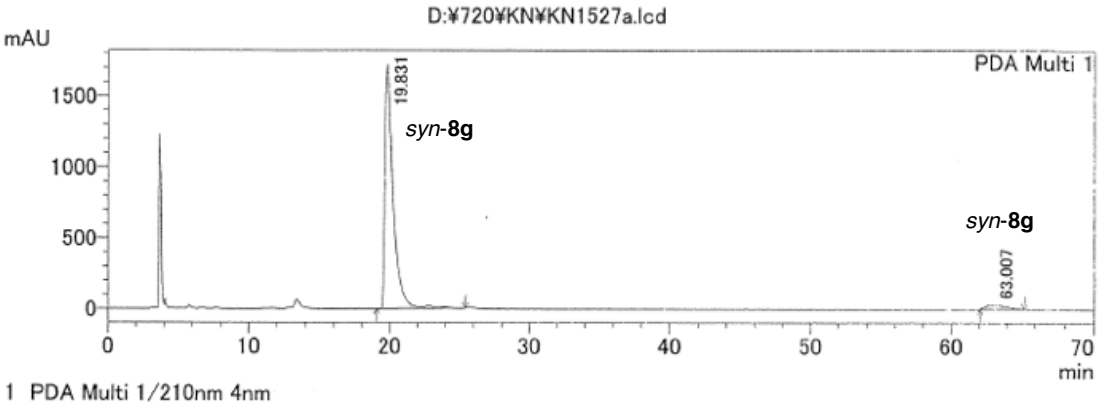

Peak Table

SPD-M20A Ch1 210nm 4nm

Peak No.	RT (min)	Area	Height (mV)	% Area
1	19.831	70970579	1604868	95.964
2	63.007	2984724	31456	4.036
Total		73955304	1636324	100.000

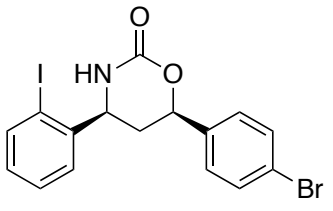

(*syn*-**8h**)

IA-3,
n-hexane/*i*-PrOH = 7/3,
1.0 mL/min, 210 nm

Racemic *syn*-**8h**

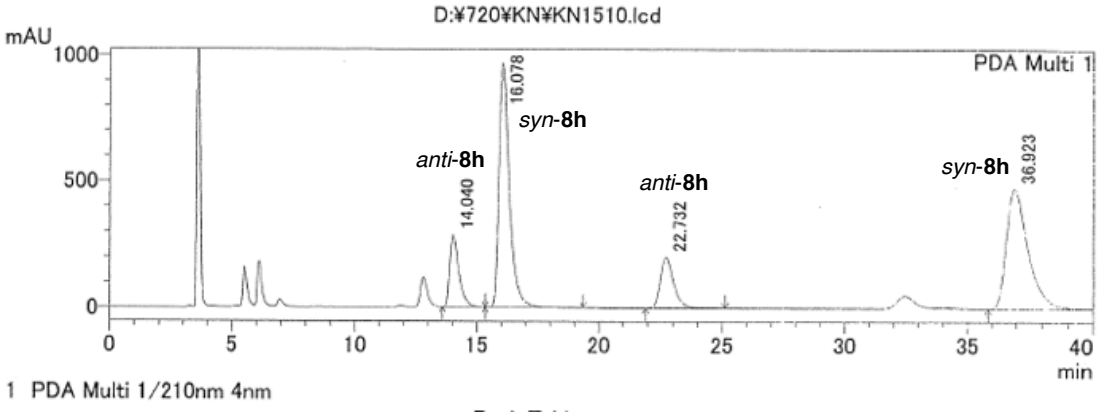

syn-**8h** by the catalysis

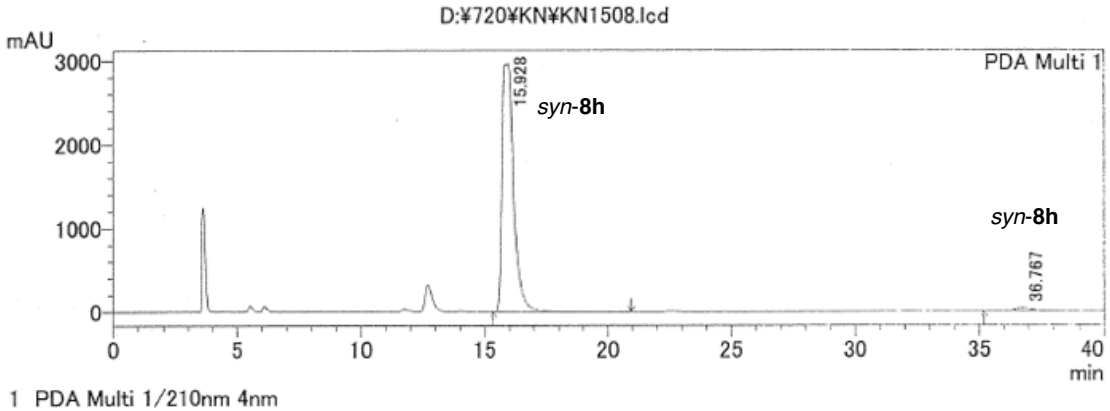

Peak Table

SPD-M20A Ch1 210nm 4nm

Peak No.	RT (min)	Area	Height (mV)	% Area
1	15.928	96967452	2951852	97.880
2	36.767	2099873	33867	2.120
Total		99067325	2985719	100.000

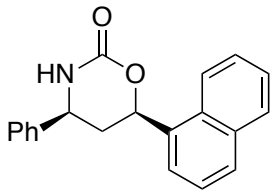

(*syn*-**8i**)

IA-3,
n-hexane/*i*-PrOH = 7/3,
1.0 mL/min, 280 nm

Racemic *syn*-**8i**

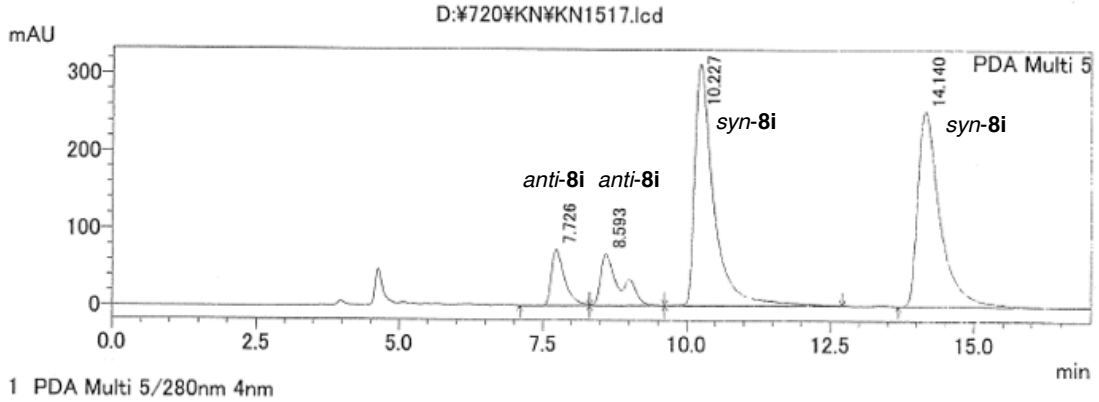

syn-**8i** by the catalysis

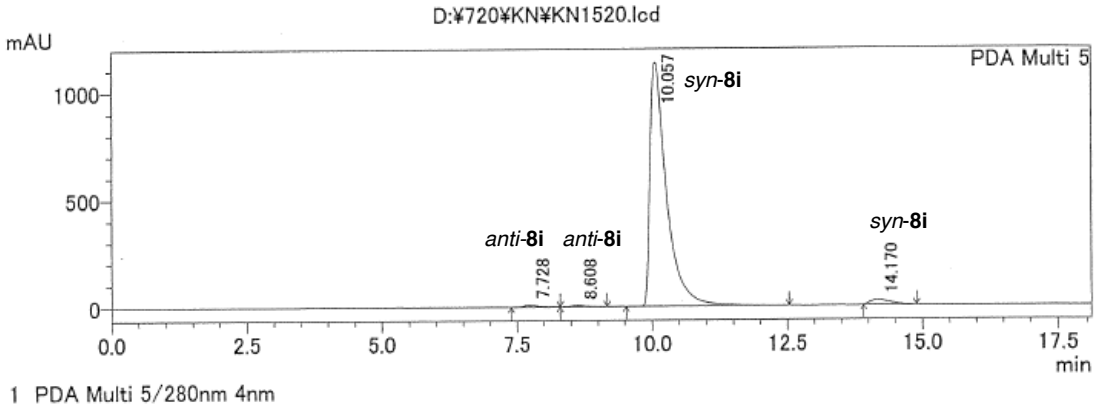

Peak Table

SPD-M20A Ch5 280nm 4nm

Peak No.	RT (min)	Area	Height (mV)	% Area
1	7.728	167577	10345	0.670
2	8.608	119279	6776	0.477
3	10.057	24175208	1132787	96.659
4	14.170	548649	22049	2.194
Total		25010713	1171958	100.000

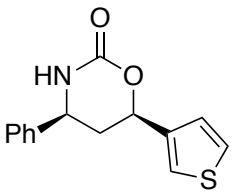

(*syn*-**8j**)

IA-3,
n-hexane/*i*-PrOH = 7/3,
1.0 mL/min, 210 nm

Racemic *syn*-**8j**

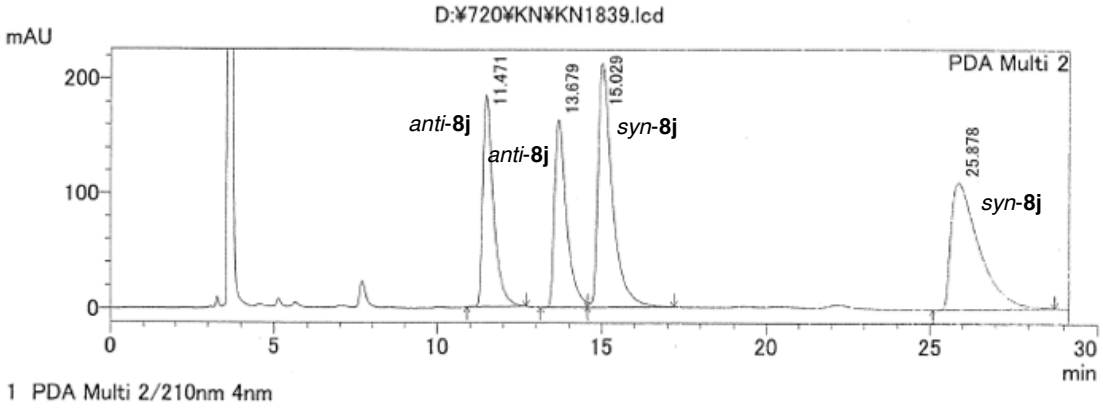

syn-**8j** by the catalysis

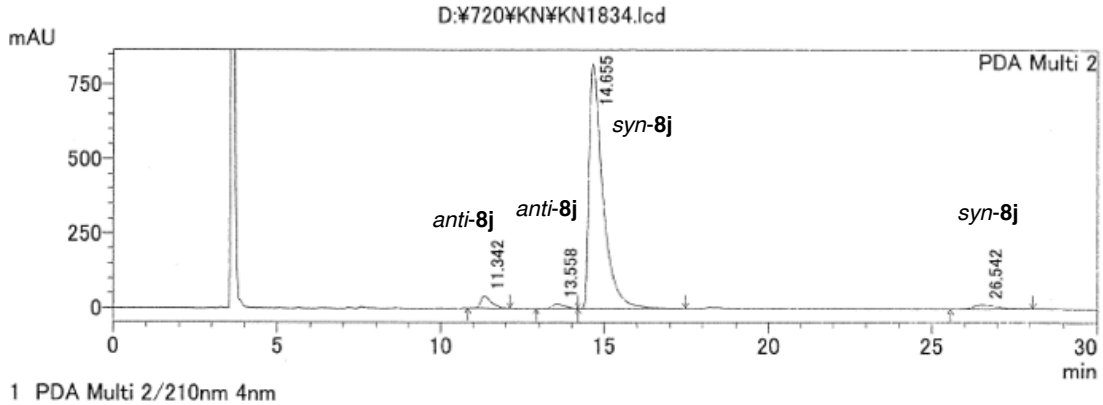

Peak Table

SPD-M20A Ch2 210nm 4nm

Peak No	RT (min)	Area	Height (mV)	% Area
1	11.342	901743	41231	3.442
2	13.558	405241	15322	1.547
3	14.655	24210188	820318	92.413
4	26.542	680724	13911	2.598
Total		26197896	890782	100.000

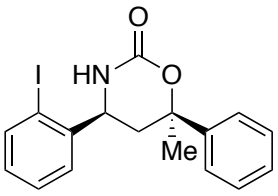

(*syn*-**10**)

IA-3,
n-hexane/*i*-PrOH = 7/3,
1.0 mL/min, 254 nm

Racemic *syn*-**10**

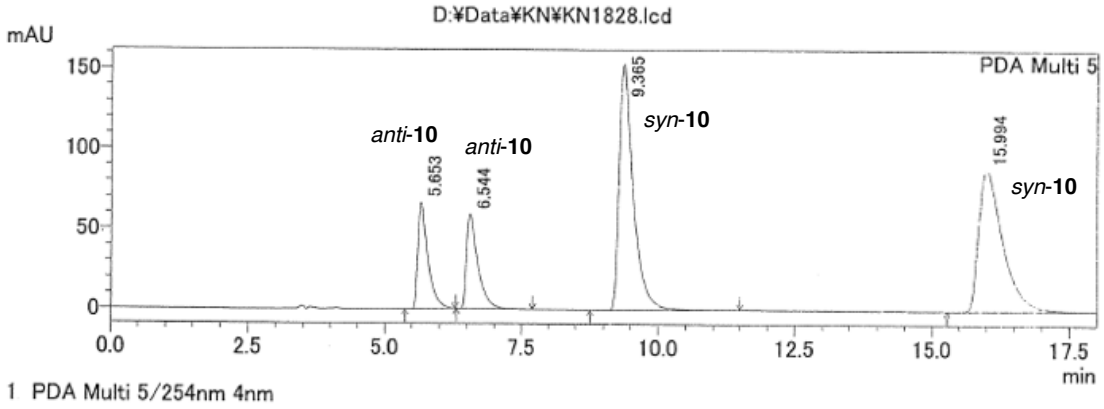

syn-**10** by the catalysis

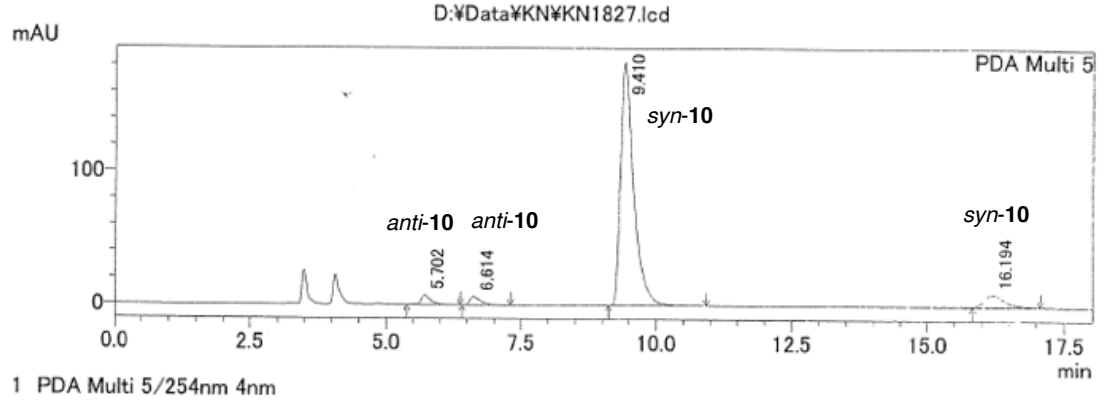

Peak Table

PDA Ch5 254nm 4nm

Peak No	RT (min)	Area	Height (mV)	% Area
1	5.702	92877	7216	2.653
2	6.614	84502	6282	2.414
3	9.410	3078028	183078	87.925
4	16.194	245318	9494	7.008
Total		3500724	206071	100.000

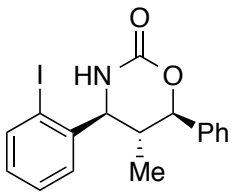

IA-3,
n-hexane/*i*-PrOH = 7/3,
1.0 mL/min, 210 nm

(1,3-*syn*-2,3-*anti*-**12**)

Racemic 1,3-*syn*-2,3-*anti*-**12**

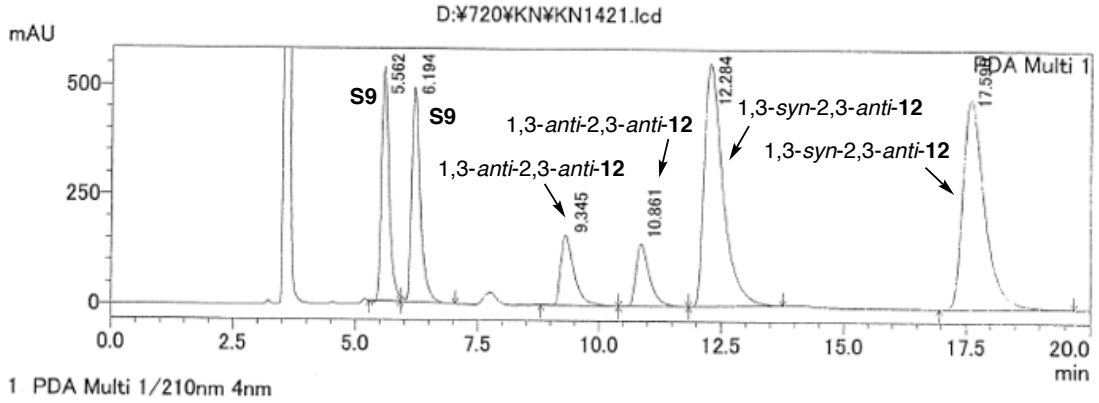

1,3-*syn*-2,3-*anti*-**12** by the catalysis

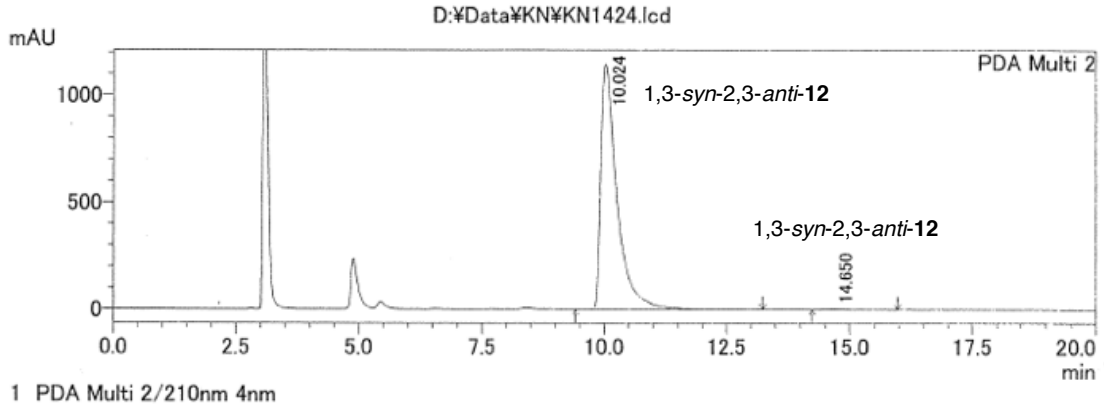

Peak Table

PDA Ch2 210nm 4nm

Peak No	RT (min)	Area	Height (mV)	% Area
1	10.024	26173999	1146300	99.651
2	14.650	91571	3537	0.349
Total		26265570	1149837	100.000

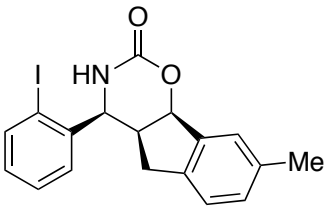

(*syn*-**14**)

IA-3,
n-hexane/*i*-PrOH = 7/3,
1.0 mL/min, 210 nm

Racemic *syn*-**14**

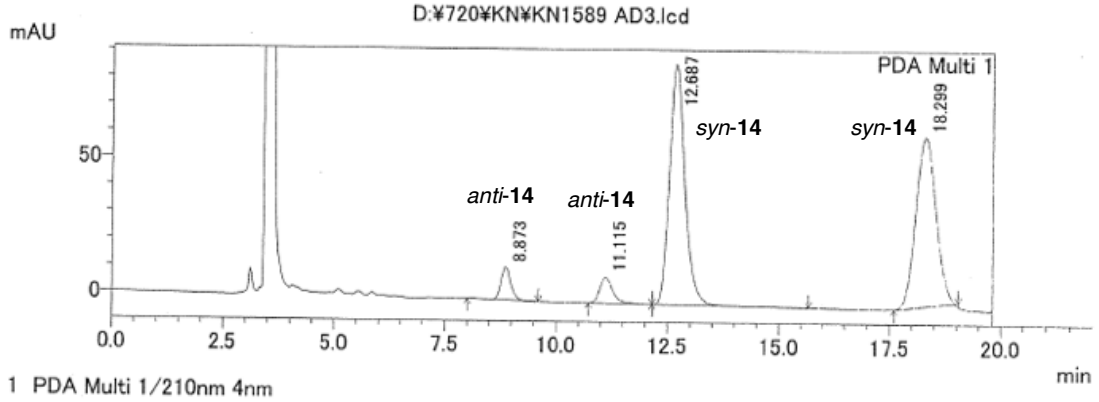

syn-**14** by the catalysis

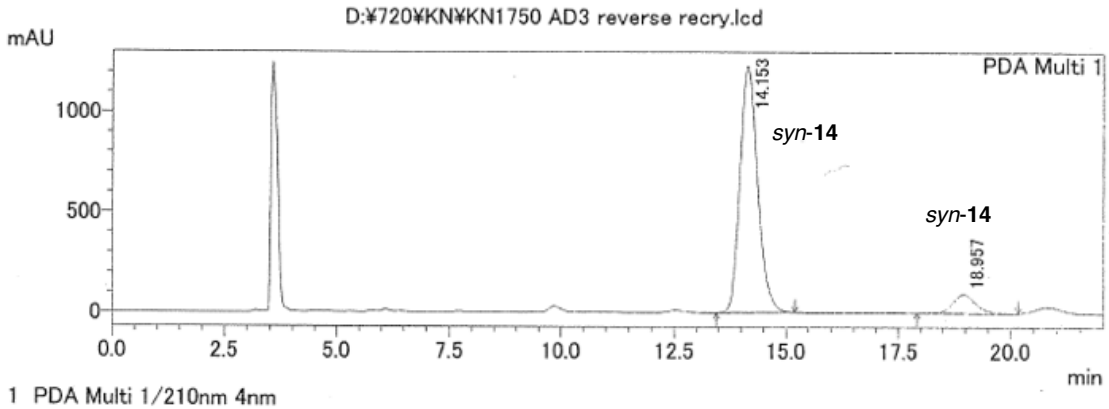

Peak Table

SPD-M20A Ch1 210nm 4nm

Peak No.	RT (min)	Area	Height (mV)	% Area
1	14.153	34066145	1182804	91.101
2	18.957	3327602	91986	8.899
Total		37393747	1274790	100.000

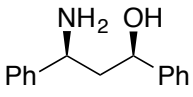

(*syn*-**15**)

OD-3,
n-hexane/*i*-PrOH = 9/1,
0.8 mL/min, 210 nm

Racemic *syn*-**15**

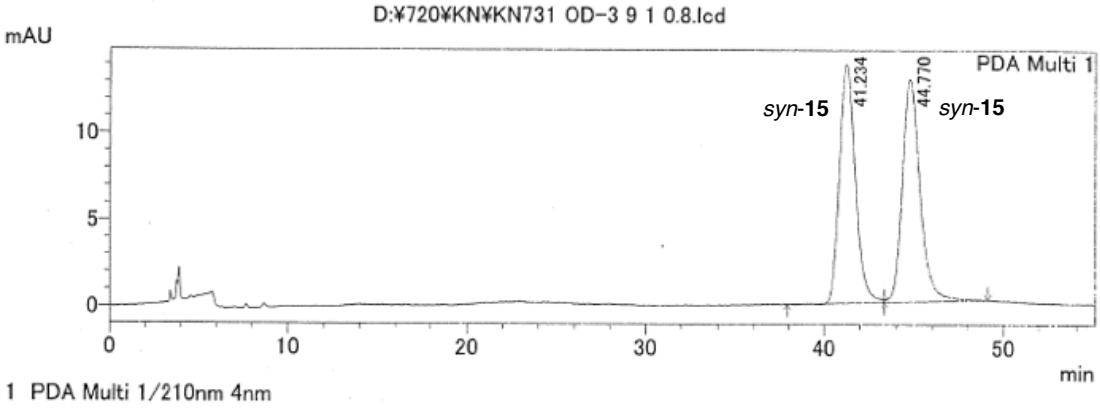

syn-**15** derived through the catalysis

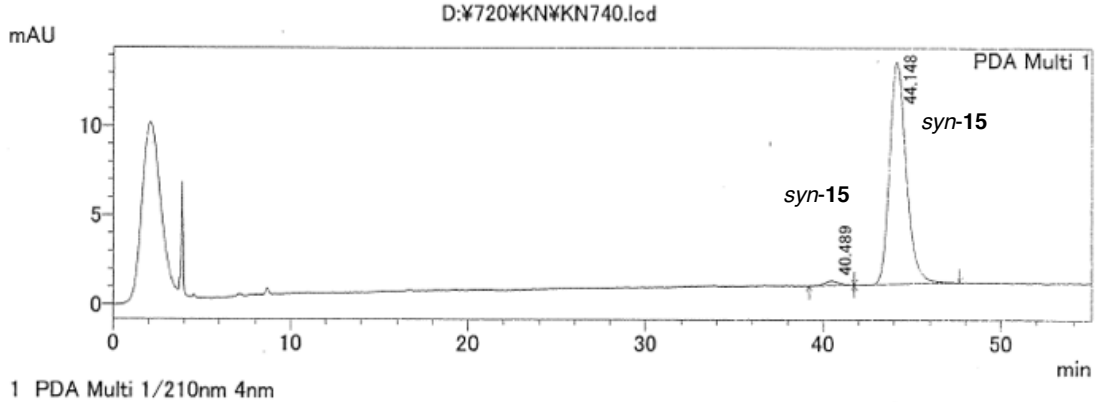

Peak Table

SPD-M20A Ch1 210nm 4nm

Peak No.	RT (min)	Area	Height (mV)	% Area
1	40.489	13722	240	1.644
2	44.148	820903	12173	98.356
Total		834625	12414	100.000

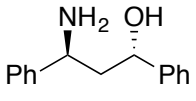

(*anti*-**15**)

OD-3,
n-hexane/*i*-PrOH = 9/1,
0.8 mL/min, 210 nm

Racemic *anti*-**15**

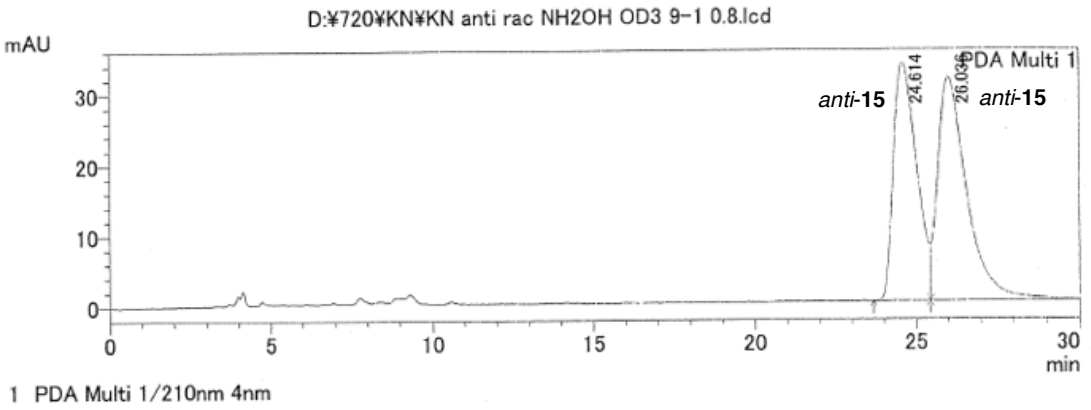

anti-**15** derived through the catalysis

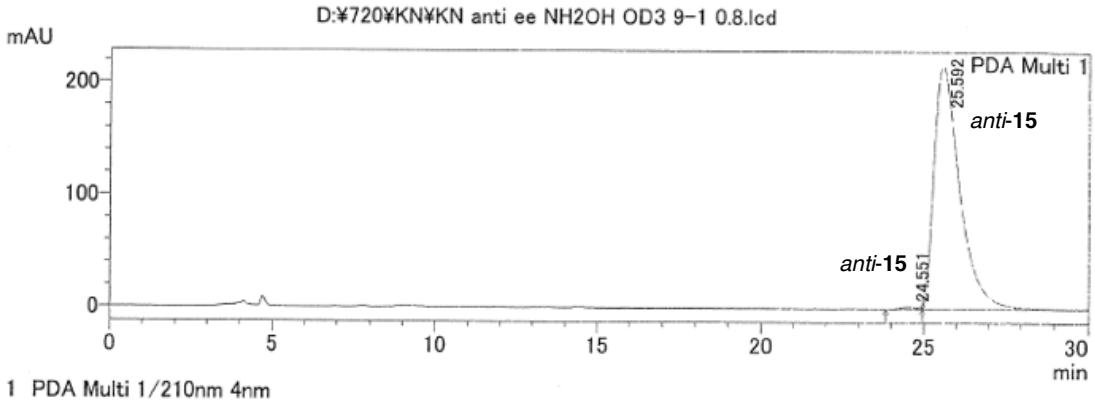

Peak Table

SPD-M20A Ch1 210nm 4nm

Peak No.	RT (min)	Area	Height (mV)	% Area
1	24.551	80264	1932	0.662
2	25.592	12036508	209714	99.338
Total		12116772	211646	100.000

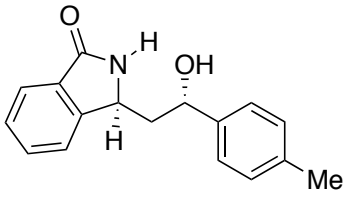

(**20**)

OD-3,
n-hexane/*i*-PrOH = 7/3,
1.0 mL/min, 254 nm

Racemic **20**

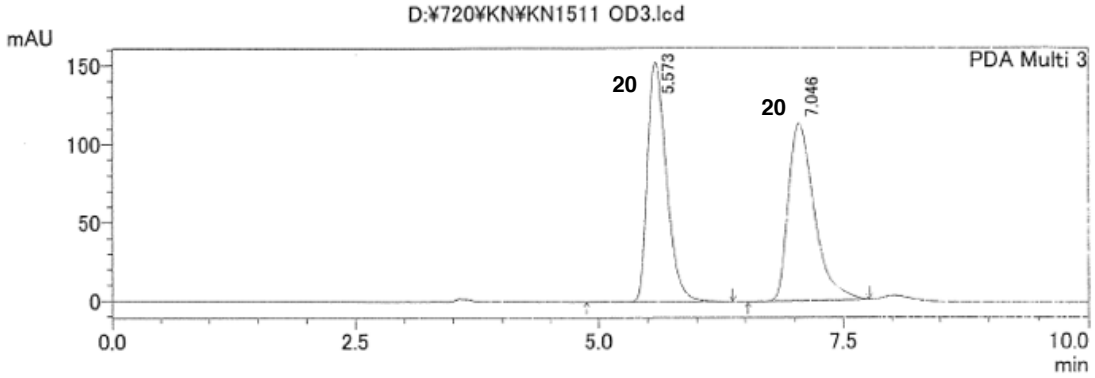

20 derived through the catalysis

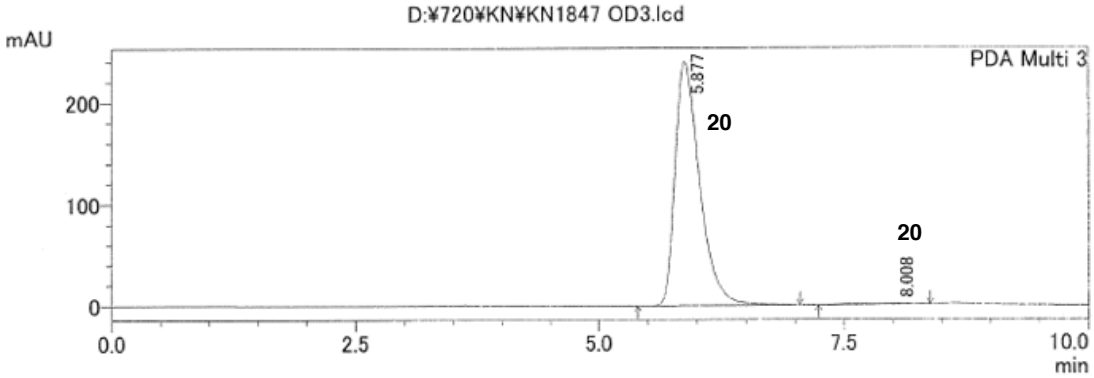

Peak Table

SPD-M20A Ch3 254nm 4nm

Peak No	RT (min)	Area	Height (mV)	% Area
1	5.877	4211456	239853	99.230
2	8.008	32685	779	0.770
Total		4244141	240631	100.000

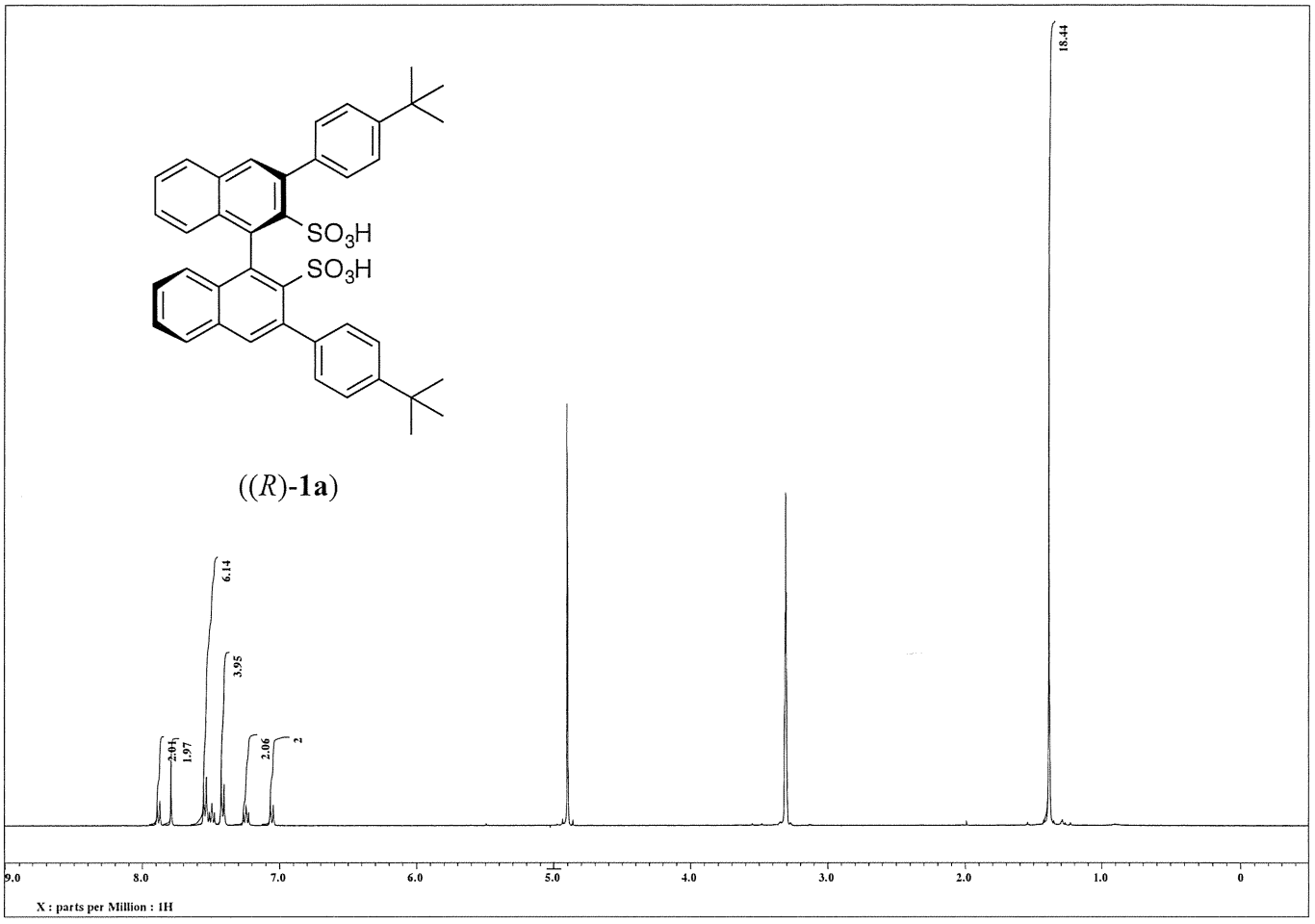

^{1}H NMR, 400 MHz, CD_3OD

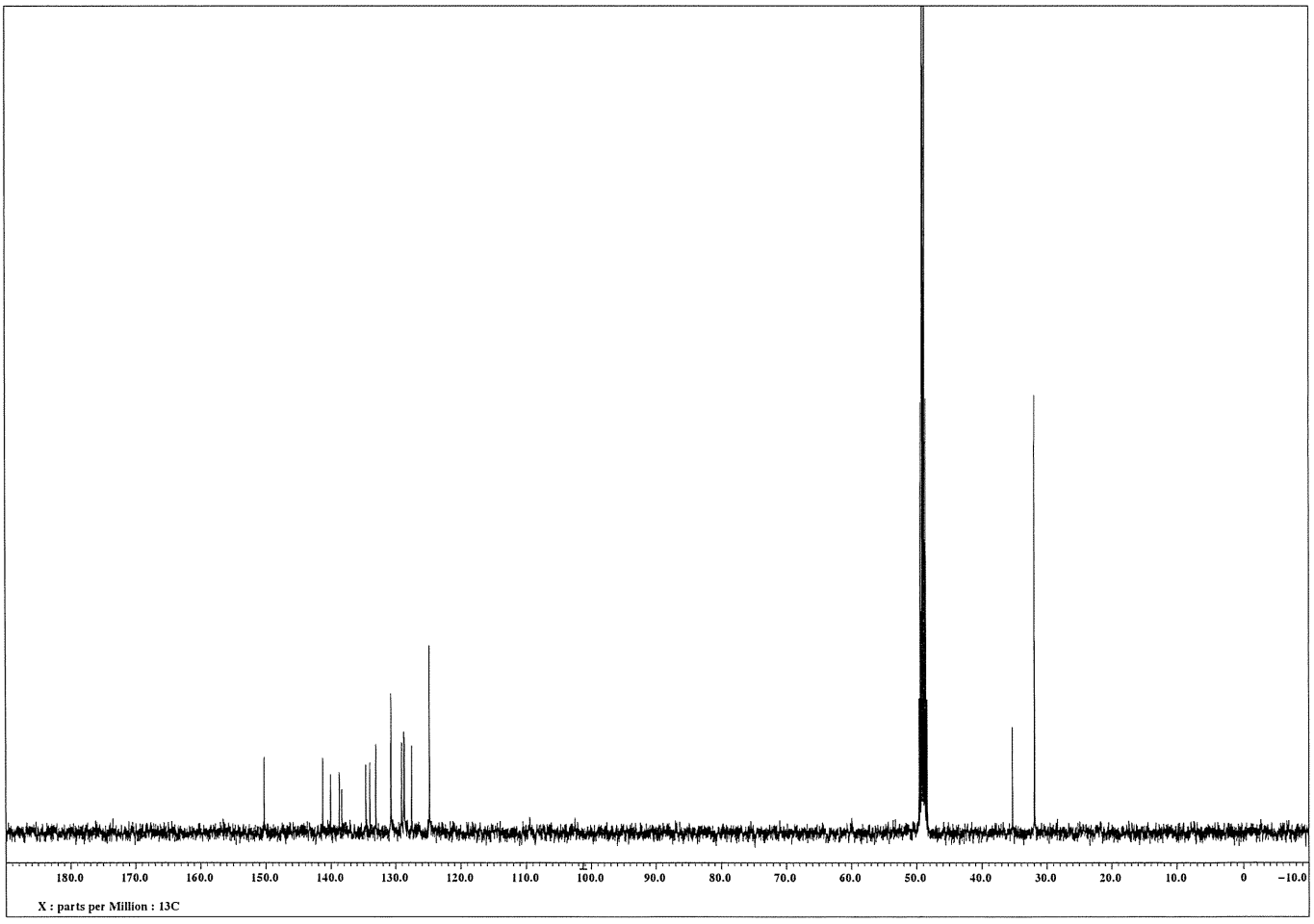

^{13}C NMR, 100 MHz, CD_3OD

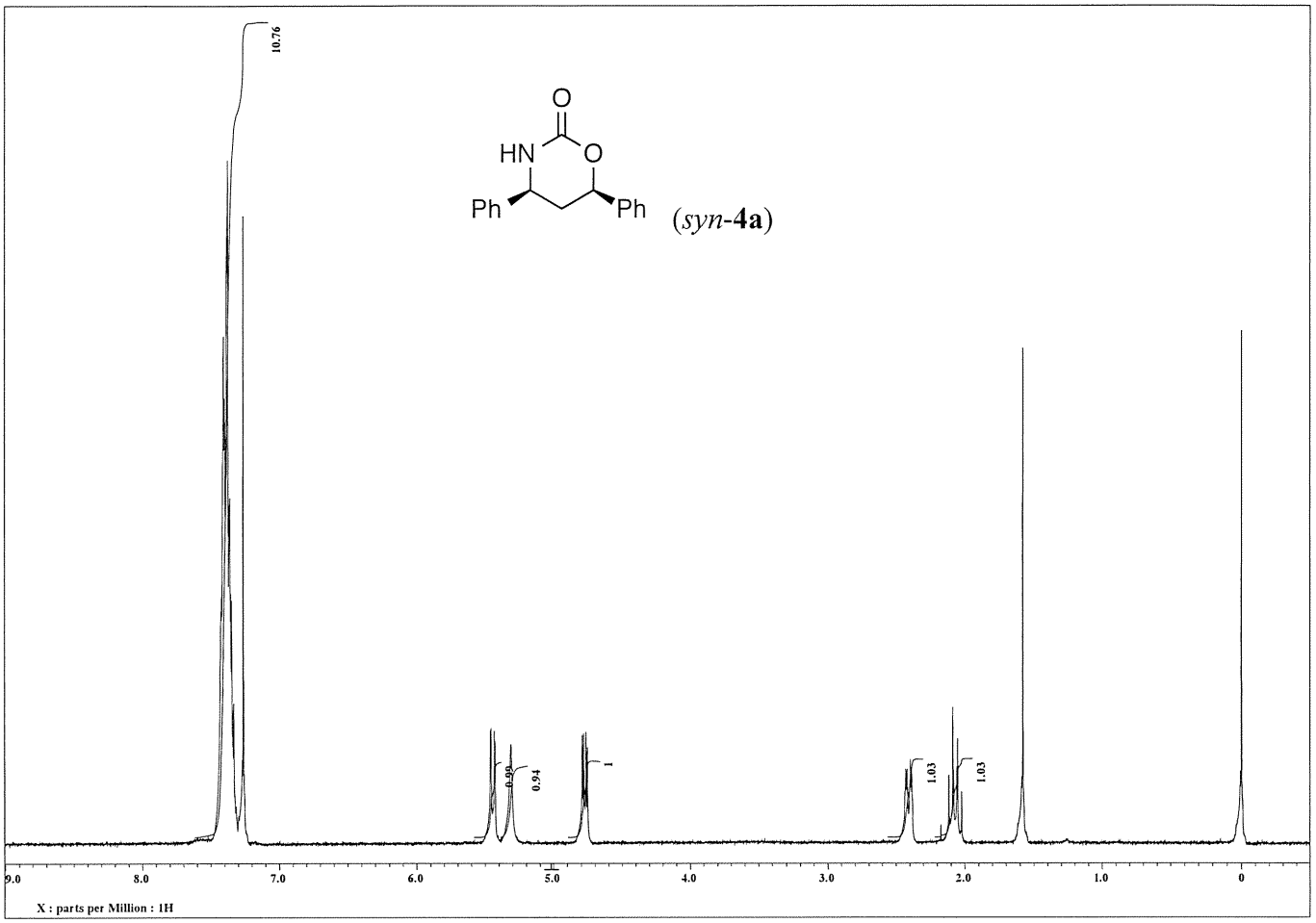

^{1}H NMR, 400 MHz, $CDCl_3$

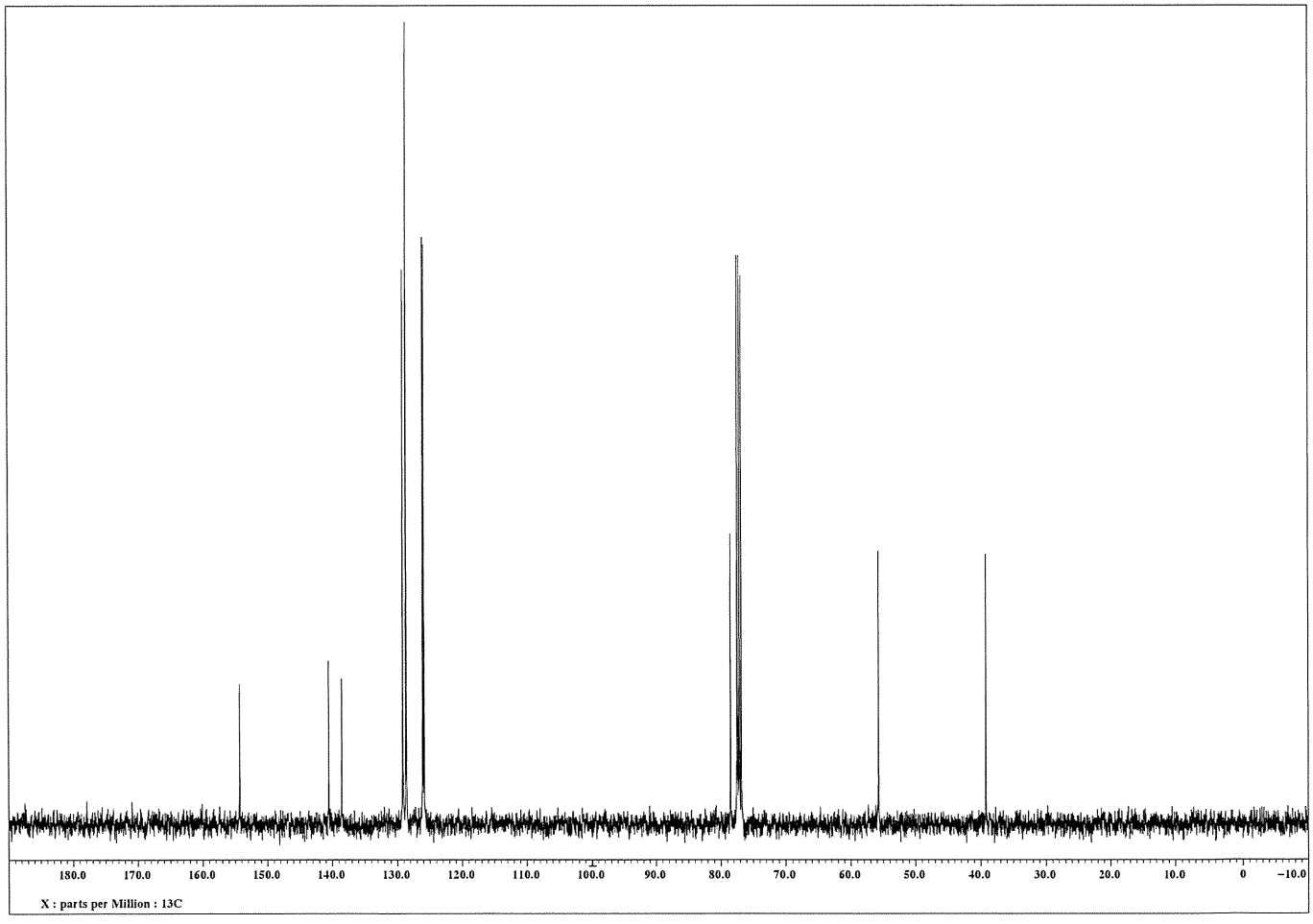

^{13}C NMR, 100 MHz, $CDCl_3$

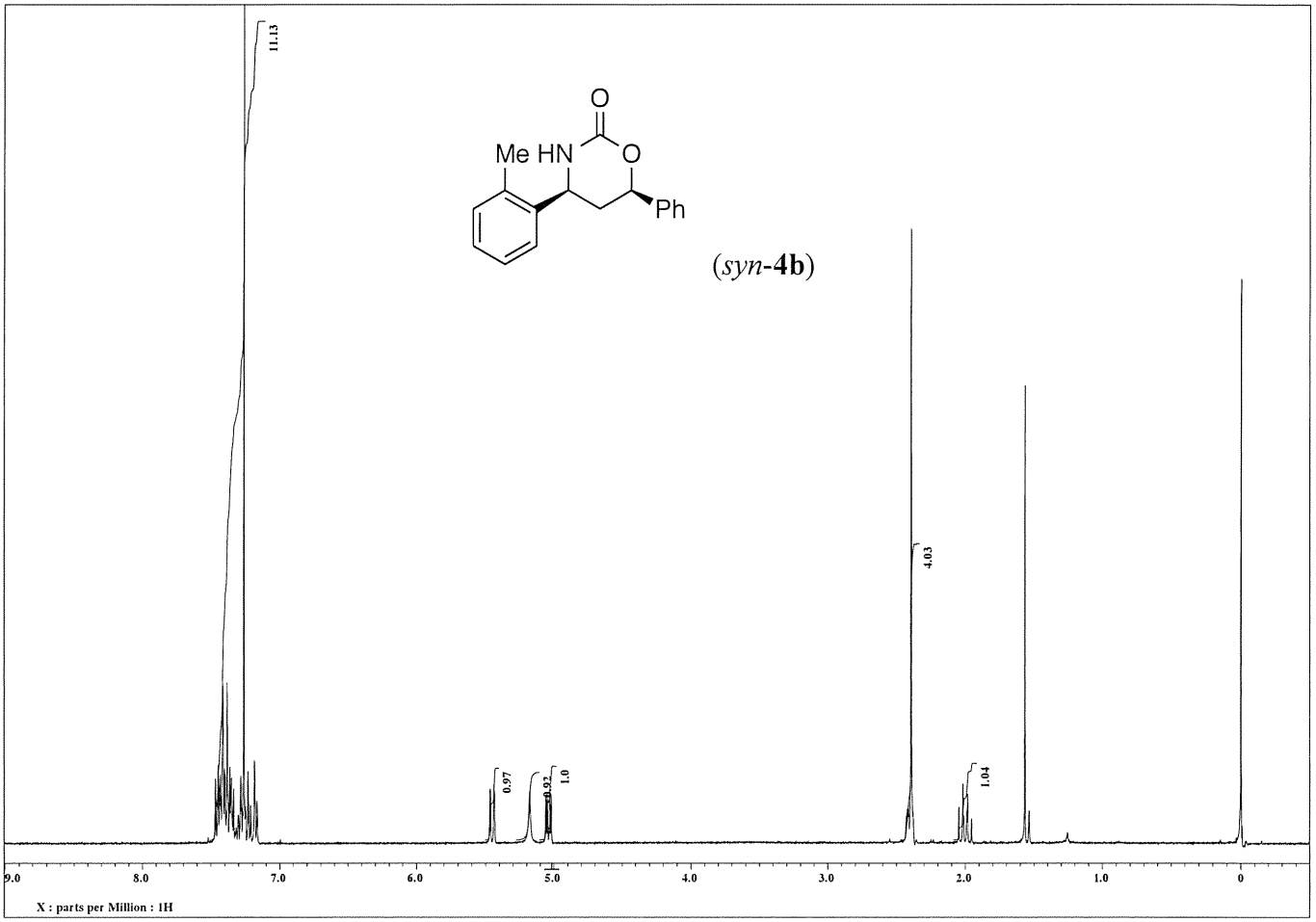

^{1}H NMR, 400 MHz, $CDCl_3$

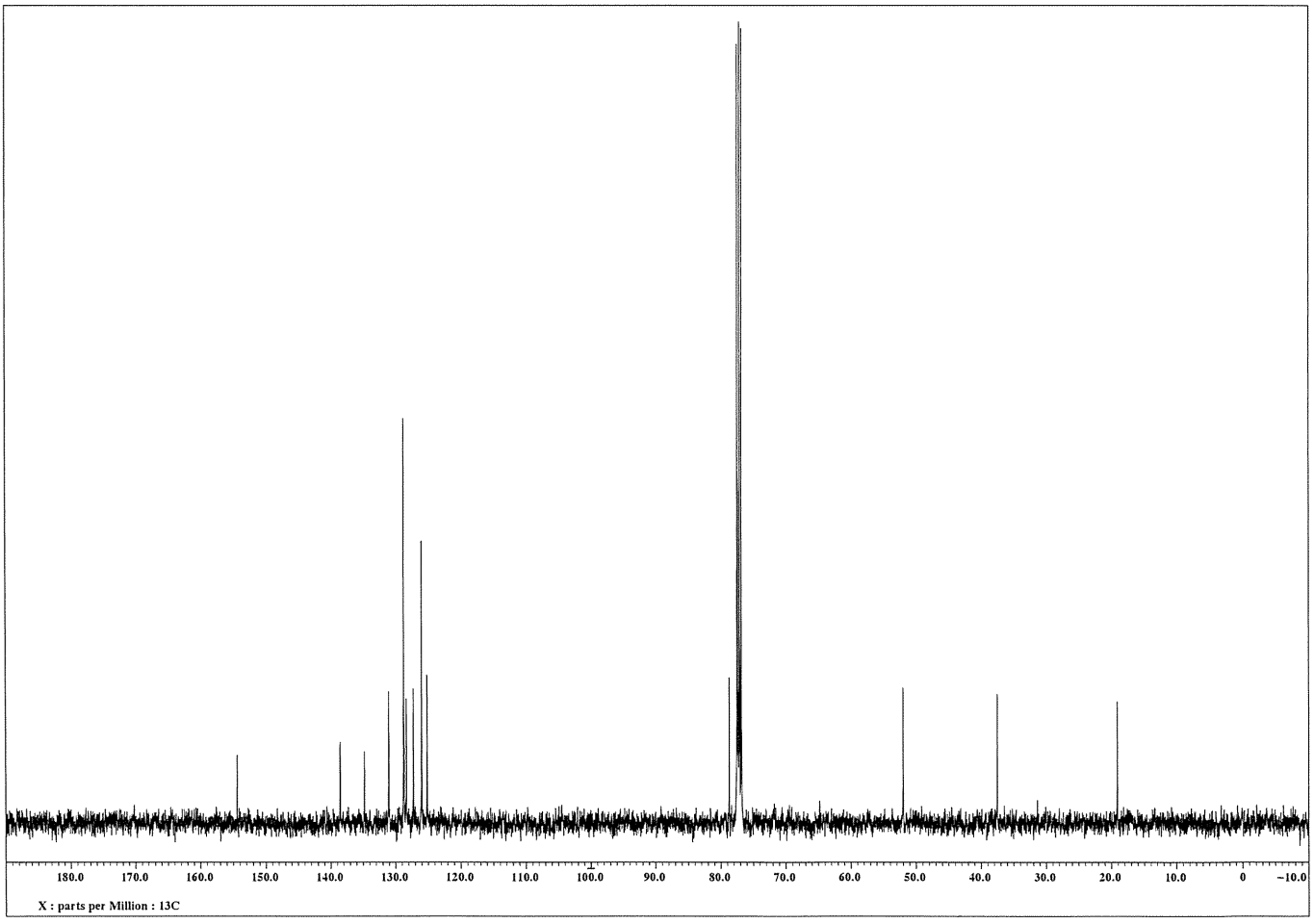

^{13}C NMR, 100 MHz, $CDCl_3$

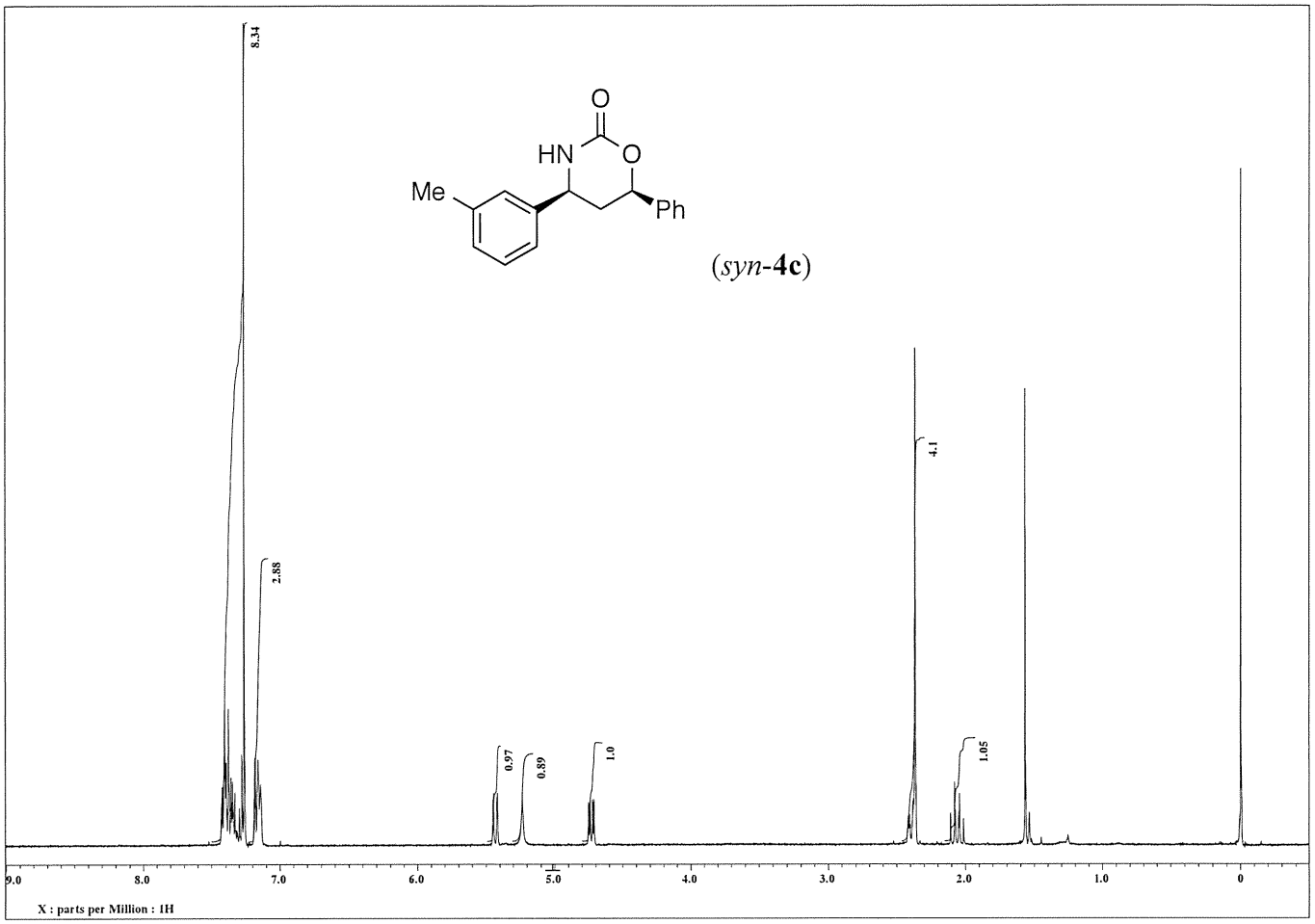

(*syn*-**4c**)

^{1}H NMR, 400 MHz, $CDCl_3$

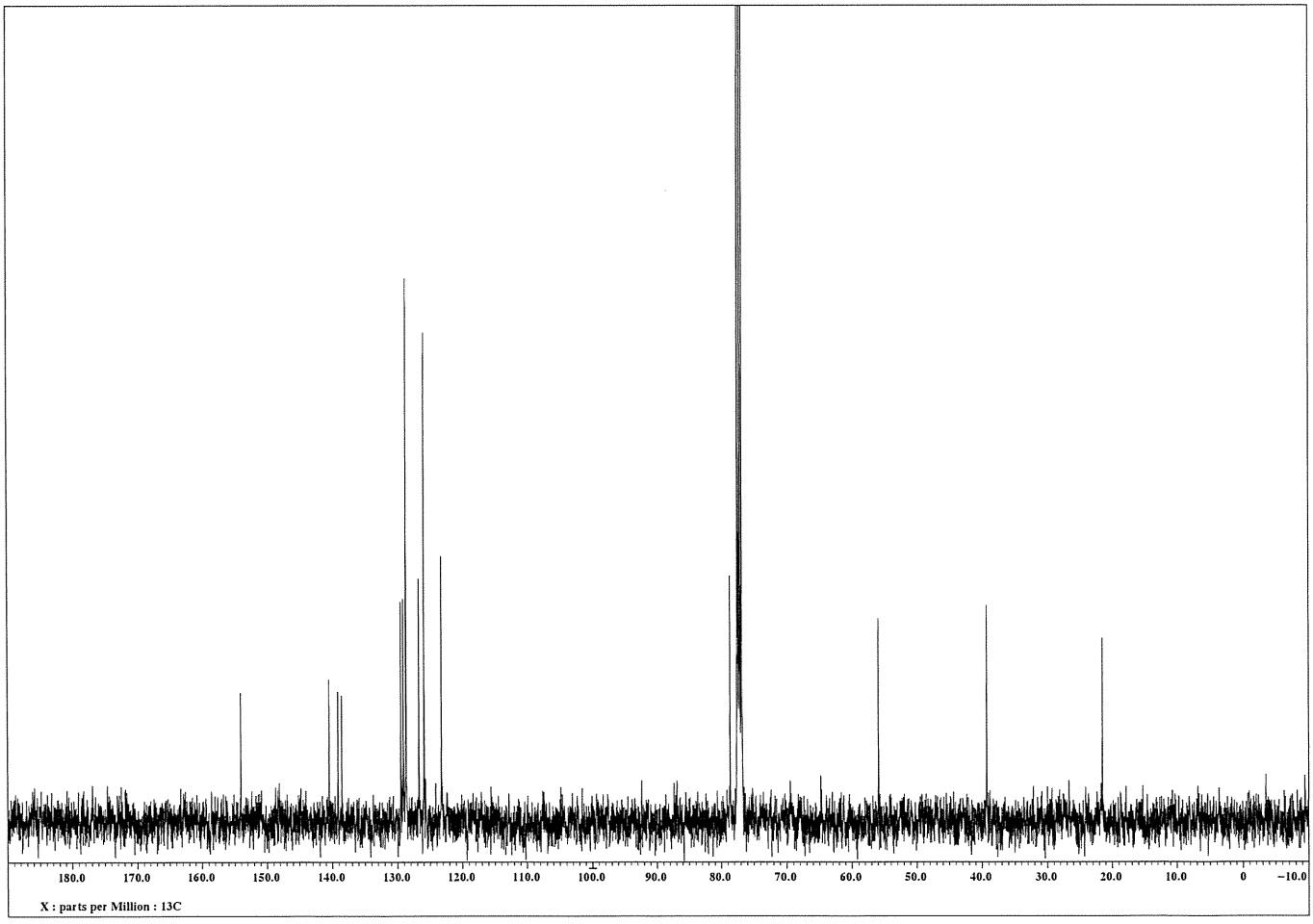

^{13}C NMR, 100 MHz, $CDCl_3$

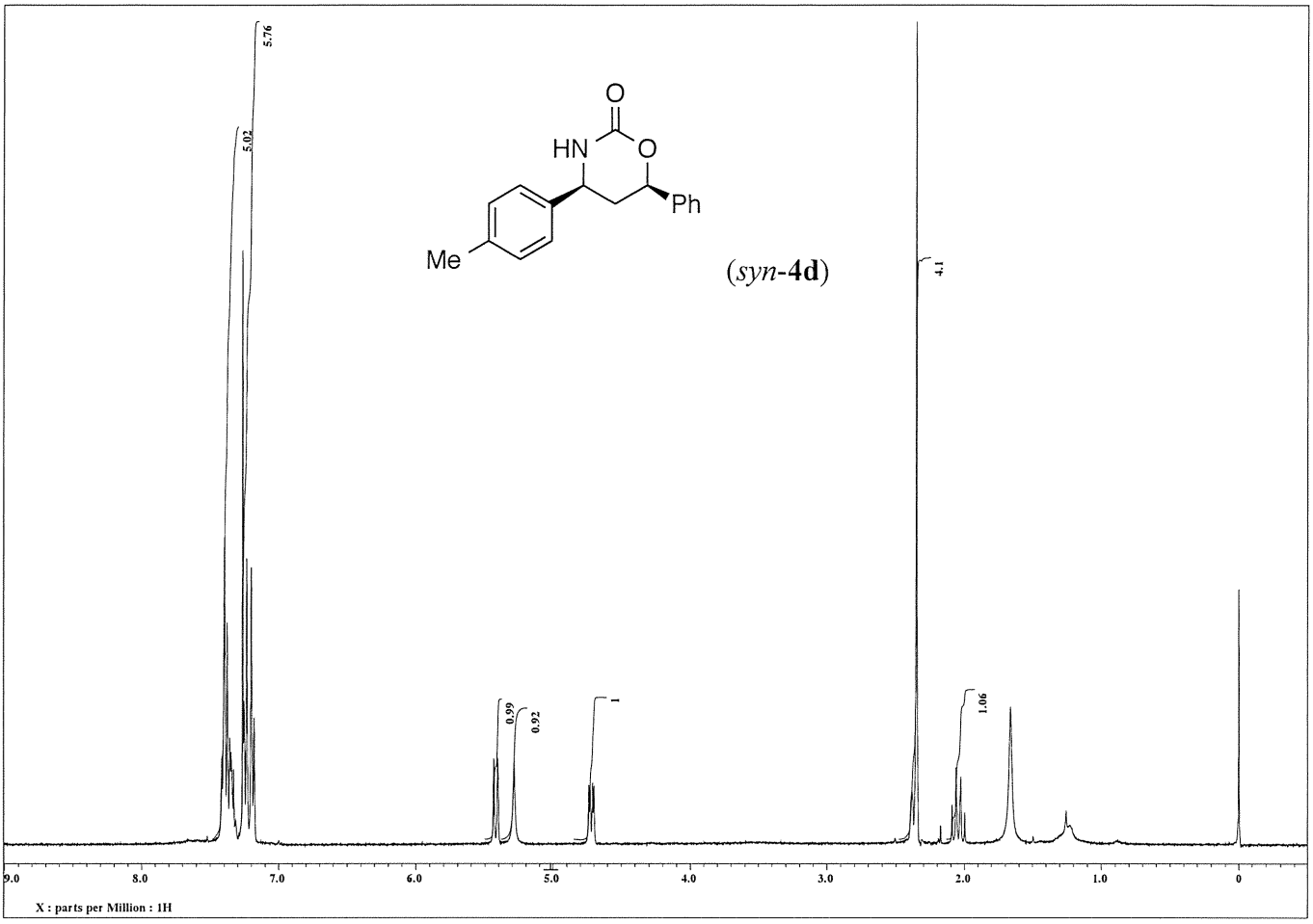

^{1}H NMR, 400 MHz, $CDCl_3$

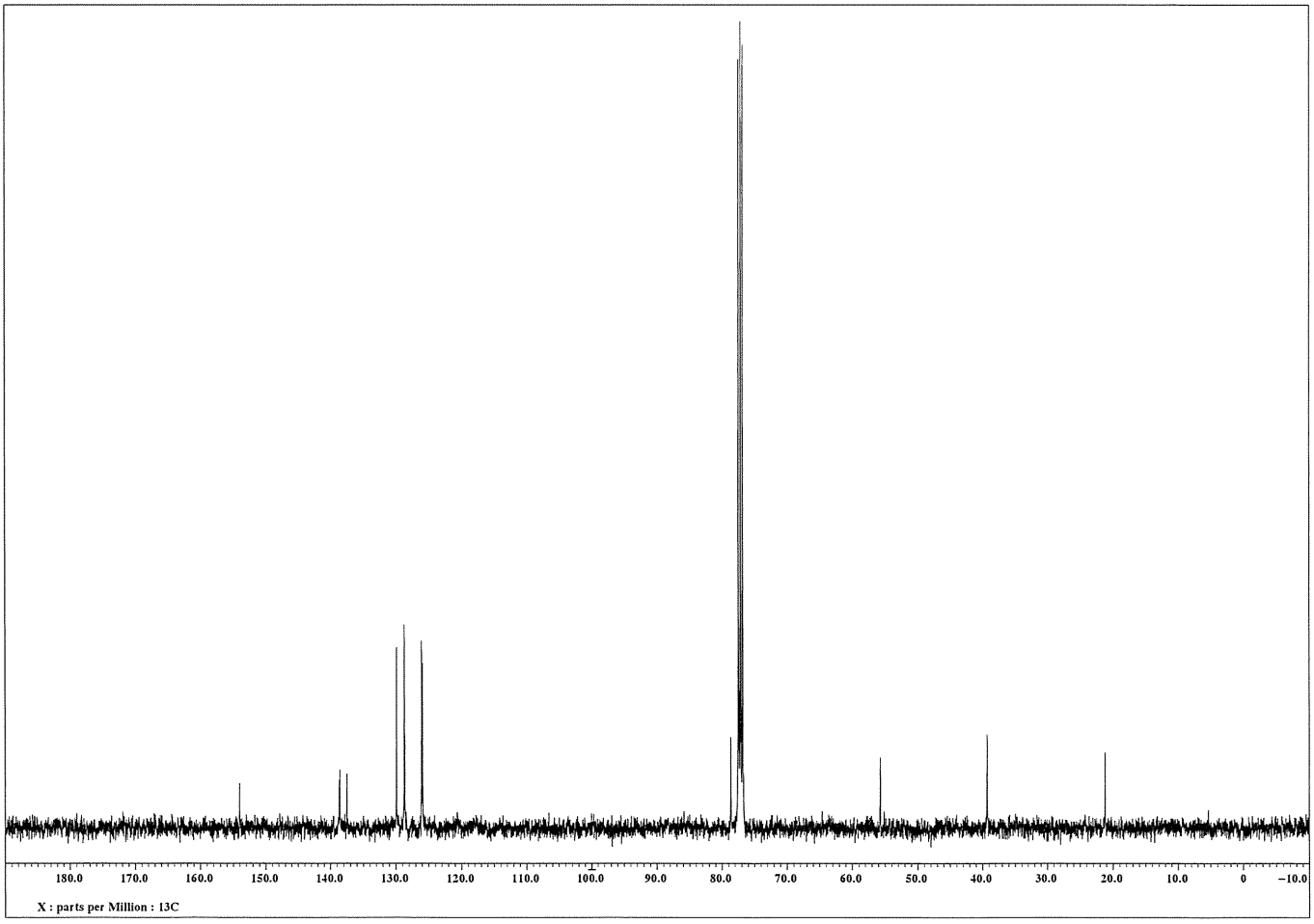

^{13}C NMR, 100 MHz, $CDCl_3$

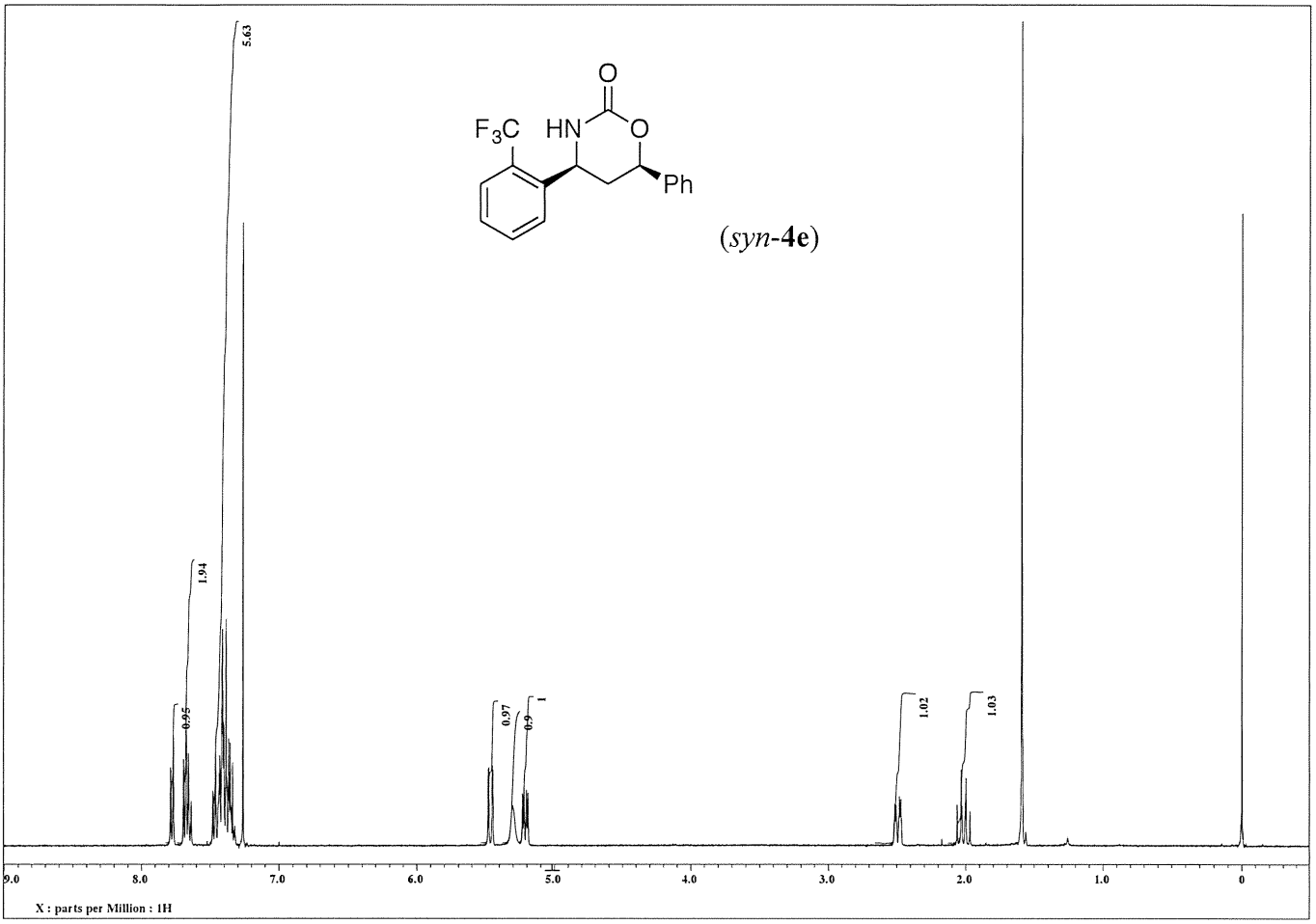

^{1}H NMR, 400 MHz, $CDCl_3$

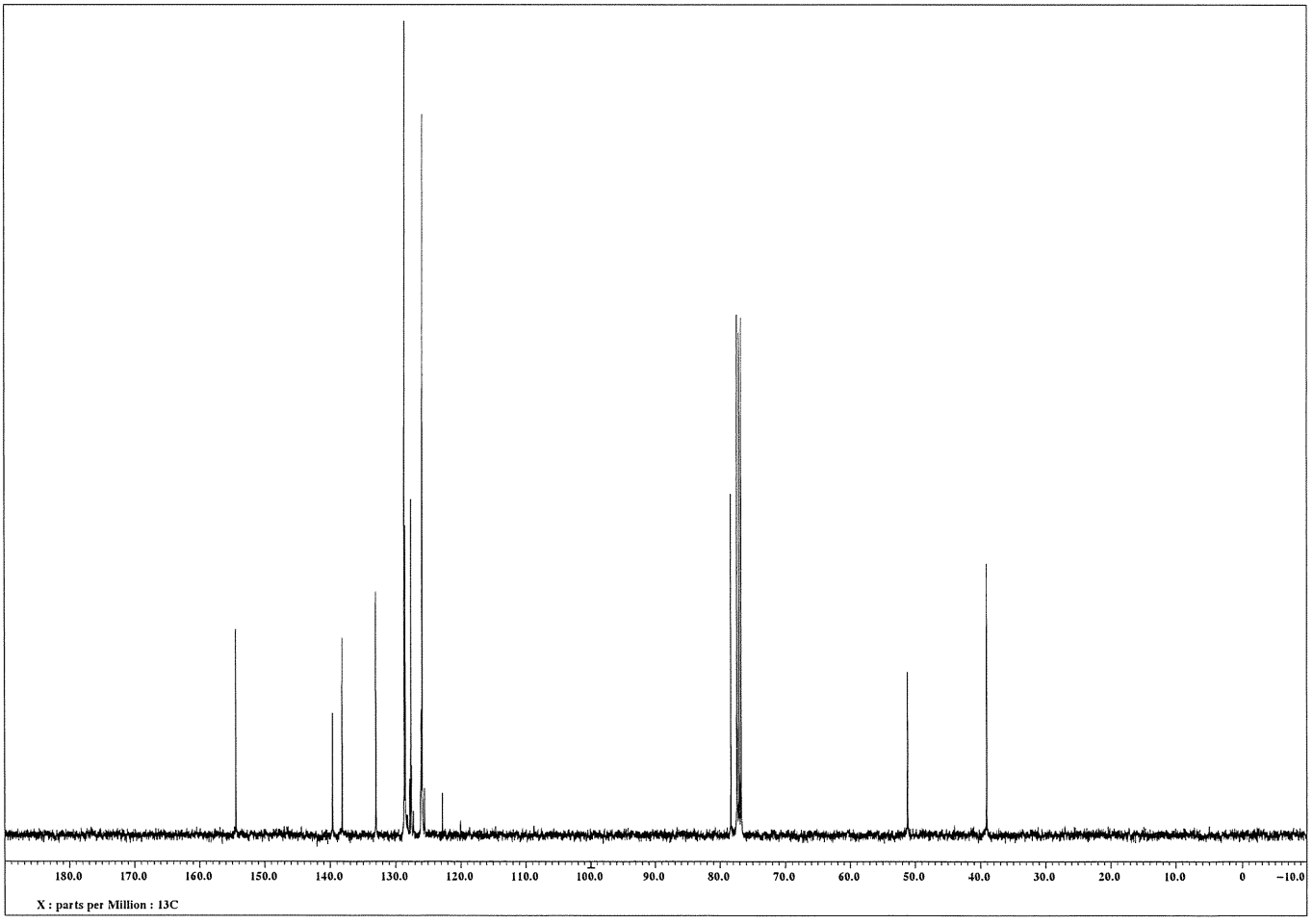

^{13}C NMR, 100 MHz, $CDCl_3$

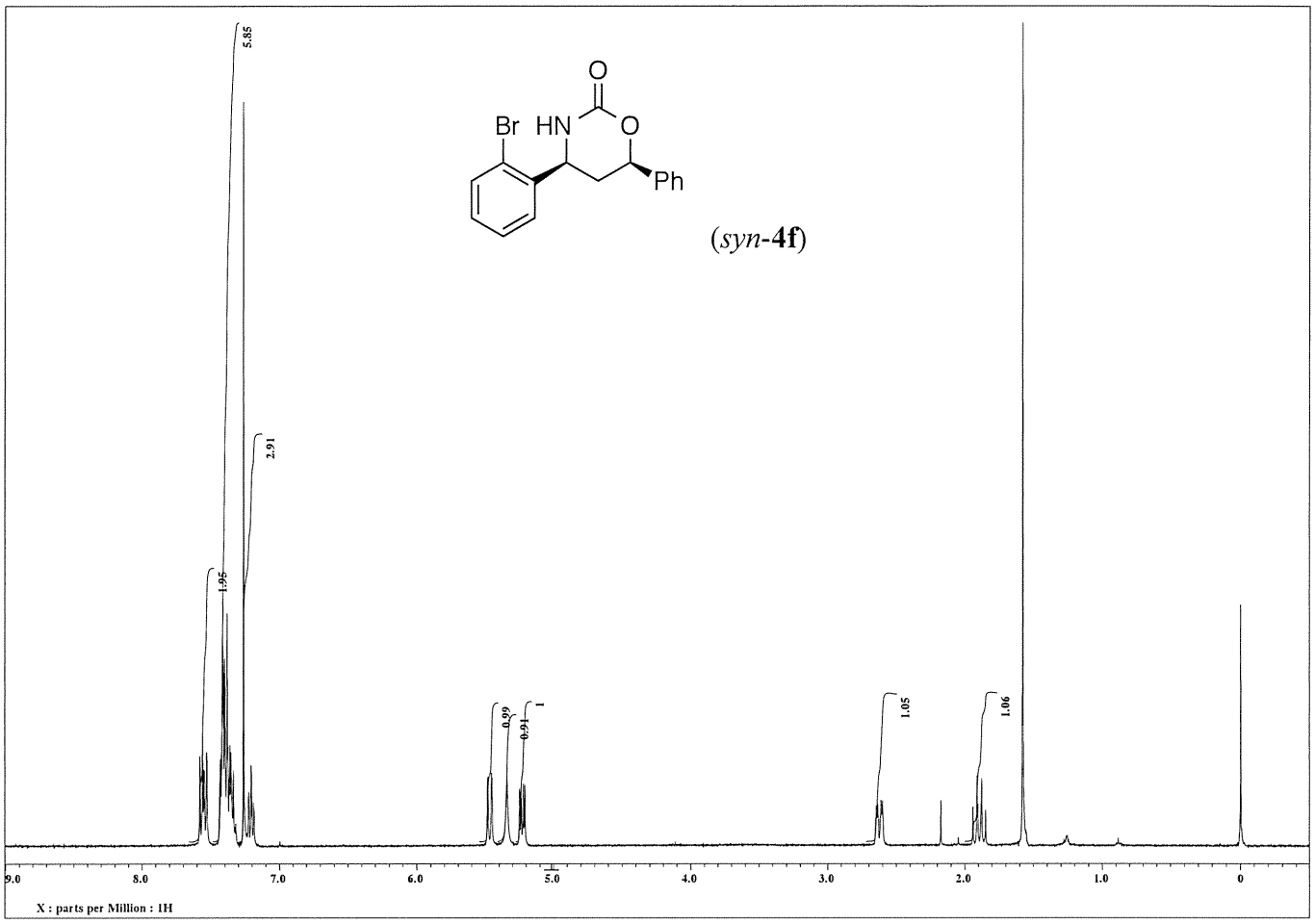

^{1}H NMR, 400 MHz, $CDCl_3$

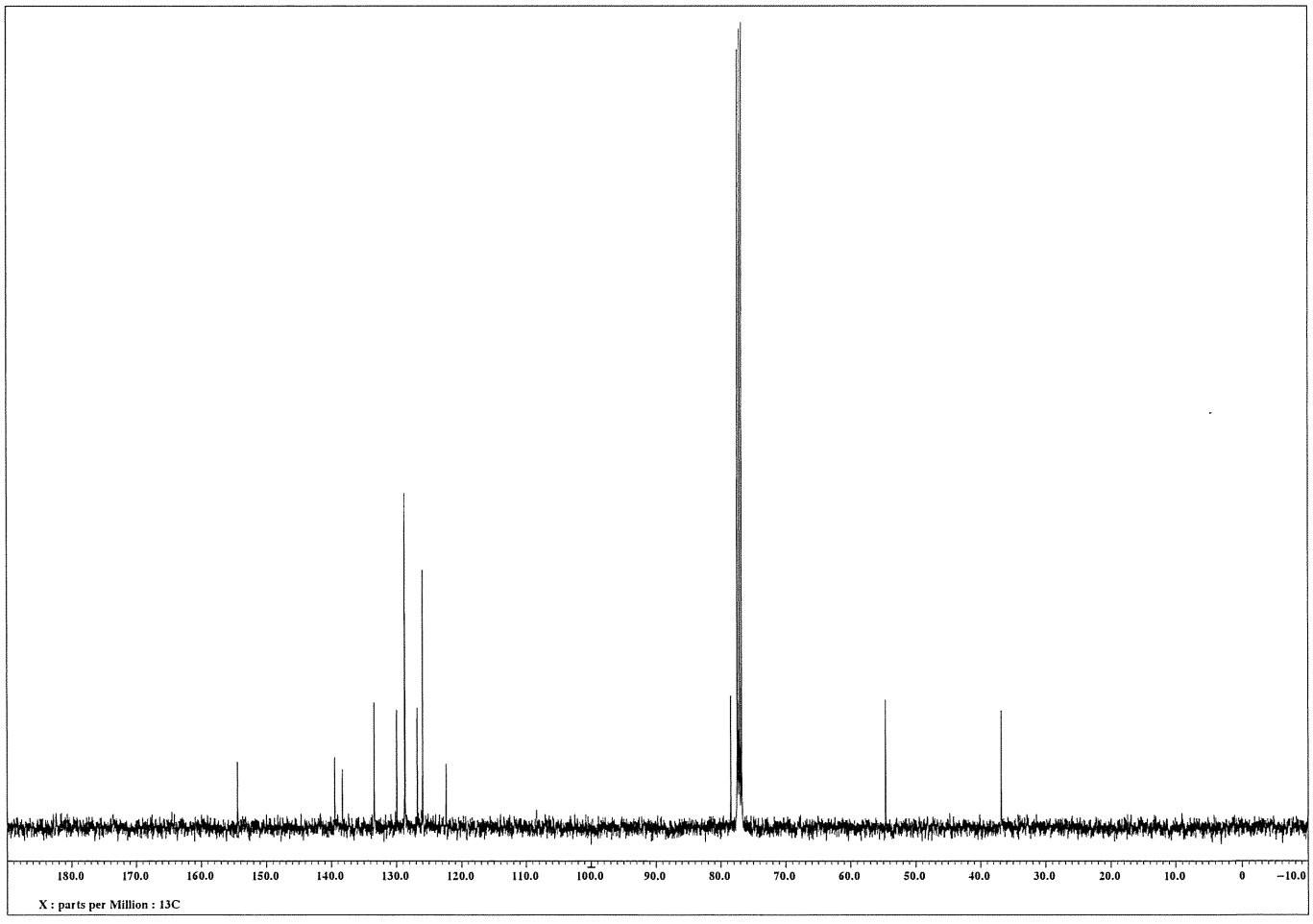

^{13}C NMR, 100 MHz, $CDCl_3$

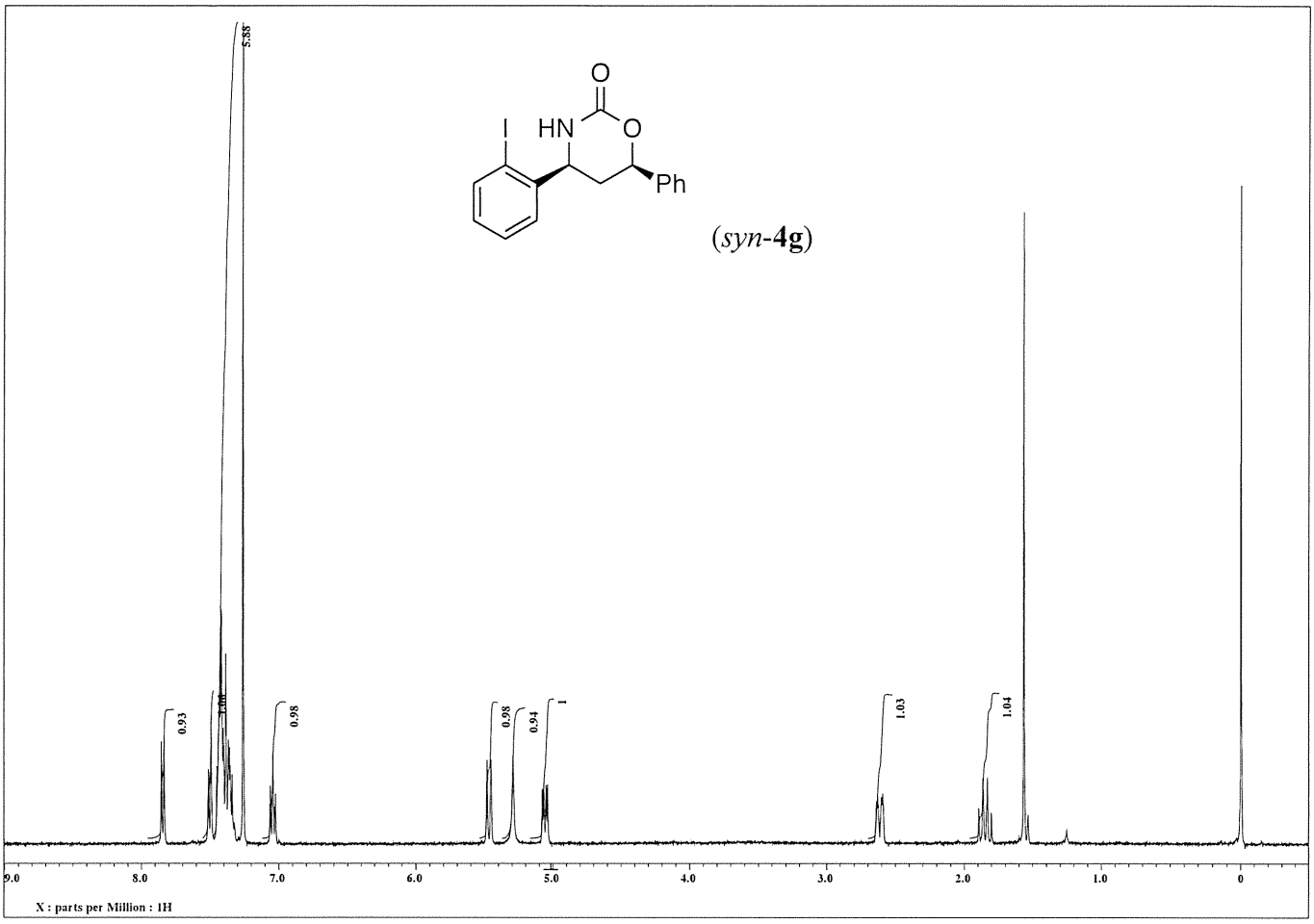

^{1}H NMR, 400 MHz, $CDCl_3$

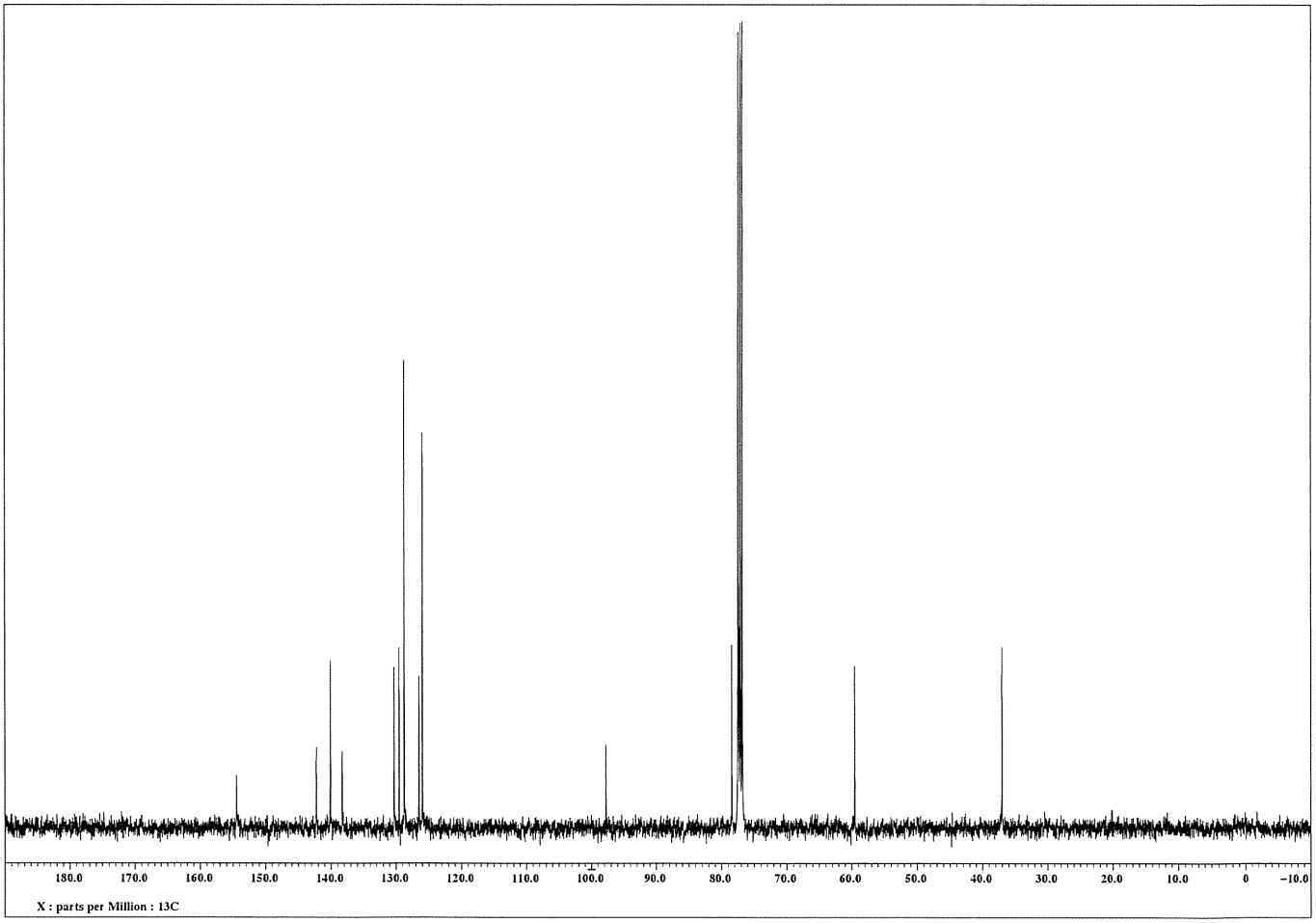

^{13}C NMR, 100 MHz, $CDCl_3$

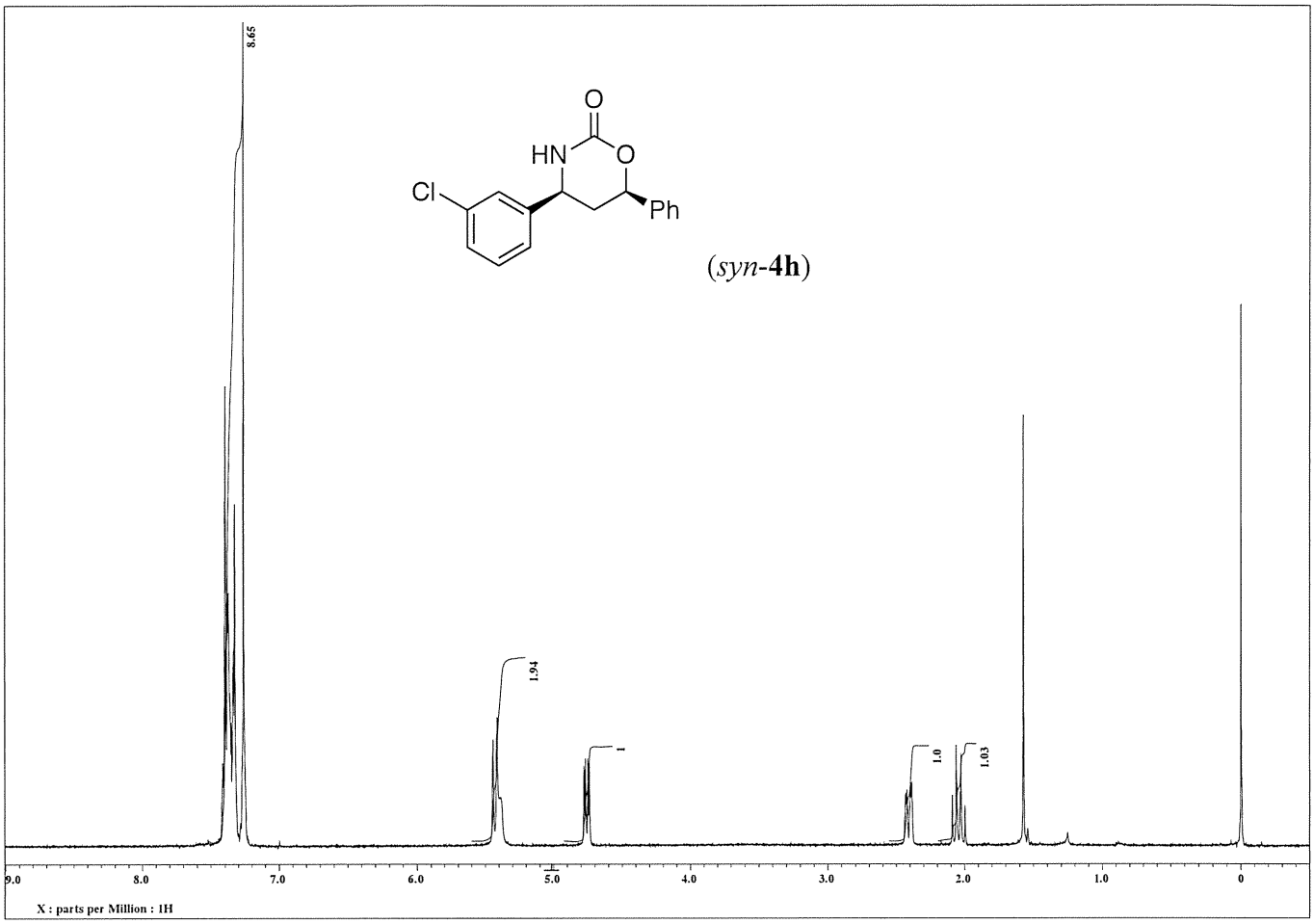

(*syn*-**4h**)

^{1}H NMR, 400 MHz, $CDCl_3$

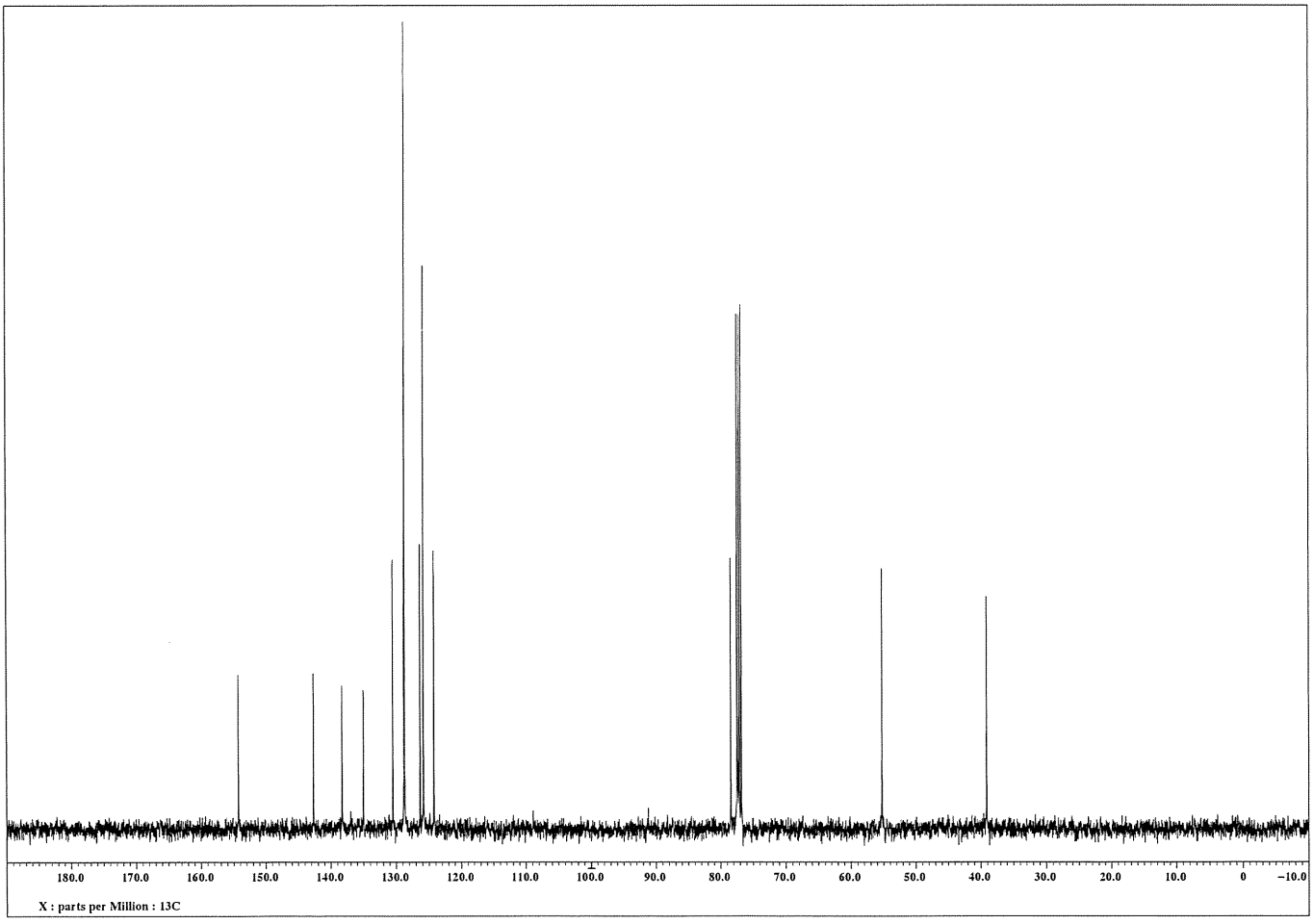

^{13}C NMR, 100 MHz, $CDCl_3$

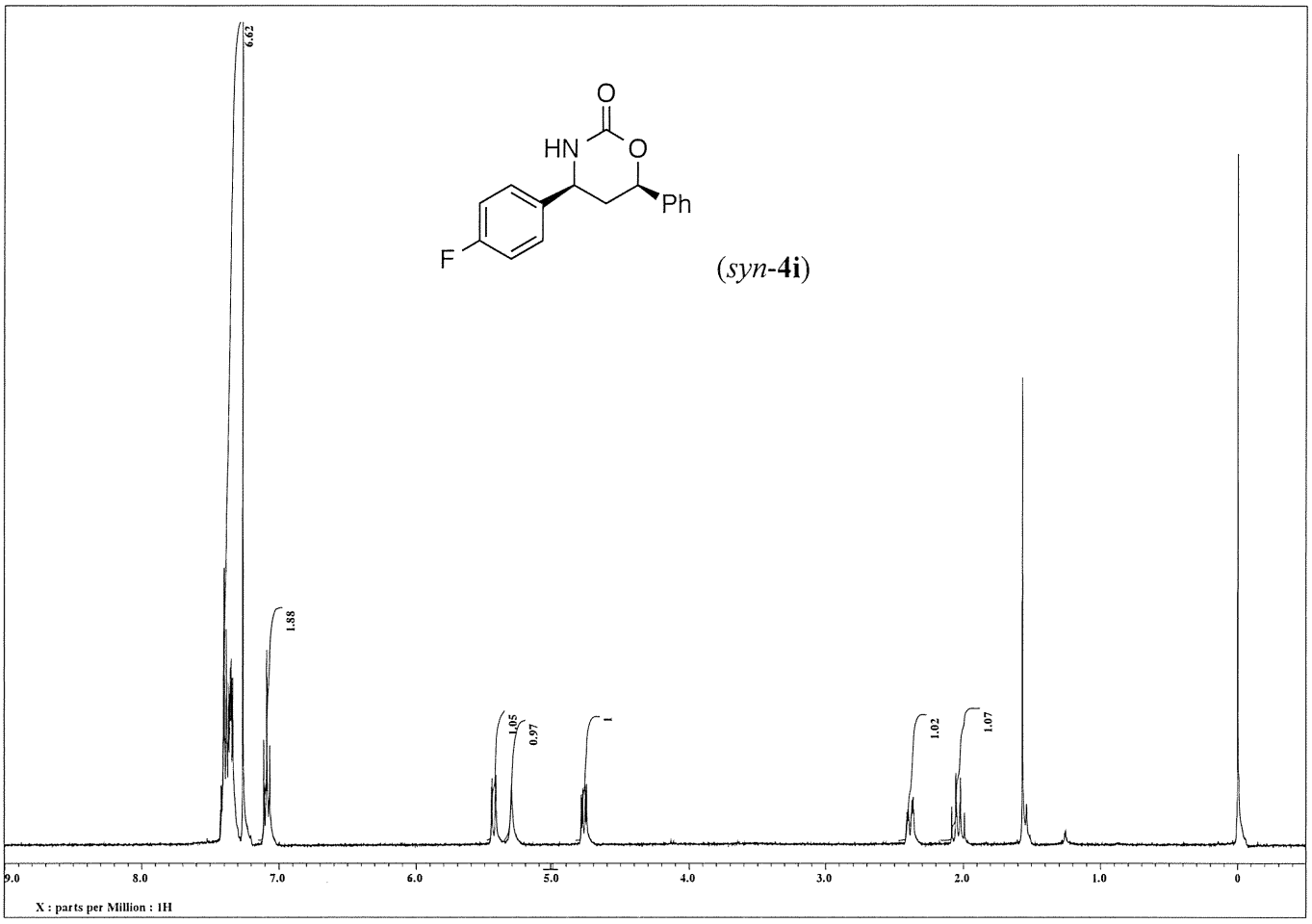

^{1}H NMR, 400 MHz, $CDCl_3$

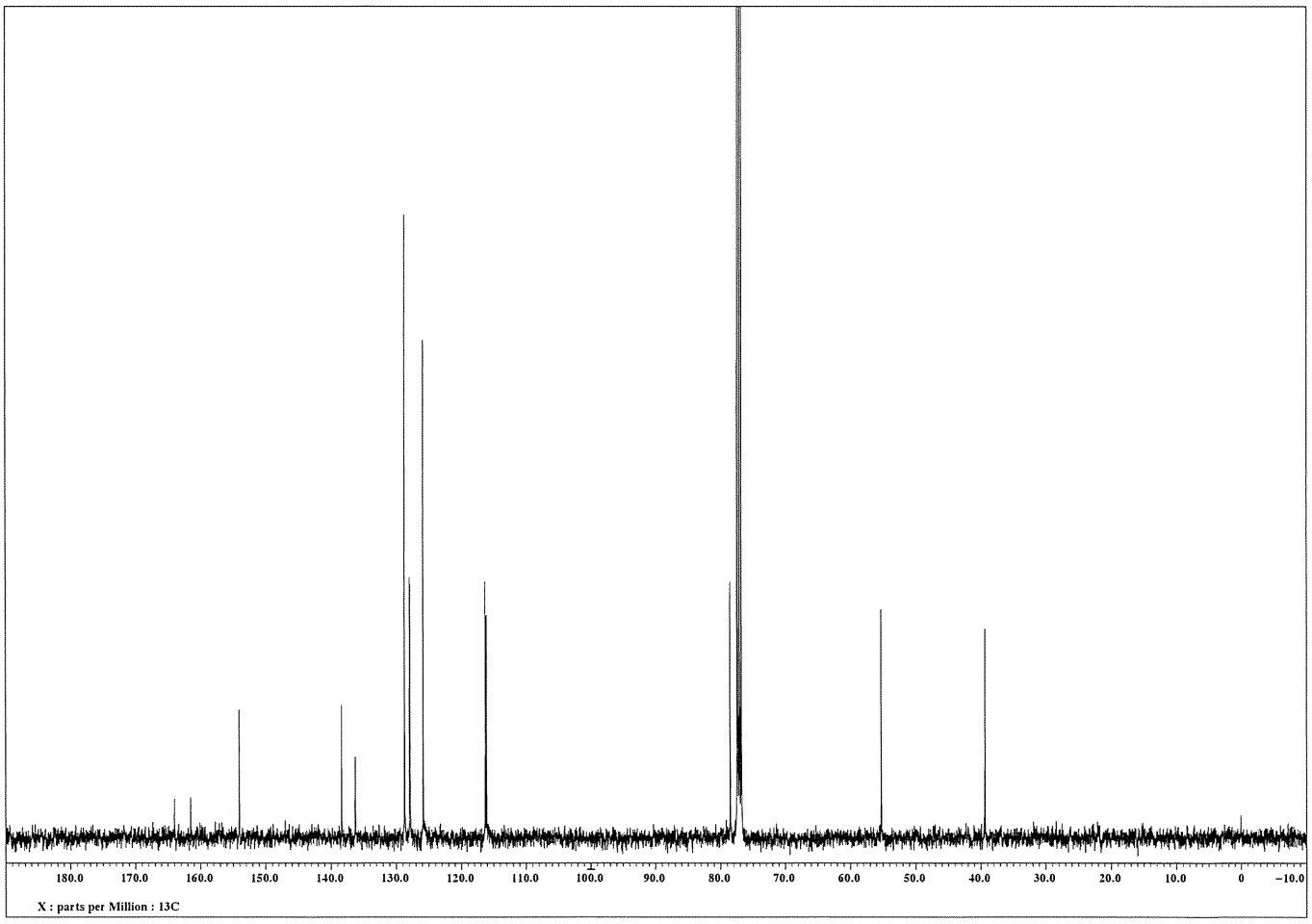

^{13}C NMR, 100 MHz, $CDCl_3$

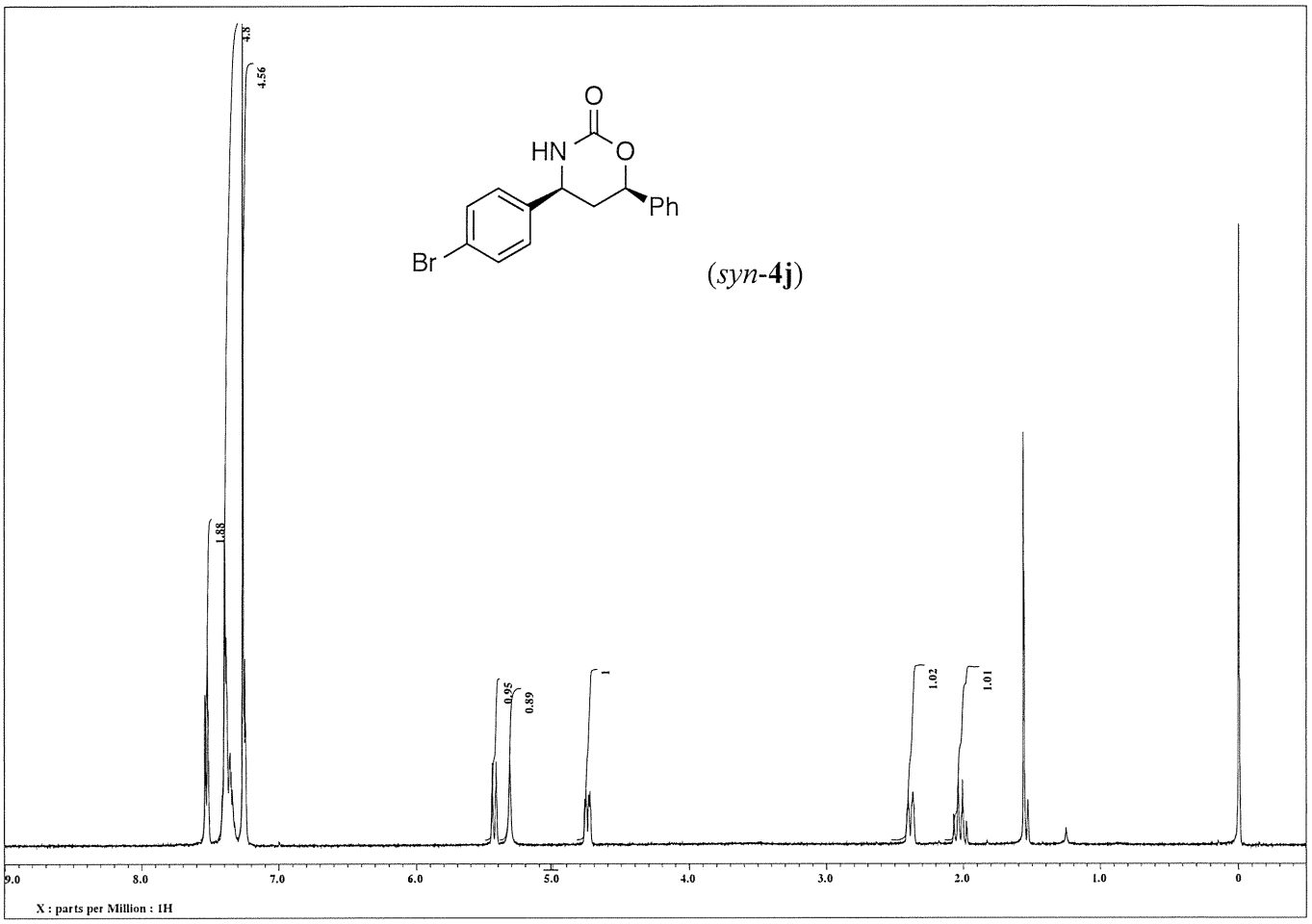

(*syn*-**4j**)

^{1}H NMR, 400 MHz, $CDCl_3$

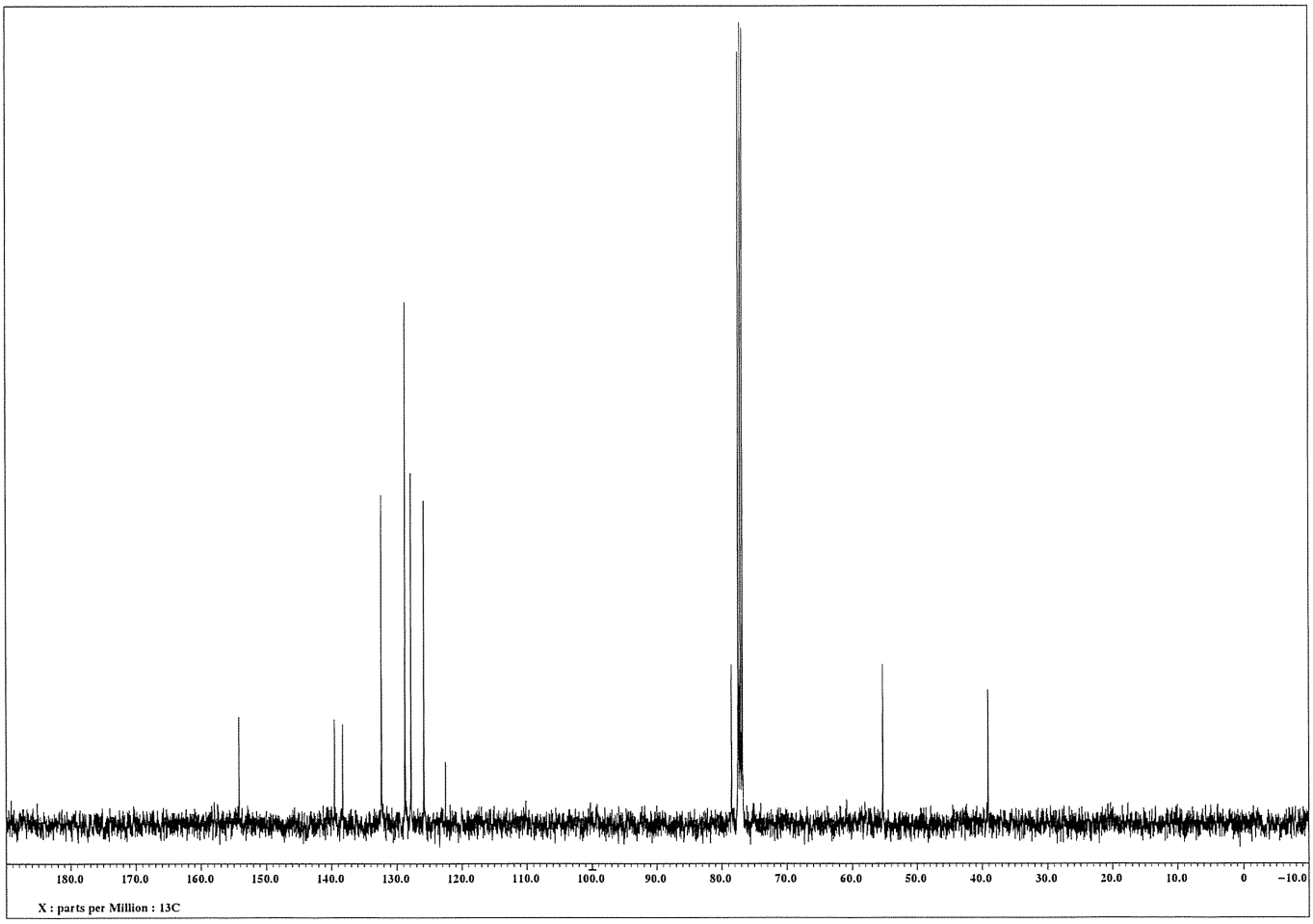

^{13}C NMR, 100 MHz, $CDCl_3$

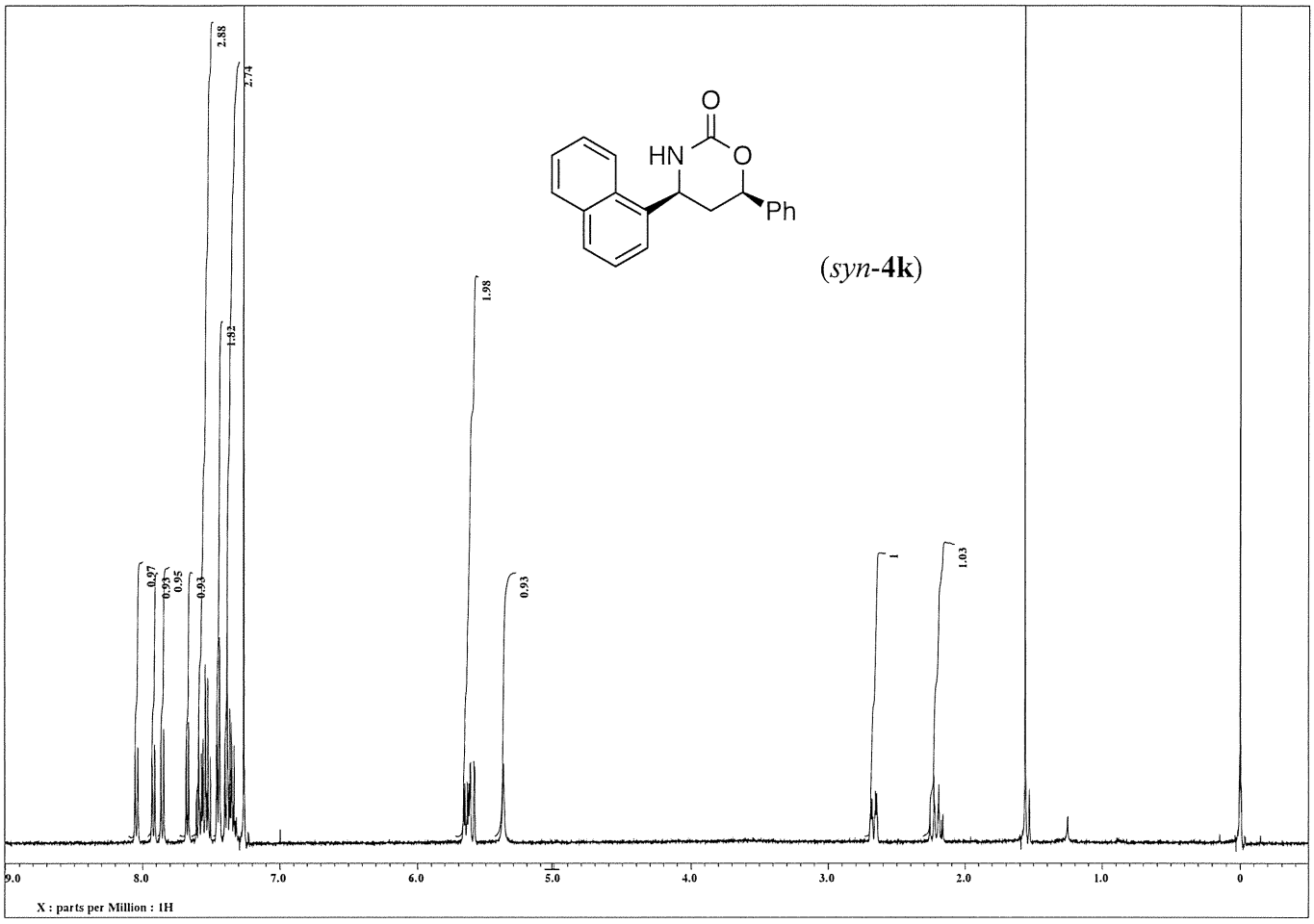

^{1}H NMR, 400 MHz, $CDCl_3$

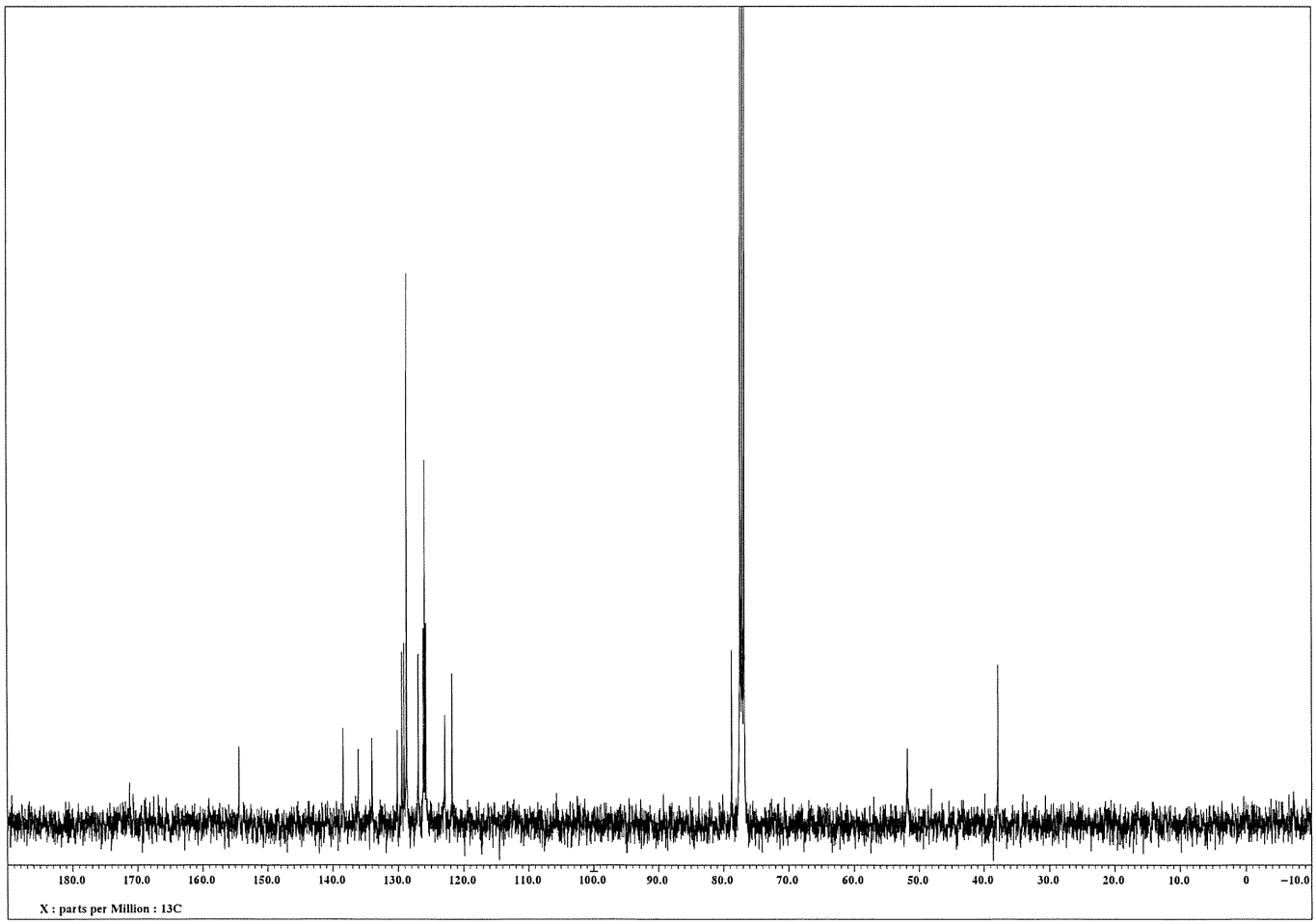

^{13}C NMR, 100 MHz, $CDCl_3$

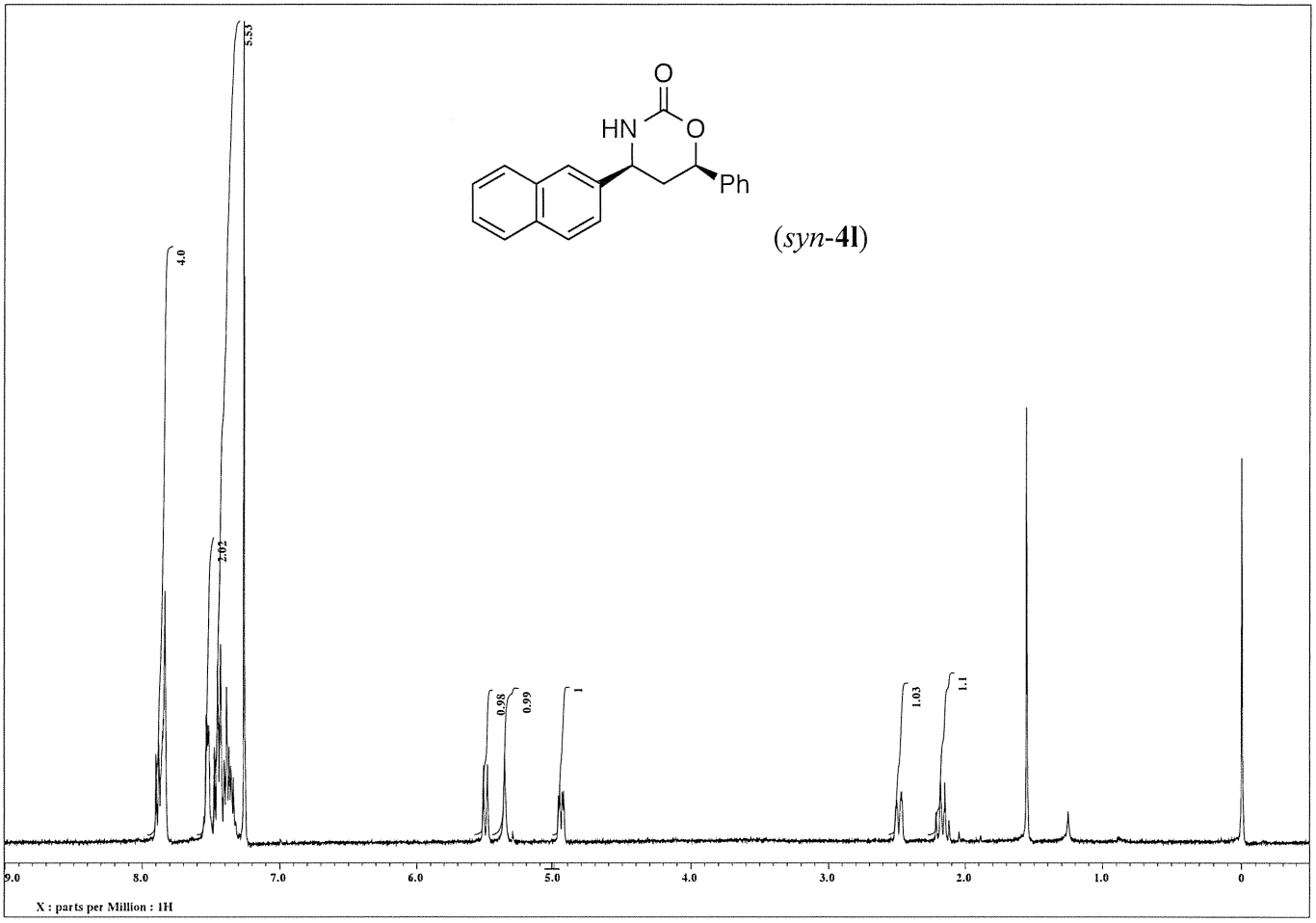

^{1}H NMR, 400 MHz, $CDCl_3$

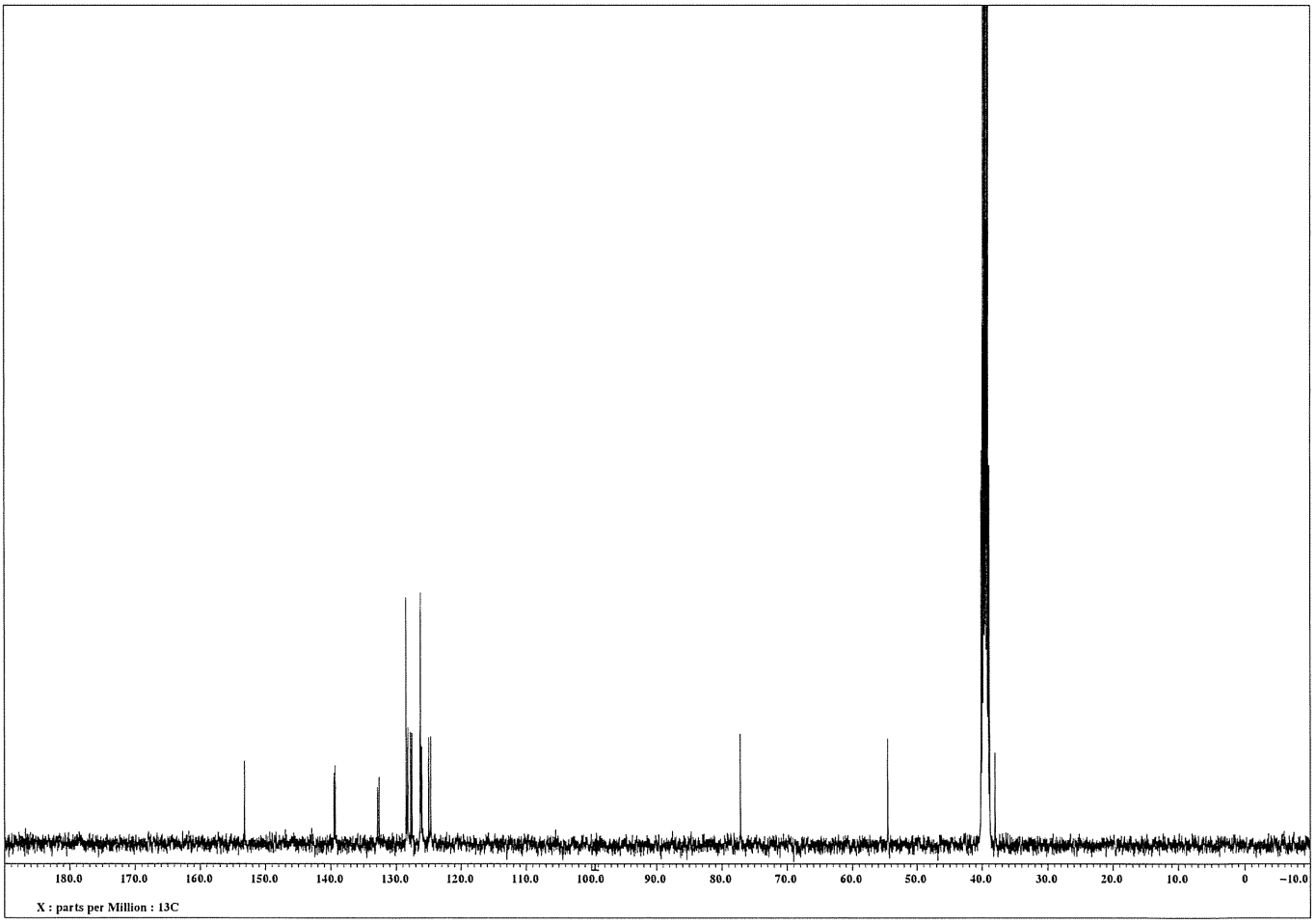

^{13}C NMR, 100 MHz, d_6-DMSO

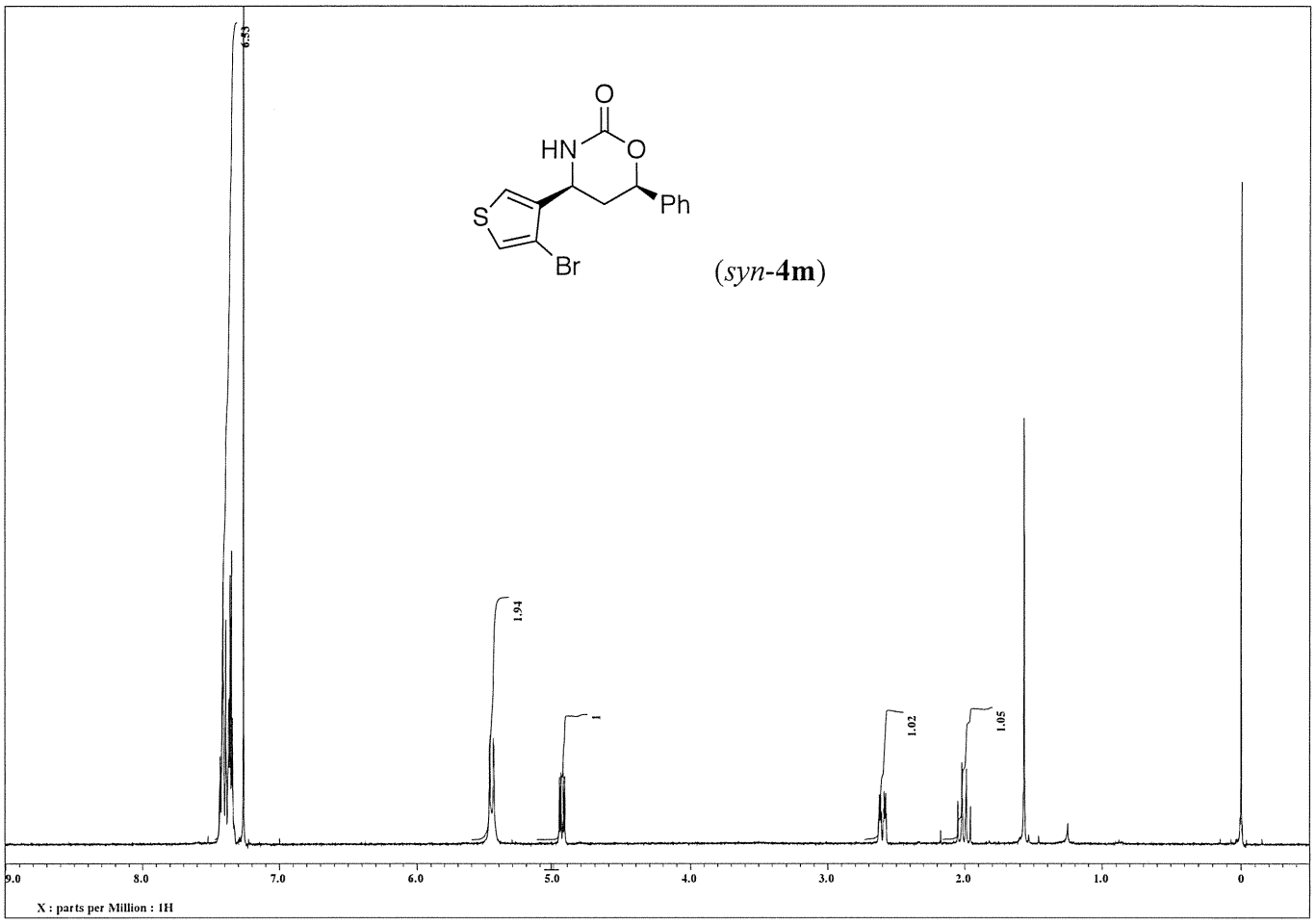

(*syn*-**4m**)

^{1}H NMR, 400 MHz, $CDCl_3$

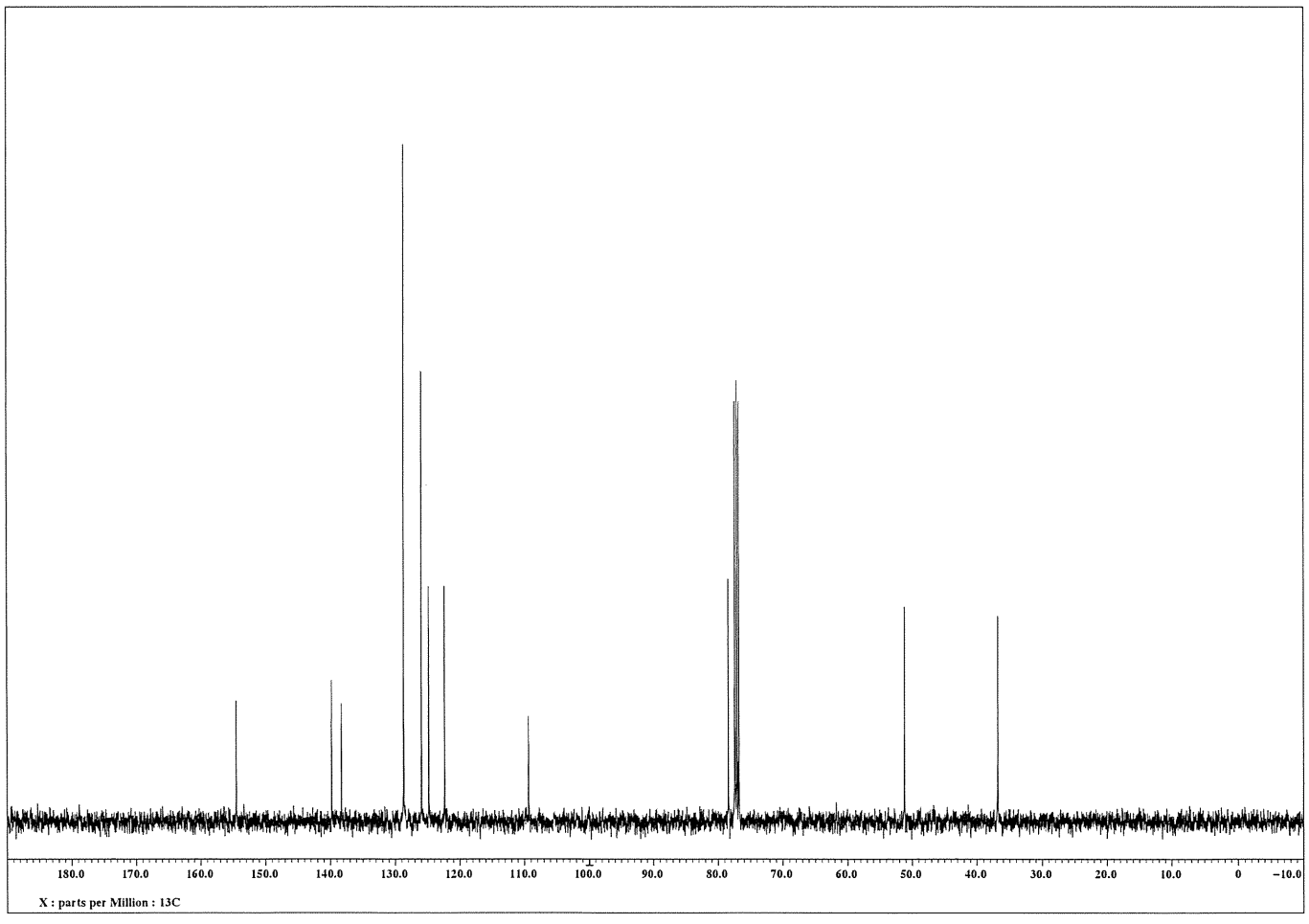

^{13}C NMR, 100 MHz, $CDCl_3$

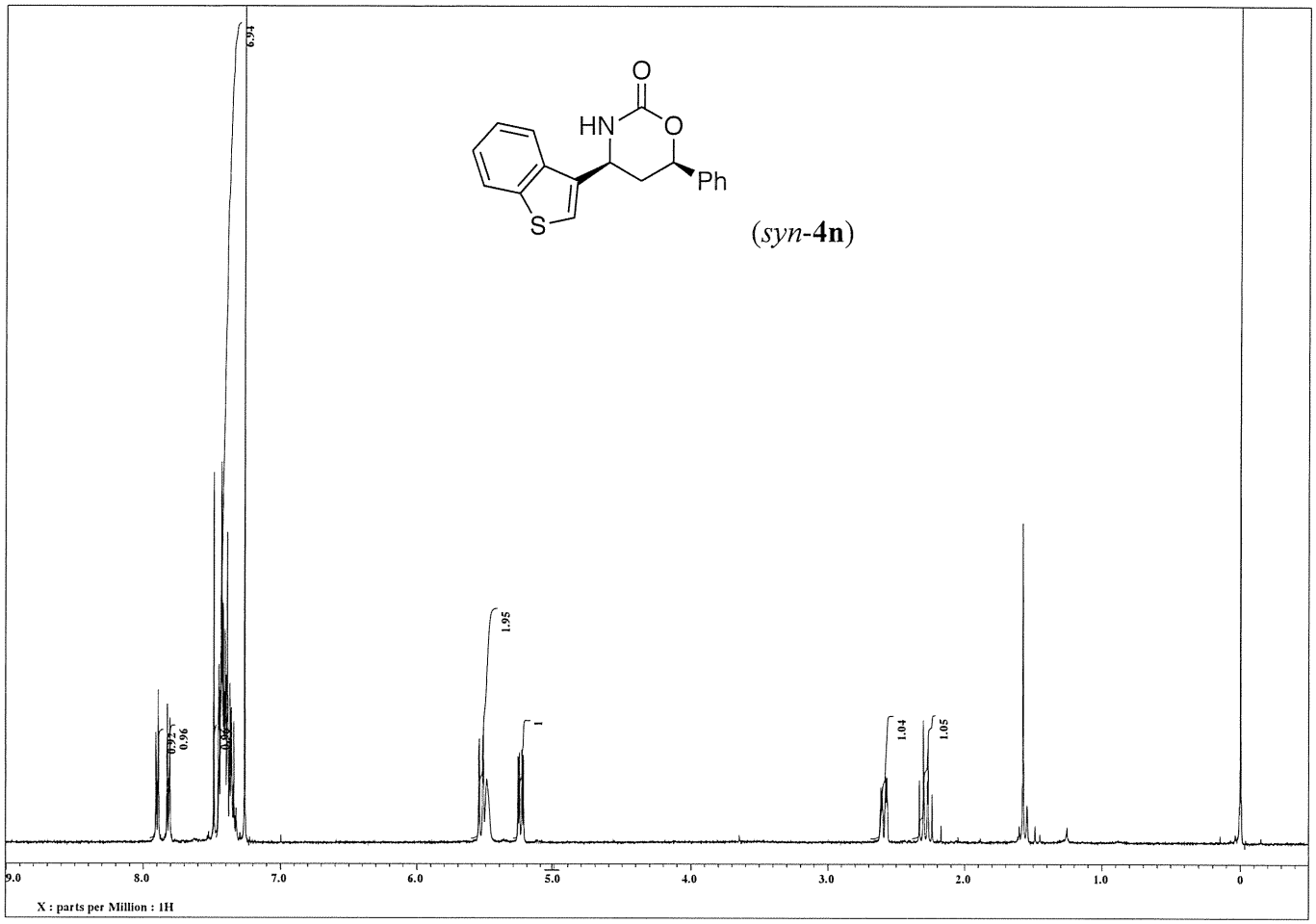

^{1}H NMR, 400 MHz, $CDCl_3$

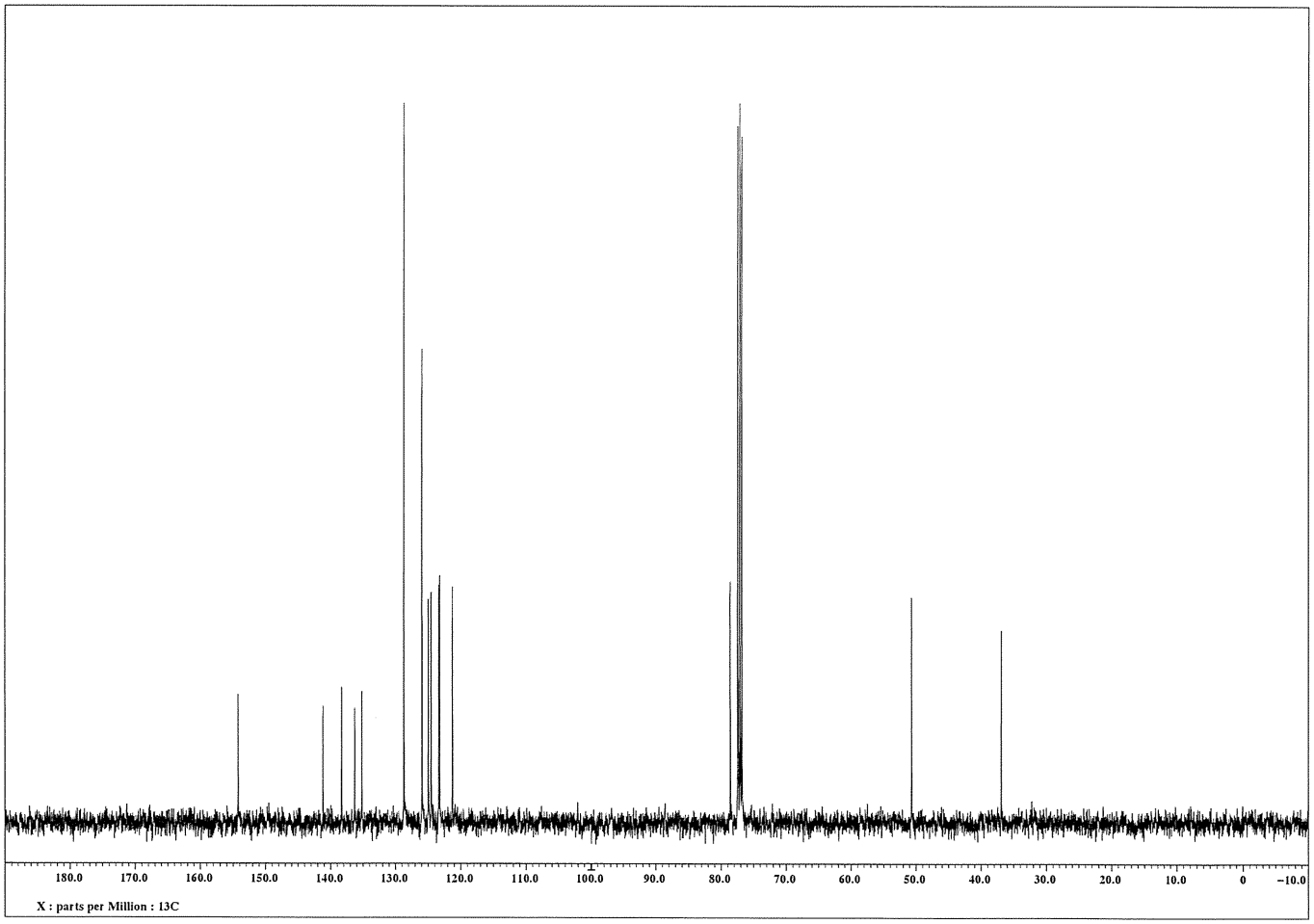

^{13}C NMR, 100 MHz, $CDCl_3$

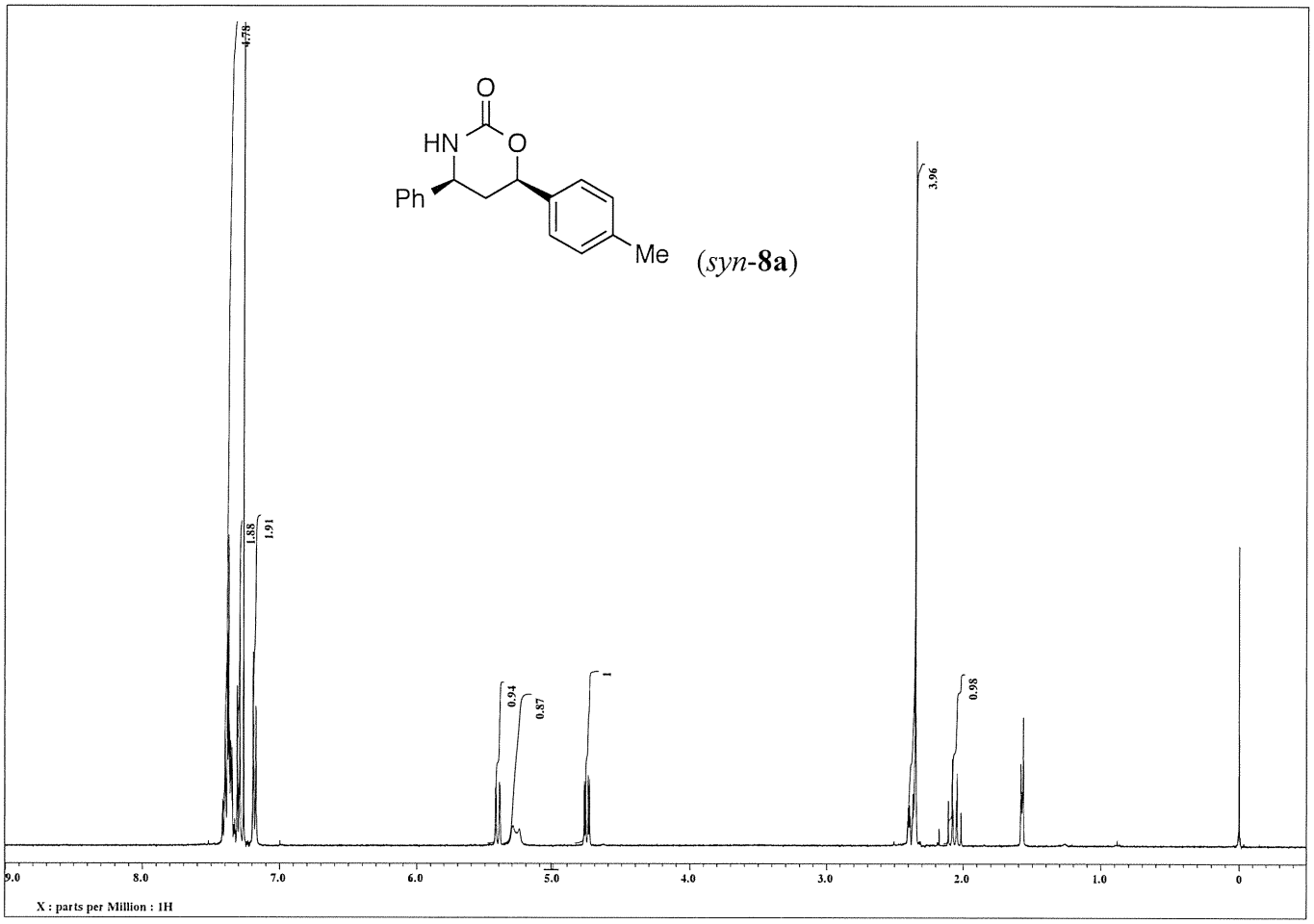

^{1}H NMR, 400 MHz, $CDCl_3$

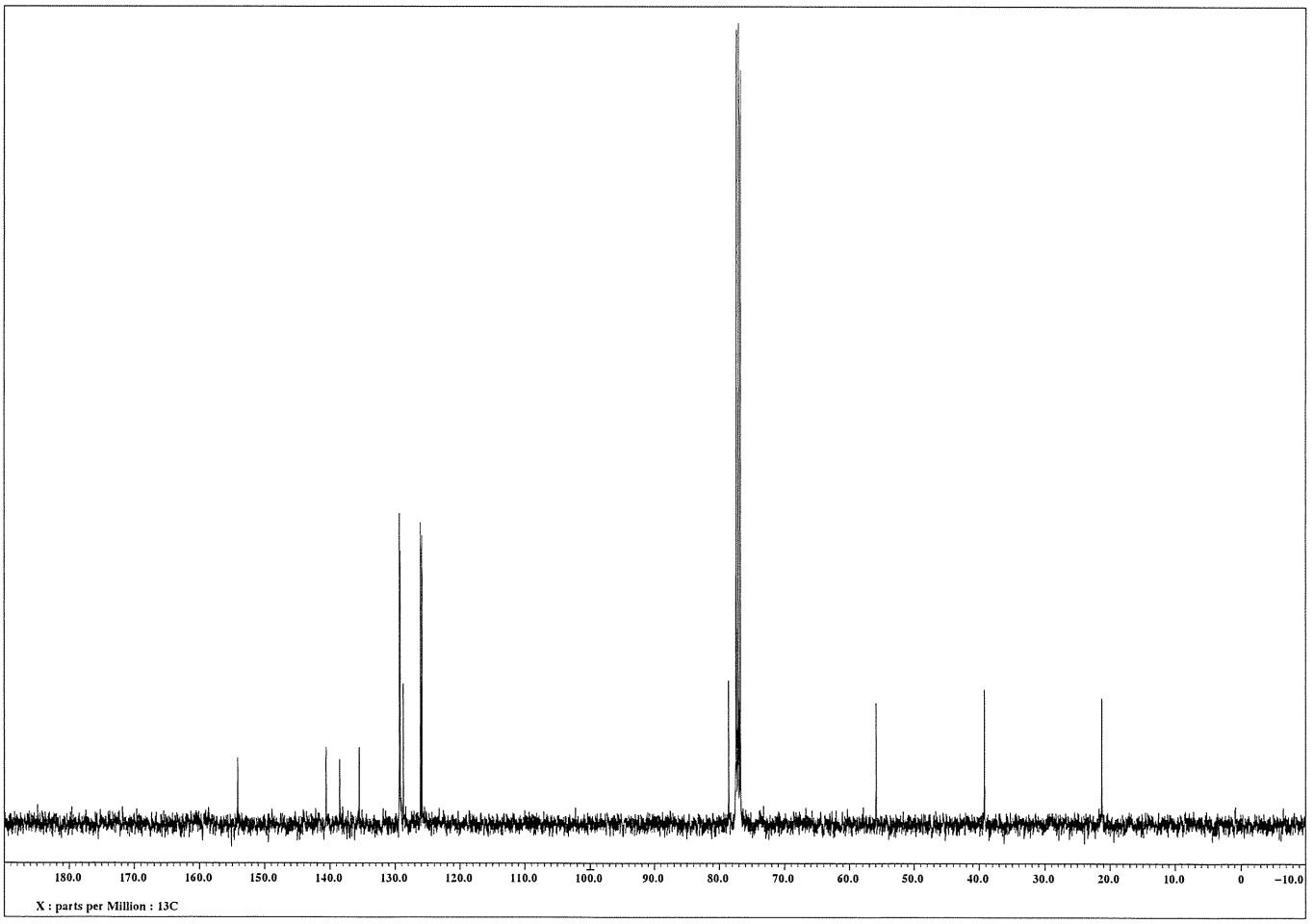

^{13}C NMR, 100 MHz, $CDCl_3$

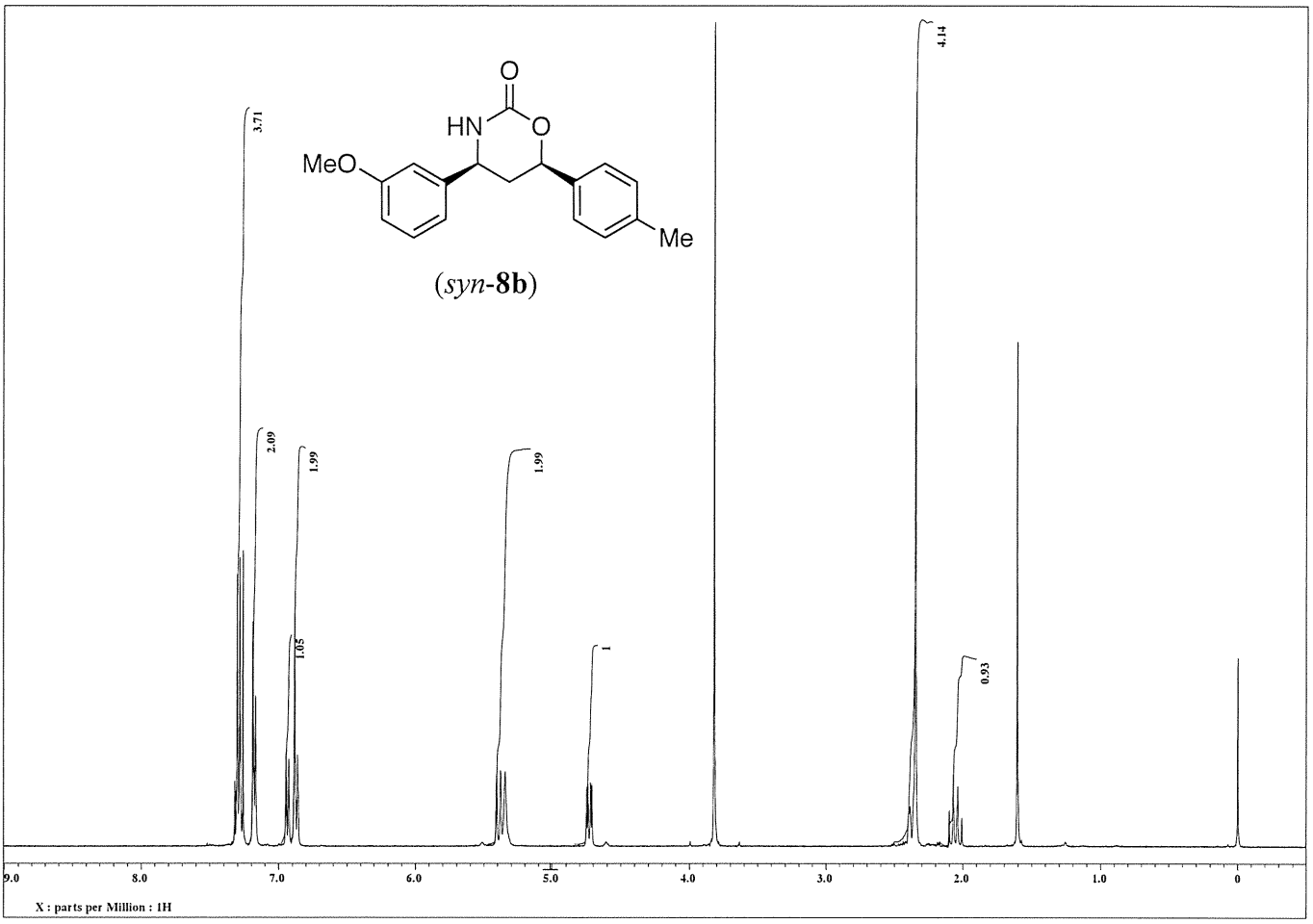

(*syn*-**8b**)

^{1}H NMR, 400 MHz, $CDCl_3$

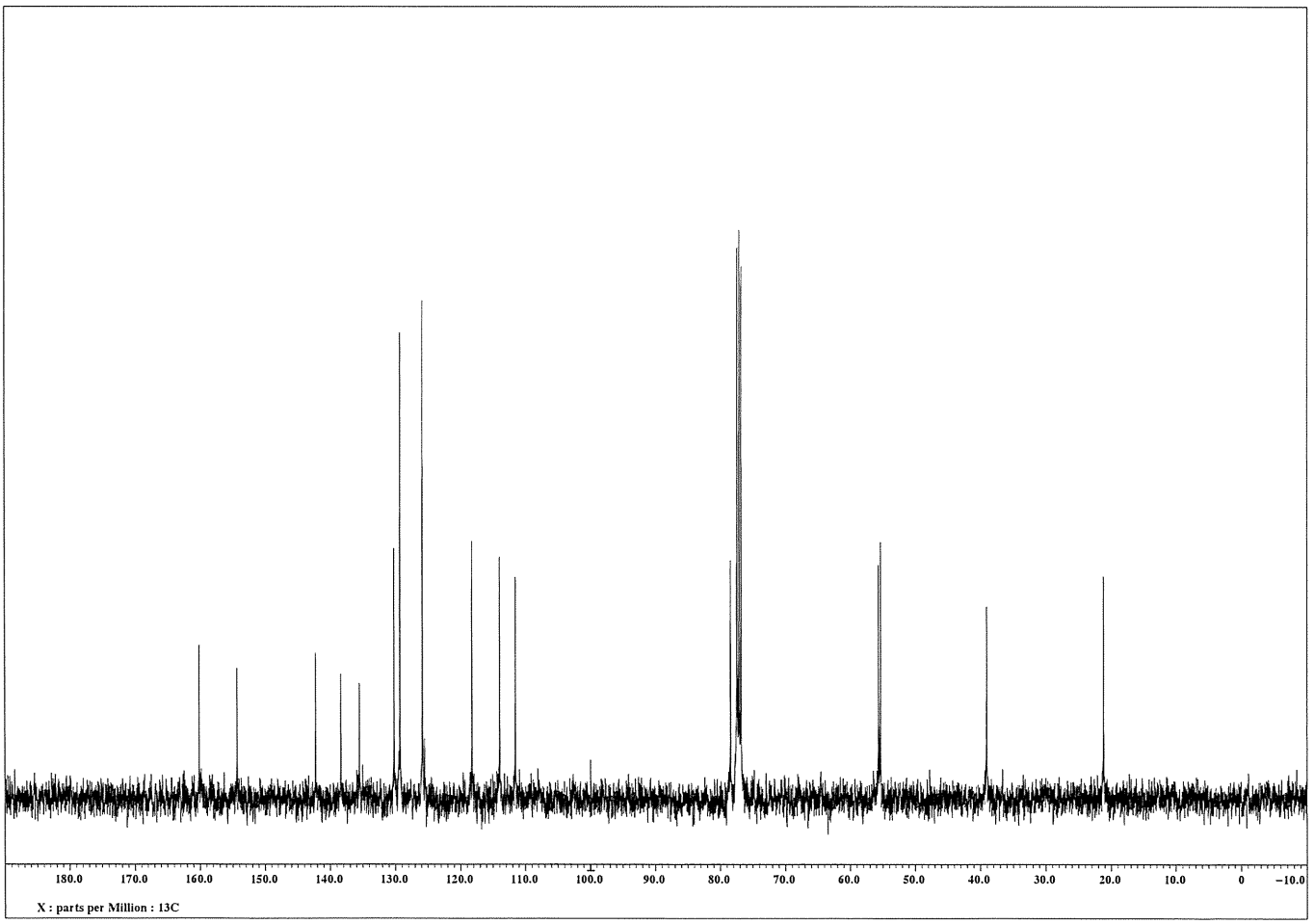

^{13}C NMR, 100 MHz, $CDCl_3$

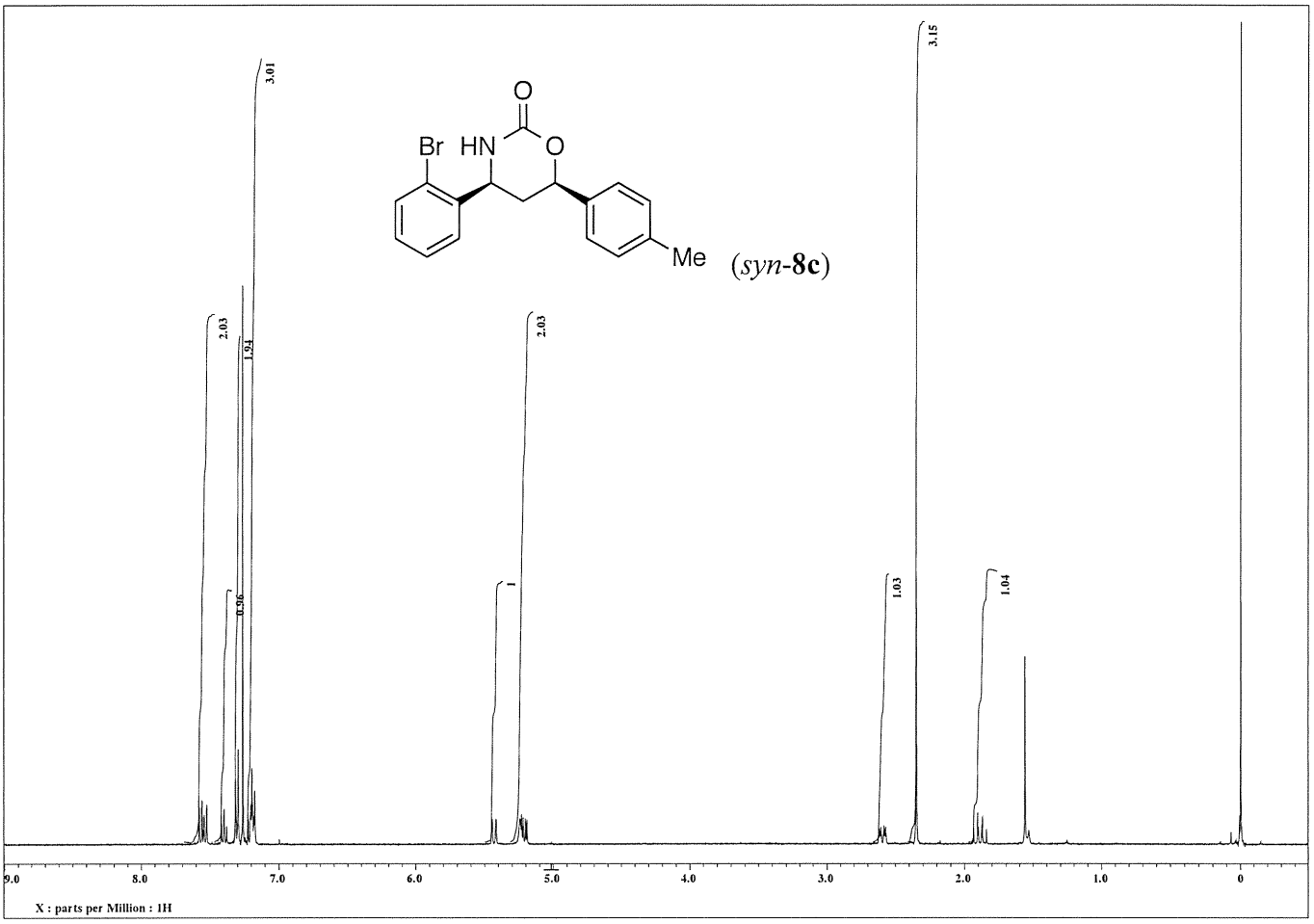

^{1}H NMR, 400 MHz, $CDCl_3$

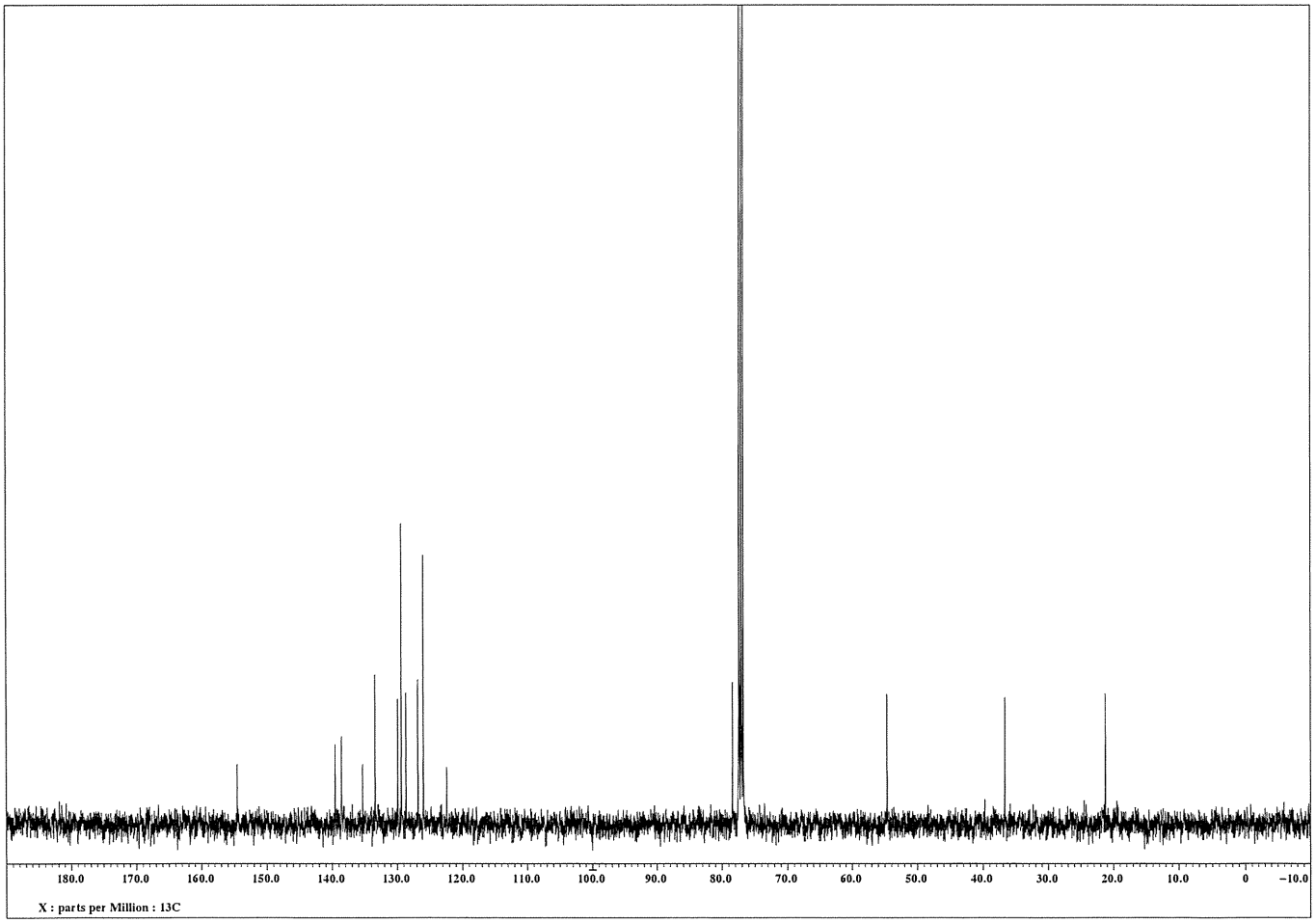

^{13}C NMR, 100 MHz, $CDCl_3$

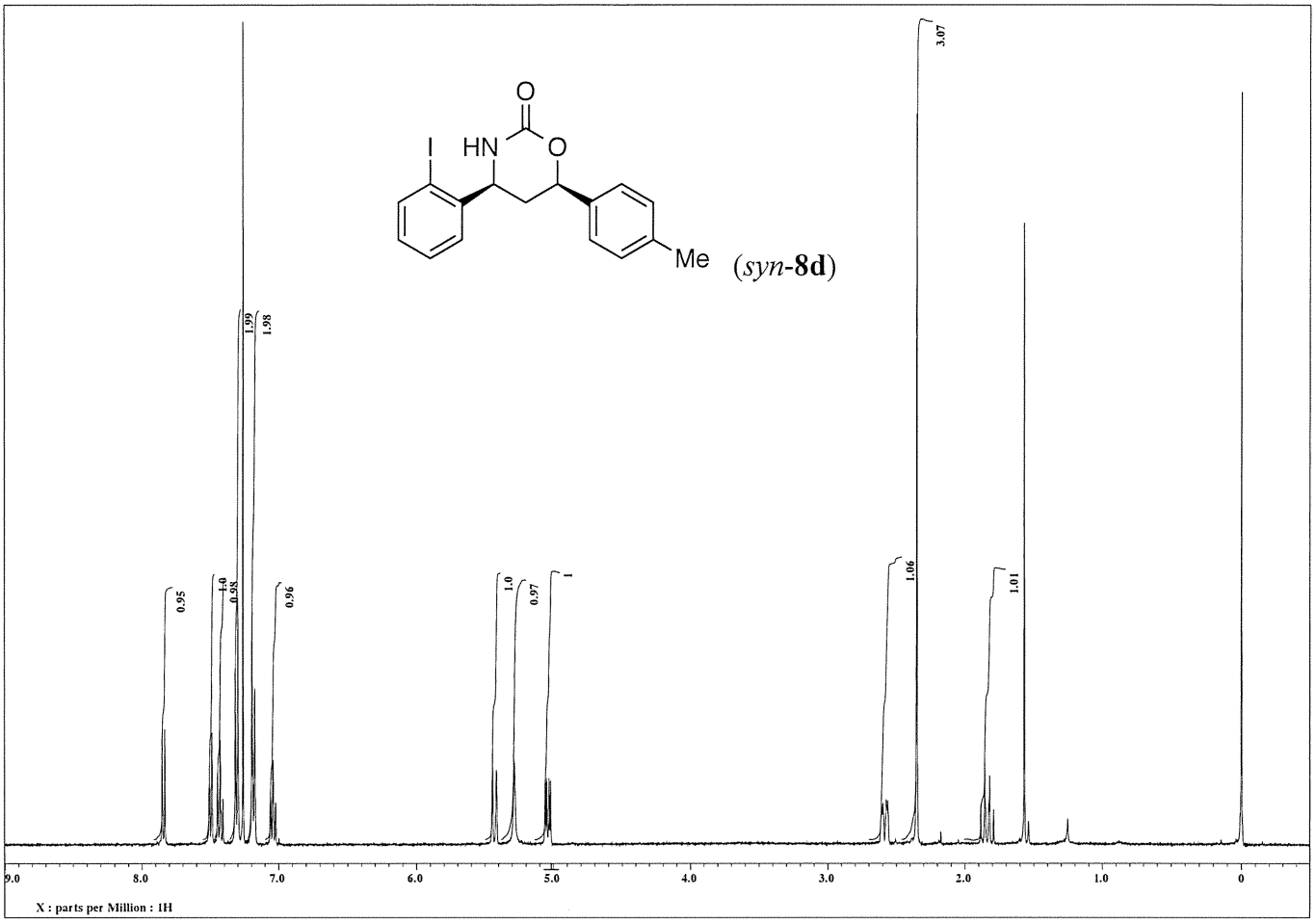

^{1}H NMR, 400 MHz, $CDCl_3$

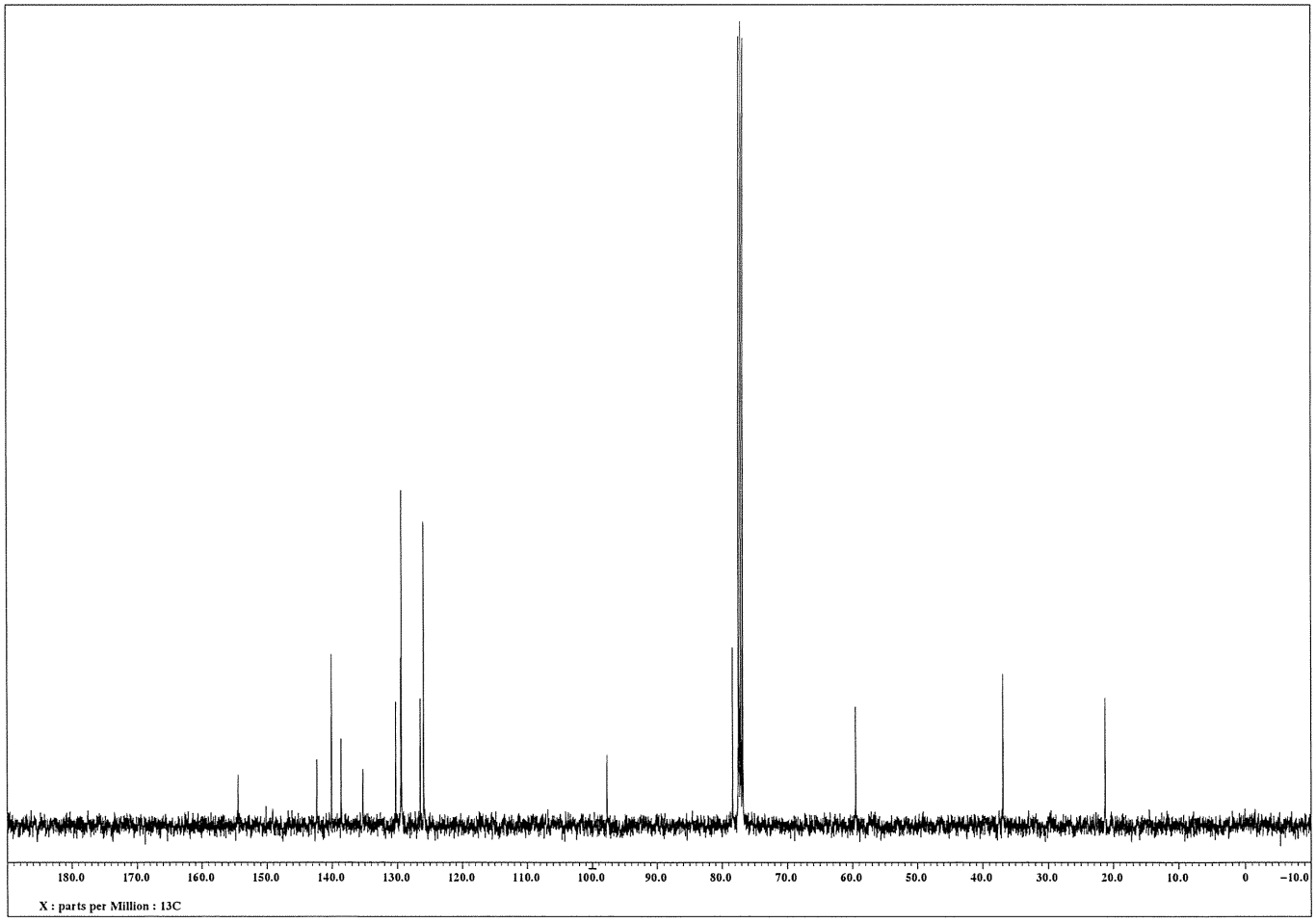

^{13}C NMR, 100 MHz, $CDCl_3$

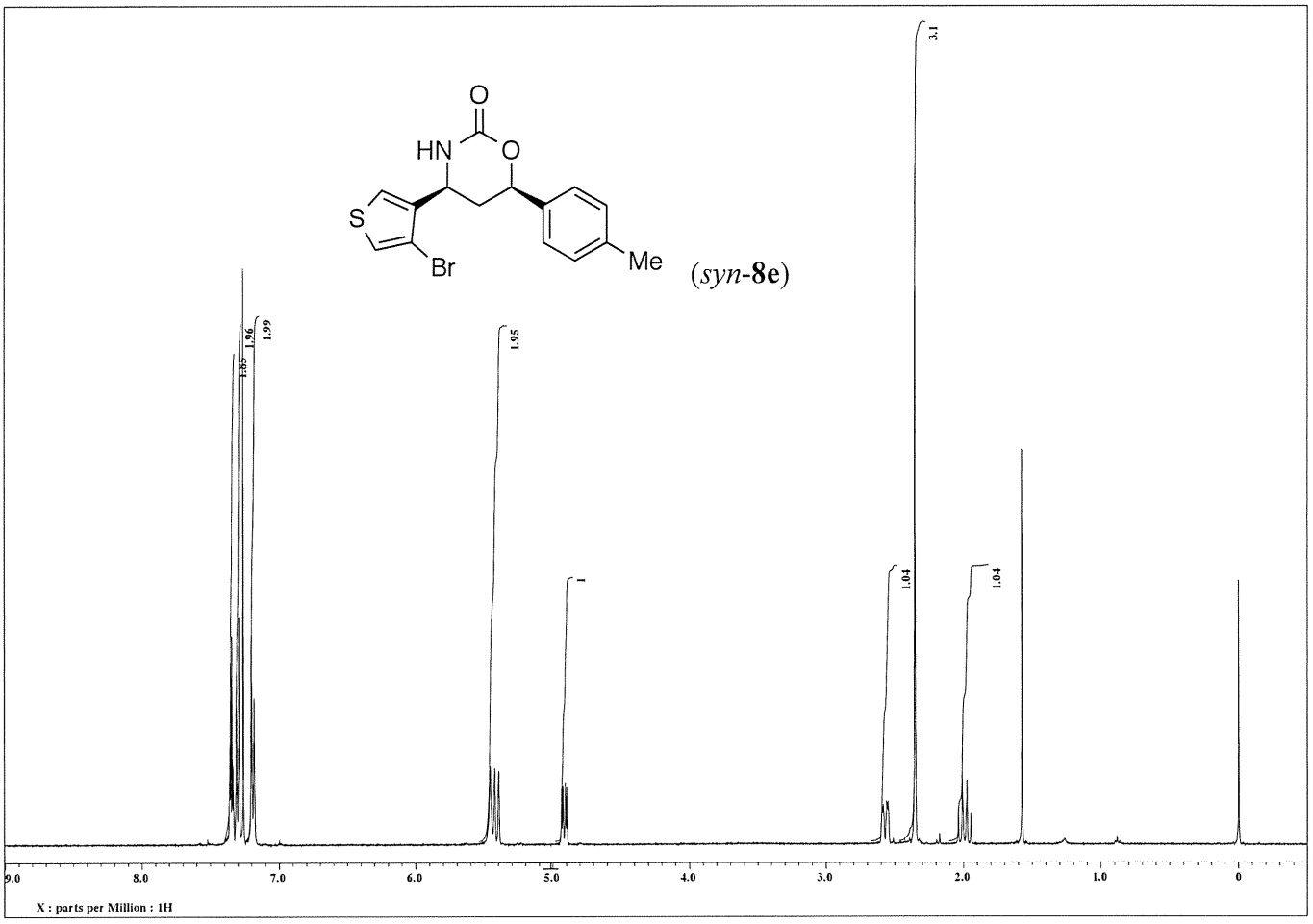

^{1}H NMR, 400 MHz, $CDCl_3$

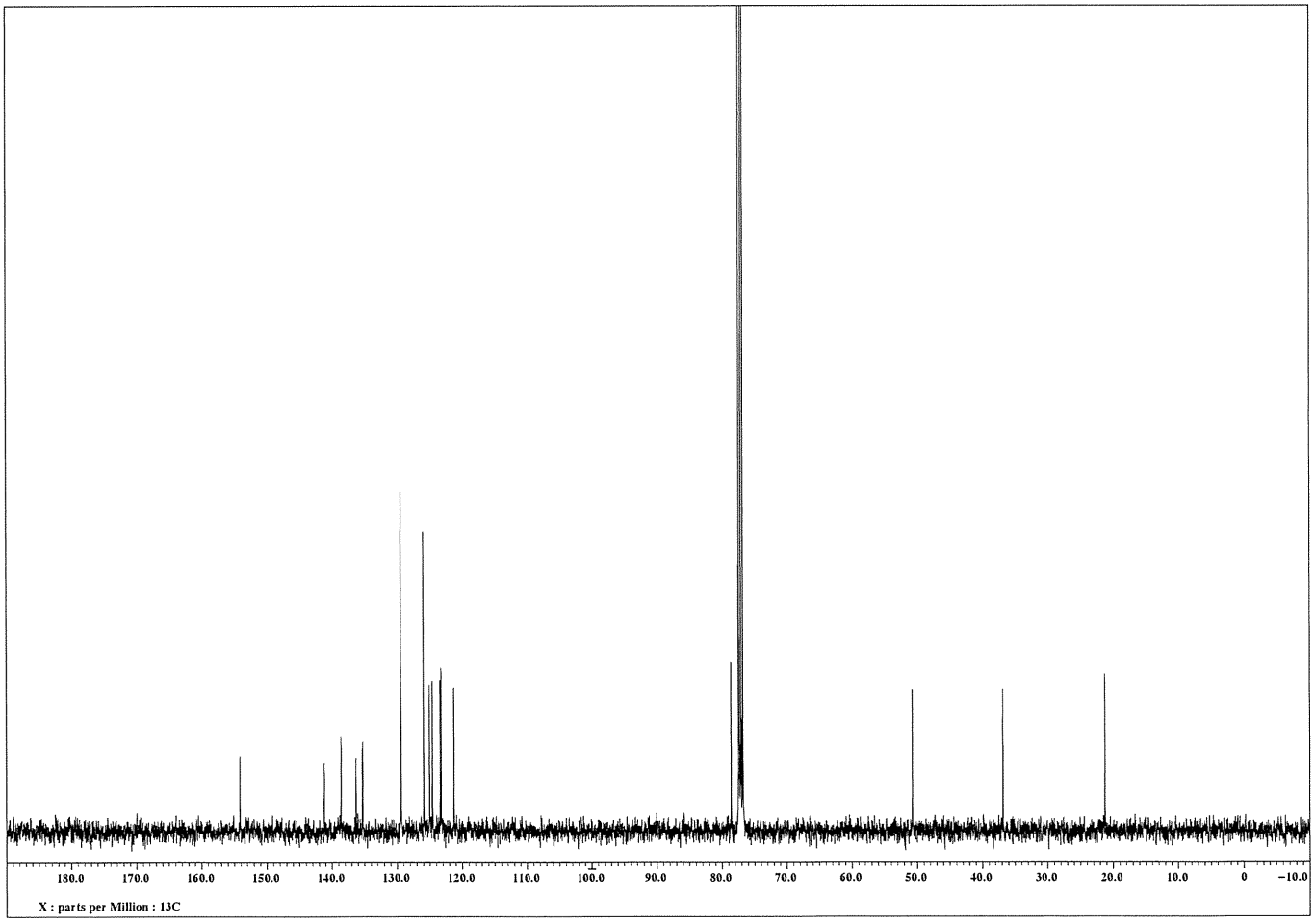

^{13}C NMR, 100 MHz, $CDCl_3$

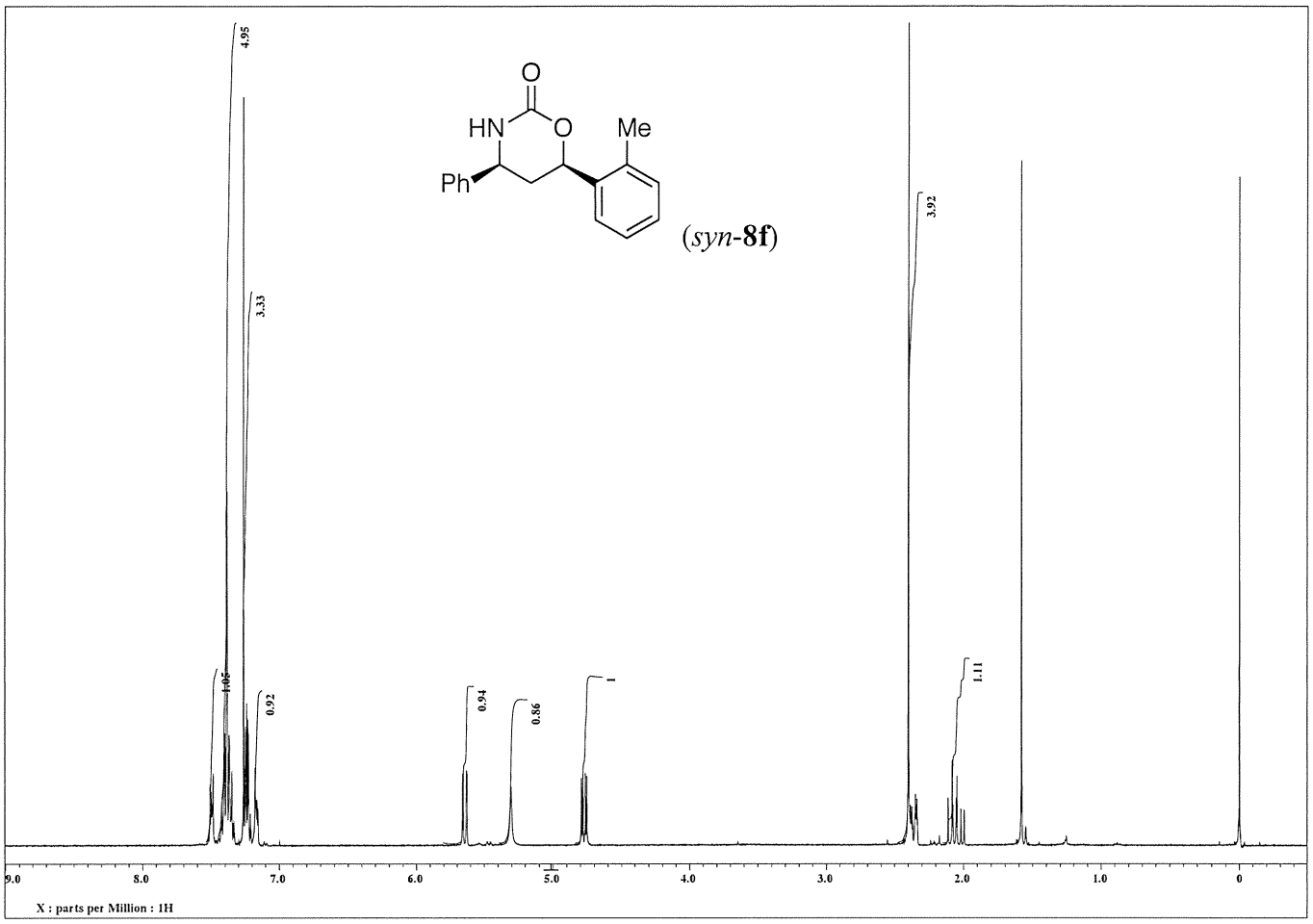

^{1}H NMR, 400 MHz, $CDCl_3$

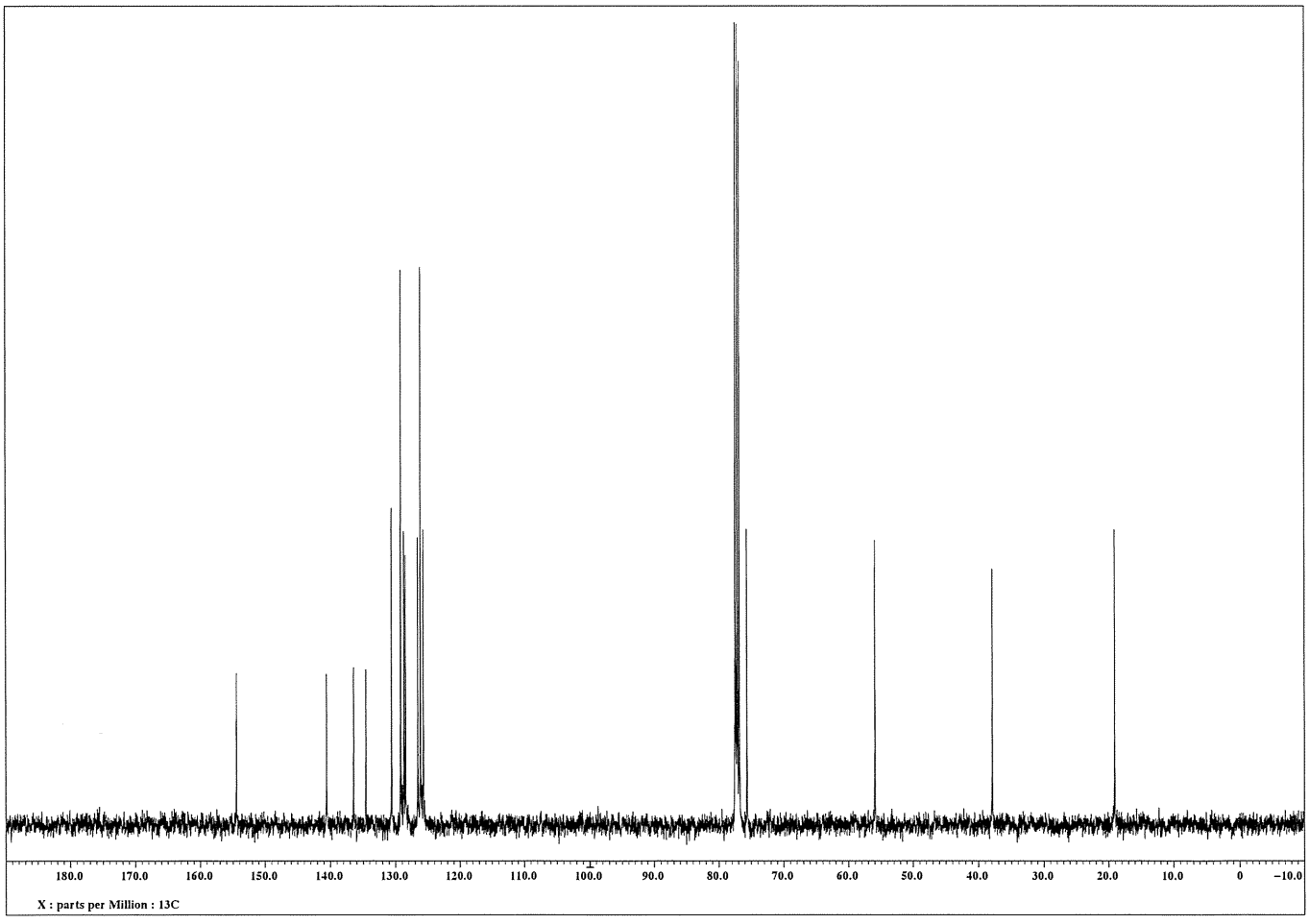

^{13}C NMR, 100 MHz, $CDCl_3$

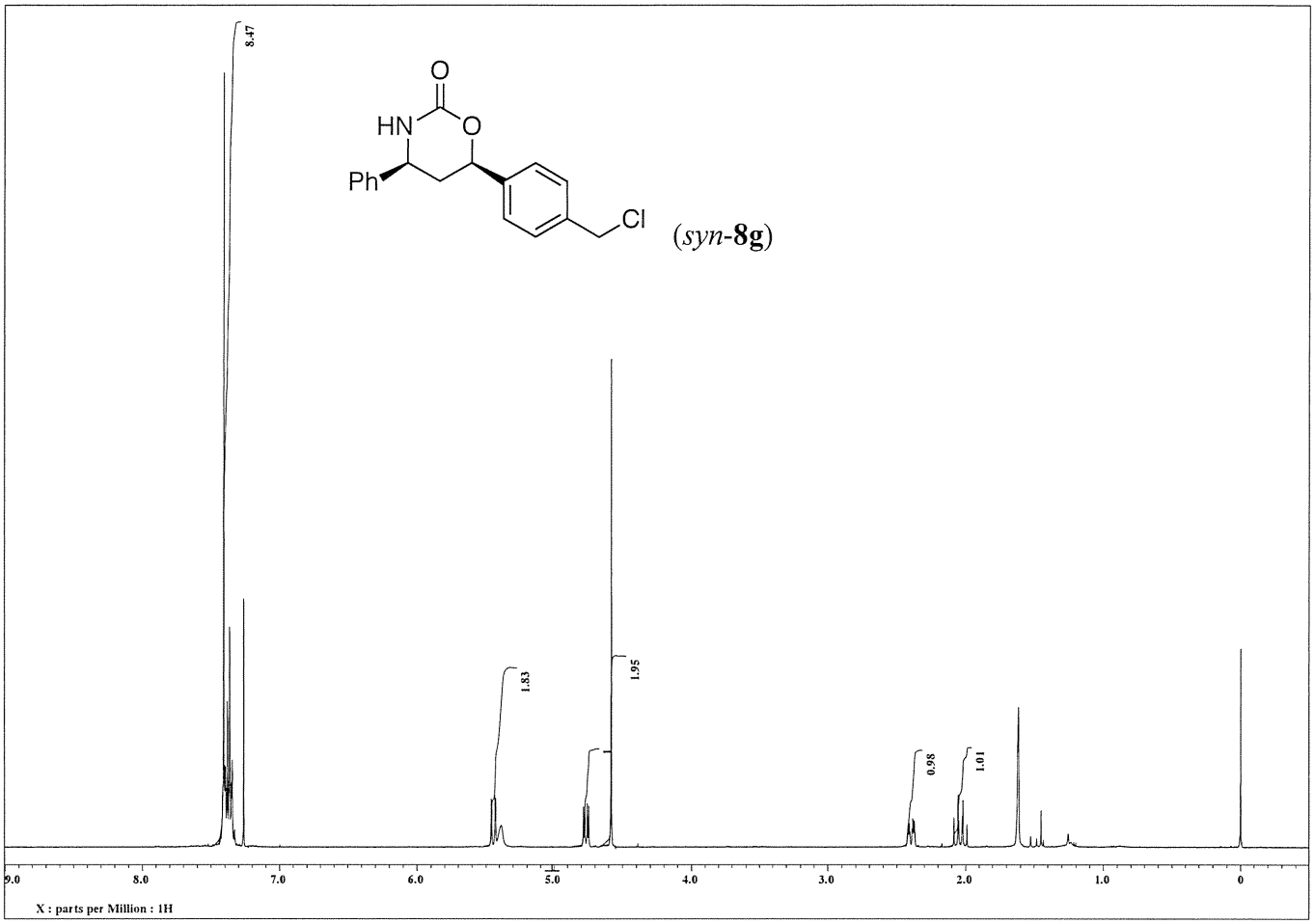

^{1}H NMR, 400 MHz, $CDCl_3$

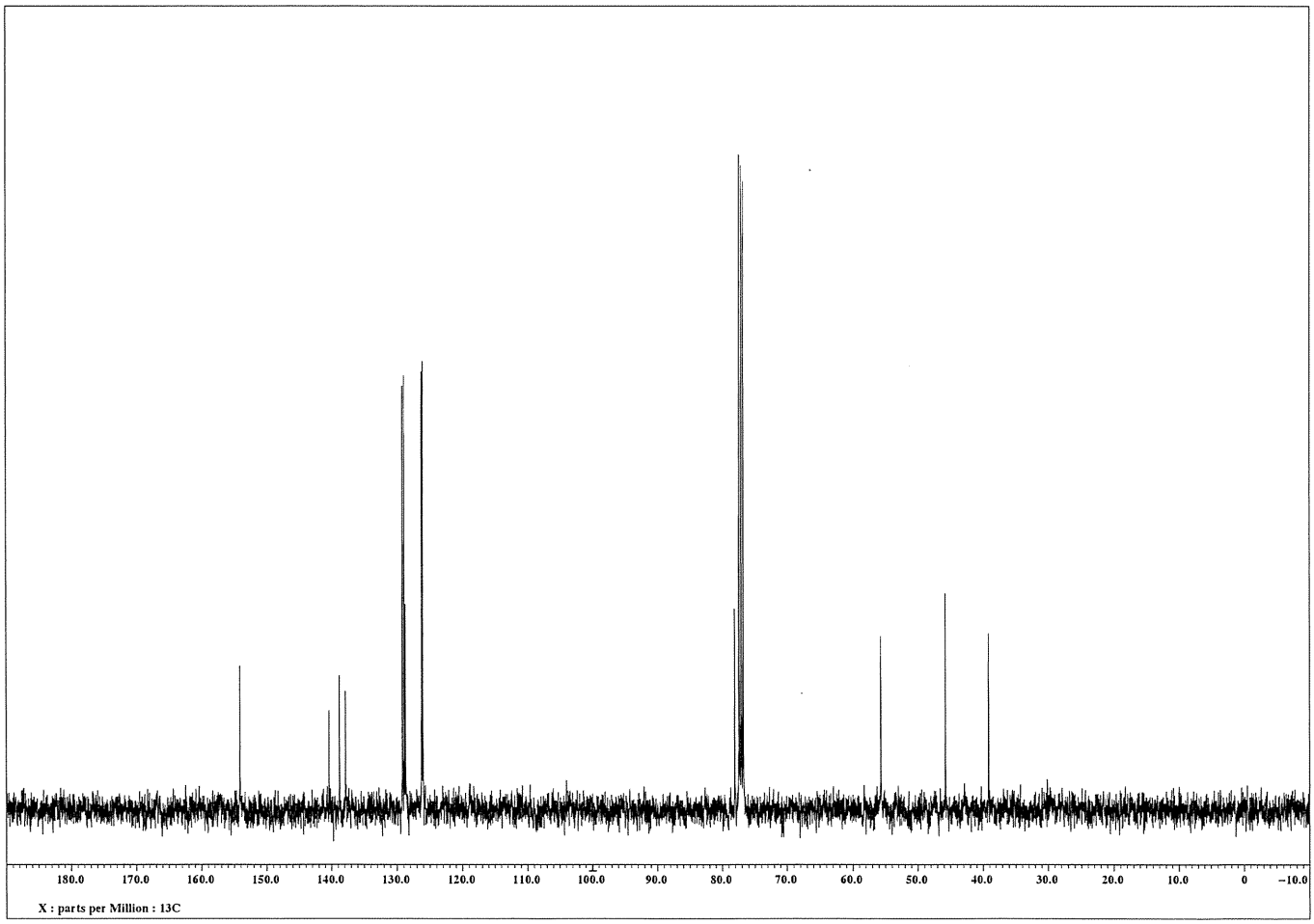

^{13}C NMR, 100 MHz, $CDCl_3$

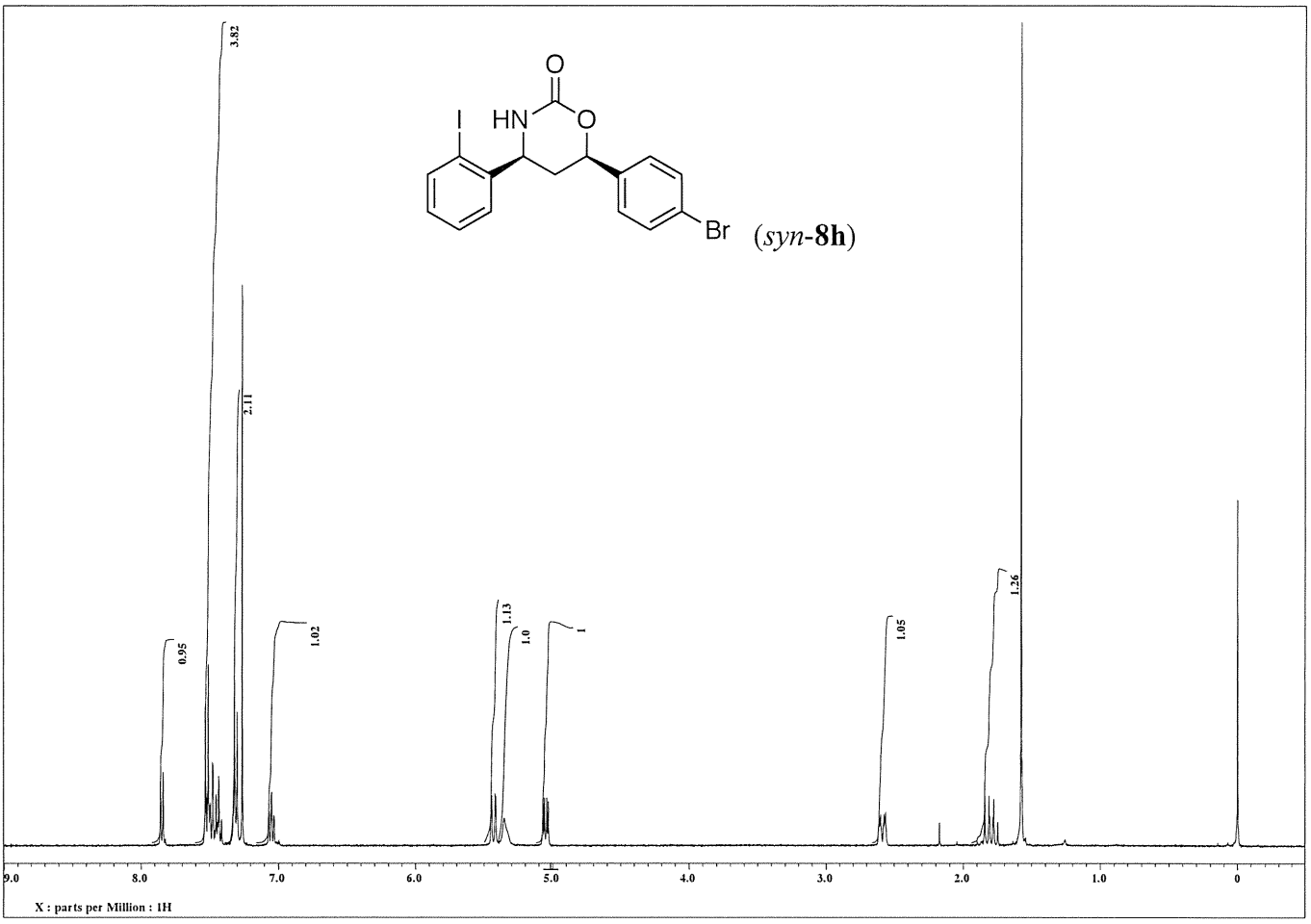

^{1}H NMR, 400 MHz, $CDCl_3$

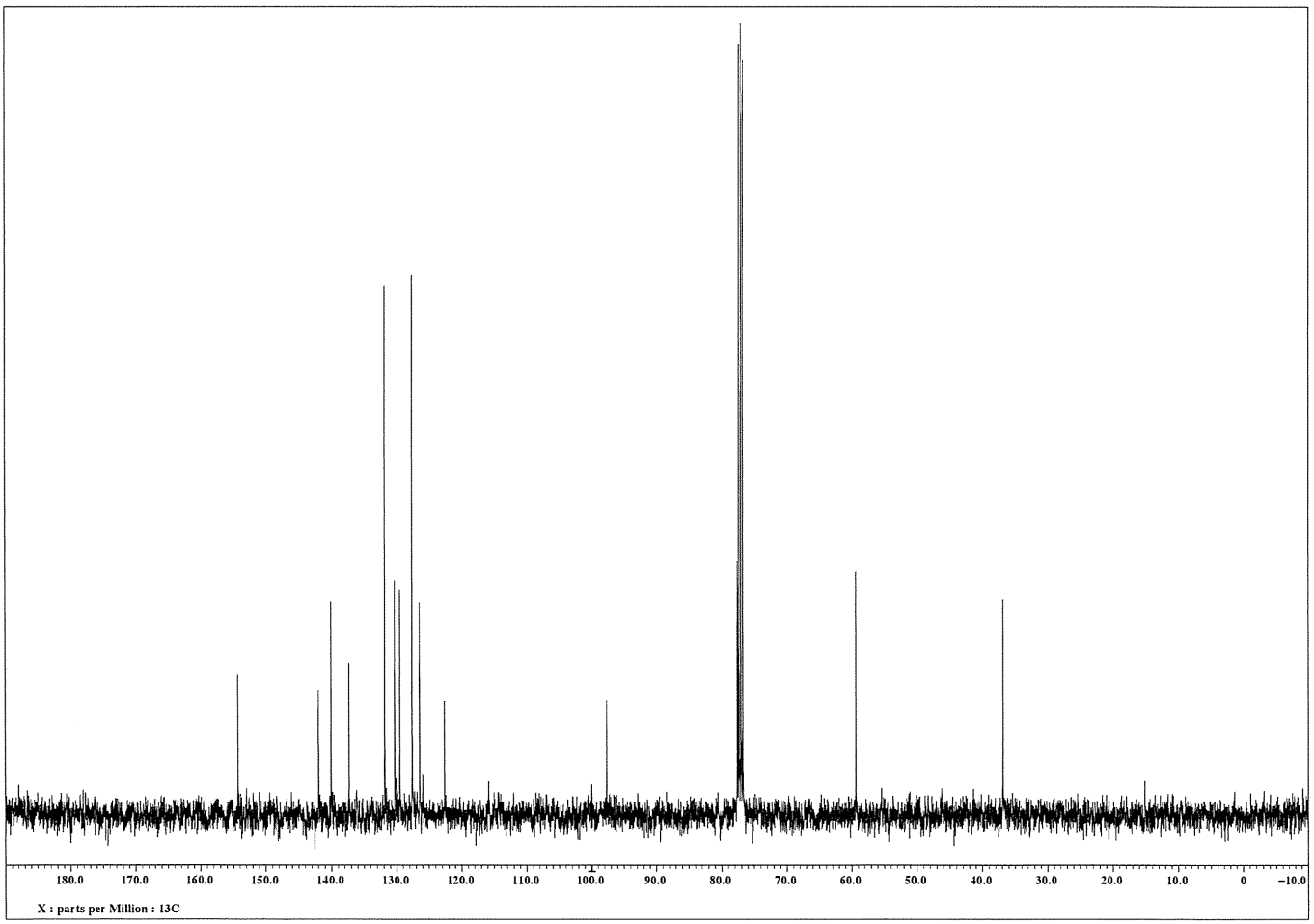

^{13}C NMR, 100 MHz, $CDCl_3$

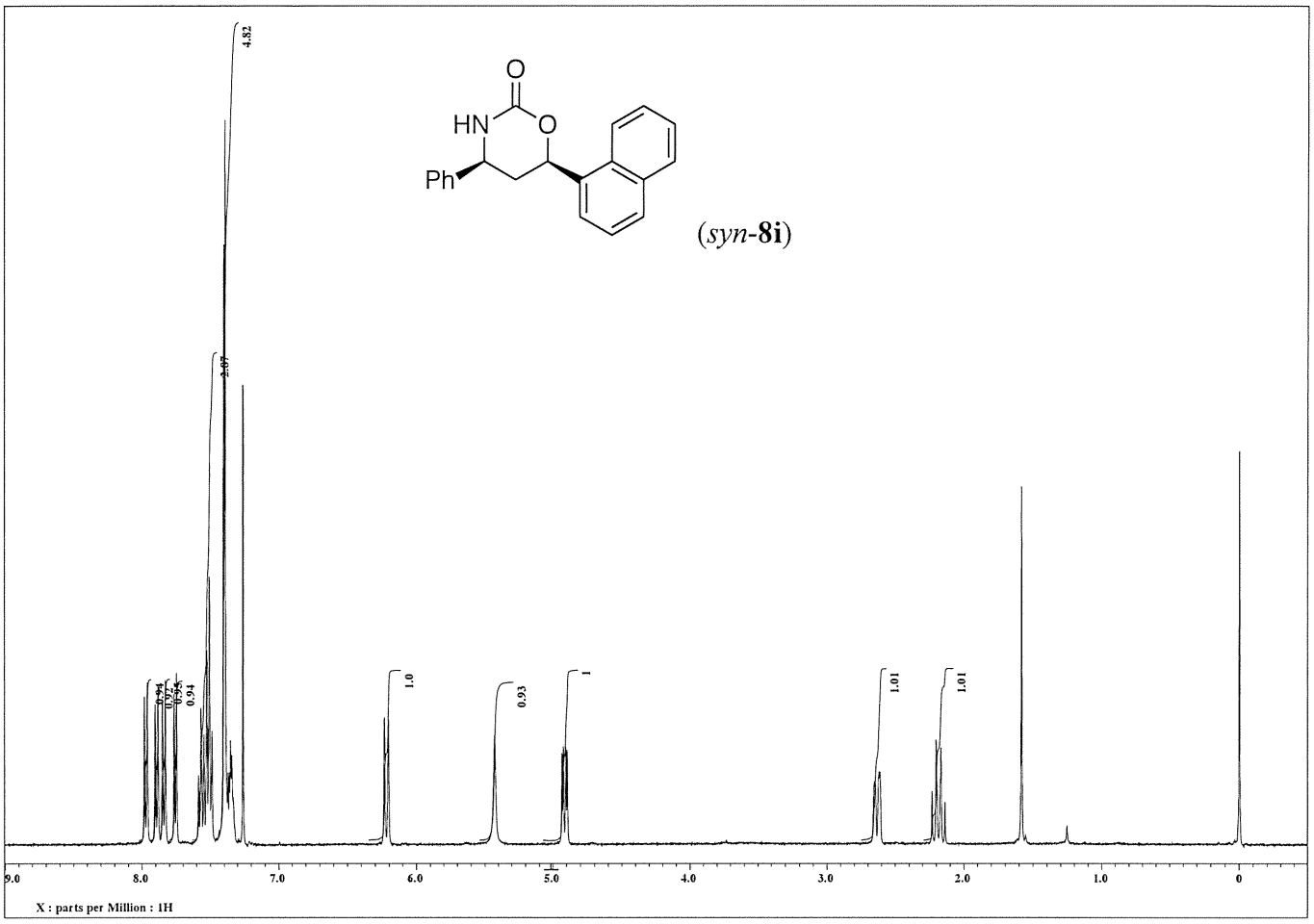

(*syn*-**8i**)

^{1}H NMR, 400 MHz, $CDCl_3$

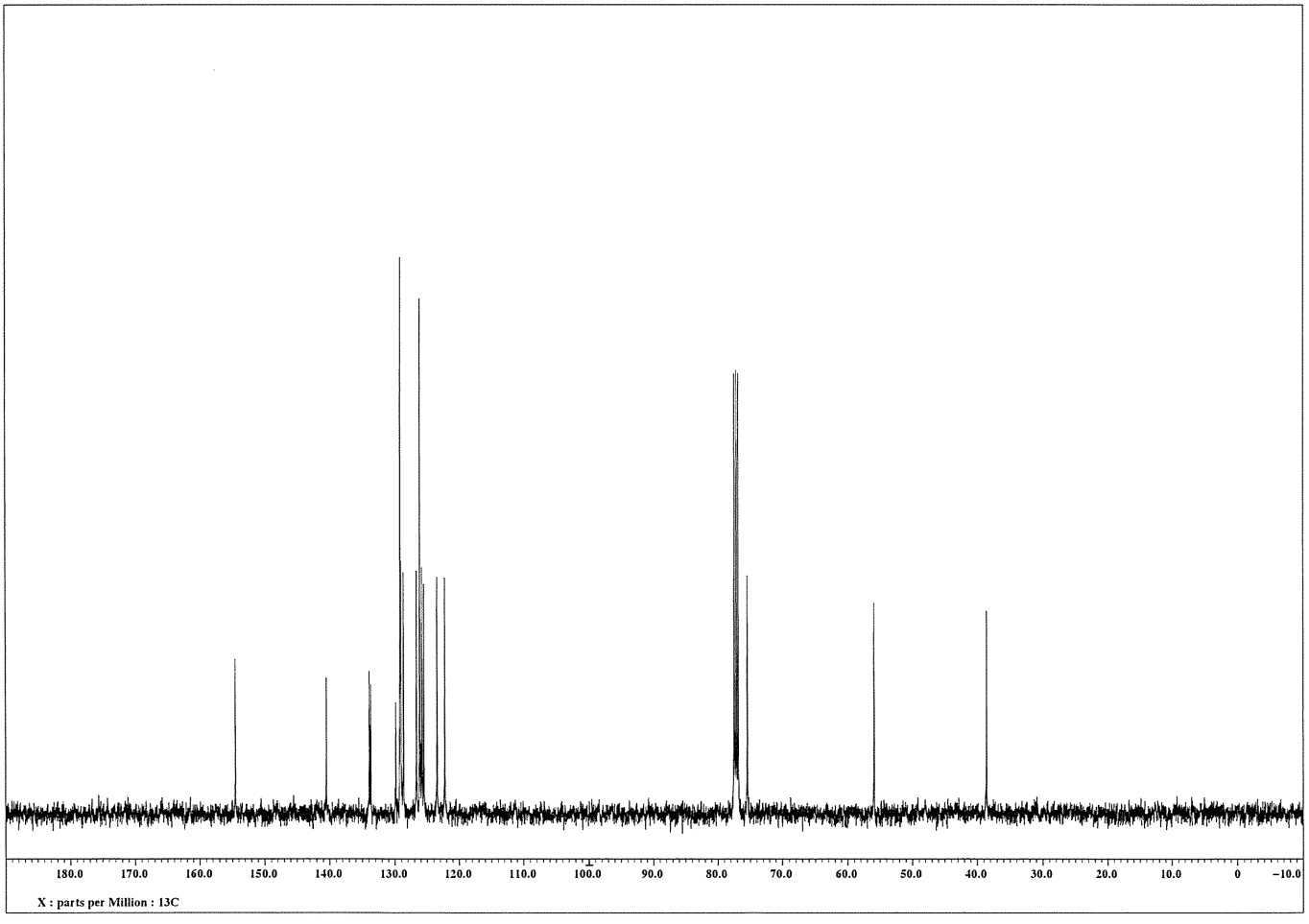

^{13}C NMR, 100 MHz, $CDCl_3$

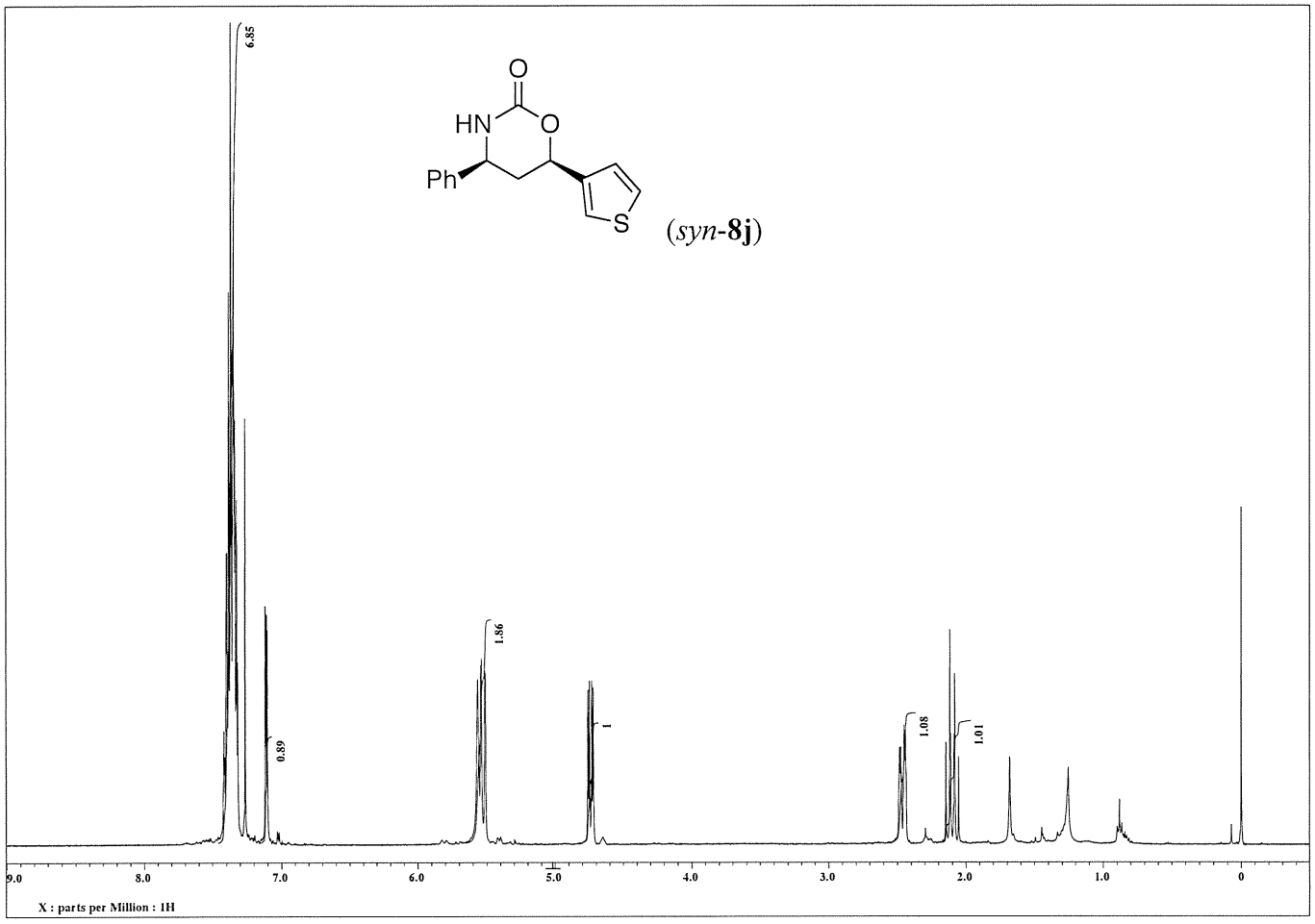

(*syn*-**8j**)

^{1}H NMR, 400 MHz, $CDCl_3$

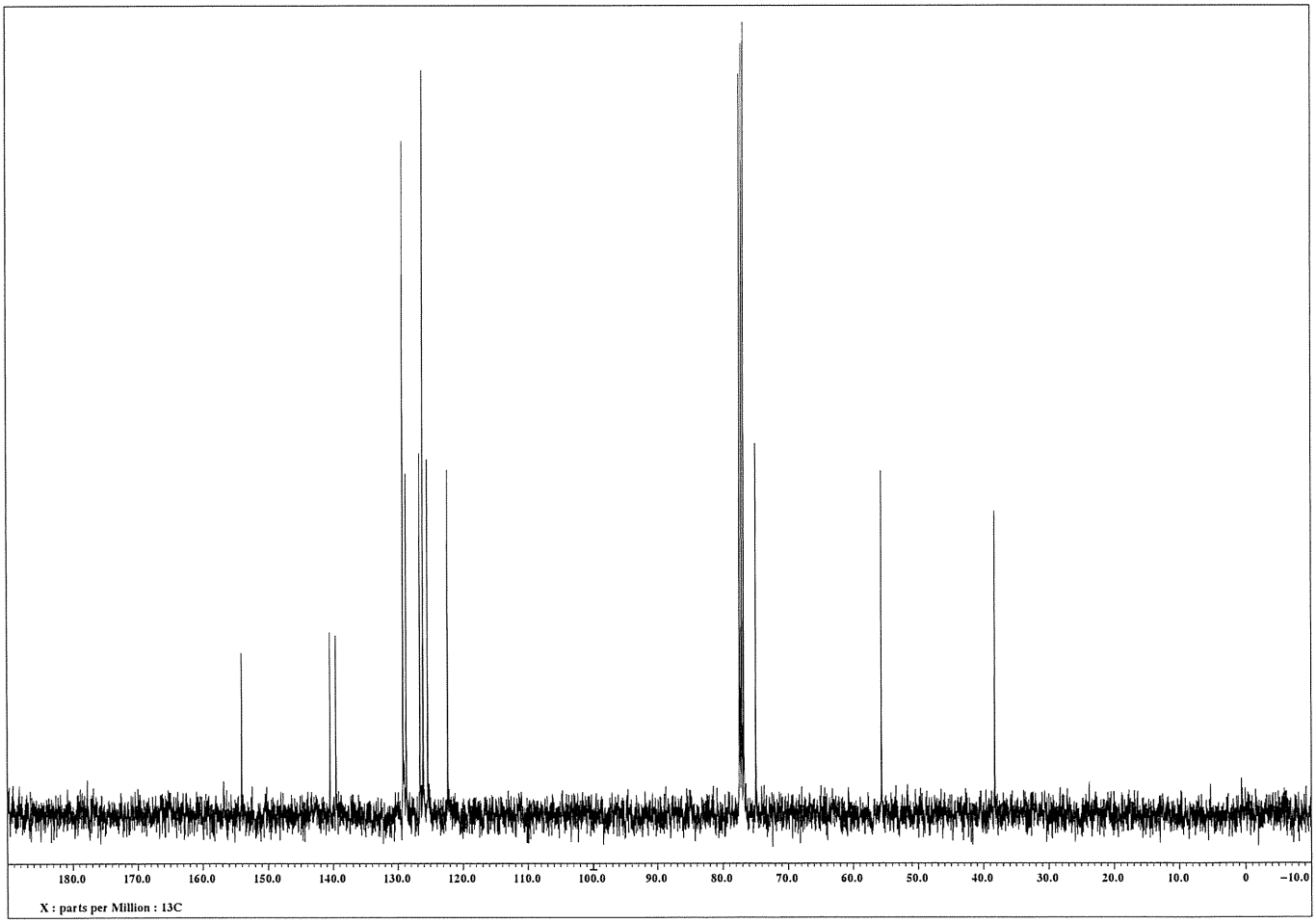

^{13}C NMR, 100 MHz, $CDCl_3$

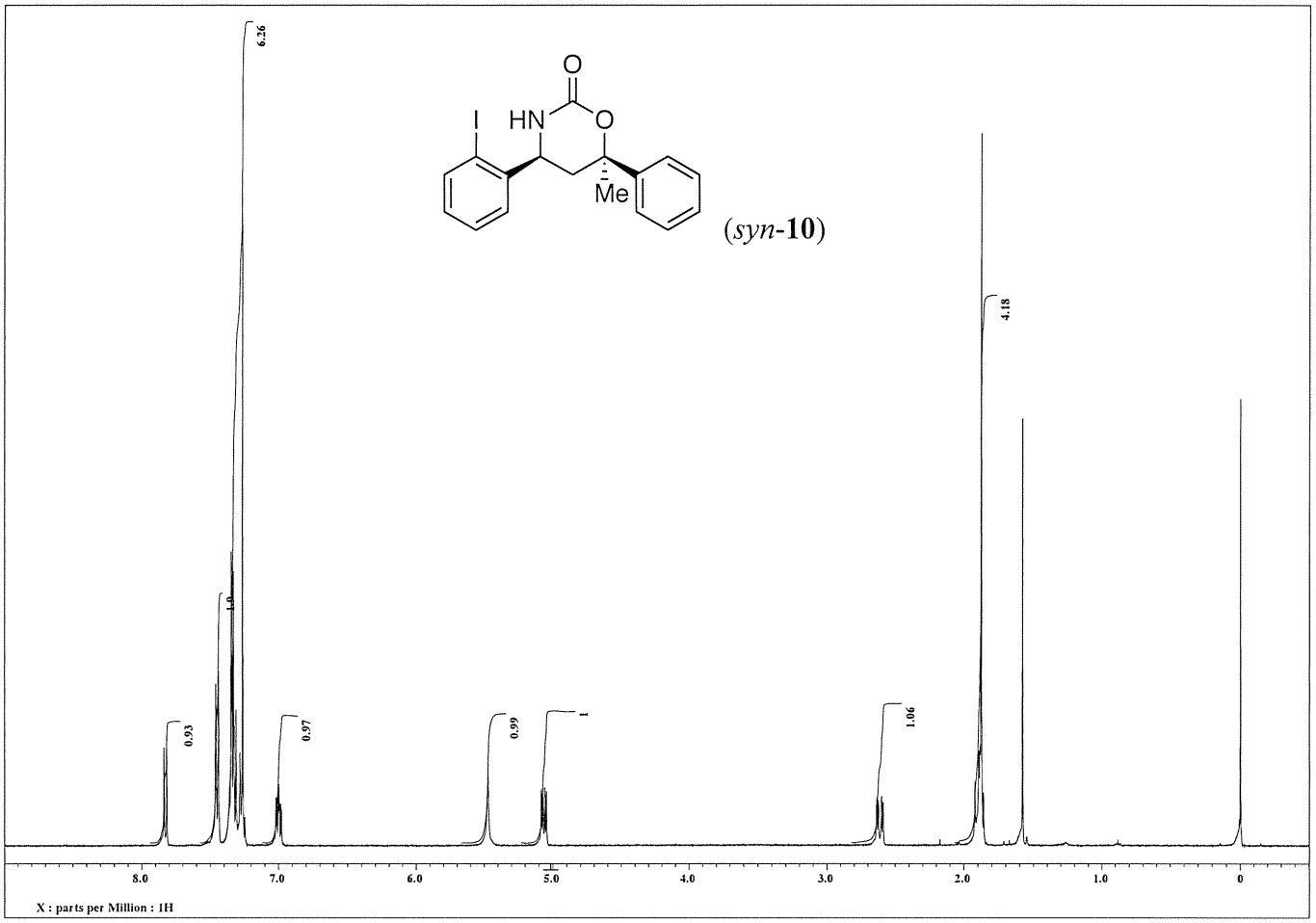

(*syn*-**10**)

^{1}H NMR, 400 MHz, $CDCl_3$

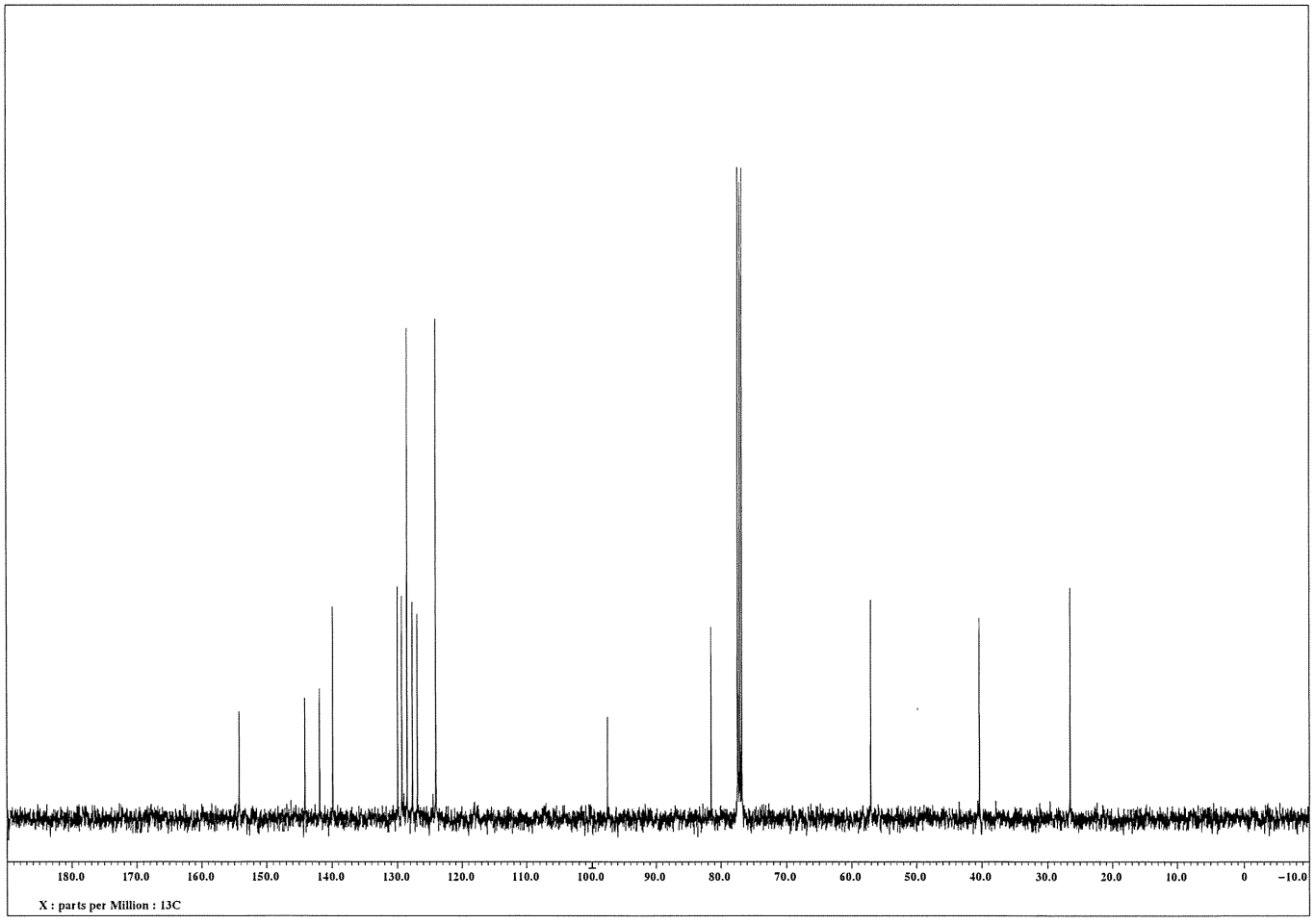

^{13}C NMR, 100 MHz, $CDCl_3$

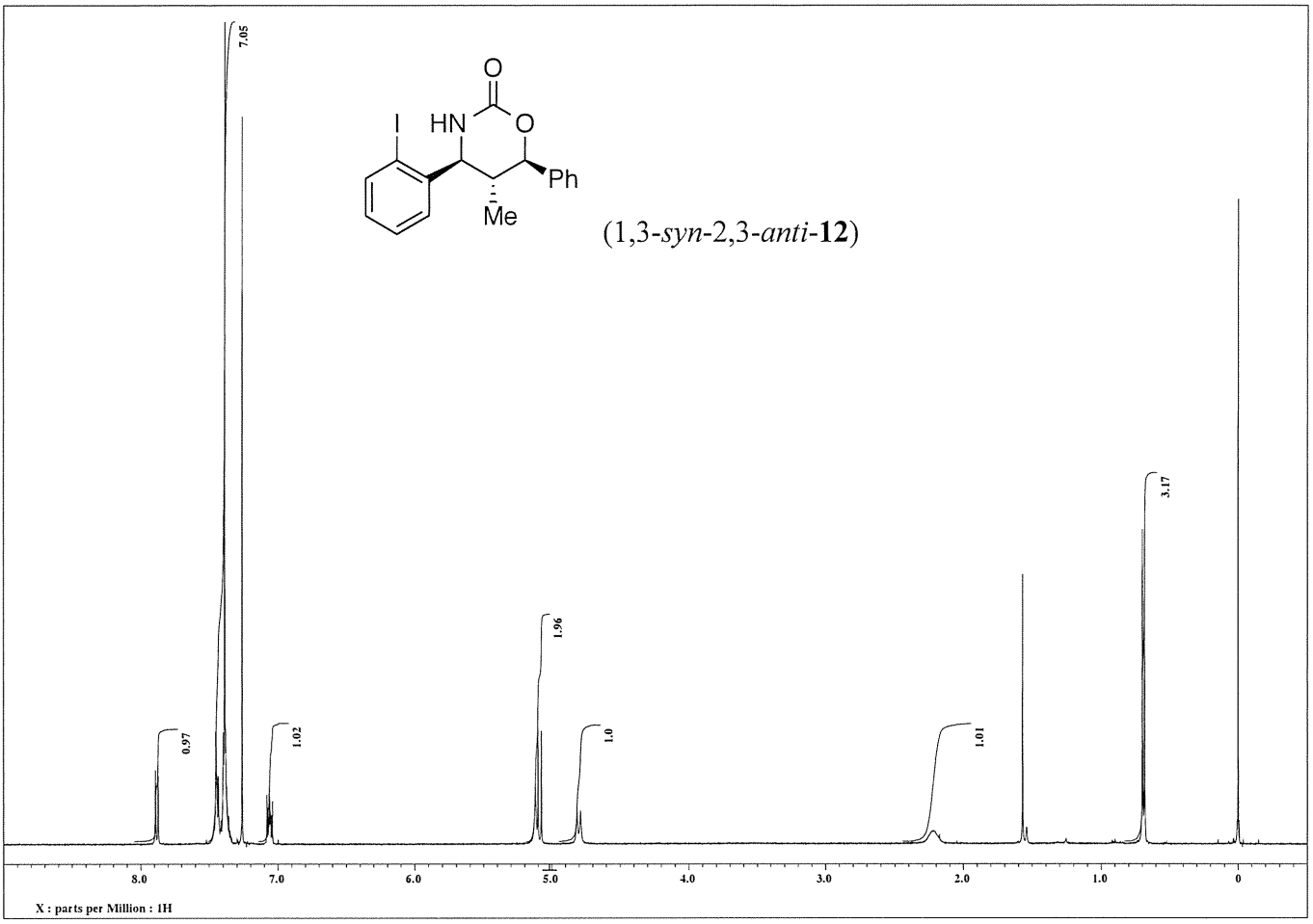

^{1}H NMR, 400 MHz, $CDCl_3$

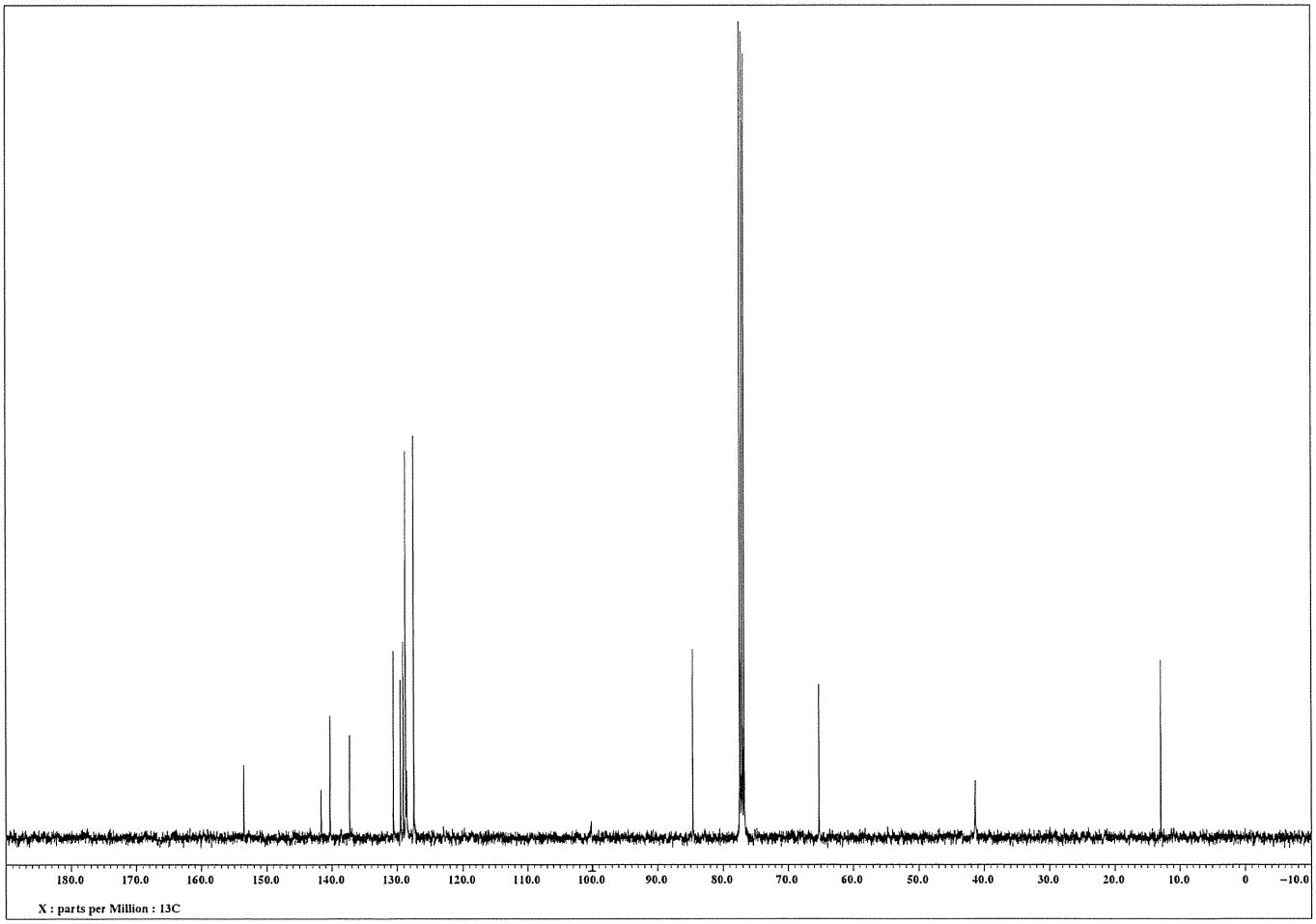

^{13}C NMR, 100 MHz, $CDCl_3$

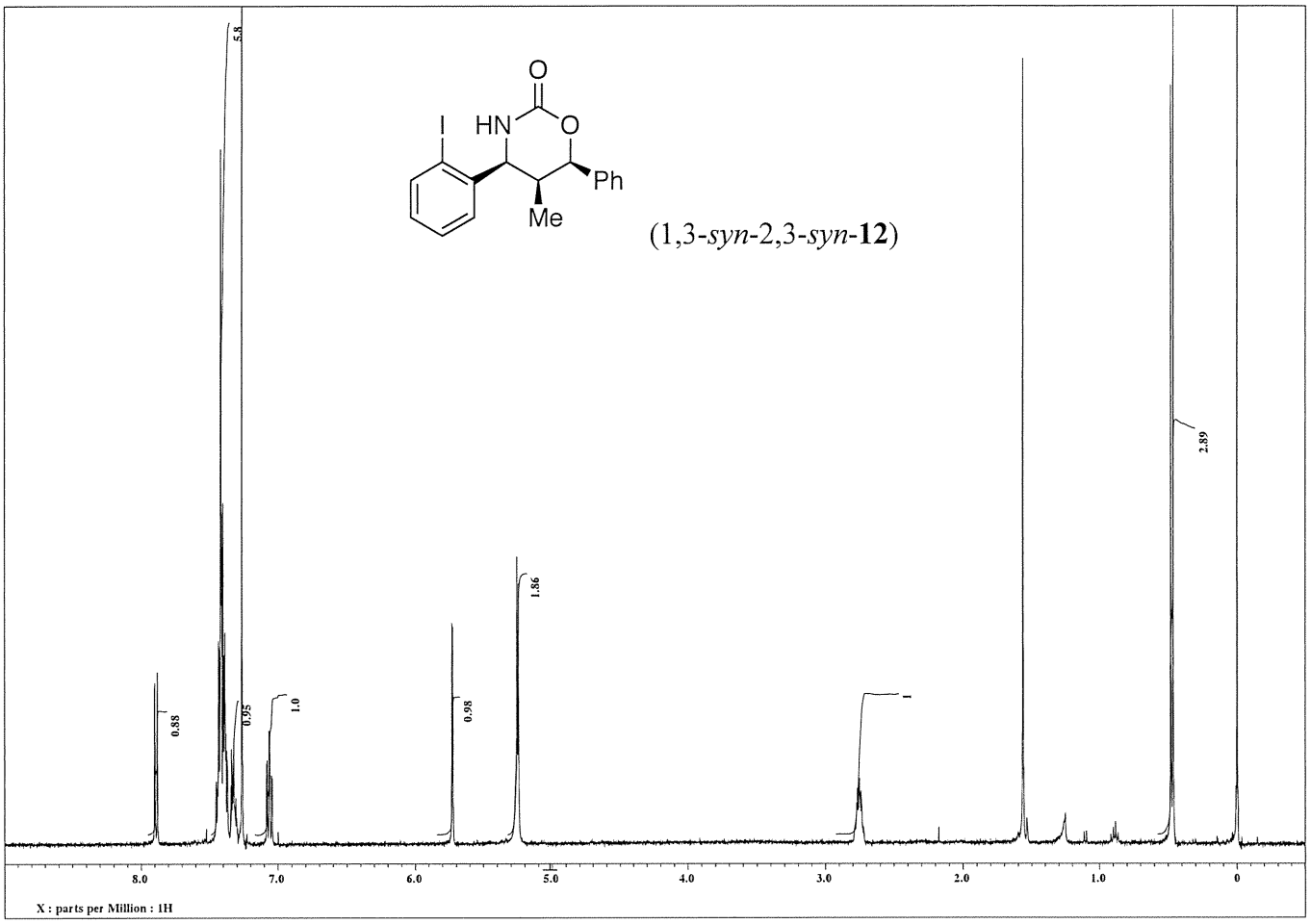

^{1}H NMR, 400 MHz, $CDCl_3$

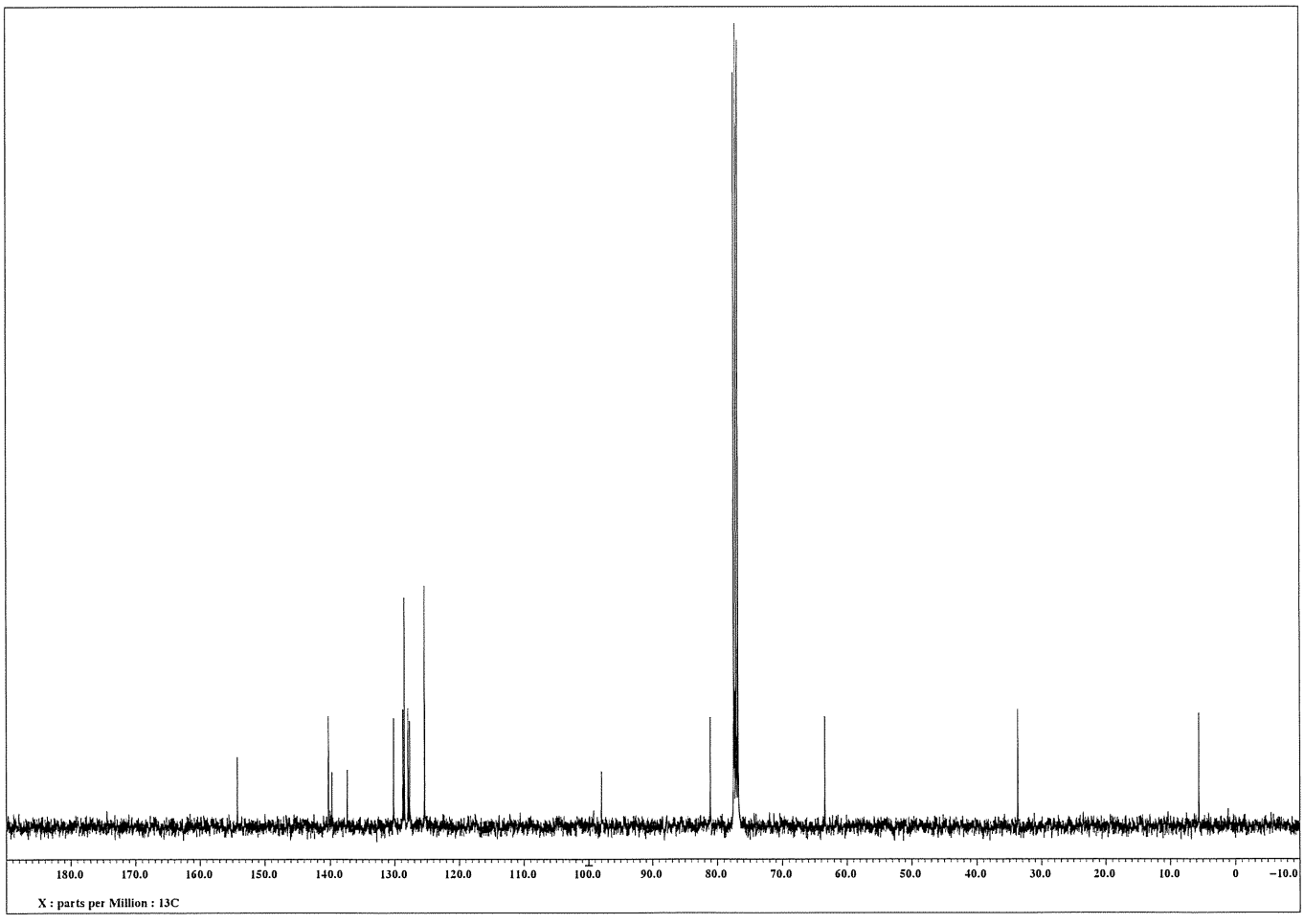

^{13}C NMR, 100 MHz, $CDCl_3$

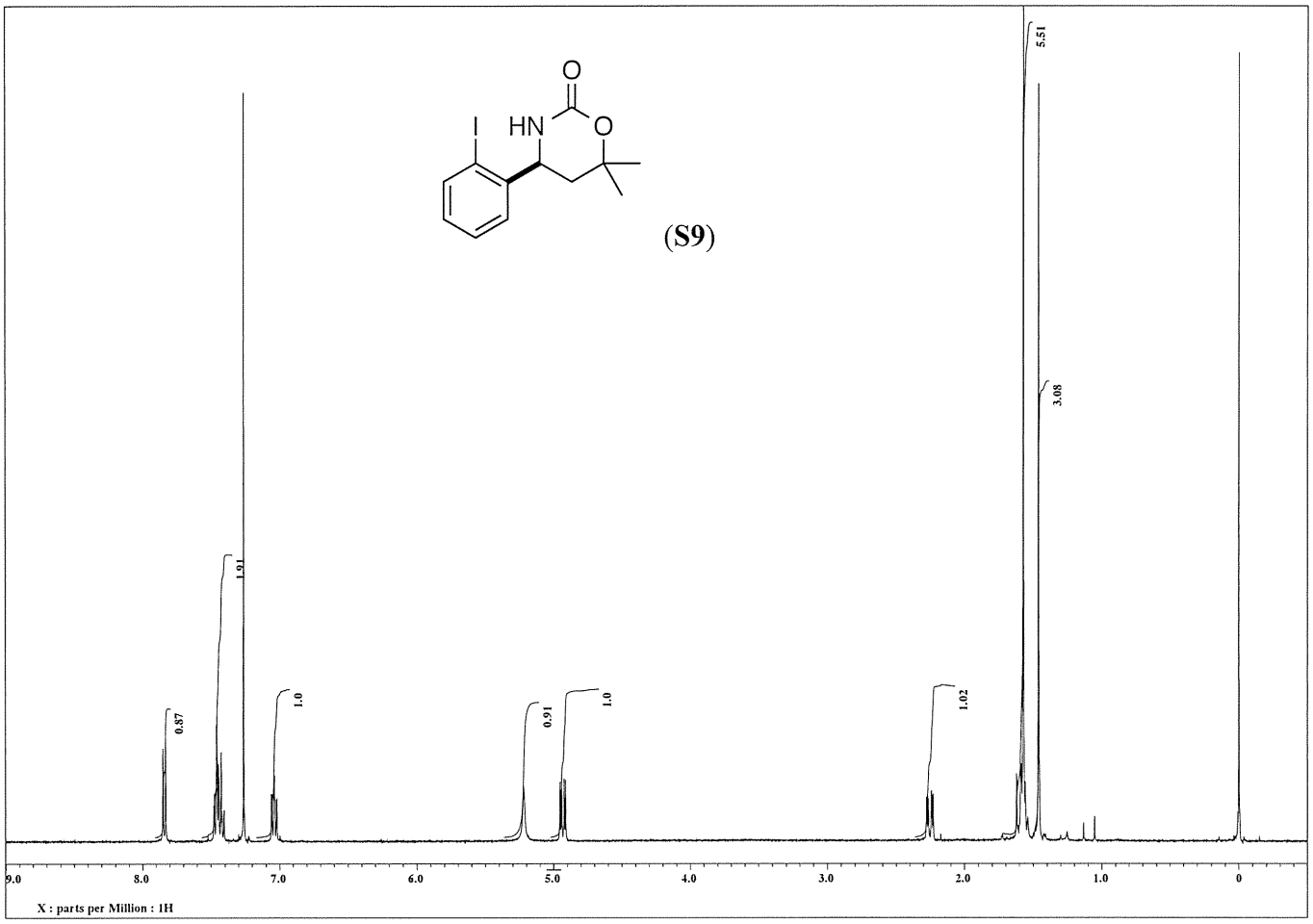

^{1}H NMR, 400 MHz, $CDCl_3$

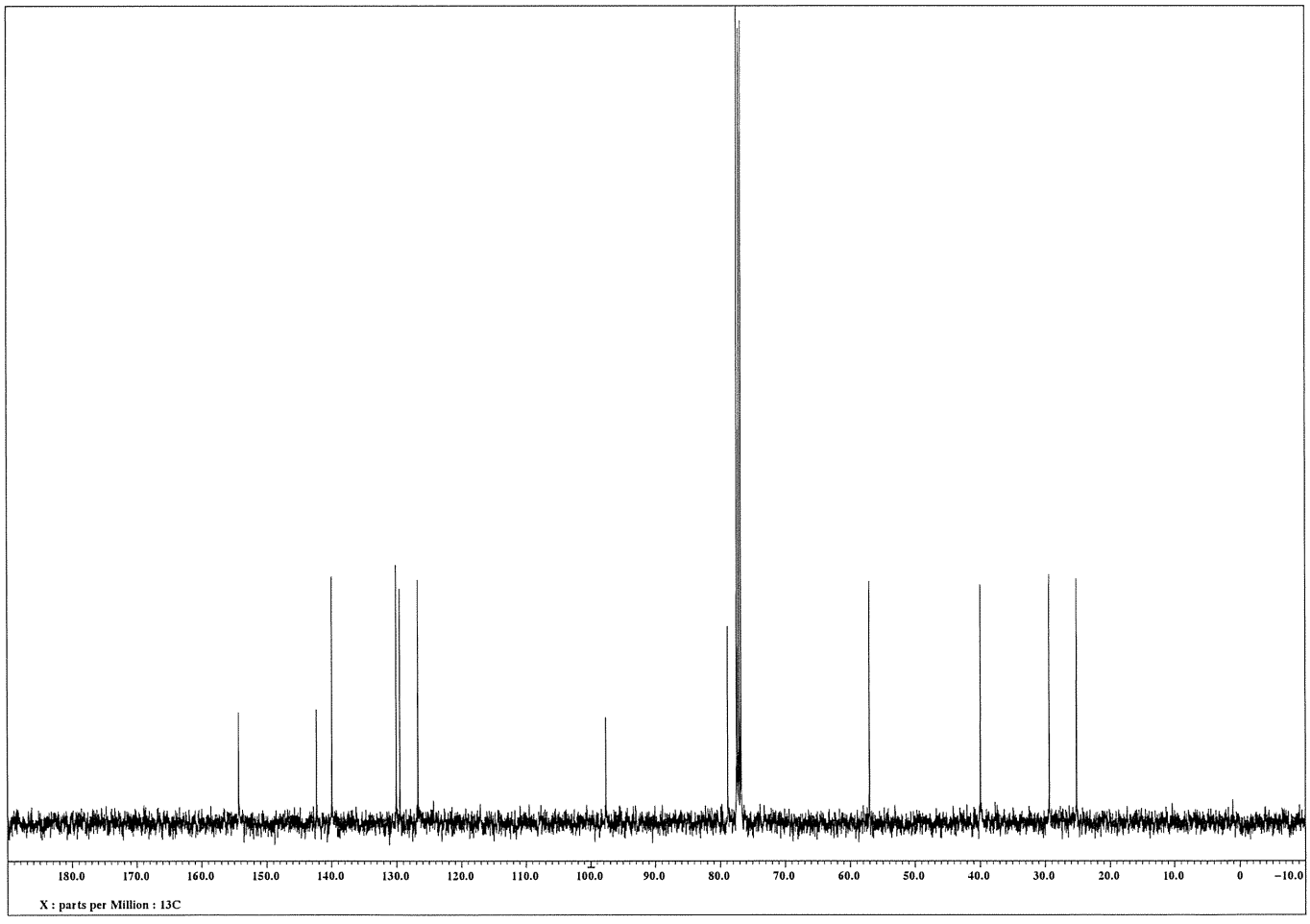

^{13}C NMR, 100 MHz, $CDCl_3$

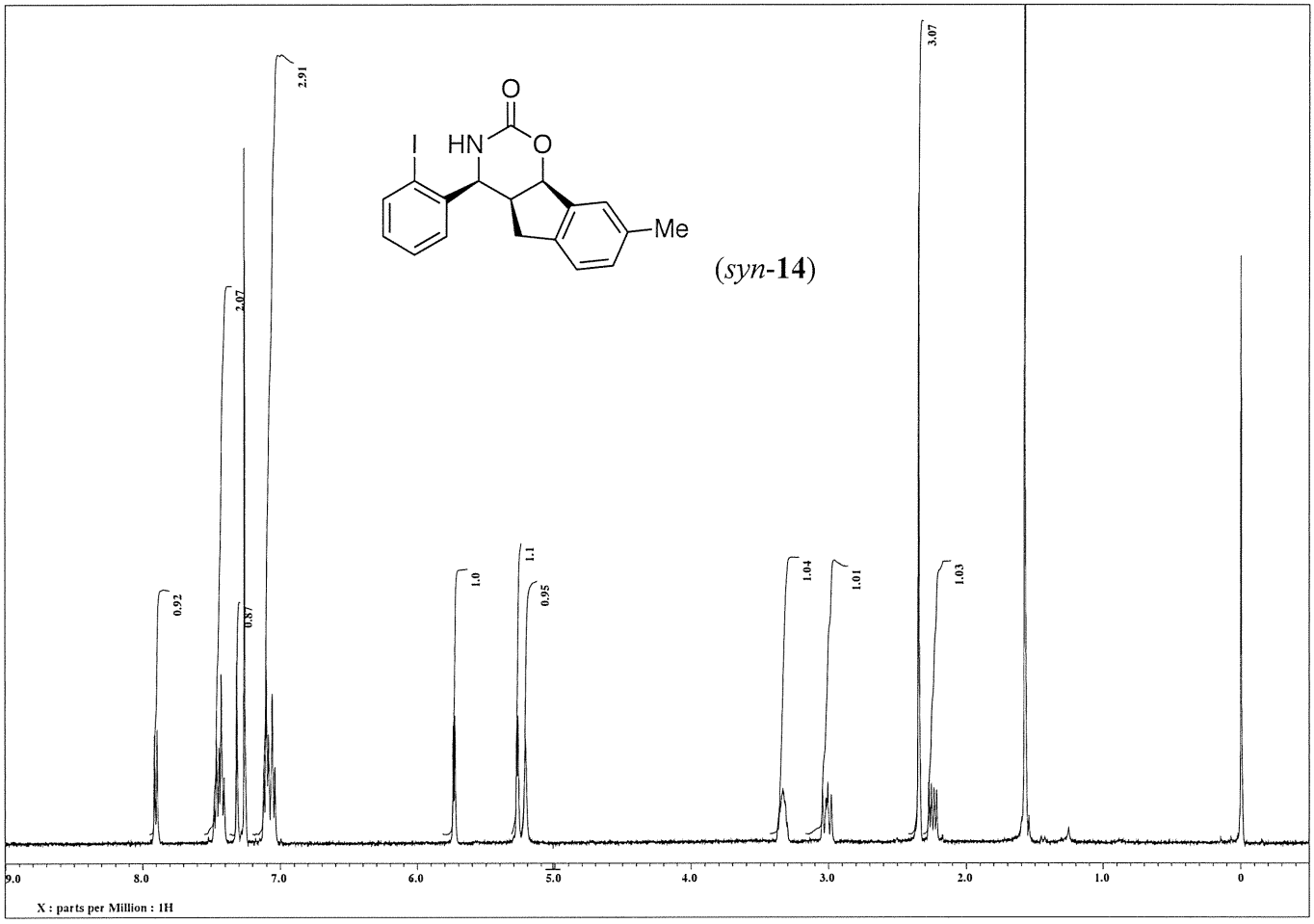

^{1}H NMR, 400 MHz, $CDCl_3$

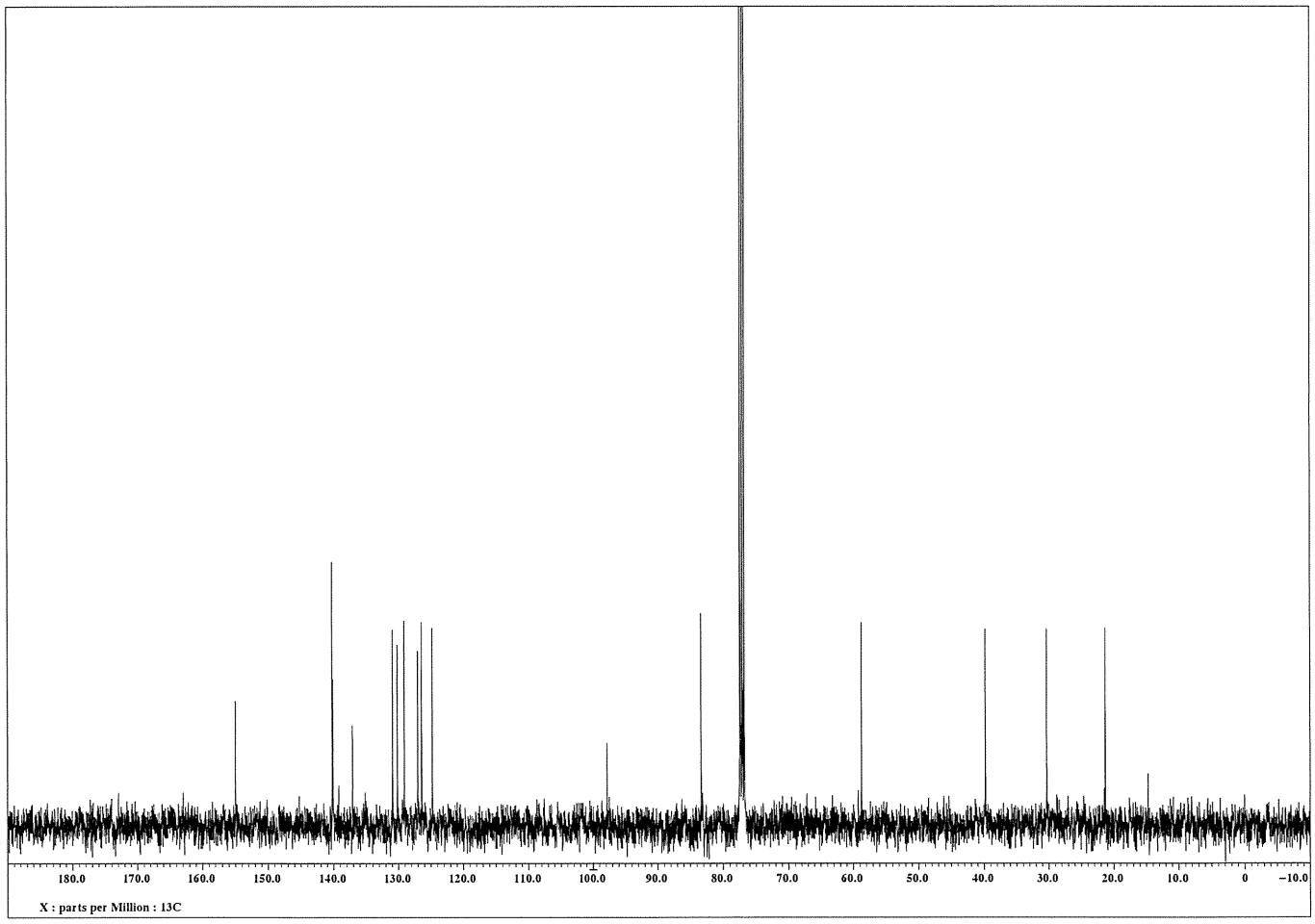

^{13}C NMR, 100 MHz, $CDCl_3$

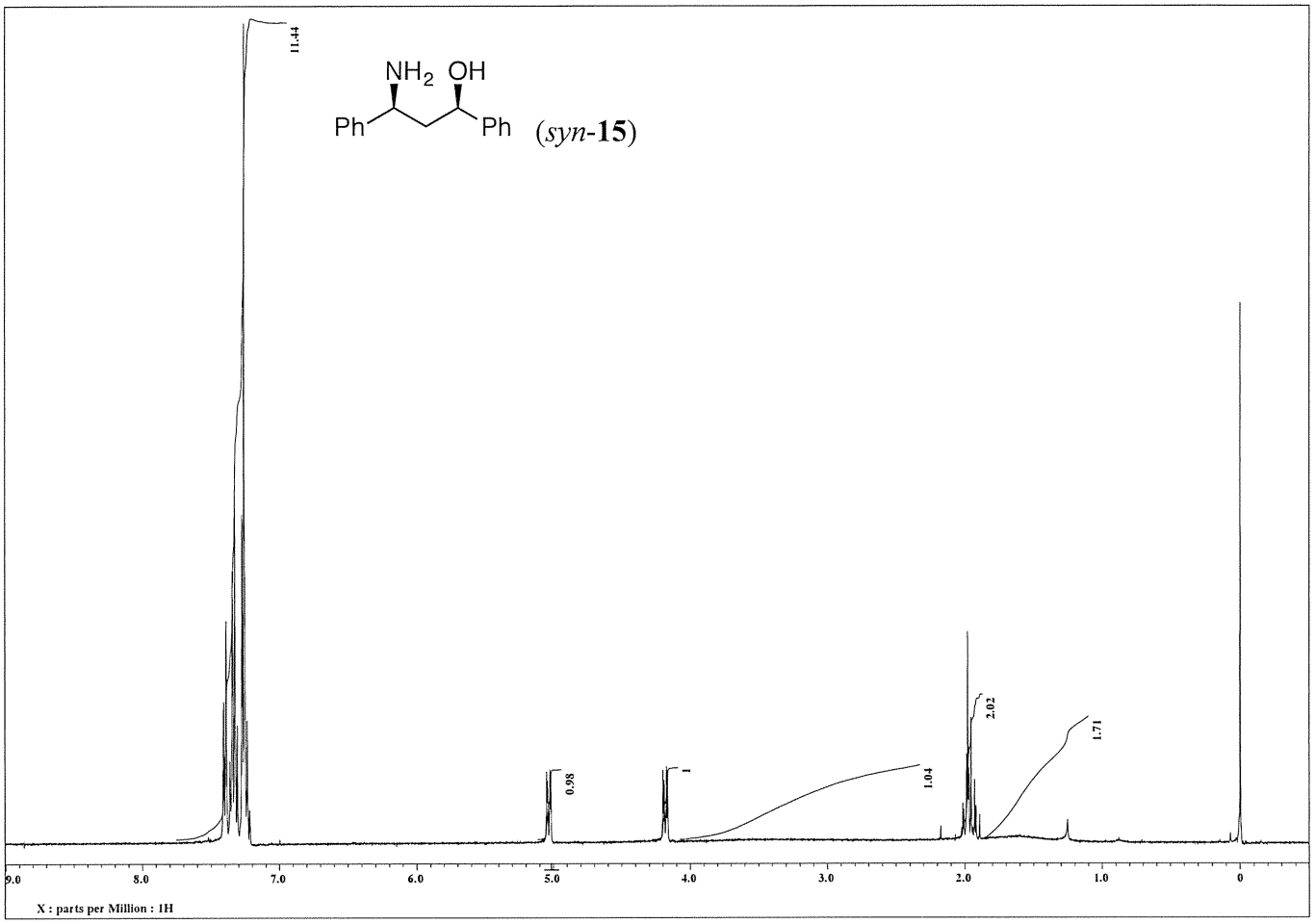

^{1}H NMR, 400 MHz, $CDCl_3$

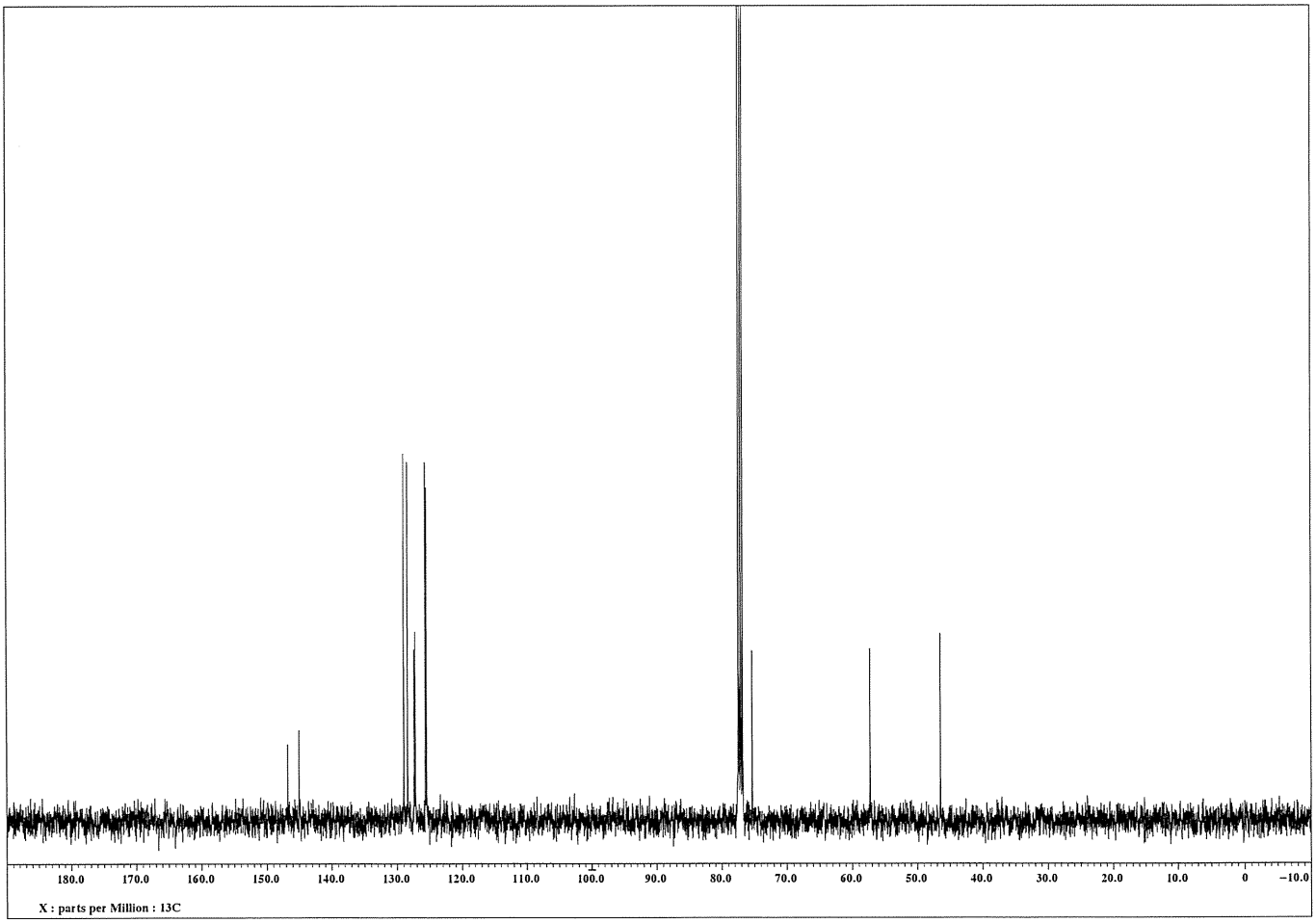

^{13}C NMR, 100 MHz, $CDCl_3$

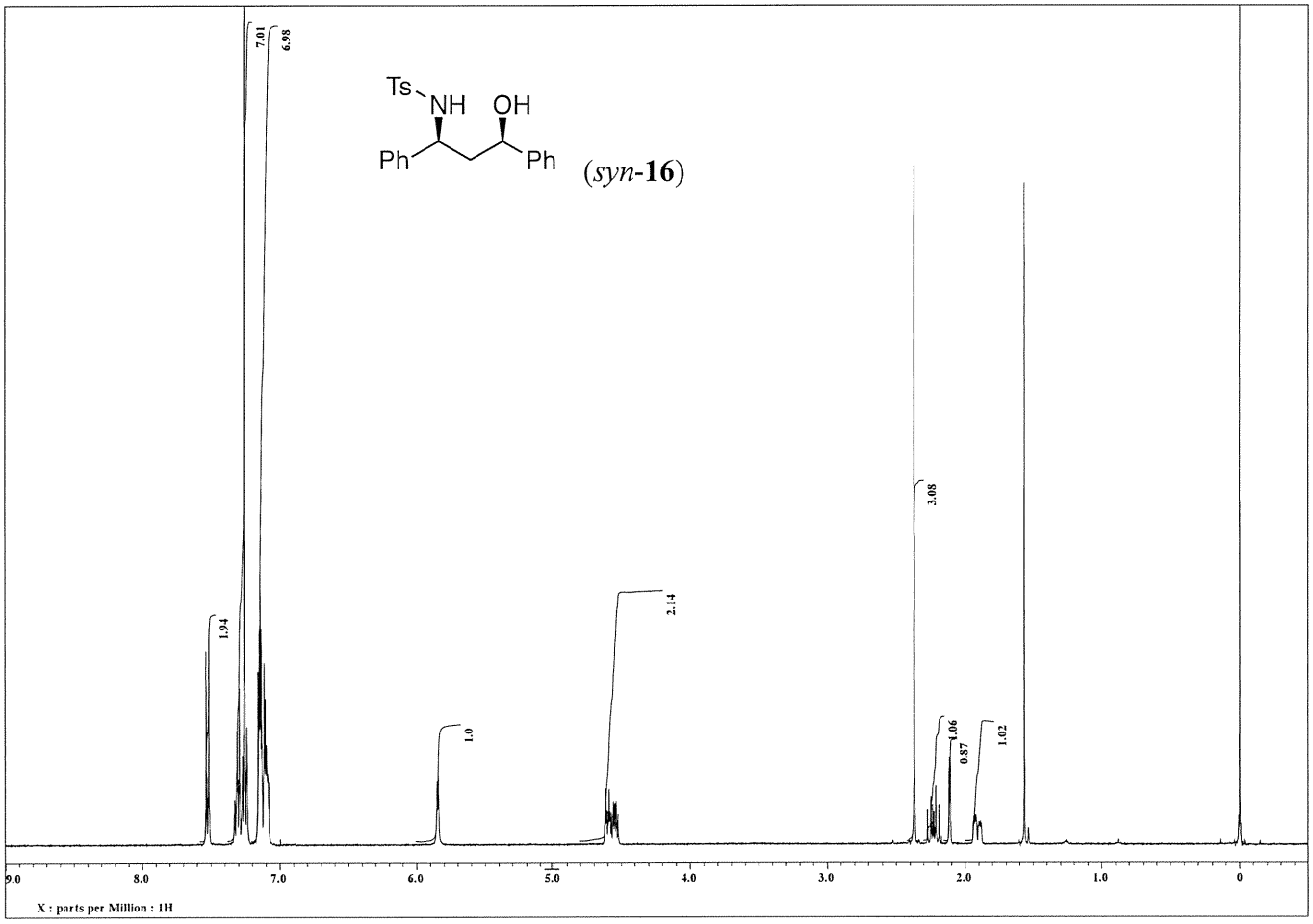

^{1}H NMR, 400 MHz, $CDCl_3$

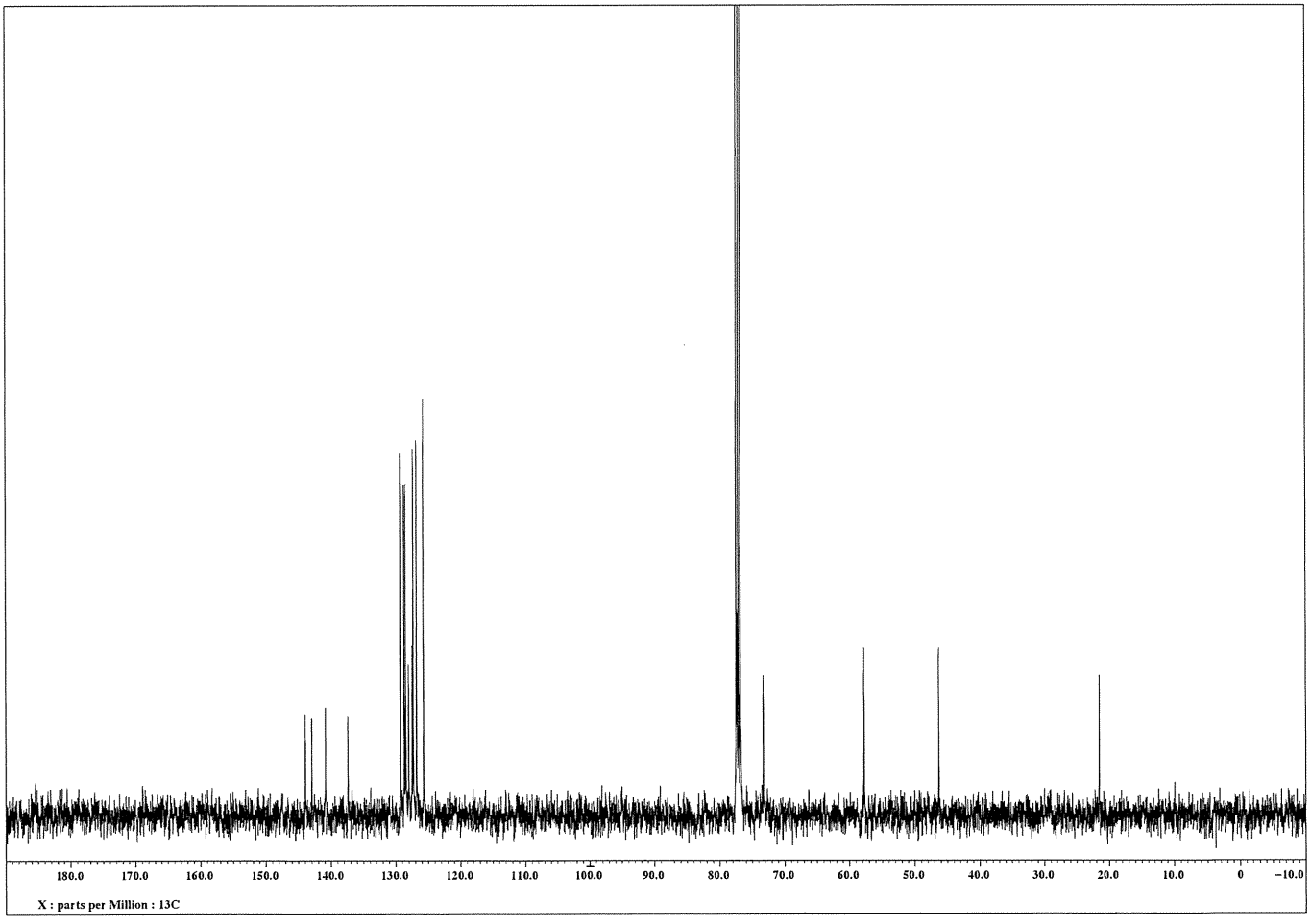

^{13}C NMR, 100 MHz, $CDCl_3$

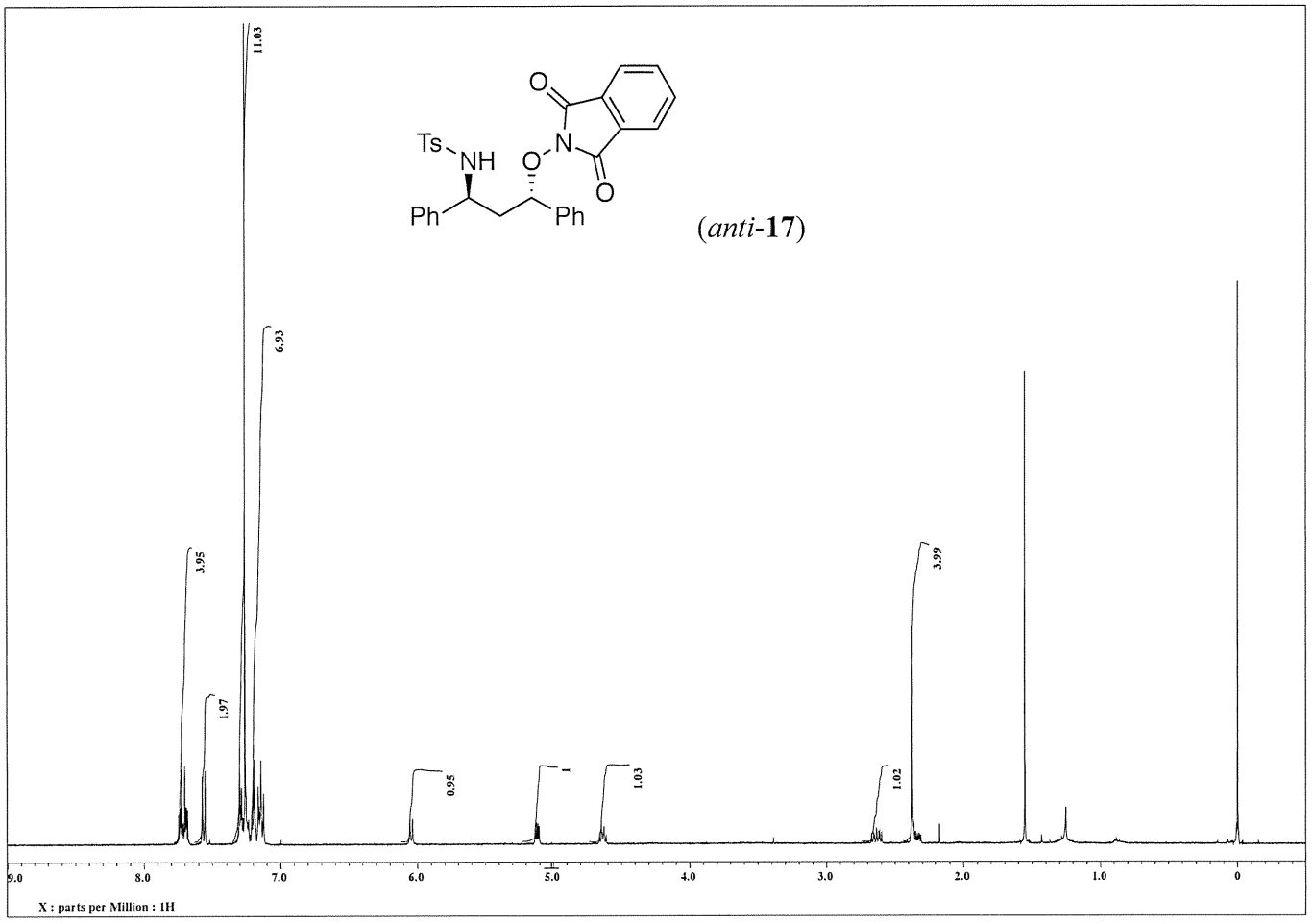

^{1}H NMR, 400 MHz, $CDCl_3$

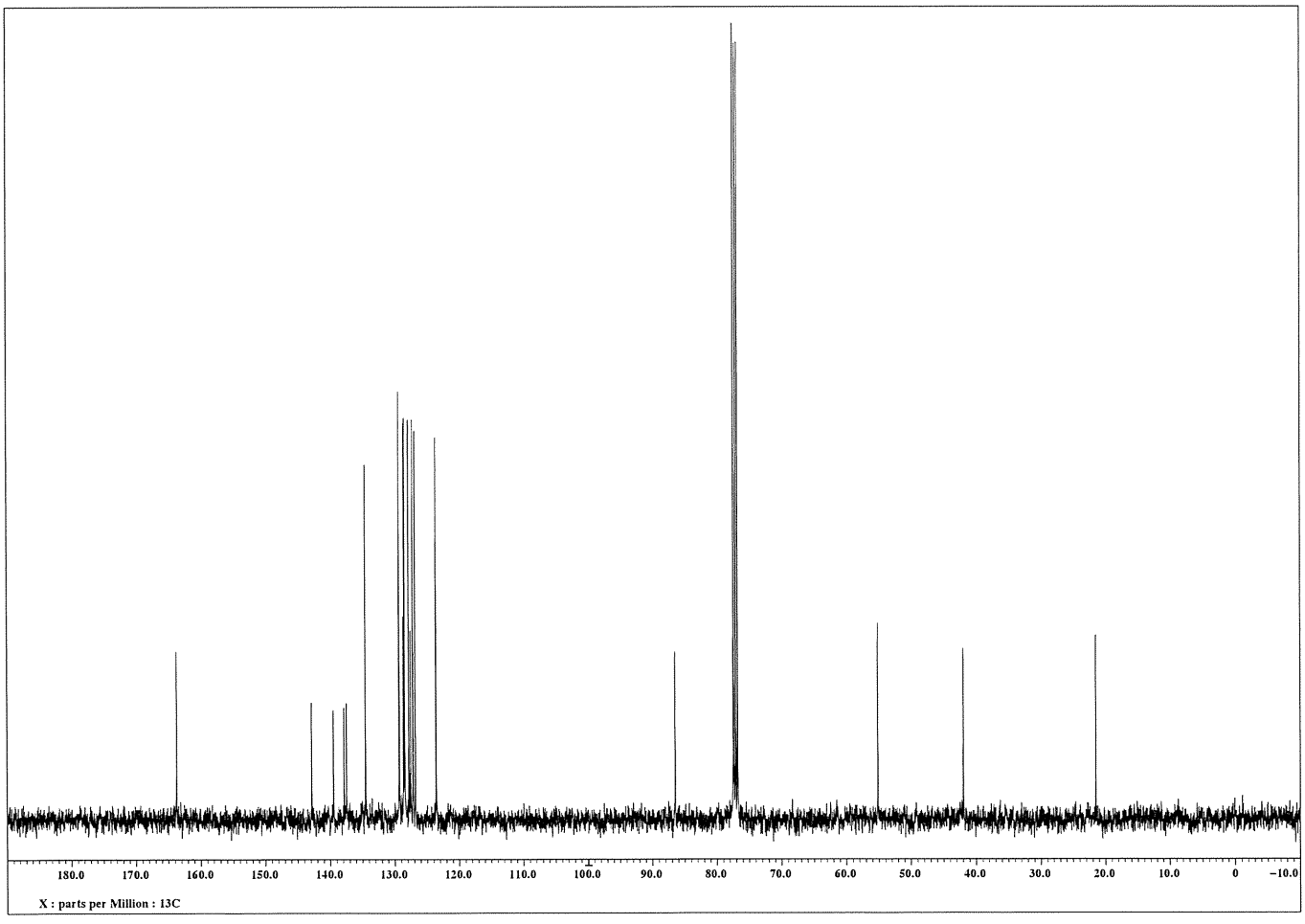

^{13}C NMR, 100 MHz, $CDCl_3$

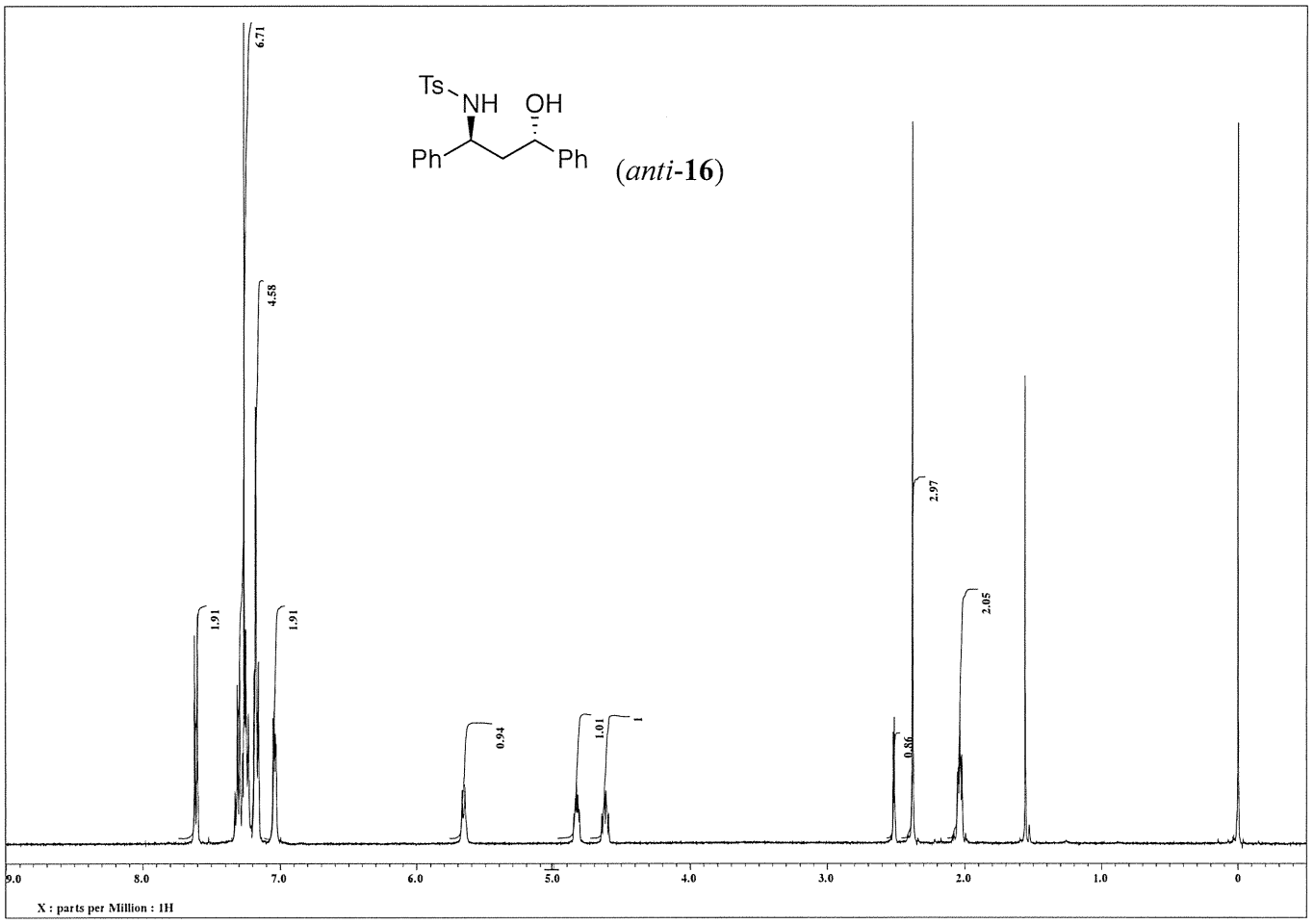

^{1}H NMR, 400 MHz, $CDCl_3$

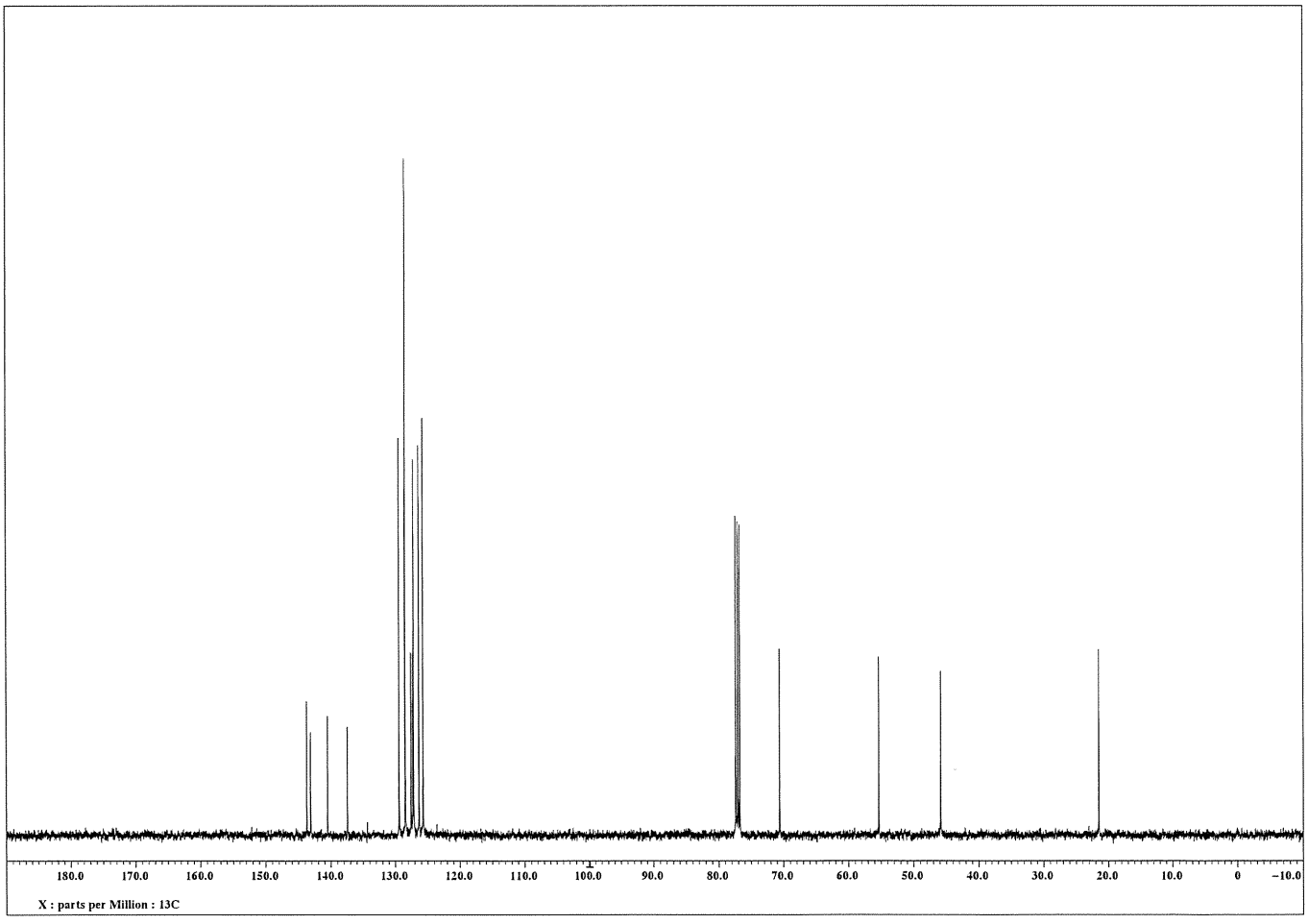

^{13}C NMR, 100 MHz, $CDCl_3$

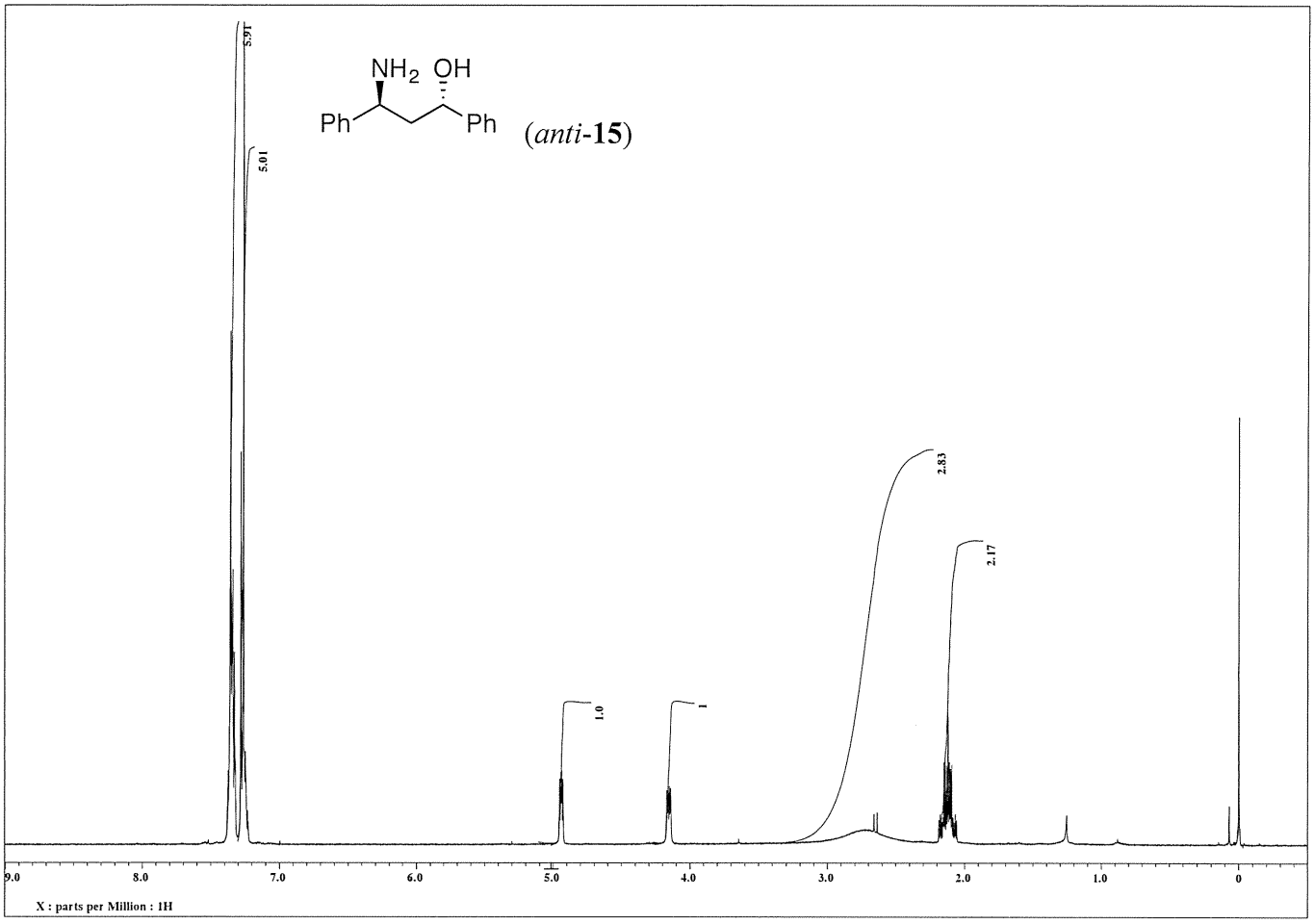

^{1}H NMR, 400 MHz, $CDCl_3$

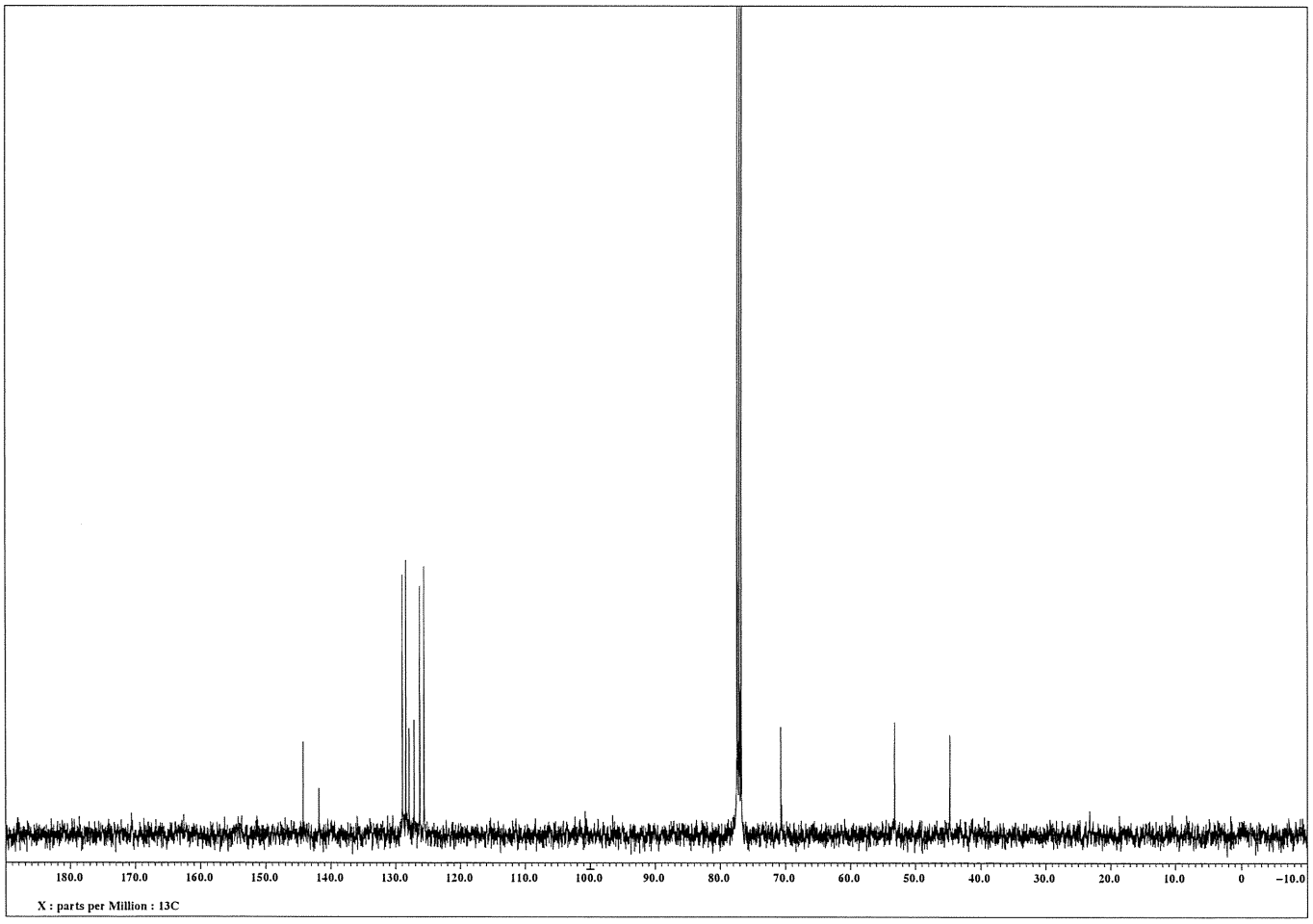

^{13}C NMR, 100 MHz, $CDCl_3$

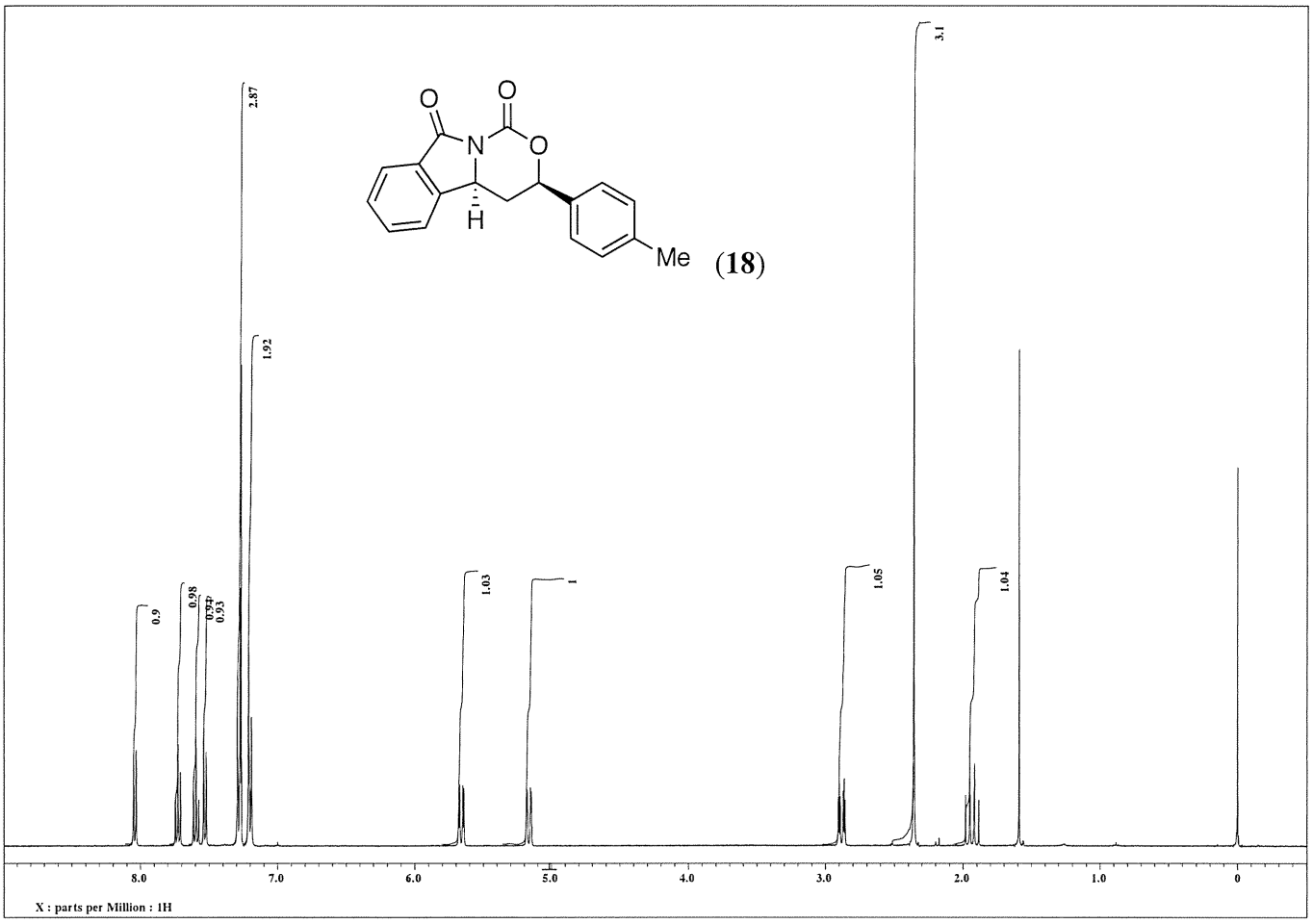

^{1}H NMR, 400 MHz, $CDCl_3$

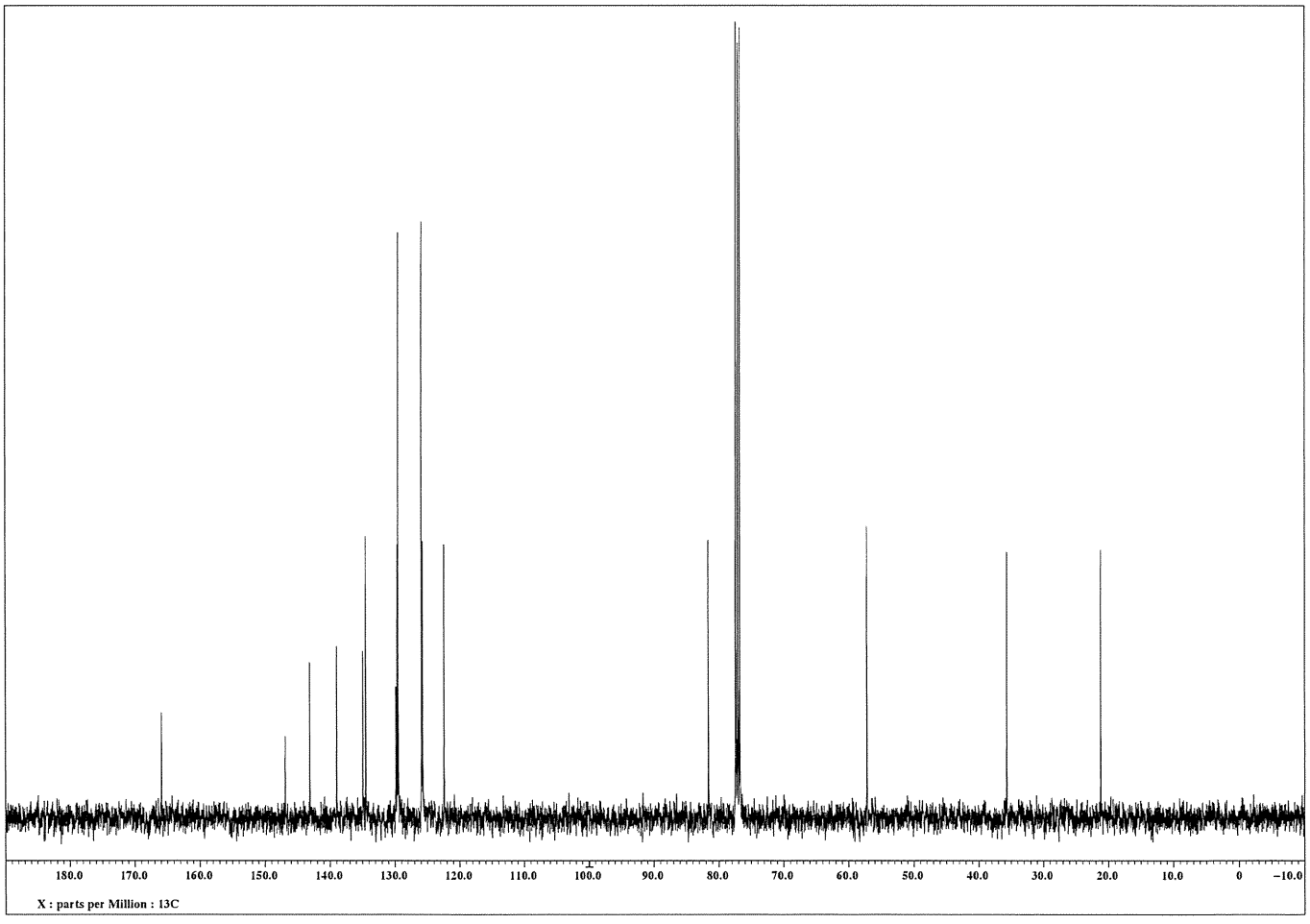

^{13}C NMR, 100 MHz, $CDCl_3$

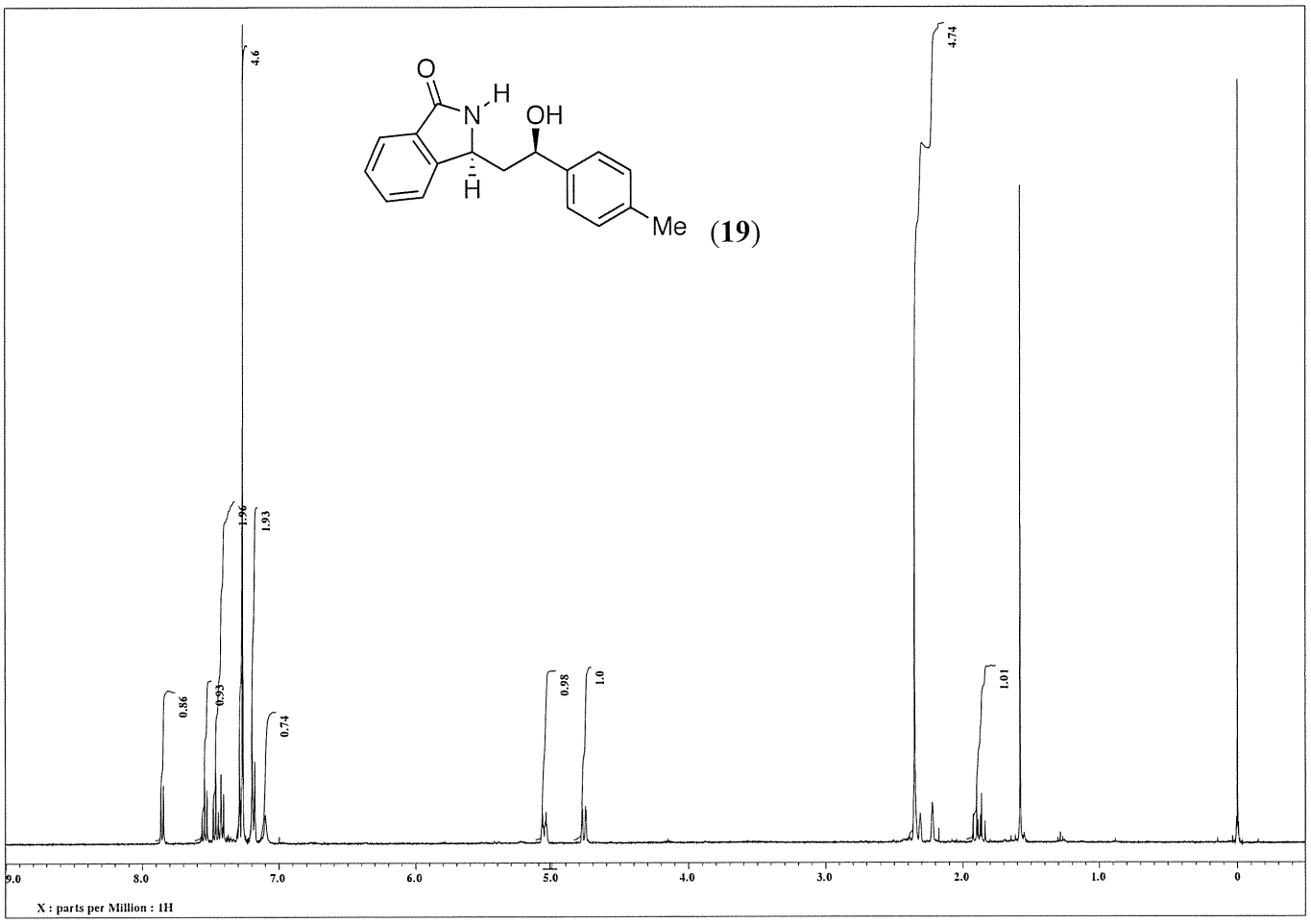

^{1}H NMR, 400 MHz, $CDCl_3$

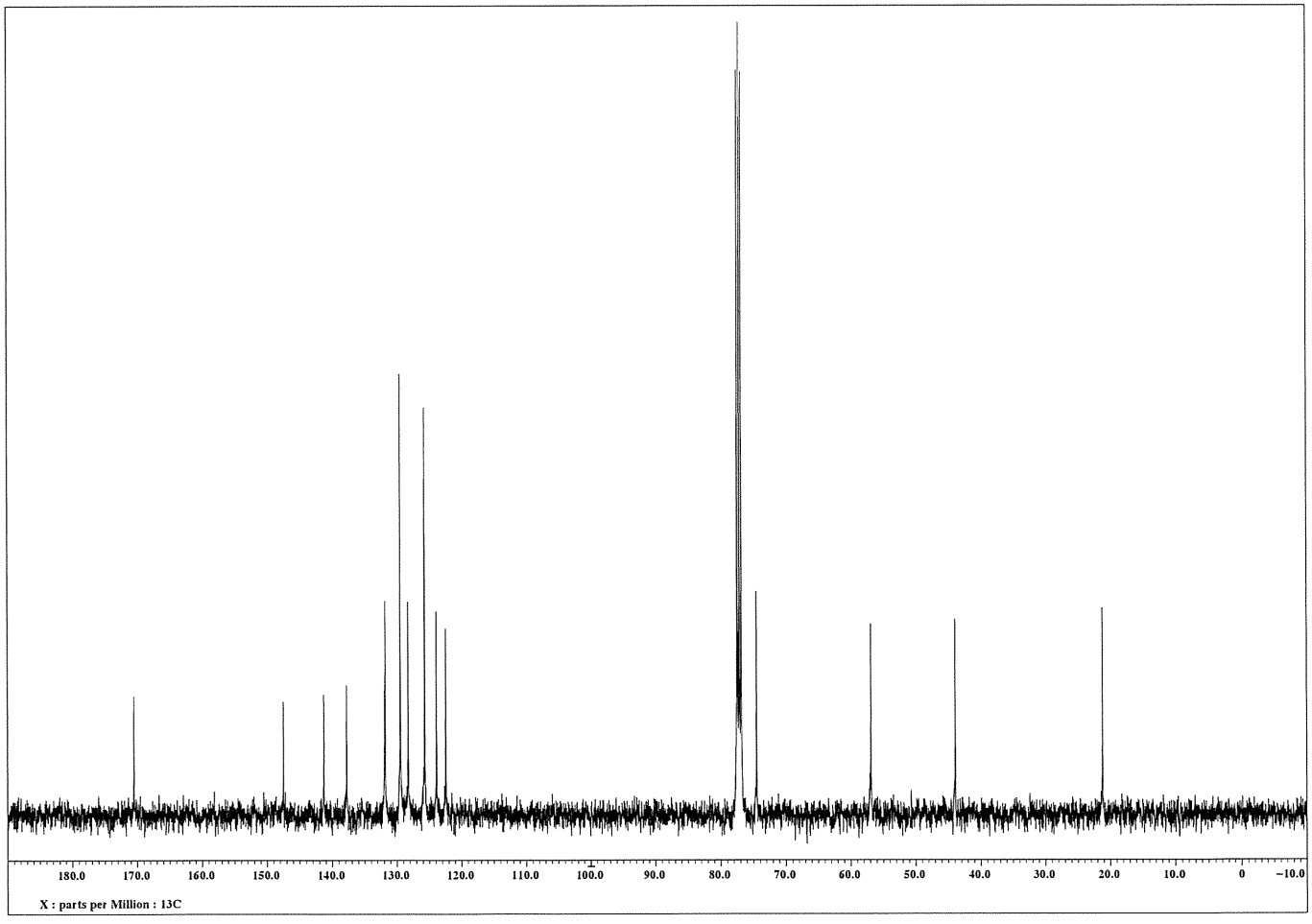

^{13}C NMR, 100 MHz, $CDCl_3$

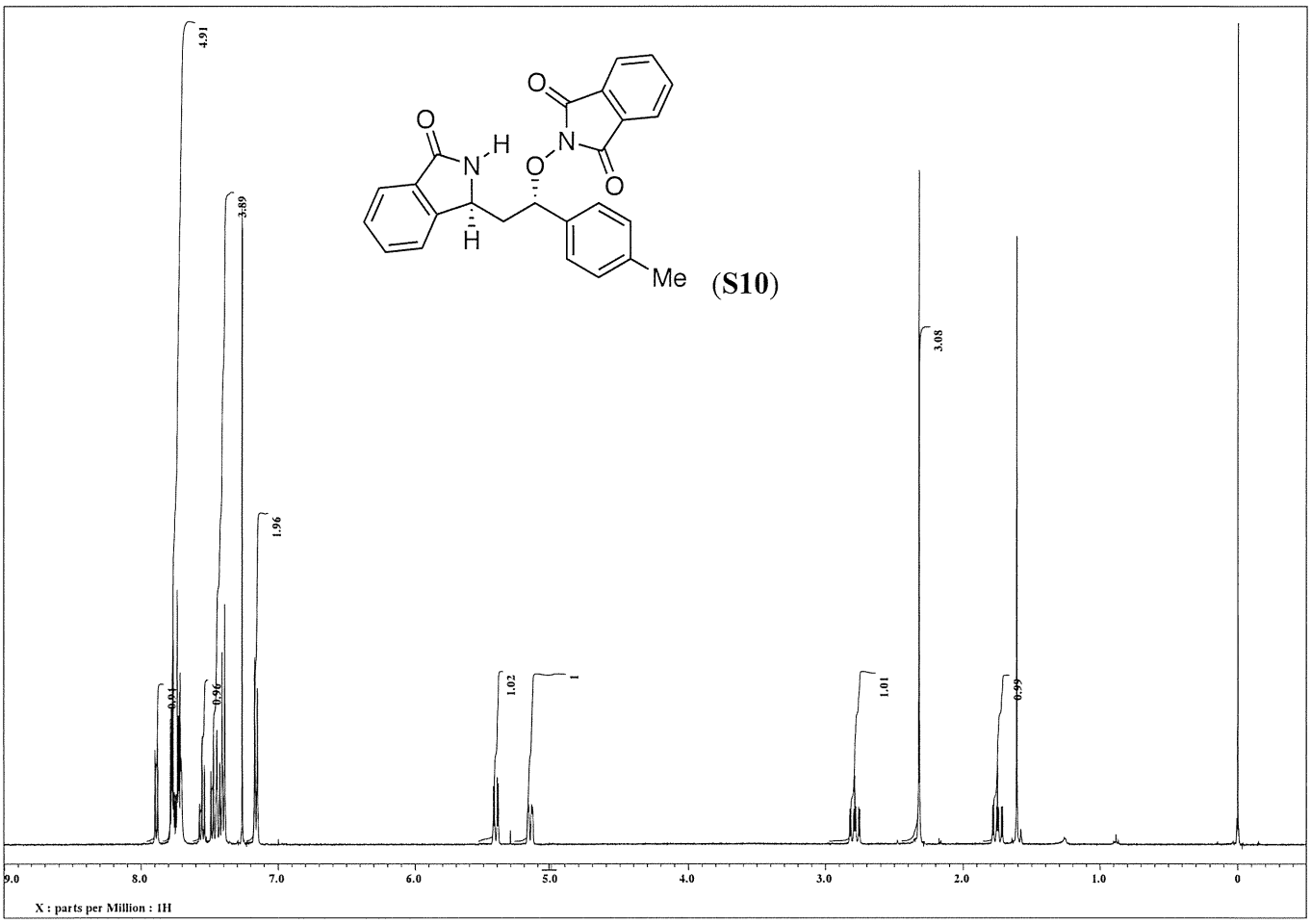

^{1}H NMR, 400 MHz, $CDCl_3$

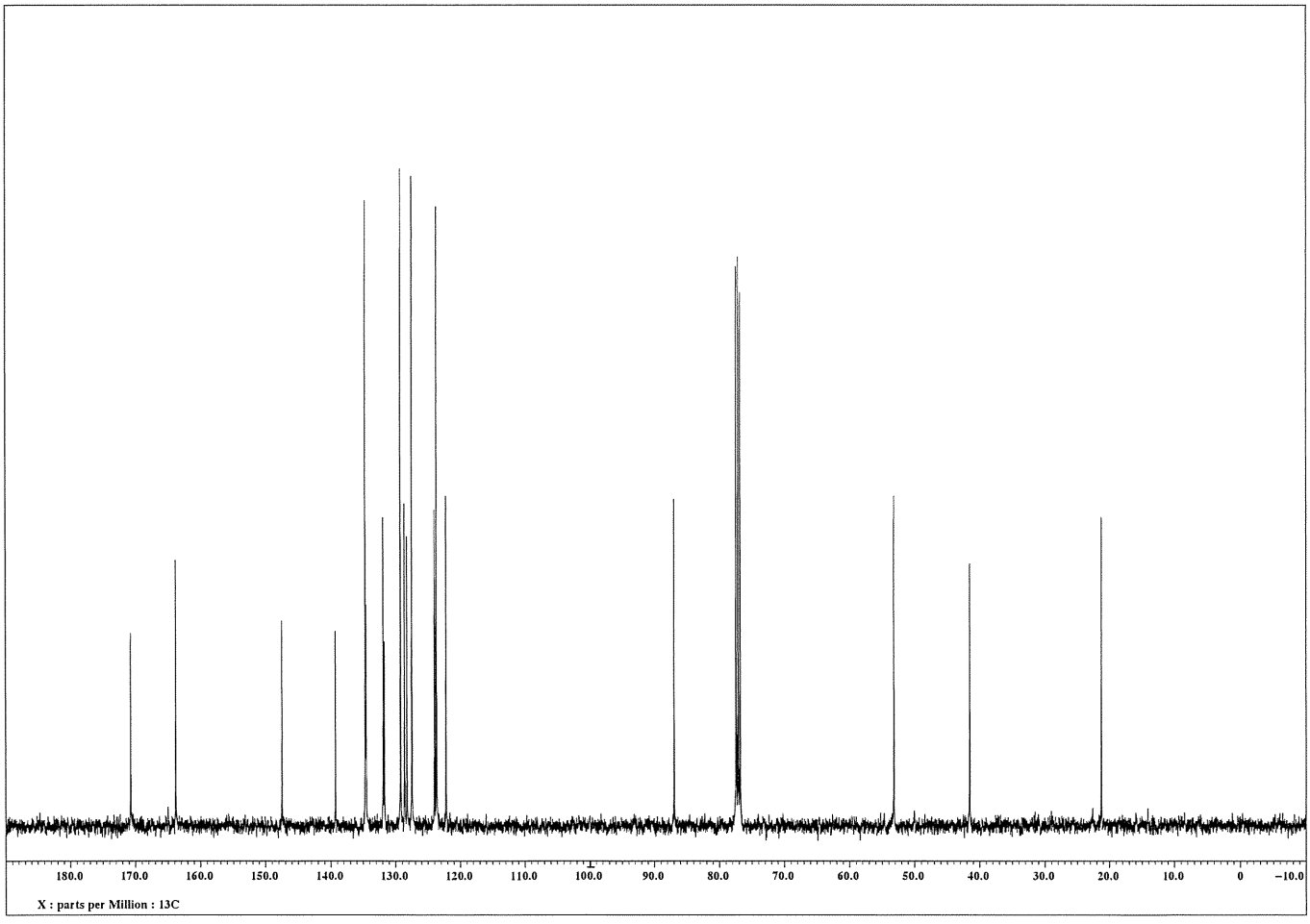

^{13}C NMR, 100 MHz, $CDCl_3$

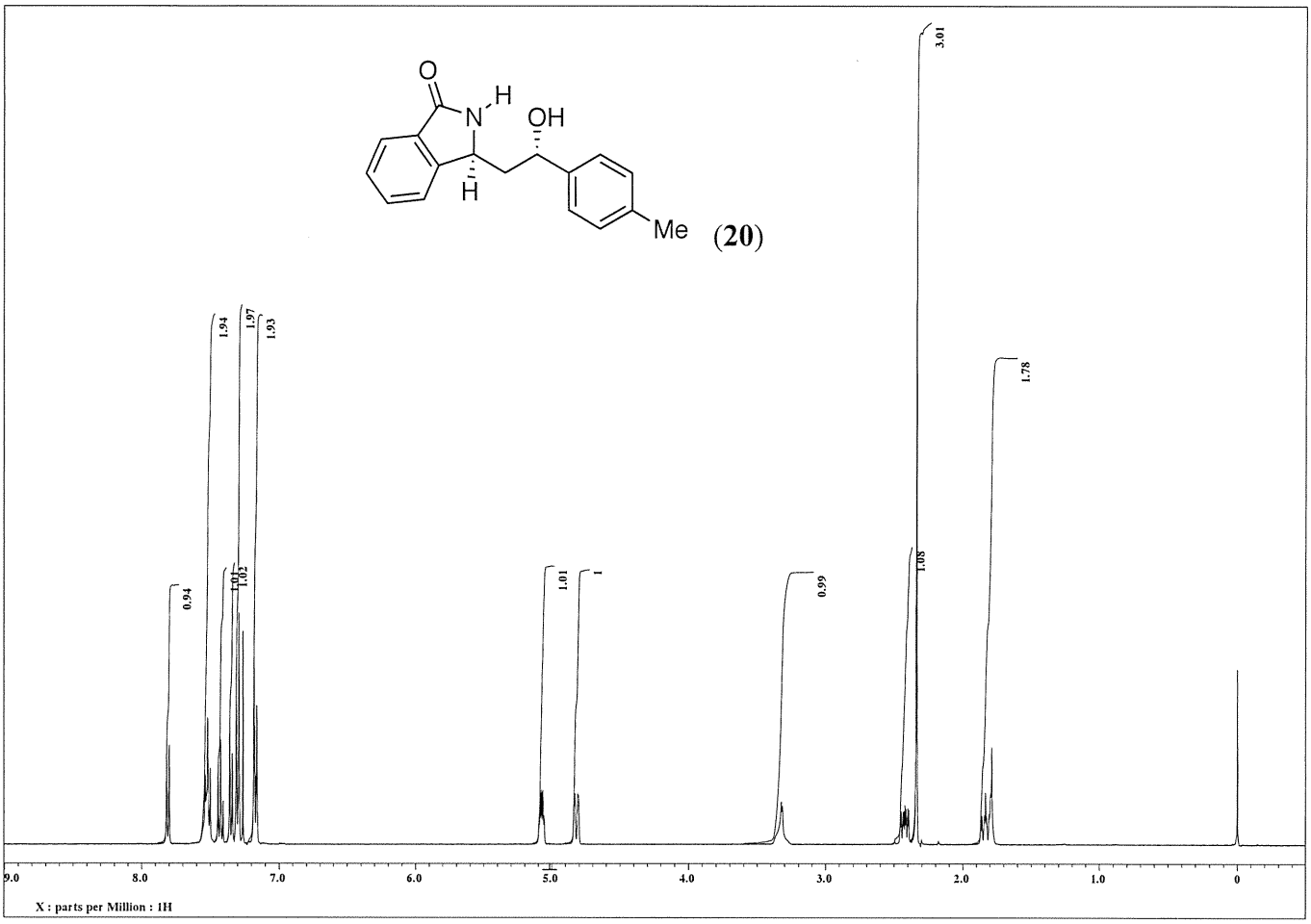

^{1}H NMR, 400 MHz, $CDCl_3$

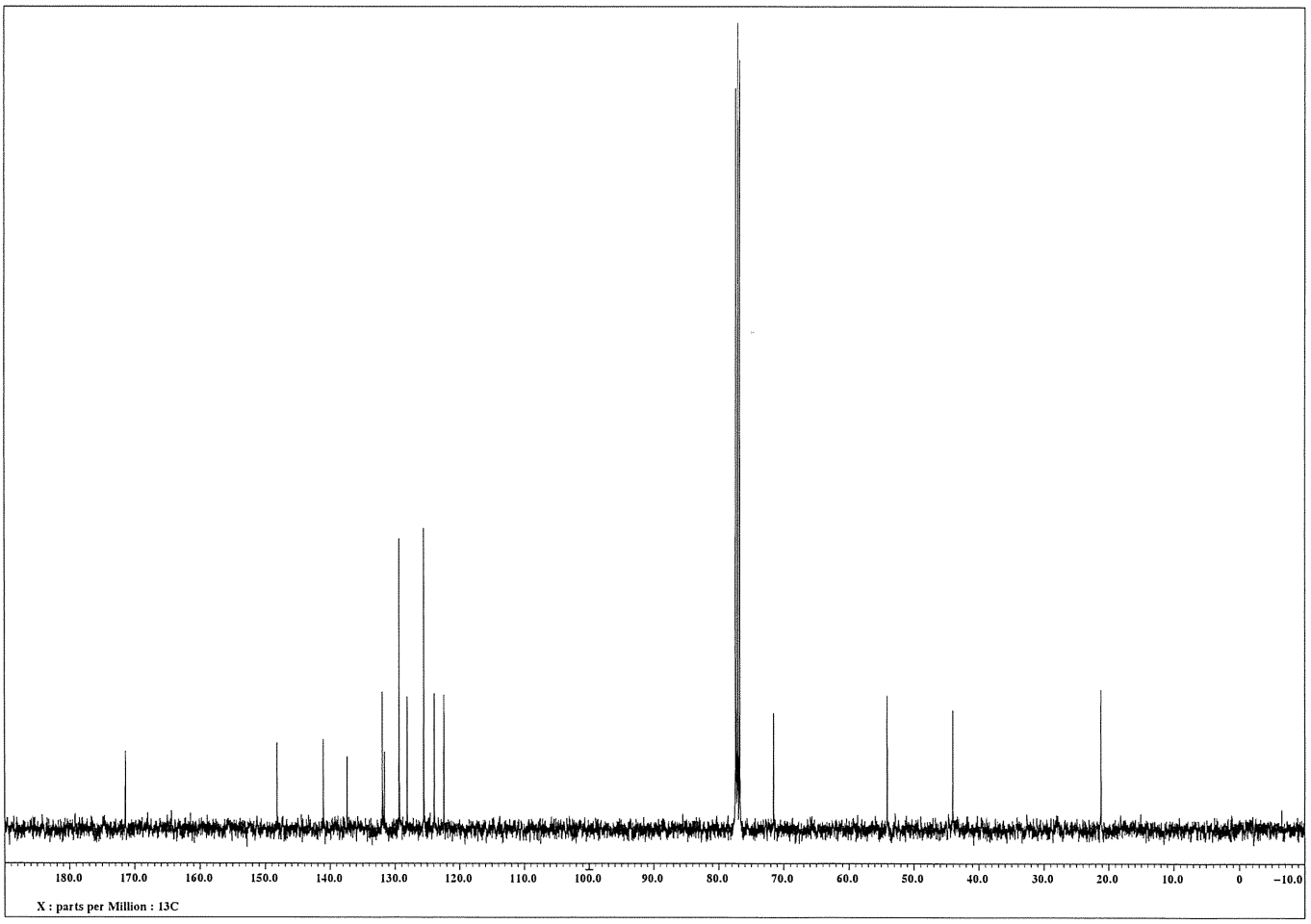

^{13}C NMR, 100 MHz, $CDCl_3$